

DESIGN AND REALIZATION OF MIXED ELEMENT
BROADBAND BANDPASS FILTERS

A THESIS SUBMITTED TO
THE GRADUATE SCHOOL OF NATURAL AND APPLIED SCIENCES
OF
THE MIDDLE EAST TECHNICAL UNIVERSITY

BY

İRFAN OKŞAR

IN PARTIAL FULFILMENT OF THE REQUIREMENTS FOR THE DEGREE OF
MASTER OF SCIENCE
IN
THE DEPARTMENT OF ELECTRICAL AND ELECTRONICS ENGINEERING

SEPTEMBER 2003

Approval of the Graduate School of Natural and Applied Sciences

Prof. Dr. Canan ÖZGEN
Director

I certify that this thesis satisfies all the requirements as a thesis for the degree of Master of Science.

Prof. Dr. Mübeccel DEMİREKLER
Head of Department

This is to certify that we have read this thesis and that in our opinion it is fully adequate, in scope and quality, as a thesis for the degree of Master of Science.

Prof. Dr. Nevzat YILDIRIM
Supervisor

Examining Committee Members

Prof. Dr. Canan TOKER (Chairman)

Prof. Dr. Nevzat YILDIRIM

Prof. Dr. Altuncan HIZAL

Assist. Prof. Dr. Şimşek DEMİR

Dilara GÜLER, M.S.E.E

ABSTRACT

DESIGN AND REALIZATION OF MIXED ELEMENT BROADBAND BANDPASS FILTERS

OKŞAR, İrfan

M.S., Department of Electrical and Electronics Engineering

Supervisor: Prof. Dr. Nevzat YILDIRIM

September 2003, 167 pages

In this thesis, a highly selective broadband hybrid bandpass filter operating between 0.4-2.0 GHz with a stopband up to 7 GHz is designed and analyzed. The realization is carried out by hybrid method, which combines both lumped and distributed element filters. In this approach, two separate filters, which are lumped highpass with 0.4 GHz corner frequency and distributed stripline lowpass with 2 GHz corner frequency, are combined to get the bandpass filter that has a passband in between 0.4 to 2.0 GHz. The usage of the lumped elements for the highpass filter resulted in a great size reduction compared to distributed element approach.

The design software FILPRO™ is used to synthesize the trial filters. More than forty filters are synthesized, and among them, the ones that have better properties are chosen for further processes. Optimization, modeling and electromagnetic simulations of the selected lumped and distributed filters are

carried out on the software GENESYS™. Distributed filters are also simulated using the software SONNET™.

After the simulations, all of the simulated filters are realized and measured, and the level of consistency with the simulations is observed. According to the results of the measurements, the filter combination that has the best combination of low insertion loss, small dimensions, high stopband attenuation and low spur levels is selected for the final bandpass filter structure and a few variants are examined to get the final structure.

Keywords: Lumped, Distributed, Stripline, Lowpass, Highpass, Quarter Wavelength Frequency, Spur, Kuroda Transformation.

ÖZ

KARMA ELEMANLI GENİŞBANT BANT GEÇİREN SÜZGEÇLERİN TASARIMI VE GERÇEKLEŞTİRİLMESİ

OKŞAR, İrfan

Yüksek Lisans, Elektrik ve Elektronik Mühendisliği Bölümü

Tez Yöneticisi : Prof. Dr. Nevzat YILDIRIM

Eylül 2003, 167 sayfa

Bu tez çalışmasında, yüksek seçicilikli geniş bantlı hibrit 0.4-2.0 GHz bantgeçiren ve 7GHz'e kadar bastırma bandı olan bir süzgeç tasarlandı ve analiz edildi. Süzgeç, toplu ve dağınk filtrelerin birleşmesiyle oluşan hibrit bir yapı ile sağlandı. Bu yaklaşımda, 0.4 GHz köşe frekanslı yüksek geçiren ve toplu elemanlardan oluşan süzgeç ile 2.0 GHz köşe frekanslı alçak geçiren ve dağınk elemanlardan oluşan iki ayrı filtre, 0.4-2.0 GHz geçirgen bandı olan filtreyi oluşturmak için birleştirildi. Yüksek geçiren filtre için toplu elemanların kullanılması dağınk eleman metoduna oranla filtre boyutlarının çok küçük tutulabilmesini sağladı.

Süzgeçleri sentezlemek için FILPRO™ programı kullanıldı. Kırtan fazla filtre sentezlendi ve aralarından daha iyi özelliklere sahip olanlar ileriki aşamalar için seçildi. Seçilen bütünleşik ve dağınk filtrelerin optimizasyonu, modellenmesi

ve elektromanyetik simülasyonları GENESYS™ programı kullanılarak gerçekleştirildi. Dağınık filtreler SONNET™ programı kullanılarak ta simüle edildi.

Simülasyonlardan sonra, simülasyonu yapılan bütün filtreler gerçekleştirildi ve ölçüldü, ve ölçümlerin simülasyon sonuçları ile olan uyumları incelendi. Ölçümlerin sonuçlarına göre, düşük araya grime kaybı, küçük boyut, yüksek bant dışı bastırma ve düşük spur seviye özelliklerini bir bütün olarak en iyi sunan filtre, bant geçiren filtreyi oluşturmak üzere seçildi ve nihayi yapıyı elde etmek için bu filtrenin birkaç değişik varyasyonu denendi.

Anahtar Kelimeler: Toplu, Dağınık, Kılavuz Hat, Alçak Geçiren, Yüksek Geçiren, Dörtte Bir Dalga Boyu, Spür, Kuroda Dönüşümü.

To My Family

ACKNOWLEDGEMENTS

I would like to express my sincere gratitude to Prof. Dr. Nevzat Yıldırım for his supervision, valuable guidance and helpful suggestions throughout the progress of the thesis.

I wish to express my sincere appreciation to İrfan Yıldız, Ahmet Kırılılar, Oral Dinçer, Serkan Sevim, Serhat Erzin, Şebnem Saygıner, İnanç Altungüneş, Dilara Bağdat, İbrahim Tekin, Zeynep Eymür and Murat Mutluol for their valuable friendship, help and support. I am also grateful to ASELSAN Inc. for facilities provided for the completion of this thesis.

I would like to extend my special appreciation and gratitude to my family for their encouragement, love and understanding of my spending lots of time on this work.

TABLE OF CONTENTS

ABSTRACT	iii
OZ.....	v
ACKNOWLEDGEMENTS.....	viii
TABLE OF CONTENTS.....	ix

CHAPTER

1. INTRODUCTION.....	1
1.1 Introduction	1
1.2 Scope of the Thesis	2
1.3 Design Tools	3
1.4 Organization of the Thesis.....	4
2. FILTER DESIGN PRINCIPLES	6
2.1 Introduction	6
2.2 Filter as a Two-Port Network	6
2.3 Typical Performance Measures	9
2.4 Types of Filters	9
2.5 Filter Design Methodology	13
2.6 Typical Performance Measures	15
2.7 Lumped and Distributed Classification	18
2.7.1 Lumped LC Filters.....	19
2.7.2 Distributed Element Filters.....	21

2.7.3 Hybrid Lumped and Distributed Filters.....	28
2.8 Waves and Impedances on Transmission Lines.....	29
2.8.1 Transmission Line Circuit Model.....	29
2.8.2 The Complex Reflection Coefficient Γ	32
2.8.3 Voltage Standing Wave Ratio (SWR) and Return Loss..	33
2.9 Commensurate Line Filters.....	36
2.10 Circuit Transformations.....	37
2.10.1 Richard's Transformation.....	37
2.10.2 Kuroda Identities	39
2.10.3 Impedance Inverters	41
2.10.4 Norton Transformations.....	42
2.11 Remarks	43
3. LUMPED HIGHPASS FILTER DESIGN TRIALS.....	44
3.1 Introduction.....	44
3.2 Design Trials of the Highpass Filter	46
3.2.1 Highpass Filter Trial 1.....	46
3.2.2 Highpass Filter Trial 2.....	49
3.2.3 Highpass Filter Trial 3.....	50
3.2.4 Highpass Filter Trial 4.....	51
3.2.5 Highpass Filter Trial 5.....	52
3.2.6 Highpass Filter Trial 6.....	53
3.2.7 Highpass Filter Trial 7.....	54
3.2.8 Highpass Filter Trial 8.....	55
3.2.9 Highpass Filter Trial 9.....	55
3.2.10 Highpass Filter Trial 10.....	56
3.2.11 Highpass Filter Trial 11.....	57
3.2.12 Highpass Filter Trial 12.....	58
3.2.13 Highpass Filter Trial 13.....	59

3.2.14 Highpass Filter Trial 14.....	60
3.2.15 Highpass Filter Trial 15.....	61
3.2.16 Highpass Filter Trial 16.....	61
4. DISTRIBUTED LOWPASS FILTER DESIGN TRIALS	64
4.1 Introduction	64
4.2 Design Trials of the Lowpass Distributed Filter	66
4.2.1 Lowpass Filter Trial 1.....	70
4.2.2 Lowpass Filter Trial 2.....	74
4.2.3 Lowpass Filter Trial 3.....	75
4.2.4 Lowpass Filter Trial 4.....	76
4.2.5 Lowpass Filter Trial 5.....	78
4.2.6 Lowpass Filter Trial 6.....	79
4.2.7 Lowpass Filter Trial 7.....	80
4.2.8 Lowpass Filter Trial 8.....	81
4.2.9 Lowpass Filter Trial 9.....	82
4.2.10 Lowpass Filter Trial 10.....	83
4.2.11 Lowpass Filter Trial 11.....	85
4.2.12 Lowpass Filter Trial 12.....	86
4.2.13 Lowpass Filter Trial 13.....	87
4.2.14 Lowpass Filter Trial 14.....	89
4.2.15 Lowpass Filter Trial 15.....	90
4.2.16 Lowpass Filter Trial 16.....	91
4.2.17 Lowpass Filter Trial 17.....	92
4.2.18 Lowpass Filter Trial 18.....	93
4.2.19 Lowpass Filter Trial 19.....	94
4.2.20 Lowpass Filter Trial 20.....	95
4.2.21 Lowpass Filter Trial 21.....	96
4.2.22 Lowpass Filter Trial 22.....	98
4.2.23 Lowpass Filter Trial 23.....	99

4.2.24 Lowpass Filter Trial 24.....	100
4.2.25 Lowpass Filter Trial 25.....	101
4.2.26 Lowpass Filter Trial 26.....	102
4.2.27 Lowpass Filter Trial 27.....	103
4.2.28 Lowpass Filter Trial 28.....	104
4.2.29 Lowpass Filter Trial 29.....	105
4.3 Selected Filter Versions	106
4.3.1 Selected Lowpass Filter 1 (Trial 11).....	106
4.3.2 Selected Lowpass Filter 2 (Trial 28).....	107
4.3.3 Selected Lowpass Filter 3 (Trial 29).....	108
5. OPTIMIZATION, SIMULATION AND REALIZATION OF THE SELECTED FILTERS	110
5.1 Introduction	110
5.2 Lumped Highpass Filter	115
5.2.1 First Layout	119
5.2.2 Second Layout	125
5.3 Selected Lowpass Filter 1	131
5.4 Selected Lowpass Filter 2	138
5.5 Selected Lowpass Filter 3	144
5.5 Combination of Lowpass and Highpass Filters to form Bandpass Filter	149
6. CONCLUSION.....	156
REFERENCES.....	159

APPENDICES

**APPENDIX A. STRIPLINE SUBSTRATE AND DRILL HOLE
DIMENSIONS.....161**

**APPENDIX B. PROPERTIES OF STRIPLINE DIELECTRIC
MATERIAL162**

APPENDIX C. PROPERTIES OF LUMPED INDUCTORS.....164

LIST OF TABLES

TABLE

3.1 Four-decade element values of the E12 series, starting value is 1 pF for capacitors and 1 nH for inductors	45
5.1 Layout and grid sizes. The dimensions are in mils	120
5.2 Layout and grid sizes. The dimensions are in mils	126
5.3 Equivalent widths of TLs and stubs	132
5.4 Layout and grid sizes. The dimensions are in mils	133
5.5 Equivalent widths of TLs and stubs	139
5.6 Layout and grid sizes. The dimensions are in mils	140
5.7 Layout and grid sizes. The dimensions are in mils	145

LIST OF FIGURES

FIGURES

1.1 Separate highpass and lowpass filters are combined to get the bandpass filter response.....	2
2.1 Filter as a two-port network with S-parameter representation.....	6
2.2 Filter types according to frequency selectivity	11
2.3 Ideal bandpass filter magnitude and phase characteristics.....	12
2.4 Typical amplitude response of a bandpass filter	12
2.5 Typical frequency response of a band-pass(or high pass) distributed filter.....	13
2.6 Basic filter design process using insertion loss method.....	14
2.7 Bessel filter amplitude response.....	15
2.8 Gaussian filter amplitude response	16
2.9 Butterworth filter amplitude response.....	16
2.10 Chebychev type-1 amplitude response.....	17
2.11 Chebychev type-2 amplitude response.....	17
2.12 Elliptic filter amplitude response	18
2.13 A typical lumped LC filter	18
2.14 A typical microstrip filter.....	19
2.15 (a) Coilcraft 1008CS inductor and (b) Philips 0603 capacitor, scales are the same.	21
2.16 Inductance vs. frequency of the 100 nH inductor	22
2.17 The 100 nH inductor has a 10% increase at around 150 MHz.....	22
2.18 Capacitance vs. frequency of the 100 pF capacitor.....	23
2.19 The 100 pF capacitor has a 10% increase at around 50 MHz.....	23
2.20 Some examples of commensurate distributed filters, (a) Parallel coupled line filter, (b) Interdigital filter and (c) Compline filter.....	26

2.21 Stub filter having O.C. and S.C. stubs	26
2.22 Equivalent representation of an incremental TL piece	29
2.23 Equivalent transmission line configurations for lumped elements	38
2.24 The four Kuroda identities	40
2.25 Equivalent circuits illustrating Kuroda identity (a) in Figure 2.22	41
2.26 Impedance inverter	42
2.27 Norton Transformations	42
3.1 Elements of Trial 1	47
3.2 Type B dual of Trial 1	48
3.3 Insertion loss characteristic of Trial 1	48
3.4 Return loss characteristic of Trial 1	48
3.5 Elements of Trial 2	49
3.6 Elements of Trial 3	50
3.7 S21 response of Trial 3	50
3.8 Elements of Trial 4	51
3.9 S21 response of Trial 4	51
3.10 Elements of Trial 5	52
3.11 S21 of Trial 5	52
3.12 Elements of Trial 6	53
3.13 S21 graph Trial 6	53
3.14 S11 plot of Trial 6	54
3.15 Elements of Trial 7	54
3.16 Elements of Trial 8	55
3.17 Elements of Trial 9	55
3.18 Elements of Trial 10	56
3.19 S21 graph. Stopband attenuation is min 102 dB	57
3.20 Elements of Trial 11	57
3.21 S21 graph. Stop attenuation is min 82 dB	58
3.22 Elements of Trial 12	58
3.23 Elements of Trial 13	59
3.24 S21 graph. Stopband attenuation is min 77 dB	59

3.25 Elements of Trial 14	60
3.26 S21 graph. Stopband attenuation is min 80 dB	60
3.27 Elements of Trial 15	61
3.28 Elements of Trial 16	61
3.29 S21 graph. Stopband attenuation is min 75 dB	62
3.30 S11 graph, inband return loss is min 19 dB	62
3.31 Monte Carlo analysis with 5% element deviation.....	63
4.1 The wide shunt stub deteriorates the quarter wavelength behavior of the adjacent series TLs	65
4.2 Basic microstrip-like structures, the thin dark surfaces are conductors while the light color sections are the dielectric layers	67
4.3 Cut-away view of a stripline filter	67
4.4 The selected topology for the distributed low pass structure	68
4.5 The lumped equivalent of the distributed lowpass filter. Six elements that are not indicated are TZs at ∞ , and they are the counterparts of the non-redundant UEs in the distributed filter	68
4.6 S21 of the distributed circuit	69
4.7 S21 of the lumped counterpart	69
4.8 (a) Kuroda transformation is used to eliminate the series short circuited stubs, (b) The shunt series short-circuited and open-circuited stub resonator is transformed to step resonator (c) The final structure where elements are easier to realize	70
4.9 Elements of Trial 1	71
4.10 S21 graph of Trial 1	71
4.11 S11 graph Trial 1	72
4.12 23.920 Ω shunt open circuited stubs are replaced by lumped capacitors	72
4.13 S21 graph of the modified circuit.....	73
4.14 23.920 Ω shunt open circuited stubs are replaced by lumped resonators	73
4.15 S21 graph when lumped resonators are used	74
4.16 Elements of Trial 2	74
4.17 S21 graph of Trial 2	75

4.18 Elements of Trial 3	76
4.19 S21 graph of Trial 3	76
4.20 Elements of Trial 4	20
4.21 S21 graph of Trial 4	21
4.22 Elements of Trial 5	78
4.23 S21 graph of Trial 5	78
4.24 Elements of Trial 6	79
4.25 S21 graph of Trial 6	79
4.26 Elements of Trial 7	80
4.27 S21 graph of Trial 7	81
4.28 Elements of Trial 8	81
4.29 S21 graph of Trial 8	82
4.30 Elements of Trial 9	83
4.31 S21 graph of Trial 9	83
4.32 Elements of Trial 10	84
4.33 S21 graph Trial 10	84
4.34 Elements of Trial 11	85
4.35 S21 graph of Trial 11	86
4.36 Elements of Trial 12	86
4.37 S21 graph of Trial 12	87
4.38 Elements of Trial 13	88
4.39 S21 graph of Trial 13	88
4.40 Elements of Trial 14	89
4.41 S21 graph of Trial 14	89
4.42 Elements of Trial 15	90
4.43 S21 graph of Trial 15	90
4.44 Elements of Trial 16	91
4.45 S21 graph Trial 16	91
4.46 Elements of Trial 17	92
4.47 S21 graph of Trial 17	93
4.48 Elements of Trial 18	93

4.49 S21 graph Trial 18	94
4.50 Elements of Trial 19 with the inner shunt stubs divided into two equal parts	94
4.51 S21 graph Trial 19	95
4.52 Elements of Trial 20	96
4.53 S21 graph Trial 20	96
4.54 Elements of Trial 21	97
4.55 S21 graph Trial 21	97
4.56 Elements of Trial 22	98
4.57 S21 graph of Trial 22	98
4.58 Elements of Trial 23	99
4.59 S21 graph of Trial 23	99
4.60 Elements of Trial 24	100
4.61 S21 graph of Trial 24	100
4.62 Elements of Trial 25	101
4.63 S21 graph of Trial 25	101
4.64 Elements of Trial 26	102
4.65 S21 graph of Trial 26	103
4.66 Elements of Trial 27	103
4.67 S21 graph Trial 27	104
4.68 Elements of Trial 28	105
4.69 S21 graph of Trial 28	105
4.70 Elements of Trial 29	106
4.71 Elements of Selected Lowpass Filter 1	107
4.72 S21 response of the Selected Lowpass Filter 1	107
4.73 Elements of Selected Lowpass Filter 2	108
4.74 S21 graph of Selected Lowpass Filter 2	108
4.75 Elements of Selected Lowpass Filter 3	109
5.1 In (a) the real structure is shown, and (b) and (c) are two different approximations that can be used in simulations.....	111
5.2 A meshing example where the grids do not fit the structure.....	112

5.3 Rectangular mesh	113
5.4 Elements of lumped highpass filter	115
5.5 Tuned filter with E12 element values using GENESYS.....	115
5.6 Ideal S21 of the highpass filter.....	116
5.7 Ideal S11 of the lowpass filter.....	117
5.8 S21 response of the optimized lowpass filter.....	117
5.9 S11 response of the optimized lowpass filter.....	118
5.10 The upper side of the first lumped HP layout	119
5.11 The bottom side of the first lumped HP layout	119
5.12 Combined view of the 0.4 GHz highpass filter.....	120
5.13 Layout parameters of the first layout	120
5.14 Insertion loss result of the EM simulation compared with the linear analysis	121
5.15 Return loss result of the EM simulation compared to linear analysis.....	121
5.16 Top view of the first 400 MHz HP filter layout.....	122
5.17 Bottom view of the first 400 MHz HP filter layout	122
5.18 Measured S21 up to 800 MHz	123
5.19 Measured S21 up to 9 GHz	123
5.20 Measured S11 up to 800 MHz	124
5.21 Measured S11 up to 9 GHz	124
5.22 Parameters of the EM simulation in GENESYS.....	125
5.23 Top view of the second HP filter layout	125
5.24 Bottom view of the second HP filter layout.....	125
5.25 Insertion loss result of the EM simulation compared with the linear analysis.	126
5.26 Return loss result of the EM simulation compared to linear analysis.....	126
5.27 Top view of the second HP filter with elements and connectors soldered ..	127
5.28 Bottom view of the second HP filter with elements and connectors soldered	127
5.29 Filter with the soldered supporting structure	127
5.30 Measured insertion loss of the second lumped HP filter up to 800 MHz	128

5.31 Measured insertion loss of the second lumped HP filter up to 9 GHz.....	128
5.32 Measured return loss of the second lumped HP filter up to 800 MHz.....	129
5.33 Measured return loss of the second lumped HP filter up to 9 GHz	129
5.34 Schematic with 0.5 pF coupling capacitors.....	130
5.35 Distortion in insertion loss due to simulated coupling.....	130
5.36 Elements of Selected Lowpass Filter 1	131
5.37 Linear scheme of Selected Lowpass Filter 1	131
5.38 Layout view of Selected Lowpass Filter 1	132
5.39 Linear analysis S21 and S11 responses of Selected Lowpass Filter 1	133
5.40 Parameters of the layout in GENESYS.....	133
5.41 EM simulation output obtained from GENESYS	134
5.42 EM simulation output obtained from SONNET	134
5.43 View of TLs and stubs of Selected Lowpass Filter 1	135
5.44 Connected view of Selected Lowpass Filter 1	135
5.45 Side view of Selected Lowpass Filter 1	136
5.46 Near the connector due to soldering the top and bottom parts may not be connected properly, the filter is resoldered to correct this error.	136
5.47 Measured insertion loss of Selected Lowpass Filter 1 up to 6 GHz	137
5.48 Measured return loss of Selected Lowpass Filter 1 up to 6 GHz.....	137
5.49 Elements of Selected Lowpass Filter 2	138
5.50 Linear scheme of Selected Lowpass Filter 2 constructed in GENESYS ...	138
5.51 Layout view of Selected Lowpass Filter 2	139
5.52 Linear analysis S21 and S11 responses of Selected Lowpass Filter 2	140
5.53 Parameters of the EM simulation in GENESYS.....	140
5.54 EM simulation output obtained from GENESYS	141
5.55 EM simulation output obtained from SONNET	141
5.56 TLs and stubs of Selected Lowpass Filter 2	142
5.57 Measured insertion loss of Selected Lowpass Filter 2 up to 6 GHz	142
5.58 Measured return loss of Selected Lowpass Filter 2 up to 6 GHz.....	143
5.59 Elements of Selected Lowpass Filter 3	144
5.60 Linear scheme of Selected Lowpass Filter 3 in GENESYS	144

5.61	Layout view of Selected Lowpass Filter 3	145
5.62	Linear analysis S21 and S11 responses of Selected Lowpass Filter 3	145
5.63	Parameters of the EM simulation in GENESYS	146
5.64	EM simulation output obtained from GENESYS	146
5.65	EM simulation output obtained from SONNET	147
5.66	TLs and stubs of Selected Lowpass Filter 3	147
5.67	Measured insertion loss of Selected Lowpass Filter 3 up to 6 GHz	148
5.68	Measured insertion loss of Selected Lowpass Filter 3 up to 6 GHz	148
5.69	Lower part's top layout before soldering	149
5.70	Lower part's top layout after soldering	149
5.71	Lower part's bottom side after soldering	150
5.72	Upper part's top side	150
5.73	Upper part's bottom side	150
5.74	Measured S21 response of the connected filters up to 6 GHz	151
5.75	Measured S11 response of the connected filters up to 6 GHz	151
5.76	Inside view of the box	152
5.77	Side view of the BP filter box	152
5.78	Top view of the BP filter box	153
5.79	Oblique view of the BP filter box	153
5.80	Measured S21 response of the final boxed BP filter up to 6 GHz	154
5.81	Measured S11 response of the final boxed BP filter up to 6 GHz	154
A.1	Dimensions of the stripline substrate and locations of the drill holes for aluminum box	161
B.1	Rogers 5870/5880 substrates	162
B.2	Material properties of Rogers 5870/5880 substrates	163
C.1	Coilcraft 0603CS inductors	164
C.2	Coilcraft 0603CS inductors' Q and L curves	165
C.3	Coilcraft 0805CS inductors	166
C.4	Coilcraft 0805CS inductors' Q and L curves	167

LIST OF ABBREVIATIONS

IL	: Insertion Loss
RL	: Return Loss
UE	: Unit Element
O/C	: Open Circuit
S/C	: Short Circuit
FTZ	: Finite Transmission Zero
TL	: Transmission Line
SRF	: Self Resonant Frequency
f_q	: Quarter wavelength frequency
TZ	: Transmission Zero
FTZ	: Finite Transmission Zero
GB	: Giga Byte
RAM	: Random Access Memory
SCSI	: Small Computer System Interface
IDE	: Integrated Device Electronics
RADAR	: Radio Detection and Ranging
EM	: Electro Magnetic
2D	: Two Dimension
3D	: Three Dimension

CHAPTER 1

INTRODUCTION

1.1 Introduction

It is desirable to have circuits capable of selectively filtering one frequency or range of frequencies out of a mix of different frequencies in a circuit. A circuit designed to perform this frequency selection is called a filter circuit, or simply a filter. The ideal filter network provides perfect transmission for all frequencies in certain passband regions and infinite attenuation in the stopband regions [8]. Filter design problem may also be defined as the achievement of a desired frequency response between a generator and a load, over a given frequency band [10].

Filters are primary elements of communication systems. Their functionality has an unavoidable significance in processing signals at a wide range of frequency spectrum. Insertion loss, return loss, impedance, phase and group delay are typical performance measures that are mostly encountered.

The aim of this thesis is to search for the design and implementation of a bandpass filter having a passband between 0.4 GHz to 2.0 GHz with some certain specifications. Using simulation tools effectively and comparing the final results with the simulation outputs to decide on the dependability of the software is aimed. Developing a highly selective filter printed on a single substrate with no external tuning, and meeting the normal electrical and environmental requirements associated with such components are also desired.

1.2 Scope of the Thesis

The following specifications are accepted for the electrical performance:

3 dB passband: 0.4 to 2 GHz

Insertion loss in pass-band: Max. 2 dB

Return loss in pass-band: Min. 10dB

Stopband attenuation: Min 60 dB at $\pm 20\%$ of the corner frequencies

Stopband up to 6 GHz

Since the filter bandwidth is very wide, 1.6 GHz passband centered at 1.2 GHz, it is found inconvenient to design the filter using a single bandpass structure transformed from a lowpass prototype. Combining a 0.4 GHz highpass filter with a 2.0 GHz lowpass filter is preferred to obtain the 0.4-2.0 GHz bandpass filter as seen in Figure 1.1 below:

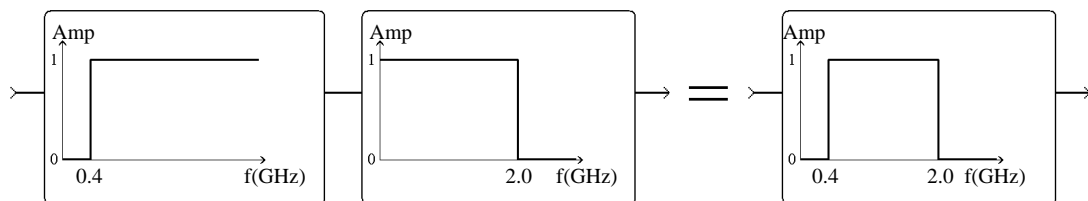


Figure 1.1: Separate highpass and lowpass filters are combined to get the bandpass filter response

The hybrid element methodology is selected to keep the size as small as possible. The frequency spectrum around 1 GHz is sometimes called the awkward transition region due to the fact that, lumped elements usually deteriorate so much after 500 MHz and size of the distributed filters gets too large below 2 GHz.

The highpass filter is realized using the lumped approach mainly because small size is achieved using this approach. Similar distributed filters would be approximately ten times larger compared to lumped counterparts.

The lowpass filter is realized in stripline form, because low loss, high stopband attenuation and high stopband frequencies can be satisfied using this structure with the simplicity of construction.

Lowpass and highpass filters are designed independently due to the fact that the combined bandpass filter is very wide band; the corner frequency of the lowpass filter (2 GHz) is 5 times the corner frequency of the highpass filter (0.4 GHz). Both of the filters are tuned and optimized until the desired specifications are met. When the highpass and lowpass filters are combined to form the bandpass filter, there was no need to tune the overall structure.

To reach the desired filter response, design, simulation, optimization, construction and measurement of different kinds of filters with distinct design parameters are investigated.

1.3 Design Tools

The design stage involves use of several synthesis, analysis, simulation and optimization tools in circuit theory and electromagnetic theory levels.

The filters are designed using FILPRO™. FILPRO is a filter synthesis, transformation and analysis software. All kinds of passive amplitude filtering networks; both lumped and distributed, can be designed using FILPRO. Optimization and Monte Carlo analysis is also included in FILPRO. This software is developed in Electrical Engineering Department of METU [1].

GENESYS™ is a linear design tool of EAGLEWARE Company. Most of the analysis, tuning and optimization of the filters are carried out using linear toolbox of GENESYS™ software. The physical dimensions of the microstrips and striplines are calculated using the TLINE tool of GENESYS™ [2]. Electromagnetic Simulations of the filters are performed using this software. This software has the

capability of combining linear and electromagnetic analysis, which is very usable especially for lumped filters.

SONNET™ is an electromagnetic analysis software, which uses method of moments (MOM) to solve the current distribution on the metallization of the circuit under consideration [3]. In this thesis SONNET™ is used for characterization of discontinuities such as tee and cross, which are also not available in CAD tools' circuit element libraries and for analysis of layout problems such as undesired couplings and parasitic effects.

HFSS™ (High Frequency Structure Simulator) is a three dimensional (3D) simulator which uses Finite Element Method (FEM). Objects are divided into small tetrahedrons for calculation [17]. One of the filters is simulated using HFSS to be able to compare the results with GENESYS and SONNET.

1.4 Organization of the Thesis

To keep synchronism with the filter design process, this thesis is organized in the order of design steps when designing a filter.

In Chapter 2, the basic building blocks of the filter design process is described. This chapter is a summary of the knowledge gained to have a basic understanding of the filter design process. This way, the work done in the succeeding chapters will easily be understood.

Chapter 3 is devoted to lumped high pass filter synthesis using FILPRO's synthesis tool. This chapter starts with the criteria that are considered for the synthesized lumped highpass filters. After that 16 filter synthesis trials are explained and compared to each other. According to the results obtained in this stage, optimum lumped filter structure is chosen for further simulation, optimization and realization processes.

In Chapter 4, some of the distributed filter criteria are introduced similar to lumped criteria. After that, some basic microstrip-like structures are shown and among them stripline structure, which will be the structure to be used, is detailed. A lumped-distributed analogy is also given before the trials. 29 filter trials are performed in this chapter. According to the resulting responses, 3 filter structures are found appropriate for further analysis.

Chapter 5 is devoted to simulation, optimization and realization of the selected filter structures. Simulations are performed using Genesys™ and SONNET™ programs. The ideal transmission lines and stubs of filters are transformed into stripline form for realization. The physical parameters of transmission lines are calculated using TLINE™ tool of GENESYS™. The resulting stripline filters are simulated and outputs of the simulation results are explained. One of the distributed filter simulations is also performed using HFSS to see the similarity between GENESYS and SONNET. Approving the responses of the filters with the simulation outputs, various forms of the filters are realized using the drilling method. The realized filters are tested and the measurements are considered. The obtained performances are compared with the simulation outputs. Finally, some optimizations are performed to tune the final bandpass filter's highpass and lowpass pairs and the final response of the bandpass filter is given.

Chapter 6 concludes the thesis with results, expectations and new ideas on the continuation of the subject.

CHAPTER 2

FILTER DESIGN PRINCIPLES

2.1 Introduction

The purpose of this introductory chapter is to give a brief discussion of filters. The basics introduced here indicate the theoretical knowledge gained during this thesis work, which helps a clear understanding of the succeeding chapters.

In this chapter, network representation of filters, filter performance measures, filter types, filter design methodology, approximating functions, lumped and distributed classification, some transmission line related topics, Richard's and Norton's Transformations and Kuroda's identities will be examined.

2.2 Filter as a Two-Port Network

A filter may be analyzed as a two-port network [15]. In Figure 2.1, a filter network embedded between a resistive source R_S and a resistive load R_L is seen:

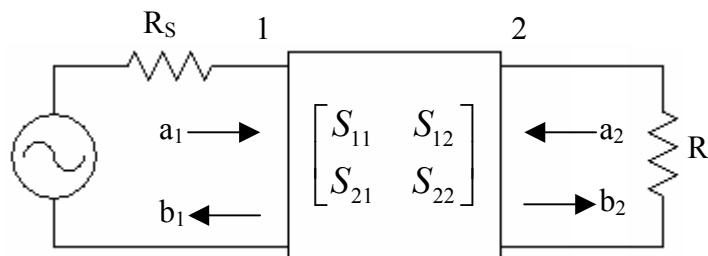


Figure 2.1: Filter as a two-port network with S-parameter representation

If we define:

E_{i1} as the incident wave from the source to the network

E_{i2} as the incident wave from the load to the network

E_{r1} as the reflected wave from to the network to the source

E_{r2} as the reflected wave from to the network to the load

then a_1 , a_2 , b_1 and b_2 are defined as [18]:

$$a_1 = \frac{E_{i1}}{\sqrt{Z_0}} \quad , \quad a_2 = \frac{E_{i2}}{\sqrt{Z_0}} \quad , \quad b_1 = \frac{E_{r1}}{\sqrt{Z_0}} \quad , \quad b_2 = \frac{E_{r2}}{\sqrt{Z_0}} \quad . \quad (2.1)$$

where; Z_0 is the characteristic impedance of the lossless transmission line

$$Z_0 = \sqrt{\frac{L}{C}}$$

which connects the network to the source and the load.

S parameters are defined as:

S_{11} : Input reflection coefficient with the output port terminated by a matched load ($R_L=Z_0$)

$$S_{11} = \left. \frac{b_1}{a_1} \right|_{a_2=0} \quad (2.2)$$

S_{22} : Output reflection coefficient with the input port terminated by a matched source ($R_S=Z_0$)

$$S_{22} = \left. \frac{b_2}{a_2} \right|_{a_1=0} \quad (2.3)$$

S_{21} : Forward transmission coefficient with the output port terminated by a matched load ($R_L=Z_0$)

$$S_{21} = \left. \frac{b_2}{a_1} \right|_{a_2=0} \quad (2.4)$$

S_{12} : Reverse transmission coefficient with the input port terminated by a matched source ($R_S=Z_0$)

$$S_{12} = \left. \frac{b_1}{a_2} \right|_{a_1=0} \quad (2.5)$$

Writing Equation (2.2), (2.3), (2.4) and (2.5) in matrix form we obtain:

$$\begin{bmatrix} b_1 \\ b_2 \end{bmatrix} = \begin{bmatrix} S_{11} & S_{12} \\ S_{21} & S_{22} \end{bmatrix} \cdot \begin{bmatrix} a_1 \\ a_2 \end{bmatrix} \quad (2.6)$$

S parameters are normalized with respect to R_S and R_L . We will choose R_S and R_L 50Ω for the filters we deal with, which is the most common impedance value for RF and microwave devices and transmission lines.

2.3 Typical Performance Measures

In practice, filter responses are specified in terms of insertion loss (IL), return loss (RL), voltage standing wave ratio (VSWR), insertion phase (Ψ) and group delay (GD) which are defined as

$$IL = 10 \log \frac{1}{|S_{21}(f)|^2} \quad (2.7)$$

$$RL = 10 \log \frac{1}{|S_{11}(f)|^2} \quad (2.8)$$

$$VSWR = \frac{1 + |S_{11}|}{1 - |S_{11}|} \quad (2.9)$$

$$\psi(f) = Phase(b_2) - Phase(a_1) \quad (2.10)$$

$$GD(f) = d \frac{\psi(f)}{df} \quad (2.11)$$

2.4 Types of Filters

In most applications, filters are required to shape only the amplitude of the transmitted signal in accordance with frequency. However, in some applications, linearity of insertion phase or in other words time delay may be important [9]. When delay of the filter at different passband frequencies is not constant, then the resulting input waveform will be distorted at the output. This affect is especially important for relatively wide-band signals with respect to filter bandwidth, where the time-domain shape of the signal has a critical importance, such as RADAR pulses. Even we do not design a linear phase filter, phase criteria should always be

kept in mind to be able to guess phase response of the designed filter to different input signals.

According to the frequency selectivity, filters are classified as:

(a) Lowpass filters: They pass low frequencies from DC up to a specified frequency (the cut-off frequency) with no or little attenuation and allow high frequencies beyond this to be attenuated (Figure 2.2.a).

(b) Highpass filters: They pass frequencies above the cut-off frequency, and substantially reject below this frequency (Figure 2.2.b).

(c) Bandpass filters: They pass one band of frequencies and rejects both higher and lower frequencies (Figure 2.2.c).

(d) Bandstop filters They eliminate or “notch” out a specific frequency or band of frequencies from the frequency spectrum (Figure 2.2.d).

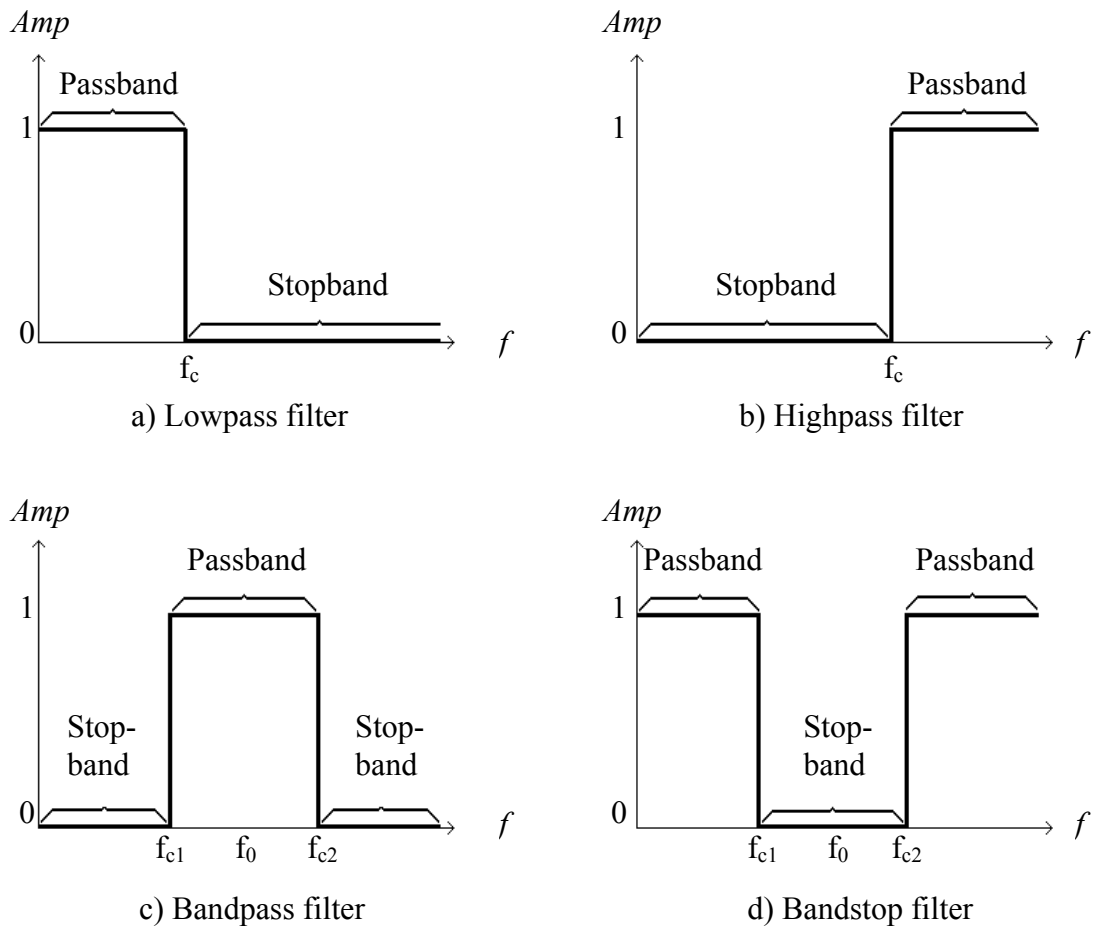


Figure 2.2: Filter types according to frequency selectivity

where; f_c is the corner frequency of the lowpass and highpass filter, f_{c1} and f_{c2} are the lower and upper corner frequencies of the bandpass and bandstop filters and f_0 is the center frequency of the pass-band and stop-band.

Note that the filter responses in Figure 2.2 are ideal; zero attenuation in passband, infinite attenuation in stopband and flat transition from passband to stopband. An ideal filter will also be the one that has a linear phase versus frequency response in the pass-band as shown in Figure 2.3:

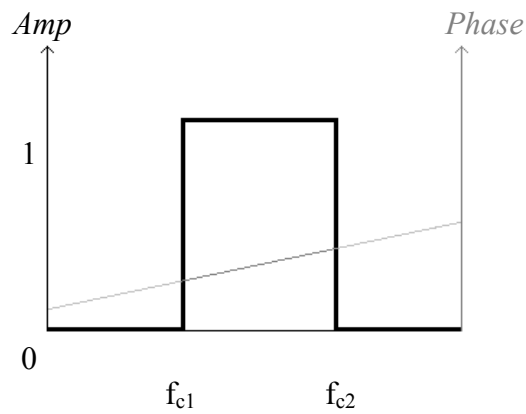


Figure 2.3: Ideal bandpass filter magnitude and phase characteristics

Such an ideal filter (brick wall filter) characteristic is not possible to obtain but ideal requirements can be approximated within an acceptable tolerance. A typical amplitude and phase response of band-pass filter is as shown in Figure 2.4:

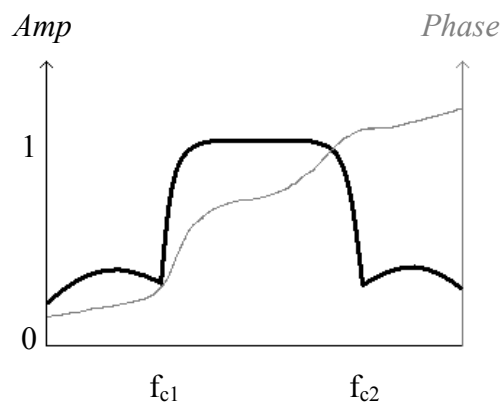


Figure 2.4: Typical amplitude response of a bandpass filter

For distributed type filters, during the synthesis stage from prototype filters, the infinite frequency is mapped to a finite frequency, which is called the quarter wavelength frequency (f_q), so this results in a repetitive frequency response as shown below (Figure 2.5):

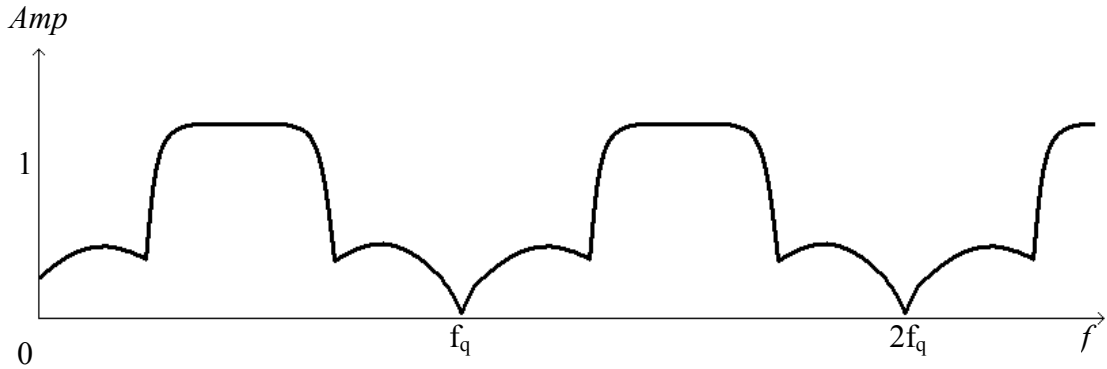


Figure 2.5: Typical frequency response of a band-pass(or high pass) distributed filter

Filters are essentially frequency selective elements. The filtering behavior results in frequency dependent reactances provided by inductors and capacitors. In microwave frequencies, lumped element inductors and capacitors usually cannot be used and thus transmission line sections are used instead which behave as inductors and capacitors. Minimizing the losses in the passband of a filter is extremely important since this does not only reduces the overall losses for a communications system but also improves the noise figure when used at the front stages of the system.

2.5 Filter Design Methodology

Filters may be designed using the image parameter or the insertion loss methods [19].

In the image parameter method, design is rather simple. The cascade of simpler two-port sections are used to provide the desired cutoff frequencies and attenuation characteristics, but do not allow the specification of a frequency response over the complete operating range. Thus, although the procedure is relatively simple, the design of filters by the image parameter method often must be iterated many times to achieve the desired results.

A more modern procedure, called the insertion loss method, uses network synthesis techniques to design filters with a completely specified frequency response. In the insertion loss method design starts with a low-pass prototype based on some mathematical functions such as Butterworth, Chebyshev, and the insertion loss in the passband as well as in the stopband can be defined and controlled based on the number of sections chosen and the components used. The design is simplified by beginning with low-pass filter prototypes that are normalized in terms of impedance and frequency. Transformations are then applied to convert the prototype designs to the desired frequency range and impedance level. A basic filter design process is shown below:

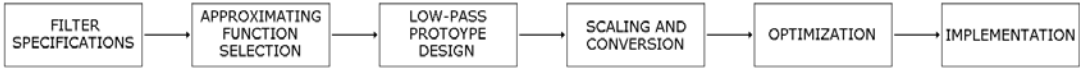


Figure 2.6: Basic filter design process using insertion loss method

With the built-in tools of FILPRO™, the above process, up to optimization, is made easy, especially with the powerful synthesis tool, virtually any type of filter up to 52 elements(selected from 177 different types of elements) can be designed and electrically analyzed, where optimization and Monte-Carlo Analysis is also possible.

With the help of accurate electromagnetic simulation tools, very realistic simulated responses can be obtained and necessary corrective changes may be performed before implementation of the filter.

2.6 Approximating Functions

The approximation problem consists of deducing a bounded real amplitude squared transfer function which approximates the required filter approximation [19]. According to the mathematical approximations used to simulate the ideal filter responses, filters are mainly classified as Bessel, Gaussian, Butterworth, Chebychev and Elliptic (also known as Cauer).

The bandpass filter responses of the approximating functions are compared to the ideal bandpass filter response, which is indicated using light gray color (Figure 2.7, 2.8, 2.9, 2.10, 2.11, 2.12).

Bessel

- Derived from Bessel Polynomial
- Small overshoot on the step and impulse response
- Rounded amplitude in passband.
- Gradual transition from passband to stopband.
- Low out-of-band rejection.
- Approximately linear passband phase (very flat group delay) and therefore low overshoot for step inputs so delays all frequency components in the passband of the filter equally in time.

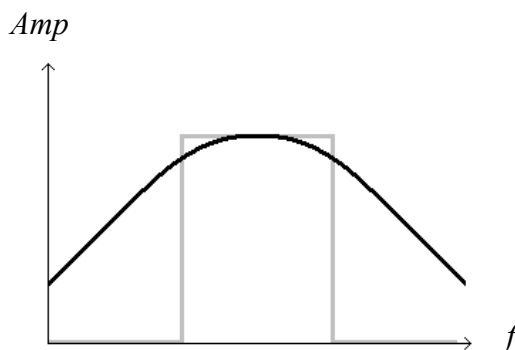


Figure 2.7: Bessel filter amplitude response

Gaussian

- Derived from Gaussian Function
- Zero overshoot on the step and impulse response
- Lowest rise times and delay
- Response close to Bessel
- Poorer selectivity and higher sensitivity than Bessel
- Rise times and delay are the lowest of the traditional transfer functions

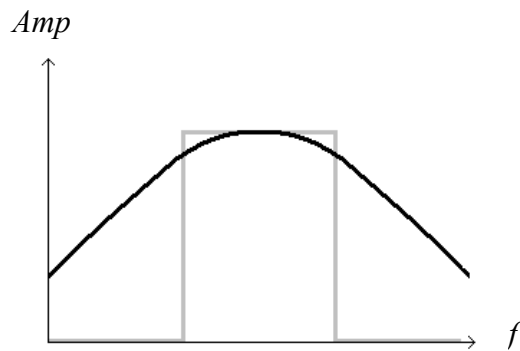


Figure 2.8: Gaussian filter amplitude response

Butterworth

- Derived from Butterworth function
- Maximally flat passband response.
- Smooth transition from passband to stopband.
- Moderate out-of-band rejection.
- Low group delay variation near center of band.
- Moderate group delay variation near band edges.
- Butterworth filters offer a compromise between the frequency selectivity of the Elliptical and Chebychev filters and the flatness of the Bessel filters.

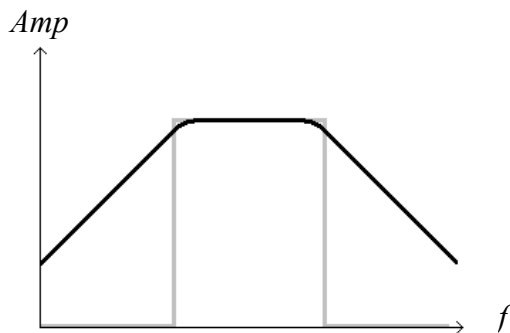


Figure 2.9: Butterworth filter amplitude response

Chebyshev

- Derived from Chebyshev equiripple function
- Equiripple in passband (Chebyshev type-1) or stopband (Chebyshev type-2, also called Inverse Chebyshev).
- Abrupt transition from passband to stopband.
- High out-of-band rejection.
- Rippled group delay near center of band.
- Large group delay variation near band edges.
- Inverse Chebyshev moves the ripple to the stopband, requires lower Q's than type-1.

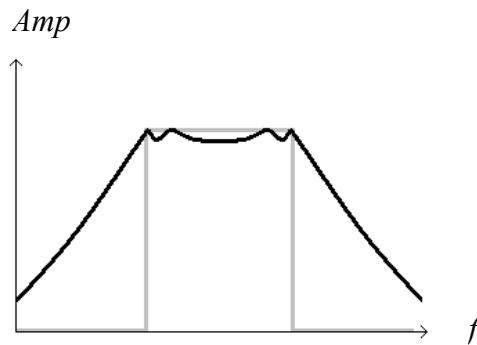


Figure 2.10: Chebyshev type-1 amplitude response

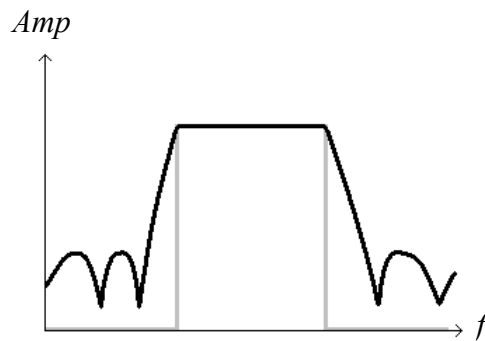


Figure 2.11: Chebyshev type-2 amplitude response

Elliptic

- Derived with the use of Jacobian elliptic functions
- Similar to Chebychev
- Equiripple both in passband and stopband.
- Transition from passband to stopband more abrupt than others
- Highest out-of-band rejection
- Poorest group delay variation
- Poor transient response

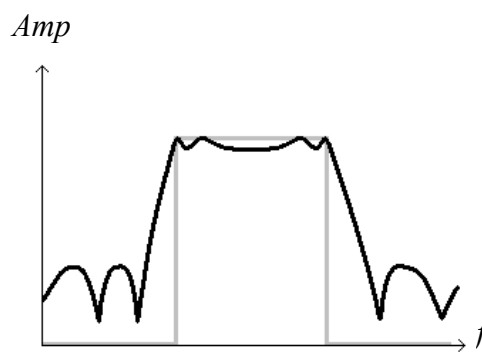


Figure 2.12: Elliptic filter amplitude response

2.7 Lumped and Distributed Classification

According to the physical structure, passive filters may be classified as [16]:

1) Lumped Filters

- a) LC Filters (Figure 2.13)
- b) Surface Acoustic Wave (SAW) Filters
- c) Ceramic Crystal Resonator Filters (Very narrowband)

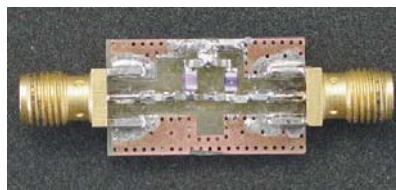


Figure 2.13: A typical lumped LC filter

2) Distributed Filters

- a) Planar/Printed Filters (Figure 2.14)
- b) Waveguide Filters

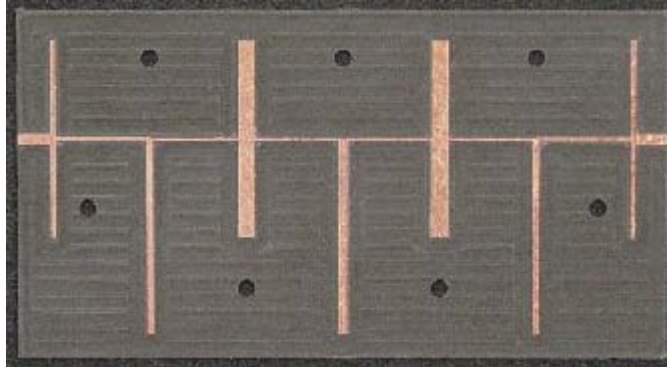


Figure 2.14: A typical microstrip filter

We will deal with LC lumped filters and a special form of planar distributed filters which is called stripline filter.

2.7.1 Lumped LC Filters:

At frequencies in the kHz region or lower MHz region, the change in phase due to finite propagation velocity of an electrical signal is usually so small that it is neglected for most physical filter structures. At these frequencies the filters are termed as lumped and so the components. The conventional passive lumped elements are inductors, capacitors and resistors [10].

Substantial progress, has been made in the past decades in the development of ferrite materials used in inductors and dielectrics used in capacitors. This permits realizing inductor Q factors of the order of 300 at low frequencies and in comparatively small physical sizes. Capacitor Q factors are significantly higher than their inductor counterparts. Cryogenic techniques or supercooling can be used in some special applications to significantly reduce the dissipative resistance losses and hence improve the Q factors [16].

Comprehensive design techniques relying on powerful and rigorous theory exists for the passive lumped filters [10]. In many practical applications an easy design procedure for lumped filters is to use the readily available LP prototypes [15] and transforming it to the desired filter response.

Because lumped structures are realizations of an exact circuit, their responses are not repetitive as in most distributed filters.

Applicable from a few Hz to the GHz range, lumped designs are very flexible. At very low frequencies below 1 MHz the inductor and capacitor values increase tremendously so active filters that use op-amps are commonly used at these frequencies which usually eliminate the use of inductors by using relatively small capacitance values. As frequencies increase, especially in broad passband or non-contiguous multiplexing applications, the lumped element topology can be easily integrated with other topologies to maximize performance in the smallest possible package volume. At high frequencies (above a few hundred MHz) the inductors and capacitors can be printed, with either single or multilayer boards being used. Such multilayer circuitry usually requires the use of plated through "via" hole technology. Some special lumped filters that have very high Q elements, may extend up to 20 GHz. Near the transition region where both lumped and distributed element filters are usable, lumped filters have the advantage of small size. Lumped filters also have relatively high broad bands and wide stop band performances.

Lumped element filters consist of discrete capacitors and inductors soldered to a substrate in various schematic configurations. These compact designs are particularly suitable for applications where size is critical. This topology is suitable for lowpass, highpass, bandpass, bandstop and multiplexing applications.

2.7.2 Distributed Element Filters

Both the image parameter and insertion loss method of filter design provide lumped-element circuits. For microwave applications such designs usually must be modified to use distributed elements consisting of transmission line sections. The Richard's transformation and the Kuroda identities provide this step. Such filters contain a wide variety of transmission types such as open and shorted sections of branch transmission lines, stepped impedances and coupled lines, tuned irises and post in wave-guide or coaxial lines, re-entrant cavities, ring filters, and direct and quarter wave coupled chambers.

As the operating frequency increases, such as at microwave frequencies, the conventional lumped elements are not feasible [10]. After a specific frequency which is called the Serial Resonance Frequency (SRF), lumped elements change their characteristic; after that frequency a capacitor turns into an inductor, and an inductor turns into a capacitor. Approaching SRF also results in change in the impedance of the lumped element. As an example, measured graphs of a Coilcraft® 1008CS 100nH inductor (Figure 2.15.a) and a Philips® 603 100pF capacitor (Figure 2.15.b) measured with a Hewlett Packard® 4291B RF Impedance and Material Analyzer with the Hewlett Packard 16191A surface mount text fixture is shown in Figures 2.16, 2.17, 2.18 and 2.19:

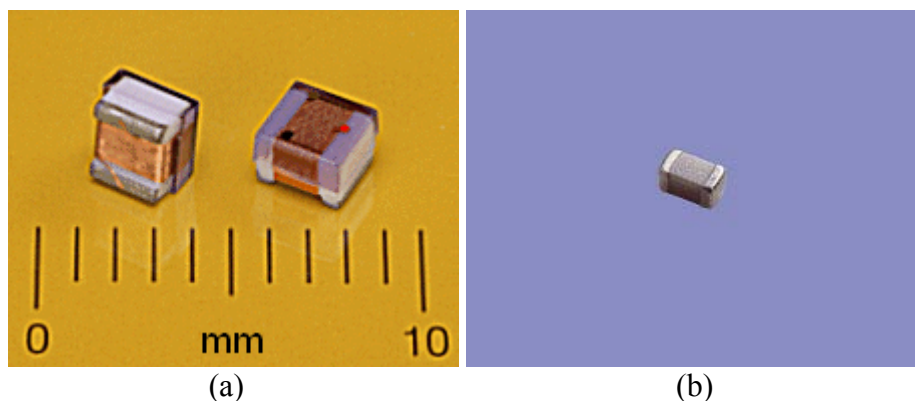


Figure 2.15: (a) Coilcraft 1008CS inductor and (b) Philips 0603 capacitor, scales are the same.

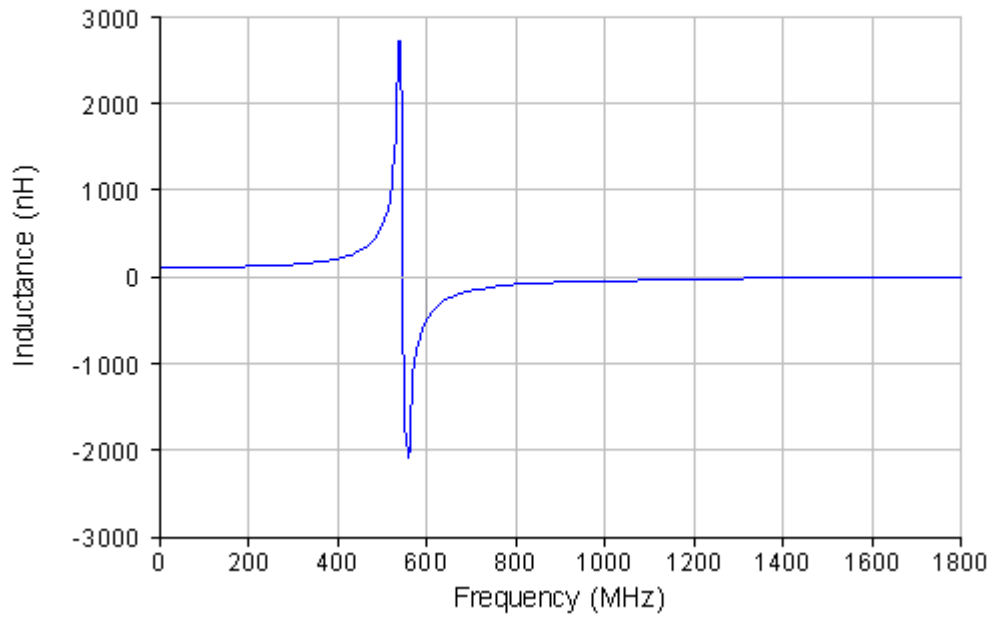


Figure 2.16: Inductance vs. frequency of the 100 nH inductor

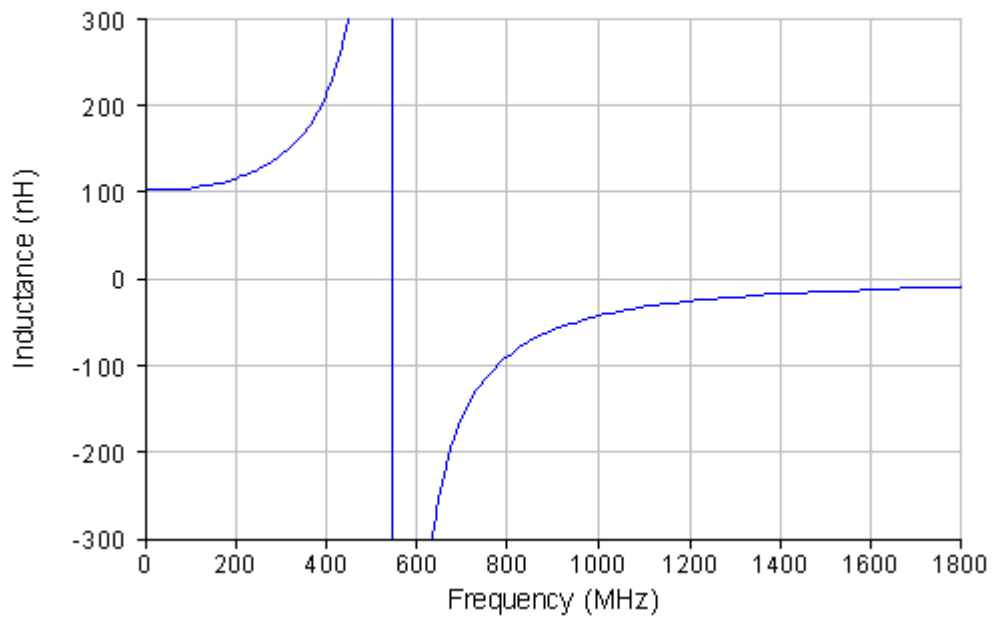


Figure 2.17: The 100 nH inductor has a 10% increase at around 150 MHz.

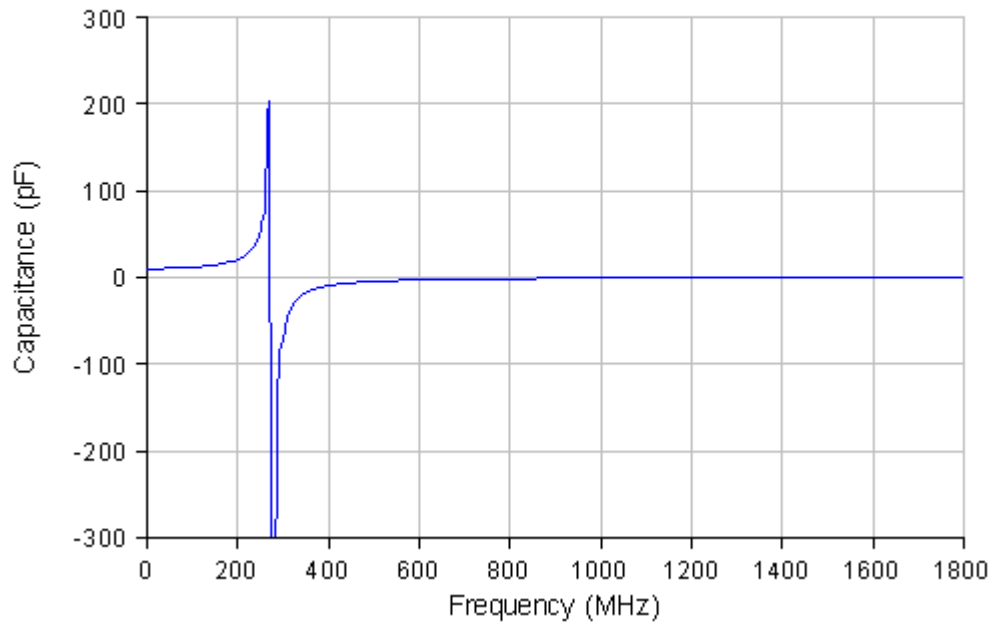


Figure 2.18: Capacitance vs. frequency of the 100 pF capacitor

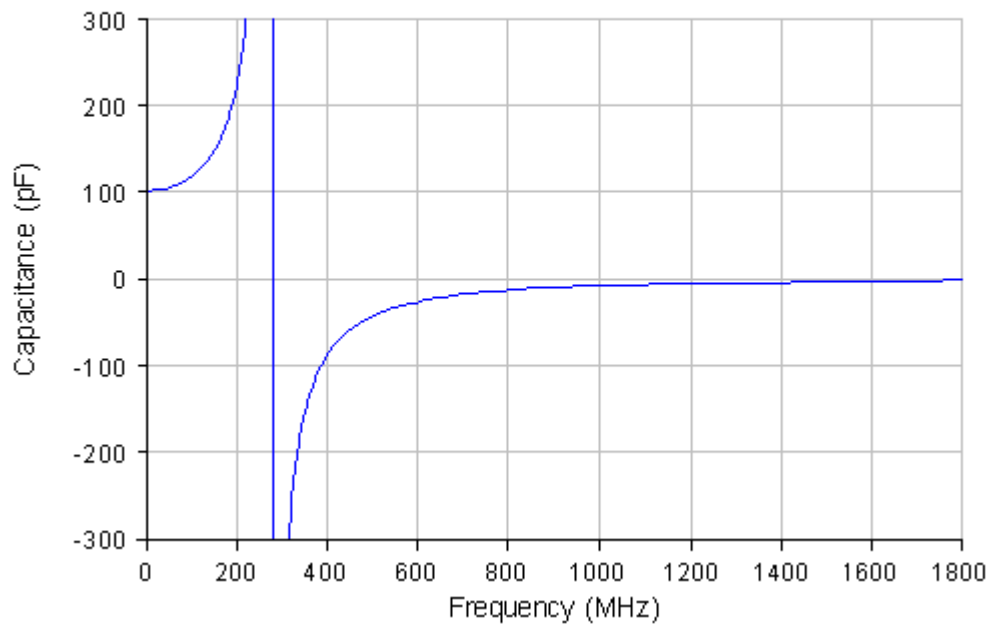


Figure 2.19: The 100 pF capacitor has a 10% increase at around 50 MHz.

As can be seen the inductor's SRF is around 540 MHz and the capacitor's SRF is around 280 MHz. The 100nH inductor reaches an inductance of 110nH at around 150 MHz and the 100pF capacitor reaches a capacitance of 110pF at around 50 MHz, we can say that these frequencies are the maximum usable frequencies for that elements if we consider 10% degradation in value without considering other factors.

Smaller the capacitor or inductor value the higher the SRF frequencies, so with smaller element values we can reach higher frequencies. Practically this limit is a few GHz for small and high quality SMD elements keeping in mind that up to 20 GHz or above is possible with special lumped elements such as specific single layer capacitors and air wounded or printed high Q inductors.

Due to these reasons, distributed element technique is usually preferred for frequencies greater than 1 GHz up to 20 GHz. In distributed element technique, printed circuit lines (transmission line pairs) are used as filter elements.

A distributed circuit is one for which the travel time of the electric signal between the components can not be neglected. The voltages and currents in such a circuit are functions of position as well as time.

As a rule of thumb:

$d/\lambda < 0.01 \rightarrow$ Lumped

$d/\lambda > 0.1 \rightarrow$ Distributed

where; d is the largest dimension of the component.

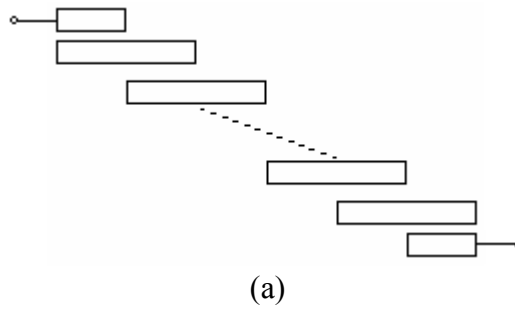
The subject of microwave filters is quite extensive, due to the importance of these components in practical systems and the wide variety of possible implementations. We give here a treatment of only the basic principles and some of the more common filter designs.

The distributed-circuit theory may be considered to have begun when Paul I. Richards published his comprehensive theory of commensurate line circuits [15]. This theory established a simple relationship between lumped and distributed circuits, which enables the entire well-developed lumped theory to be applied to distributed circuits using a simple transformation:

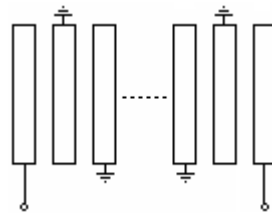
$$w \rightarrow \tan\left(\frac{w}{v_p} d\right) \quad (2.12)$$

Due to this periodic mapping, all responses of commensurate distributed filters are inherently periodic with respect to w . Hence, use of commensurate line filters is restricted to situations where such periodicity of the frequency response is acceptable [14]

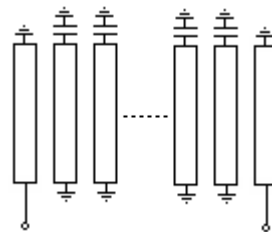
Coupling between the transmission lines in distributed circuits may be allowed resulting in different subclasses of commensurate distributed filters. One subclass of commensurate distributed filters depends on the coupling between the lines. Some examples are parallel-coupled line filters, interdigital filters and combline filters (Figure 2.20) [10].



(a)



(b)



(c)

Figure 2.20: Some examples of commensurate distributed filters, (a) Parallel coupled line filter, (b) Interdigital filter and (c) Combline filter.

Another subclass of commensurate distributed circuit, which does not allow the coupling between the lines, is called stub filters. These stubs may be open-circuited or short-circuited. One example of this kind is given in Figure 2.21.

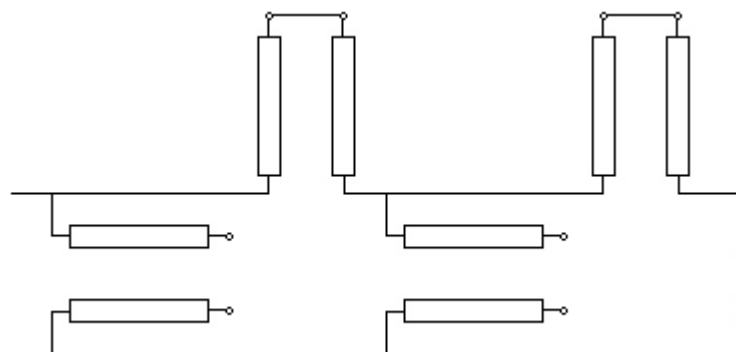


Figure 2.21: Stub filter having O.C. and S.C. stubs

In the exact design approach of Wenzel [12], quarter-wave unit elements are used to serve only to spatially separate adjacent distributed stubs so that their fields do not interact. These kinds of filters are redundant in electrical sense, since the unit elements do not contribute to the response. However, the increased number of elements may cause unacceptable insertion loss in the pass band, particularly when a microstrip version is used.

On the other hand, distributed microwave filters based on non-redundant design technique contain unit elements that contribute to the response as well as achieving physical separation of the stubs.

Another class of distributed filters is the stepped impedance method; stepped impedance filters arbitrarily uses two fixed values of line impedance, and varies the lengths as necessary. One of the impedances is high in value (thin line) which shows an inductive behavior, and the other impedance is low in value, which shows a capacitive behavior (thick line). Due to the structure, stepped impedance filters are preferred for constructing low-pass filters.

Modern microwave receiver systems have a clear requirement for small and highly selective filters. Hence, the needs for reduced size and weight and for low fabrication cost render a printed circuit configuration particularly favorable for microwave filters. There exist various printed circuit forms, like microstrip, stripline to realize a microwave circuit physically. Each type has its own advantages and disadvantages over the others and must be considered when deciding the realization form of the circuit.

The difficulties in realizing practical microwave filter structures can perhaps be appreciated when one considers that, for shielded TEM structures, the range of realizable impedances is roughly 10 to 500. Compare this with lumped elements for which parameter values are available over a range of greater than 10^6 .

We will deal with “planar” distributed filters, which have the advantage of easy construction and small size. Microstrip, stripline and suspended-substrate stripline filters are the most common planar filters.

For many years some types of microwave filters have been built in microstrip form. As mentioned in [13], these have normally been used in cases where the selectivity has not been severe. Microstrip filters also suffer limitations on stopband loss due to quasi-surface modes, high in-band dissipation loss, and a low range of impedance values that may be realized. Undesired couplings are also a problem for microstrip filters [4].

Suspended substrate stripline has the advantage of low loss and it has high range of impedance values. On the other hand, mechanical construction is difficult and grounding to the metal walls (to decrease the spurs) is very critical and sensitive.

Stripline is the sandwiched version of the microstrip. With the availability of low loss dielectric substrates and inherent immunity to radiation and coupling, stripline loss may be kept small. Stopband loss is less, compared to microstrip. Ease of mechanical construction makes stripline a good choice if limited impedance range, compared to suspended substrate stripline, may be tolerated. Due to this reasons stripline is selected to be used for the distributed filter construction.

2.7.3 Hybrid Lumped and Distributed Combination Filters

Filters employing both lumped and distributed elements are regarded as hybrid types employing the advantages of both lumped and distributed elements particularly in the “awkward frequency spectrum” between about 100 MHz to 1 GHz [16]. In this range, lumped-element parasitics become objectionable and the wavelength is comparatively long for distributed filters. So mixed usage of lumped and distributed elements may be advantageous.

2.8 Waves and Impedances on Transmission Lines

2.8.1 Transmission Line Circuit Model

A transmission line may be considered to consist of incremental elements as shown below:

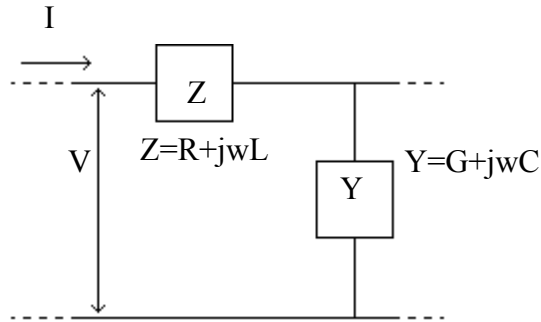


Figure 2.22: Equivalent representation of an incremental TL piece

Z and Y are the impedance and admittance per unit length Δz .

$$Z = R + j\omega L \quad Y = G + j\omega C \quad (2.13)$$

where;

R is the series resistance per unit length Δz , Ω/m

L is the series inductance per unit length Δz , H/m

G is the shunt conductance per unit length Δz , S/m

C is the shunt capacitance per unit length Δz , F/m

The equation for voltage (V) and current (I) are:

$$\frac{dV}{dz} = -ZI \quad \text{and} \quad \frac{dI}{dz} = -YV \quad (2.14)$$

simultaneous solution of which yields;

$$\frac{d^2V}{dz^2} = ZYV \quad \text{and} \quad \frac{d^2I}{dz^2} = ZYI \quad (2.15)$$

where; z represents distance along the transmission line.

The solution of these equations is in the form of waves in the +z and -z direction, which for sinusoidal excitation take the form

$$V(z) = V_+ e^{wt - j\gamma z} + V_- e^{wt + j\gamma z} \quad \text{and} \quad I(z) = I_+ e^{wt - j\gamma z} + I_- e^{wt + j\gamma z} \quad (2.16)$$

where; the propagation constant γ is given by

$$\gamma = \alpha + j\beta = \sqrt{ZY} \quad (2.17)$$

For $\omega L \gg R$ and $\omega C \gg G$ (α small or zero; low or zero loss case),

$$\beta = \omega \sqrt{LC} \quad (2.18)$$

The voltage and current functions represents waves in each direction such that successive peaks move at a velocity

$$v = \frac{\omega}{\beta} = f\lambda \quad \text{so} \quad \beta = \frac{2\pi}{\lambda} \quad (2.19)$$

To distinguish it from the free space wavelength nomenclature λ or λ_0 , the waveguide on a coaxial or a transmission line is often referred to as the guide

wavelength λ_g . For a single wave solution in one direction, the ratio $V(z)/I(z)$ is the same everywhere on the line, and is defined as the *characteristic impedance* Z_0 , which for a lossless line is a real number:

$$Z_0 = \frac{V_+}{I_+} = \sqrt{\frac{Z}{Y}} = \sqrt{\frac{L}{C}} \quad (2.20)$$

where; L and C are the inductance and capacitance per unit length respectively.

Thus, we can rewrite the current equation as

$$I(z) = I_+ e^{wt-j\beta z} + I_- e^{wt+j\beta z} = \frac{V_+}{Z_0} e^{wt-j\beta z} - \frac{V_-}{Z_0} e^{wt+j\beta z} \quad (2.21)$$

where; the minus sign reflects the fact that the magnetic field, and hence the current, of the negative-going propagation is reversed compared to that of a positive-going wave.

If both waves exist, the instantaneous voltage or current as function of location is the sum of voltages or currents of both waves. The characteristic impedance Z_0 is the ratio of voltage to current of either wave independently.

2.8.2 The Complex Reflection Coefficient Γ

We can express the total voltage and current resulting from waves traveling in both directions:

$$V(z) = V_+ e^{wt-j\beta z} + V_- e^{wt+j\beta z} \quad (2.22)$$

$$I(z) = \frac{V_+}{Z_0} e^{wt-j\beta z} - \frac{V_-}{Z_0} e^{wt+j\beta z} \quad (2.23)$$

A mismatched load may be either lumped impedance or a finite transmission line of a different Z_0 . If we consider a complex load impedance Z_L terminating a transmission line Z_0 , the magnitude of the $-z$ wave is related to that of the $+z$ wave at the termination by a complex quantity defined as the *reflection coefficient* Γ_L , defined such that

$$V_- = \Gamma_L V_+ \quad (2.24)$$

where;

$$\Gamma_L = \frac{V_-}{V_+} = \frac{-I_-}{I_+} = |\Gamma_L| e^{j\theta} = \rho e^{j\theta} \quad (2.25)$$

The relationship between the incident wave, the reflected wave and the transmitted wave arising from such a discontinuity such as a lumped load is expressed in terms of the reflection coefficient, so that the reflected wave voltage phasor at the point of reflection is

$$V_- = \Gamma_L V_+ \quad (2.26)$$

$$V_L = V_+ + V_- = V_+ (1 + \Gamma_L) \quad (2.27)$$

2.8.3 Voltage Standing Wave Ratio (SWR) and Return Loss

We can identify the maximum and minimum voltages V_{\max} and V_{\min} (normalized to V_+) by inspection of the above Equation (2.27). The ratio of these magnitudes is a real number, the voltage *standing wave ratio* (SWR, or VSWR), given by

$$VSWR = S = \frac{V_{\max}}{V_{\min}} = \frac{1 + |\Gamma_L|}{1 - |\Gamma_L|} = \frac{1 + \rho}{1 - \rho} \quad (2.28)$$

Note that this can be solved for ρ , yielding

$$\rho = \frac{S - 1}{S + 1} \quad (2.29)$$

Therefore, if we know VSWR we know ρ .

For a matched load $\rho=0$, $SWR = 1$ and the voltage on the line is just $V(d) = V_+$ for all d ; under such a condition the line is termed *flat*. The ratio of the power in the reflected wave to that in the incident wave, termed the *return loss*, is

$$\frac{P_-}{P_+} = \frac{V_-^2}{V_+^2} = \rho^2 \quad (2.30)$$

Or, expressed as a loss (a positive number) in dB

$$RL = -10 \log_{10} \rho^2 = -20 \log_{10} \rho \quad (2.31)$$

For a transmission line of characteristic impedance Z_0 and load impedance Z_L the reflection coefficient Γ_L is

$$\Gamma_L = \frac{Z_L - Z_0}{Z_L + Z_0} = \frac{\frac{Z_L}{Z_0} - 1}{\frac{Z_L}{Z_0} + 1} \quad (2.32)$$

Defining

$$z_L = \frac{Z_L}{Z_0} \quad (2.33)$$

$$\Gamma_L = \frac{z_L - 1}{z_L + 1} \quad (2.34)$$

At any distance from the load we have:

$$\Gamma(d) = \Gamma_L e^{-2j\beta d} = \frac{z(d) - 1}{z(d) + 1} \quad (2.35)$$

where;

$z=R+jX$; (impedance (z), resistance (R) and reactance (X) are normalized to Z_0).

Solving Equation (2.35) for z , we have the value of z for any measured Γ at any point d :

$$z(d) = \frac{1 + \Gamma(d)}{1 - \Gamma(d)} \quad (2.36)$$

This can be expressed in the very useful form which is the famous Telegrapher's Equation that defines the input impedance of a line of length d , characteristic impedance of Z_0 and terminated by a load Z_L .

$$Z_{in} = Z_0 \frac{Z_L + jZ_0 \tan \beta d}{Z_0 + jZ_L \tan \beta d} \quad (2.37)$$

We will use this equation to obtain pure capacitive or inductive behaviors from some specific transmission line pairs.

The impedance of the shorted transmission line of impedance Z_0 and length d is

$$X = Z_{in} = jZ_0 \tan \beta d \quad (2.38)$$

$$\tan \beta d = \tan \frac{2\pi}{\lambda_g} d = \tan \frac{2\pi f}{\lambda_g f} d = \tan \frac{\omega}{v_p} d \quad (2.39)$$

$$X = jZ_0 \tan \frac{\omega}{v_p} d \quad (2.40)$$

The impedance of a lumped inductor is

$$X = jL\omega \quad (2.41)$$

We see that the reactance of shorted transmission line is very similar to that of an inductor, with the difference of having nonlinear frequency dependence instead of linear frequency dependence of the lumped inductor.

The impedance of an open ended transmission line of impedance Z_0 and length d is

$$X = Z_{in} = \frac{1}{jZ_0 \tan \beta d} \quad (2.42)$$

$$X = \frac{1}{jZ_0 \tan \frac{\omega}{v_p} d} \quad (2.43)$$

The impedance of a lumped capacitor is

$$X = \frac{1}{jC\omega} \quad (2.44)$$

We see that the reactance of open-ended transmission line is very similar to that of a capacitor, with the difference of having nonlinear frequency dependence instead of linear frequency dependence of the lumped capacitor.

2.9 Commensurate line filters

From the previous section, it can be seen that both the line length and characteristic impedance may be varied to produce a desired inductance or capacitance as described in Equation (2.37). The stepped impedance filter arbitrarily uses just two fixed values of line impedance, and varies the lengths as necessary. An alternative method that is frequently used, but which is ultimately no less arbitrary, involves the use of commensurate lines. The term refers to the equality of line lengths used to implement the filter elements. As with the stepped impedance filter, short segments of shorted line implement inductors, and short pieces of open circuited line acts as capacitors. In Richard's original description of the method, "short" is specifically taken to mean an eighth of a wavelength at the cutoff frequency. That is, each inductor or capacitor of a lumped prototype is replaced by a $\lambda/8$ length of transmission line, whose characteristic impedance is varied to produce the desired component value. For this particular choice the resulting filter response is periodic in frequency, and may be considered the result of aliasing the lumped prototypes response.

2.10 Circuit Transformations

Richard's Transformation and Kuroda's Identities focus on uses of $\lambda/8$ lines, for which $X_L = jZ_0$ and $X_C = 1/jZ_0$ as shown below:

$$X_{L, \frac{\lambda}{8}} = jZ_0 \tan \beta d = jZ_0 \tan \frac{2\pi}{\lambda_g} \frac{\lambda_g}{8} = jZ_0 \tan \frac{\pi}{4} = jZ_0 \quad (2.45)$$

$$X_{C, \frac{\lambda}{8}} = \frac{1}{jZ_0 \tan \beta d} = \frac{1}{jZ_0 \tan \frac{2\pi}{\lambda_g} \frac{\lambda_g}{8}} = \frac{1}{jZ_0 \tan \frac{\pi}{4}} = \frac{1}{jZ_0} \quad (2.46)$$

2.10.1 Richard's Transformation

Richard's transformation is used to convert lumped elements to transmission line section. The transformation

$$\Omega = \tan \beta d = \tan \left(\frac{w}{v_p} d \right) \quad (2.47)$$

maps the w plane to the Ω plane, which repeats with a period of $w/v_p = \pi$. This transformation was introduced by P. Richard to synthesize an LC network using open- and short-circuited transmission lines [11].

Richard's idea is to use variable Z_0 (for example changing the widths of microstrip-lines) to create lumped elements from transmission lines. A lumped low-pass prototype filter can be implemented using $\lambda/8$ lines of appropriate Z_0 to replace lumped L and C elements.

So if we need an inductance of L for a prototype filter normalized to cutoff frequency, using Equation (2.41) and (2.45) we can substitute a $\lambda/8$ short-circuited transmission line stub that has $Z_0 = L w_{\lambda/8}$. Similarly to obtain a capacitance C , from Equation (2.44) and (2.46), we need a $\lambda/8$ open-circuited transmission line stub that

has $Z_0 = C w_{\lambda/8}$ (Figure 2.23).

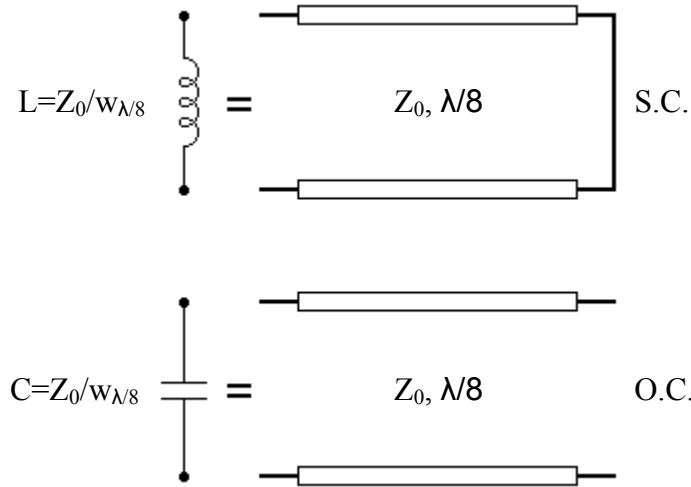


Figure 2.23: Equivalent transmission line configurations for lumped elements

The $\lambda/8$ transmission line sections are called commensurate lines, since they are all the same length in a given filter.

$\tan\left(\frac{w}{v_p} d\right)$ goes to infinity when the frequency doubles:

$$\tan\left(\frac{w}{v_p} d\right) = \tan\left(\frac{2\pi f}{f\lambda} d\right) = \tan\left(\frac{2\pi}{\lambda} \frac{\lambda_f}{8}\right) \xrightarrow{f=2f} \tan\left(\frac{2\pi}{\lambda_f/2} \frac{\lambda_f}{8}\right) = \tan\frac{\pi}{2} = \infty \quad (2.48)$$

The frequency where $\tan(wd/v_p)$ goes to infinity is called the quarter wavelength frequency ($f_q=2f$), since at that frequency the commensurate lines may be considered of $\lambda/4$ length, which were $\lambda/8$ length at half the quarter wavelength frequency. Due to mapping, the frequency f_q of distributed filters is similar to infinite frequency of lumped ones.

One can not specify arbitrarily high characteristic impedances, of course, because there is always a lower bound on the width of lines that may be fabricated

reliably. Assuming a typical manufacturing tolerance of 2 mils ($50.8\mu\text{m}$), and supposing that this variation is allowed to represent at most 20% of the total width, one may assume a minimal practical line width of 10 mils ($254\mu\text{m}$). Hence on 30 mils $\epsilon=2.2$ dielectric material, practical line impedances rarely exceed about $200\ \Omega$.

There are also practical bounds on the maximum width of the lines because, again, all linear dimensions of a microstrip element must be small compared to wavelength at all frequencies of interest for close approximation to lumped element behavior. The associated implicit lower bound on impedance depends on the operational frequency range, but as a general rule, characteristic impedances below approximately $10\text{-}15\ \Omega$ are rarely used. In realizing microstrip filters, then it is important to keep in mind that practical impedance levels are thus generally within about a factor of four of 50Ω .

One practical consideration is that following Richard's prescription precisely requires the use of shorted lines to implement inductances. However, it is inconvenient to implement shorts in microstrip, because one would generally would like to the use of grounding vias if at all possible. Fortunately, we may again use transmission line behavior to transform inductors into capacitors, and thus avoid the need for shorted sections.

2.10.2 Kuroda Identities

The four Kuroda identities use redundant transmission line sections to achieve a more practical microwave filter implementation by performing any of the following operations:

- Physically separate transmission line stubs
- Transform series stubs into shunt stubs, or vice versa
- Change impractical characteristic impedances into more realizable ones

The additional transmission line sections are called unit elements and a $\lambda/8$ long at f_c , the unit elements are thus commensurate with the stubs used to implement the inductors and capacitors of the prototype design.

The four identities are illustrated in Figure 2.24, where each box represents a unit element (transmission line) of the indicated characteristic impedance and length ($\lambda/8$ at f_c). The inductors and capacitors represent short-circuit and open-circuit stubs, respectively. The first identity (a) in Figure 2.24 can be redrawn as shown in Figure 2.25.

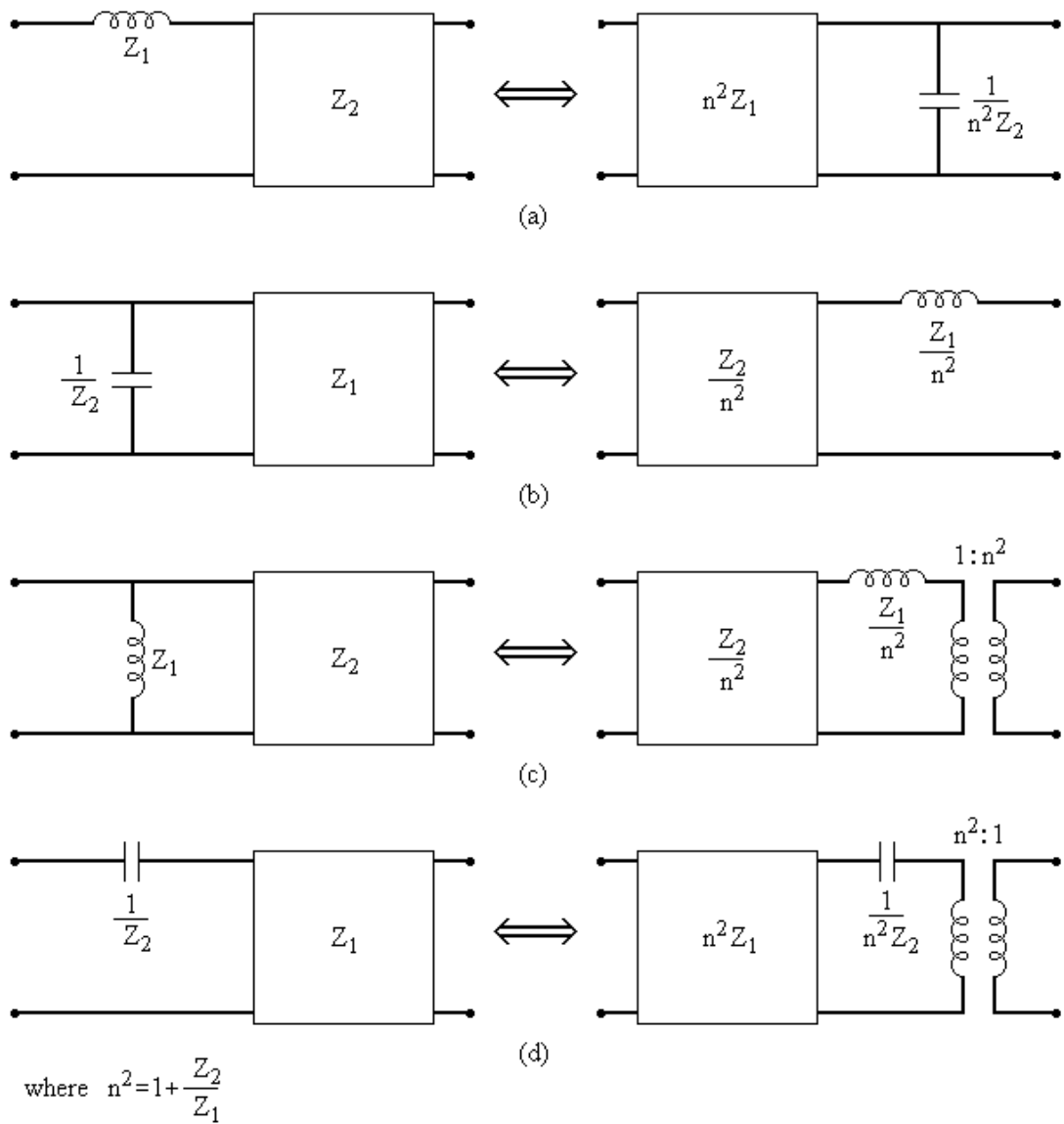


Figure 2.24: The four Kuroda identities

The first identity in the above figure may be detailed as shown in Figure 2.23. As can be seen a series short circuited stub is transformed in to a shunt open circuited stub which is easier to construct.

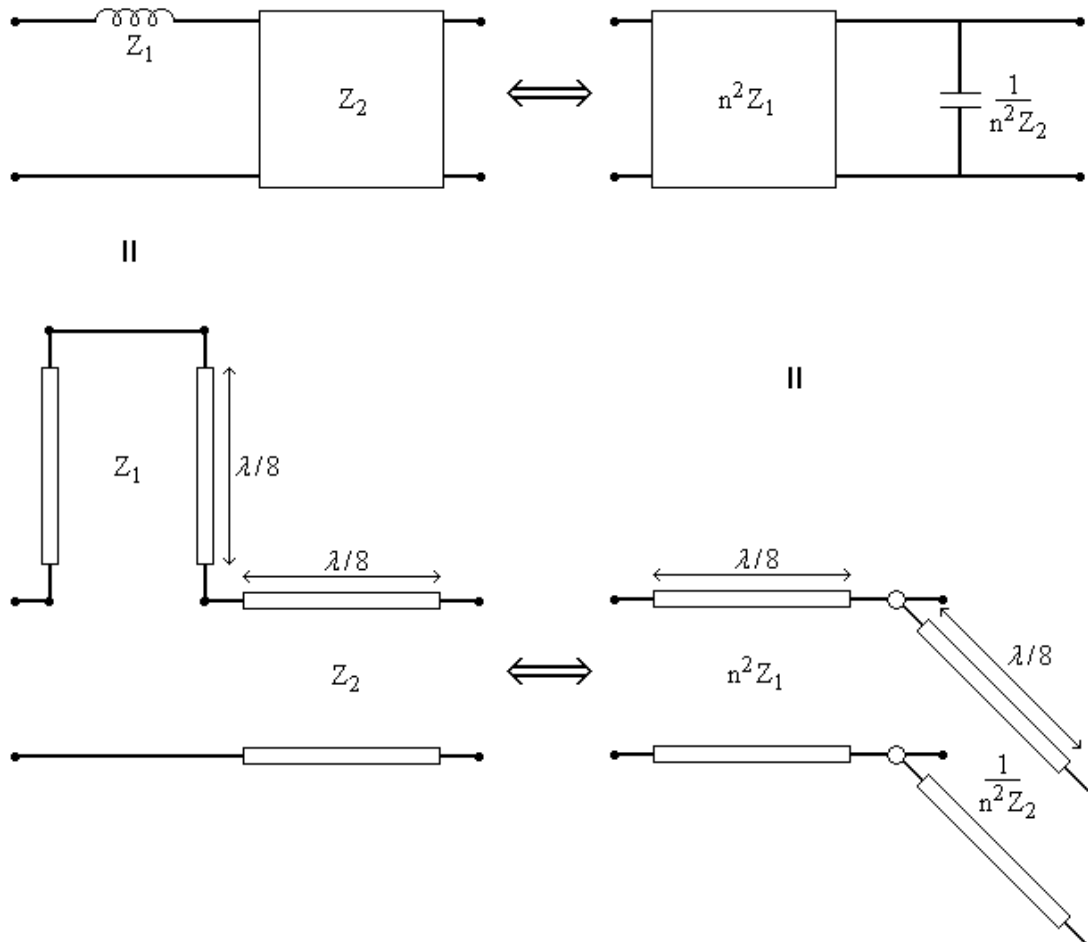


Figure 2.25: Equivalent circuits illustrating Kuroda identity (a) in Figure 2.22

2.10.3 Impedance Inverters

It is usually desirable to use only series, or only shunt elements when implementing filters with a particular type of transmission line. The Kuroda Identities can be used for conversions of this form, but another possibility is to use impedance inverters (Figure 2.26). Such inverters are especially useful for bandpass or bandstop filters with narrow bandwidths (smaller than 10% of the center frequency).

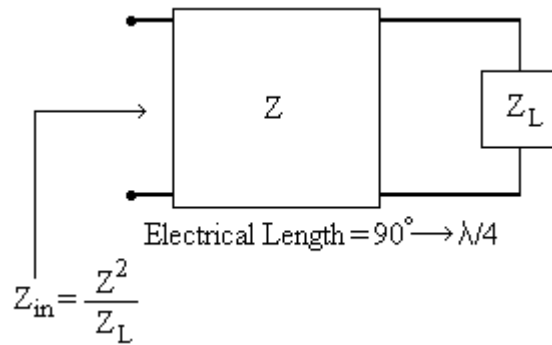


Figure 2.26: Impedance inverter

Impedance inverters, as shown in the above figure, as their names imply, can produce an input impedance or admittance that is inversely proportional to the impedance or admittance of the attached load. They can be used to transform series-connected elements to shunt-connected elements, or vice-versa.

2.10.4 Norton Transformations

Norton transformations are the basis of most of the circuit transformations, which enable us to form a variety of equivalent circuits [1].

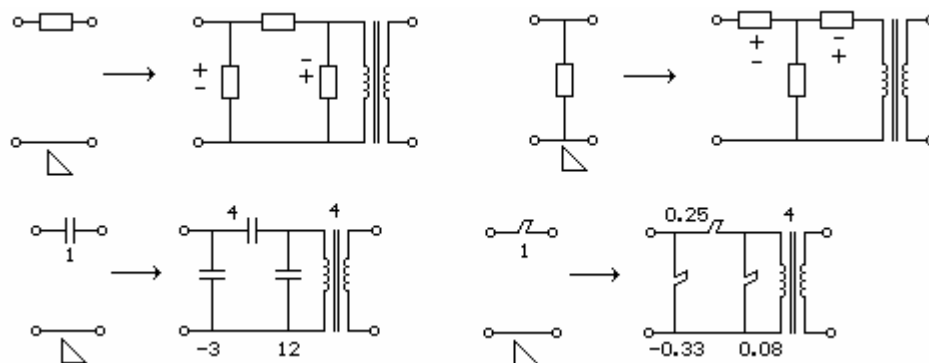


Figure 2.27: Norton Transformations

The two basic Norton transformations are shown in Figure 2.27. In these transformations a single series (shunt) element (lumped elements or stubs) is replaced by a Tee (Pi) network together with a transformer. Depending on whether the transformer ratio k is greater or less than one, either the left or the right element

of Tee and Pi sections will be negative. The negative element has to be absorbed by the neighboring positive elements.

The Norton Transformations can be used in scaling some element values in bandpass filters at the expense of increasing number of elements in the circuit.

2.11 Remarks

In this chapter we shortly discussed common filter terms and design principles, the most related items from the literature are selected. The material presented here forms the basics of the work that will be performed in the following chapters. In the next two chapters, FILPRO, which has built in tools to make the necessary transformations of the filter design process, will be used to synthesize and analyze the filters.

CHAPTER 3

LUMPED HIGHPASS FILTER DESIGN TRIALS

3.1 Introduction

In order to obtain proper filter structures for the highpass filters, many trials are done using the FILPRO program. According to the resulting responses, the best filter is chosen. FILPRO manuals are mainly used to have a basic understanding of different filter types.

The filter trials are considered according to the following criteria:

- **The element values:** Using small inductance and capacitance values in a filter structure is a plus for the lumped element filters. SRF (Self Resonant Frequency) of small valued elements is higher, which increases the maximum usable frequency (MUF) of the filters.
- **Range of element values:** Distribution of element values is important; it is desired to have filter elements that are close in values. Especially at higher frequencies, the dispersion of element values makes filters impractical to realize because the properties of the elements differ so much if the element values differ too much.
- **Closeness of the element values to standard values for the lumped HP filter:** Most of the inductor and capacitor vendors prefer to produce standard

element values. For most commercial products, E12 standard values are preferred (Table 1). E12 series have 12 values (1, 1.2, 1.5, 1.8, 2.2, 2.7, 3.3, 3.9, 4.7, 5.6, 6.8 and 8.2) for a decade. The closeness of the synthesized filter element values to standard values is a plus; since with less tuning the filter may be transformed to a realizable one. Parasitics should also be considered making this consideration. The repetitive usage of same elements values is a plus since the variety of elements decrease by this way, which is very important for mass production.

1	1.2	1.5	1.8	2.2	2.7	3.3	3.9	4.7	5.6	6.8	8.2
10	12	15	18	22	27	33	39	47	56	68	82
100	120	150	180	220	270	330	390	470	560	680	820
1000	1200	1500	1800	2200	2700	3300	3900	4700	5600	6800	8200

Table 3.1: Four-decade element values of the E12 series, starting value is 1 pF for capacitors and 1 nH for inductors

- **Sensitivity of the filter response to element tolerances:** Since elements deviate from the indicated standard element values within the specified tolerance range, deviation from the indicated values should not effect the filter response so much, which is also the main factor effecting the production repeatability of the filters.
- **The order/complexity of the filter:** The order of the filter directly affects the size and the loss of the filter. Filters with order greater than 15 are rarely used.

Lumped highpass filter structures will be considered in this chapter. According to the results, appropriate filters will be selected for realization.

The 0.4 GHz high pass filter is selected to be of lumped type mainly due to two reasons:

- The size of the distributed element filters gets too large at 0.4 GHz.
- High-pass filter elements are more difficult to realize (compared to lowpass ones) since filter syntheses outputs series open circuited stubs or coupled lines.

In the following designs, the passband edges are defined as the frequencies at which the loss starts to increase more than the indicated ripple value.

3.2 Design Trials of the Highpass Filter

3.2.1 Highpass Filter Trial 1

The first lumped element HP filter consists of four finite TZs and three TZs at zero:

Type	Lumped, Highpass, Equiripple, Type A
Ripple(dB)	0.1
Corner Frequency(MHz)	400
Order	11
Transmission Zeros with order of extraction (MHz)	Zero, Zero, 250, 360, 360, 320, Zero

In passband max 0.1 dB insertion-loss ripple corresponds to maximum -16.4 dB return loss (Figure 3.9.b). -16.4 dB is a moderate value, when the filter is realized this value degrades, but in most cases, it guarantees insertion loss less than 10 dB. Smaller the ripple better the insertion loss is, so 0.1 dB will be the maximum ripple value we will use.

Putting higher frequency FTZs (360 MHz ones) in the middle of the circuit is done intentionally. The lower frequency FTZs are less problematic due to lumped elements' frequency dependant characteristic, so putting them close to source and load side may be safer. But this may not a dominant affect.

The synthesized filter's element values are as shown in Figure 3.1, the responses are shown in Figure 3.3 and 3.4. As seen in Figure 3.9, stopband attenuation is min 71 dB. Two of the finite TZs are equal so we have three stopband ripples with four finite TZs.

For all filter trials, return losses are measured from the inputs (S_{11}), which are very similar to output return losses (S_{22}). Insertion losses are from input to output, which is also called forward insertion loss.

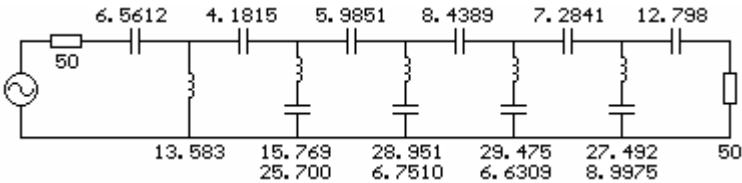


Figure 3.1: Elements of **Trial 1**

Selecting Type A topology results in a filter structure that starts with serial elements. The reason to use Type A filters is to decrease the number of inductors, because capacitors are more advantageous to use due to the following reasoning:

1. Capacitors usually have higher Q values compared to inductors
2. In general capacitors are smaller in size
3. The E field inside the capacitors is confined in the structure while for linear inductors the H field makes a loop from outside the inductors so mutual coupling between inductors may be problematic, so it should be taken care of.
4. Paralleling capacitors is easier than making serial connections between inductors.
5. Wire wound inductors have sometimes limited and non-standard values.

Using “Find Dual” command of FILPRO we may get the Type B equivalent (Figure 3.8) of the above filter. This filter has the same response but it starts with shunt elements (which are inductors), so the number of inductors increases by five while the number of capacitors decreases by the same amount. Due to the increasing number of inductors, a Type B filter is not preferred.

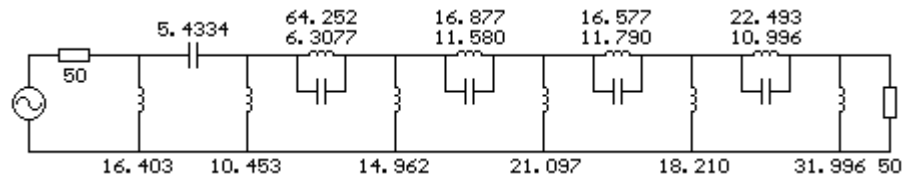


Figure 3.2: Type B dual of **Trial 1**

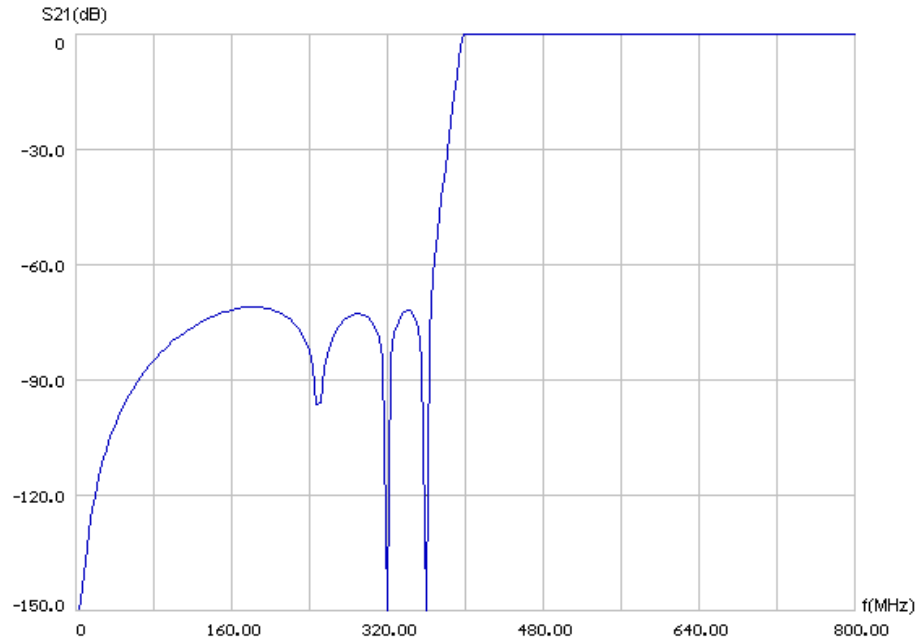


Figure 3.3: Insertion loss characteristic of **Trial 1**

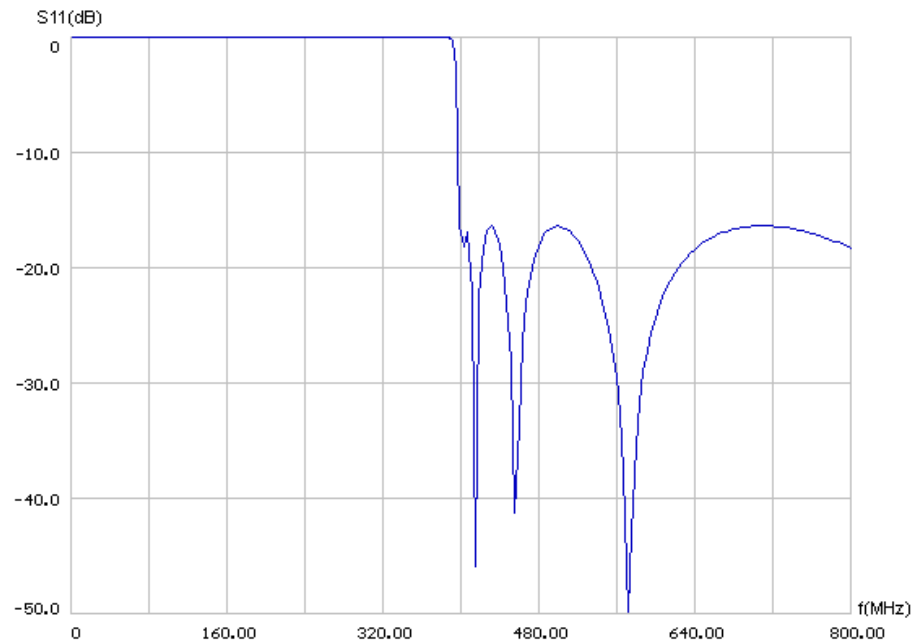


Figure 3.4: Return loss characteristic of **Trial 1**

3.2.2 Highpass Filter Trial 2

This filter's specifications are same with the previous filter. The only difference is the extraction order of the finite transmission zeros. The response is same but the element values have changed (Figure 3.5).

Type	Lumped, Highpass, Equiripple, Type A
Ripple(dB)	0.1
Corner Frequency(MHz)	400
Order	11
Transmission Zeros with order of extraction (MHz)	Zero, Zero, 360, 250, 320, 360, Zero

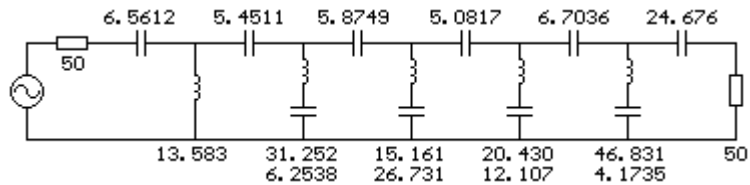


Figure 3.5: Elements of **Trial 2**

The maximum inductor value has increased to 46.831 nH from 29.475 nH of the previous filter, which may be considered as an undesired result.

Up to now, we have seen 3 filters with the same response; **Trial 1**, Type B equivalent of **Trial 1** and this trial which has different extraction order, and all of the filters have different elements. This shows us that even if we decide on a filter's specifications such as ripple, number of TZs and TZ frequencies: we should also consider type and extraction order because this affects the element values and arrangements. Since there are many variations in filter synthesis, there are no general rules for the optimum filters and different variations should be considered to get the optimum form.

3.2.3 Highpass Filter Trial 3

Compared to the previous filter, finite transmission zeros are changed to see the affect on element values.

Type	Lumped, Highpass, Equiripple, Type A
Ripple(dB)	0.1
Corner Frequency(MHz)	400
Order	11
Transmission Zeros with order of extraction (MHz)	Zero, Zero, 356, 240, 316, 356, Zero

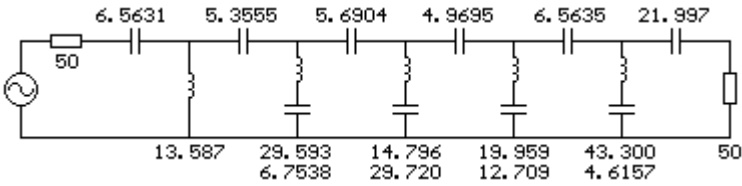


Figure 3.6: Elements of **Trial 3**

Although the stopband attenuation has increased, min 74 dB (Figure 3.7), we got smaller element values (Figure 3.6). The drawback is the decreased sharpness of the skirt.

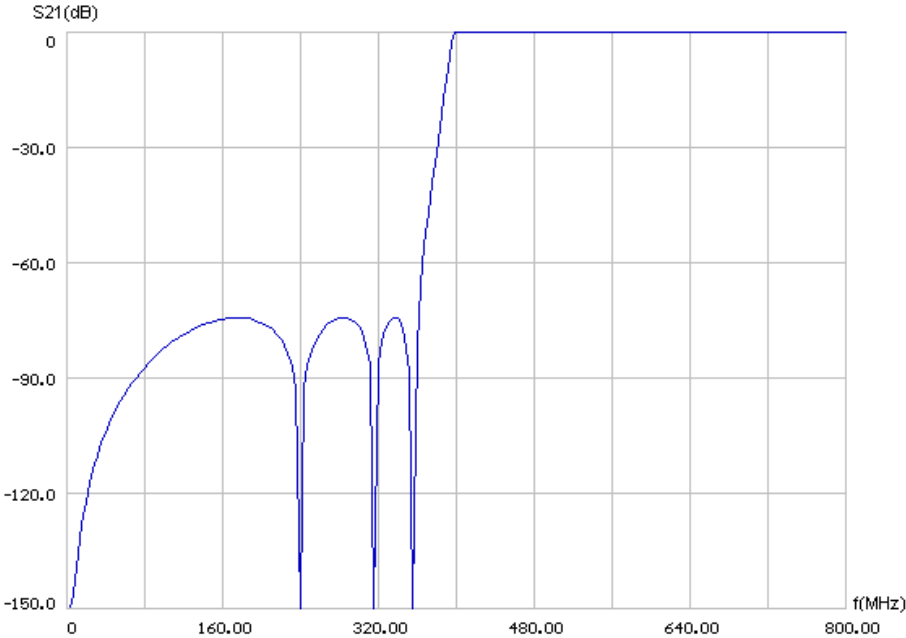


Figure 3.7: S21 response of **Trial 3**

3.2.4 Highpass Filter Trial 4

In previous examples, there were three TZs at zero. In this example we have five TZs at zero, and the stop band attenuation is increased to 90 dB (Figure 3.9) as a result of increasing order.

Type	Lumped, Highpass, Equiripple, Type A
Ripple(dB)	0.1
Corner Frequency(MHz)	400
Order	13
Transmission Zeros with order of extraction (MHz)	Zero, Zero, 268, 356, 356, 325, Zero, Zero, Zero

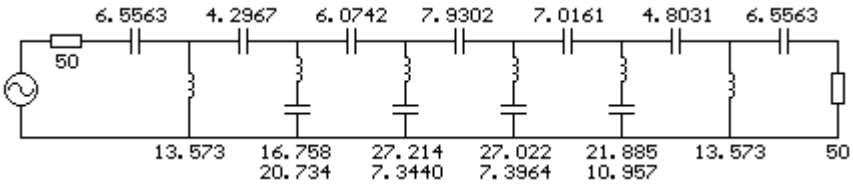


Figure 3.8: Elements of **Trial 4**

The arrangement of elements is symmetric, but since the TZs other than the 356 MHz pair are not equal, there is not a total symmetry in element values. The resulting element values maybe considered acceptable.

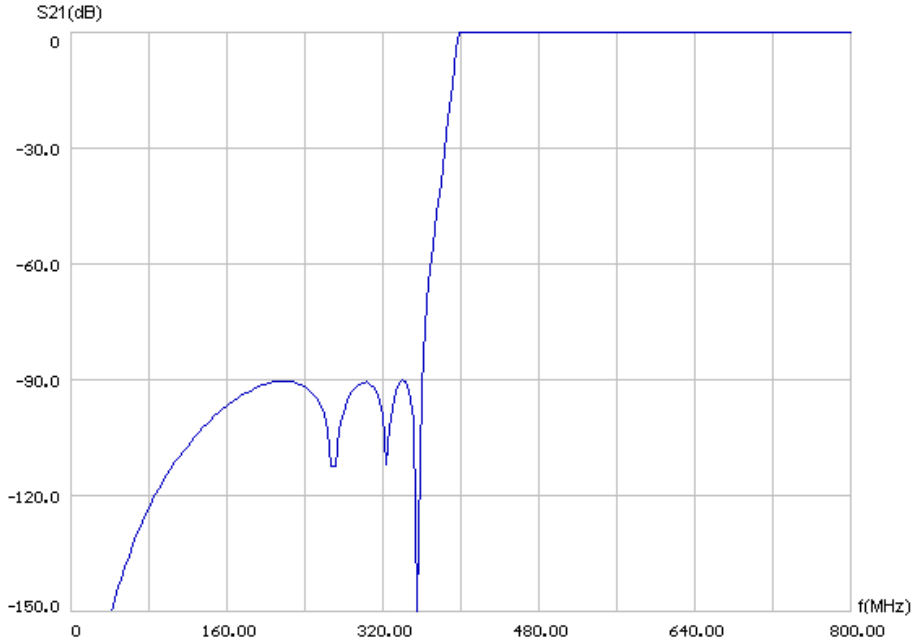


Figure 3.9: S21 response of **Trial 4**

3.2.5 Highpass Filter Trial 5

To obtain a symmetric version of the previous filter structure with similar response, the lower FTZs are also selected equal to each other as the upper ones.

Type	Lumped, Highpass, Equiripple, Type A
Ripple(dB)	0.1
Corner Frequency(MHz)	400
Order	13
Transmission Zeros with order of extraction (MHz)	Zero, Zero, 298, 352, 352, 298, Zero, Zero, Zero

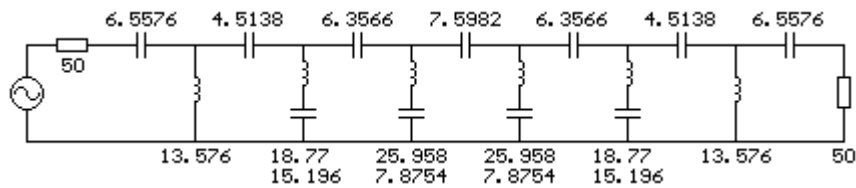


Figure 3.10: Elements of **Trial 5**

As shown above (Figure 3.10), the filter is fully symmetric; center of symmetry is the 7.5982 pF capacitor at the middle. Symmetric filters are mainly preferred due to the decreasing number of element variety. The element values are similar with the previous filter.

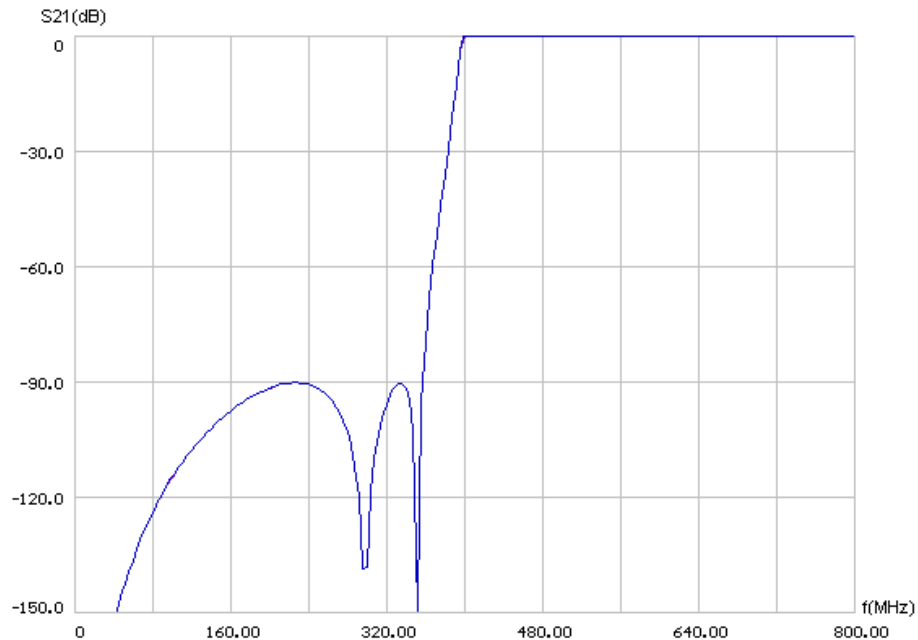


Figure 3.11: S21 of **Trial 5**

To preserve minimum 90 dB stopband attenuation, there is a slight decrease in the sharpness of the skirt (Figure 3.11).

3.2.6 Highpass Filter Trial 6

In this trial a filter with three finite transmission zeros having 0.01 dB passband ripple is examined. The number of TZs at zero is five. Stopband attenuation is min 82 dB (Figure 3.13). 0.01 dB passband ripple resulted in a return loss around 26 dB in the passband region (Figure 3.14).

Type	Lumped, Highpass, Equiripple, Type A
Ripple(dB)	0.01
Corner Frequency(MHz)	400
Order	11
Transmission Zeros with order of extraction (MHz)	Zero, Zero, 310, Zero, 250, Zero, 310, Zero

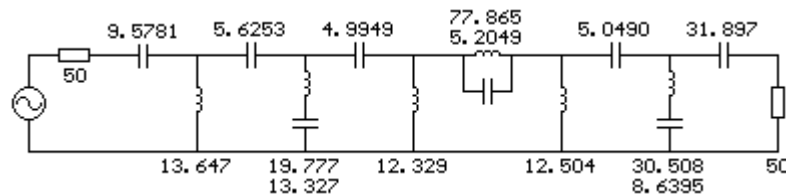


Figure 3.12: Elements of **Trial 6**

The extraction order resulted in a series resonator. The upper transmission zeros are far below 400 MHz, so the sharpness of the filter is low.

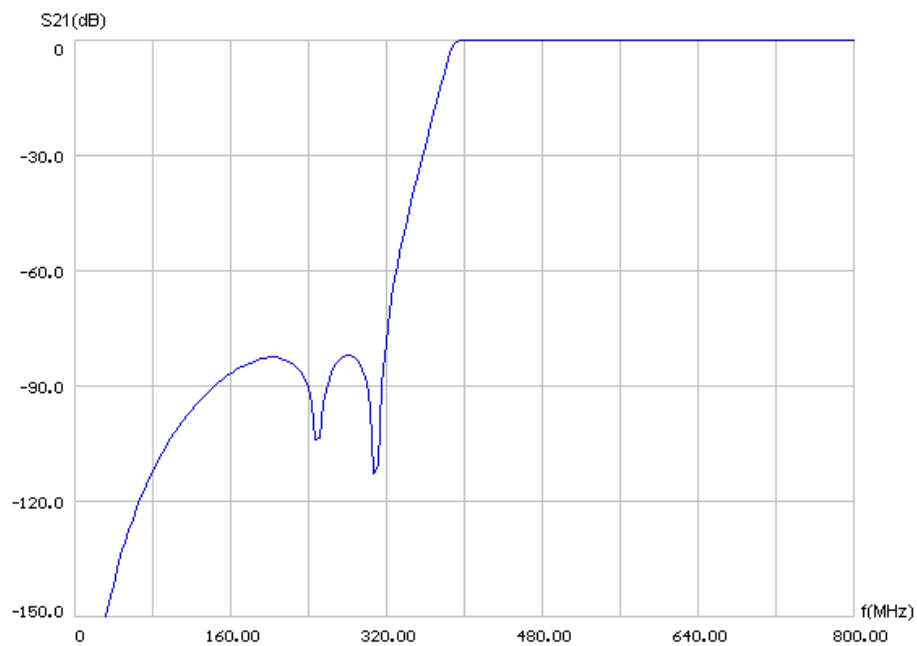


Figure 3.13: S21 graph **Trial 6**

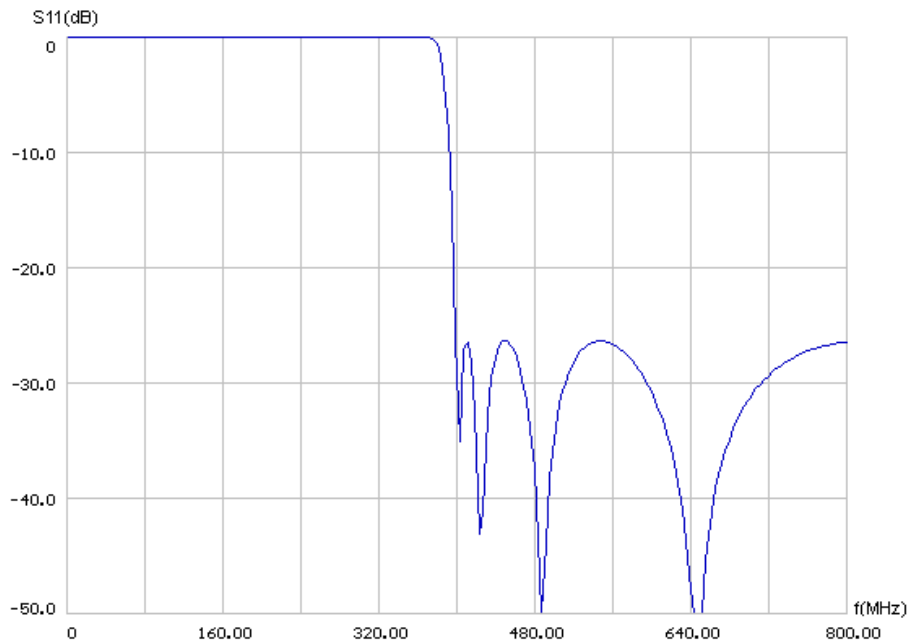


Figure 3.14: S11 plot of **Trial 6**

3.2.7 Highpass Filter Trial 7

The difference with the previous filter is only the extraction order. The extraction order is adjusted to eliminate the series resonator (Figure 3.15).

Type	Lumped, Highpass, Equiripple, Type A
Ripple(dB)	0.01
Corner Frequency(MHz)	400
Order	11
Transmission Zeros with order of extraction (MHz)	Zero, Zero, 310, Zero, Zero, 250, 310, Zero

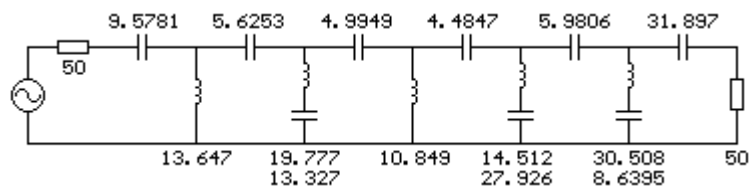


Figure 3.15: Elements of **Trial 7**

In this extraction order, we eliminated the series resonator that appeared in the previous filter, which resulted in a uniform filter with better element values.

3.2.8 Highpass Filter Trial 8

In this trial the separated finite TZs of the previous example are extracted side by side. With 250 Mhz FTZ at the middle we obtain a symmetric circuit (Figure 3.16).

Type	Lumped, Highpass, Equiripple, Type A
Ripple(dB)	0.01
Corner Frequency(MHz)	400
Order	11
Transmission Zeros with order of extraction (MHz)	Zero, Zero, 310, 250, 310, Zero, Zero, Zero

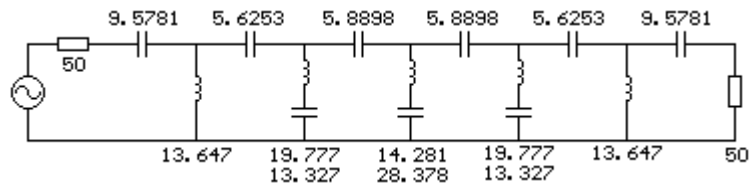


Figure 3.16: Elements of **Trial 8**

This filter has better element values compared to the previous one. Response is same with **Trial 6** (Figure 3.14).

3.2.9 Highpass Filter Trial 9

Different from the previous three trials, the ripple value is selected 0.1 dB here, where all other parameters are the same.

Type	Lumped, Highpass, Equiripple, Type A
Ripple(dB)	0.1
Corner Frequency(MHz)	400
Order	11
Transmission Zeros with order of extraction (MHz)	Zero, Zero, 310, 250, 310, Zero, Zero, Zero

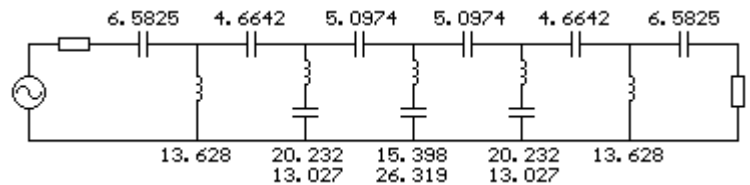


Figure 3.17: Elements of **Trial 9**

The increase in ripple (being 0.1 instead of 0.01), mainly changed the series capacitors at the source and load side, they reduced 30% (Figure 3.17). Considering parasitics, decrease in the outermost capacitor value may increase the upper boundary of the passband, so for the following lumped highpass filters, 0.01 dB ripple will not be preferred.

3.2.10 Highpass Filter Trial 10

In this trial, the order of the filter is 15, and the resulting stopband attenuation is min 102 dB (Figure 3.19).

Type	Lumped, Highpass, Equiripple, Type A
Ripple(dB)	0.1
Corner Frequency(MHz)	400
Order	15
Transmission Zeros with order of extraction (MHz)	Zero, Zero, 265, 333, 260, 333, 365, Zero, Zero

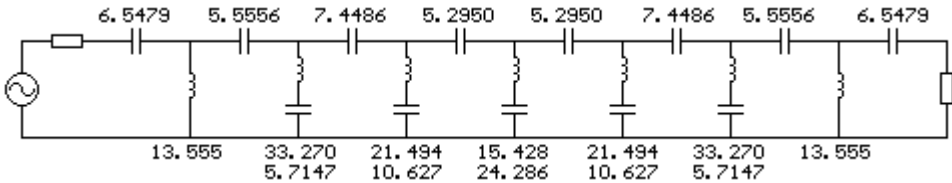


Figure 3.18: Elements of **Trial 10**

The element values may be considered moderate. Compared to **Trial 9**, the 33.270 nH inductors may be high in value. The stopband attenuation is very high at the expense of increasing order.

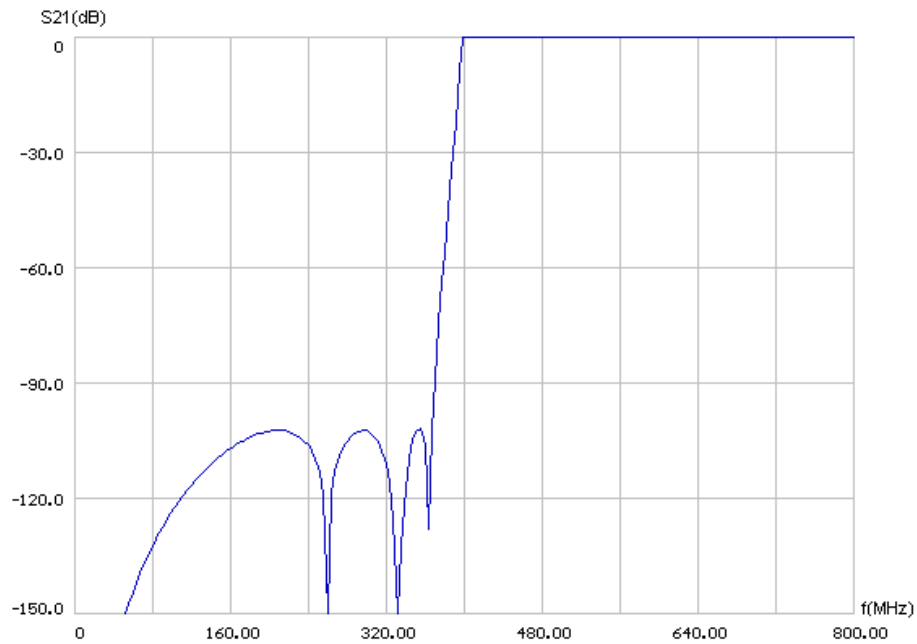


Figure 3.19: S21 graph. Stopband attenuation is min 102 dB.

3.2.11 Highpass Filter Trial 11

The order is decreased and the response is adjusted to have maximum stopband attenuation with min 60 dB loss at -20% of the corner frequency (Figure 3.21).

Type	Lumped, Highpass, Equiripple, Type A
Ripple(dB)	0.1
Corner Frequency(MHz)	400
Order	9
Transmission Zeros with order of extraction (MHz)	308, 130, 226, 284, Zero

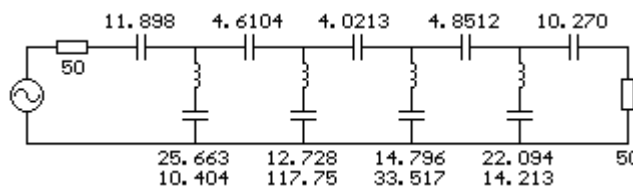


Figure 3.20: Elements of **Trial 11**

The resonator at 130 MHz includes a 117.75 pF capacitor (Figure 3.26) which is very high for a filter that should have a passband up to 2 GHz.

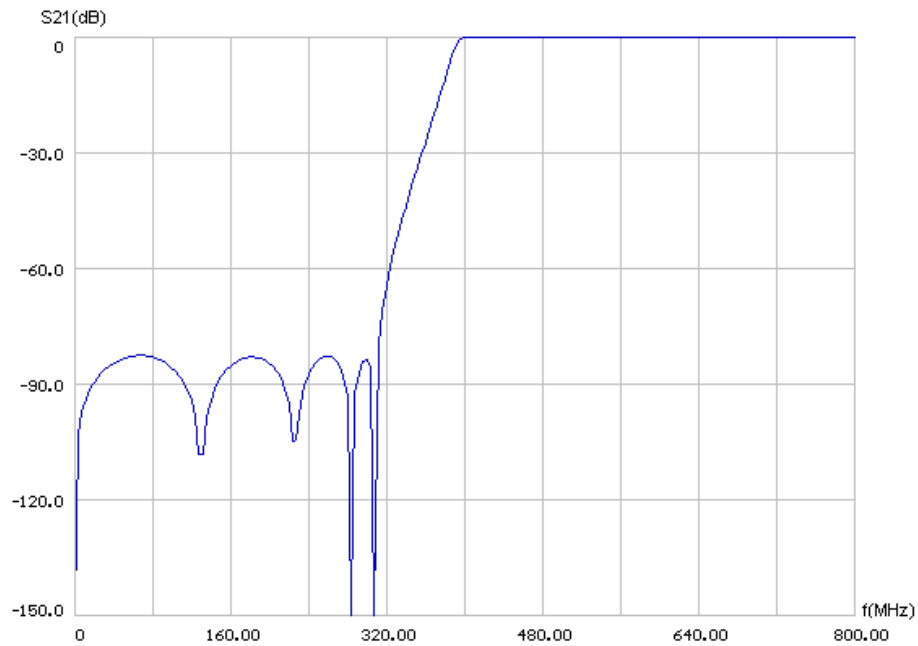


Figure 3.21: S21 graph. Stop attenuation is min 82 dB

Since the order of the filter is nine, the slope of the skirt is not sharp compared to previous filters.

3.2.12 Highpass Filter Trial 12

In this trial, the extraction order is changed compared to the previous filter.

Type	Lumped, Highpass, Equiripple, Type A
Ripple(dB)	0.1
Corner Frequency(MHz)	400
Order	9
Transmission Zeros with order of extraction (MHz)	130, 226, 284, 308, Zero

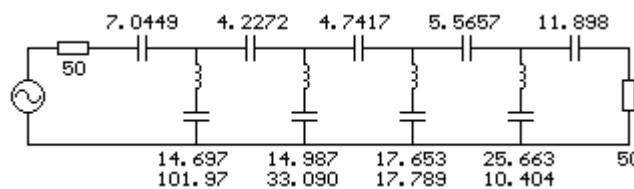


Figure 3.22: Elements of **Trial 12**

Both the inductor and the capacitor values have decreased (Figure 3.28) compared to the previous filter (Figure 3.20).

Response is same with **Trial 11** (Figure 3.21).

3.2.13 Highpass Filter Trial 13

The finite TZs are adjusted in order to have two pairs (Figure 3.23).

Type	Lumped, Highpass, Equiripple, Type A
Ripple(dB)	0.1
Corner Frequency(MHz)	400
Order	9
Transmission Zeros with order of extraction (MHz)	300, 187, 187, 300, Zero

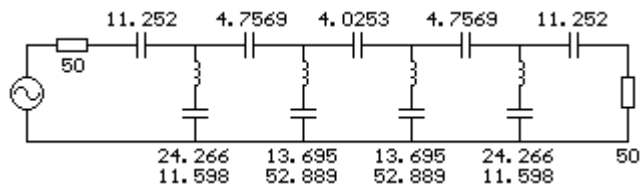


Figure 3.23: Elements of **Trial 13**

The filter is fully symmetric, 52.889 pF capacitances may be considered high in value.

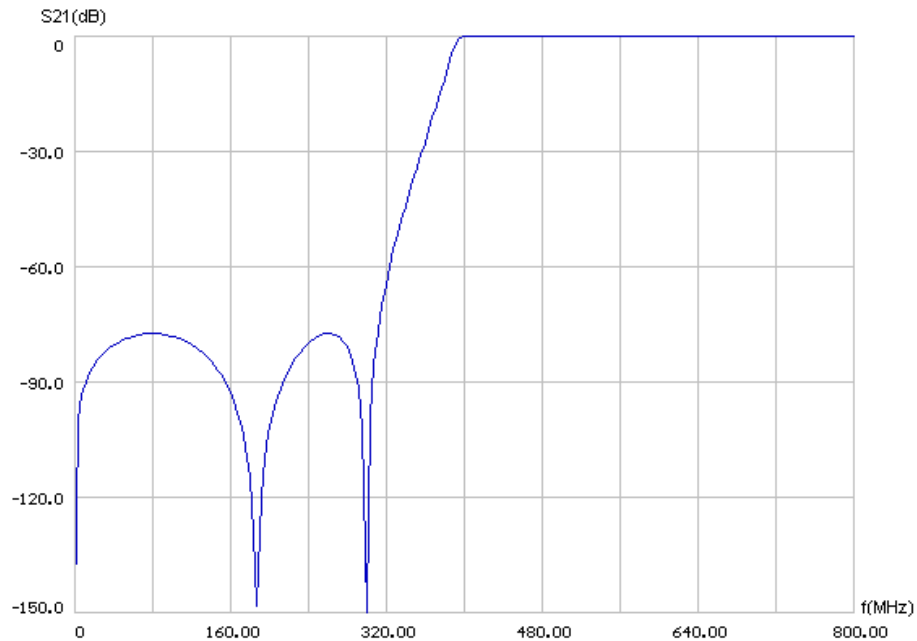


Figure 3.24: S21 graph. Stopband attenuation is min 77 dB

The slope of the skirt is relatively low, which is similar to the selectivity of **Trial 11** (Figure 3.21), but the unequal FTZs of **Trial 11** gives a little better stopband attenuation.

3.2.14 Highpass Filter Trial 14

Adding two finite TZs we obtain a sharper response. The drawback of adding two finite TZs is losing symmetry (Figure 3.25).

Type	Lumped, Highpass, Equiripple, Type A
Ripple(dB)	0.1
Corner Frequency(MHz)	400
Order	11
Transmission Zeros with order of extraction (MHz)	340, 266, 266, 340, Zero, Zero, Zero

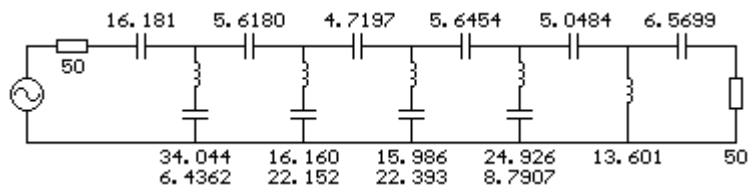


Figure 3.25: Elements of **Trial 14**

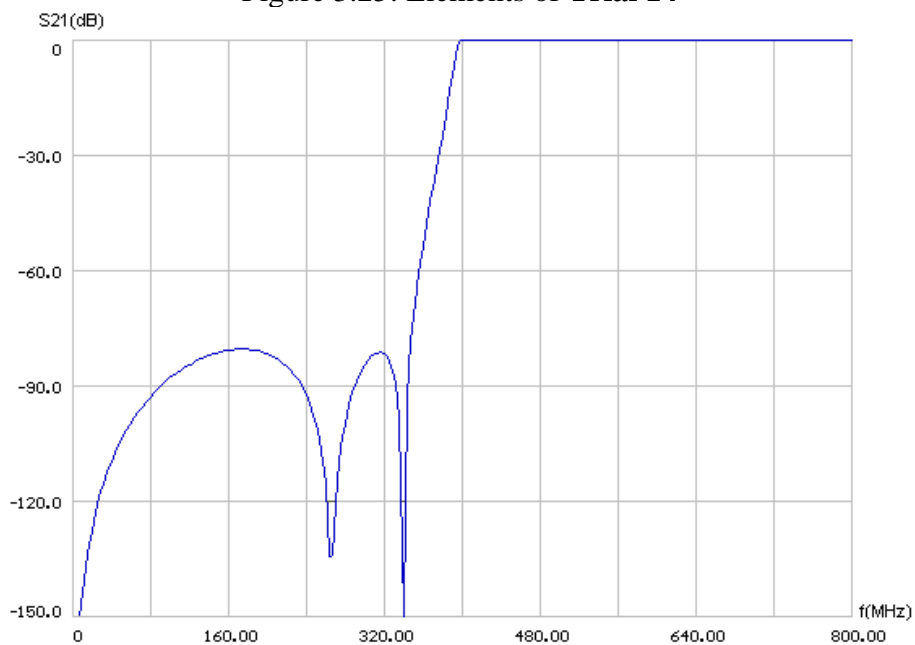


Figure 3.26: S21 graph. Stopband attenuation is min 80 dB.

The response is better compared to the previous trial.

3.2.15 Highpass Filter Trial 15

The extraction order is changed to see the affect on element values.

Type	Lumped, Highpass, Equiripple, Type A
Ripple(dB)	0.1
Corner Frequency(MHz)	400
Order	11
Transmission Zeros with order of extraction (MHz)	Zero, Zero, 266, 340, 340, 266, Zero

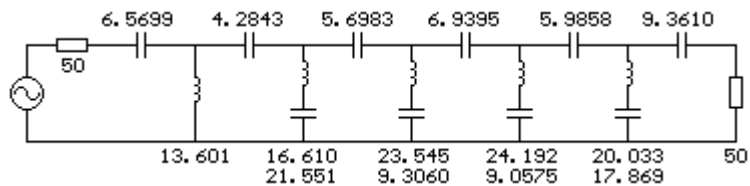


Figure 3.27: Elements of **Trial 15**

Having three transmission zeros at the initial stages results in decrease in element values, so the practical passband limit increases.

3.2.16 Highpass Filter Trial 16

Compared to the previous filter, by moving the finite TZs to higher frequencies we obtain a sharper roll-off at the expense of decreased stopband attenuation (Figure 3.29). The passband ripple is selected as 0.05 dB to have an S11 around 20 dB (Figure 3.30).

Type	Lumped, Highpass, Equiripple, Type A
Ripple(dB)	0.05
Corner Frequency(MHz)	400
Order	11
Transmission Zeros with order of extraction (MHz)	Zero, Zero, 270, 345, 345, 270, Zero

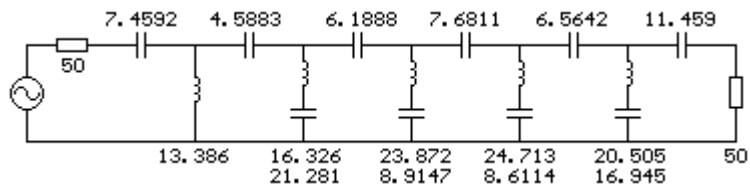


Figure 3.28: Elements of **Trial 16**

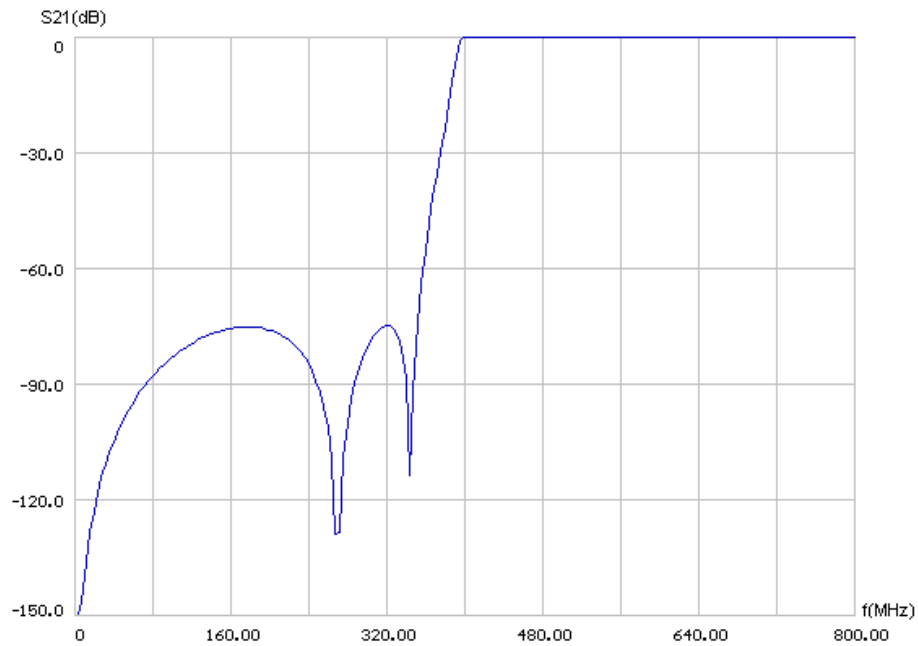


Figure 3.29: S21 graph. Stopband attenuation is min 75 dB

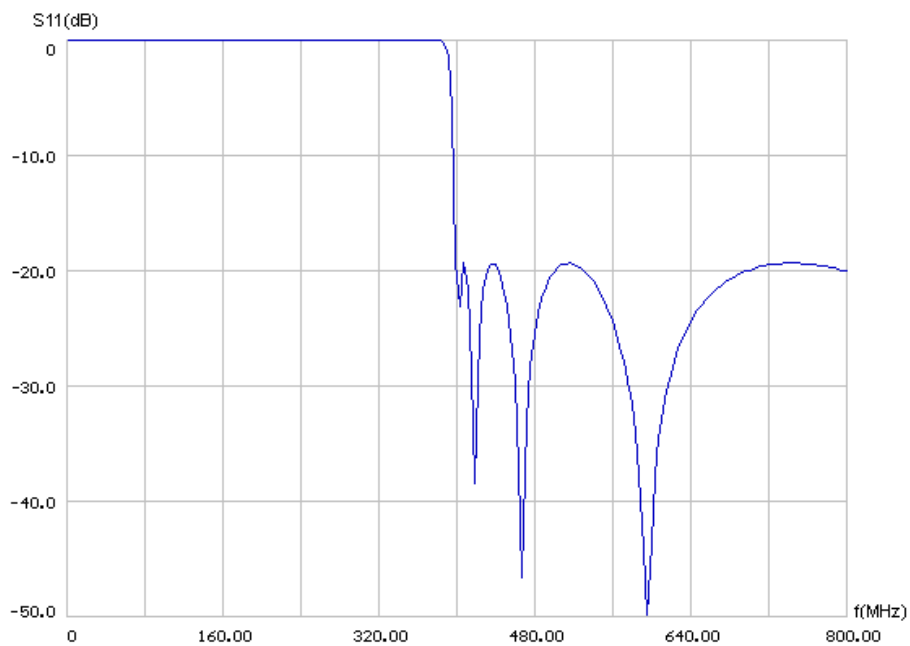


Figure 3.30: S11 graph, inband return loss is min 19 dB

After 16 trials, this filter is found proper to be used for the highpass section of the hybrid bandpass structure. The element values are relatively small and they are feasible with standard values. The sensitivity of this filter to element values is examined using Filpro's Monte Carlo analysis tool, the element deviation is selected as 5%.

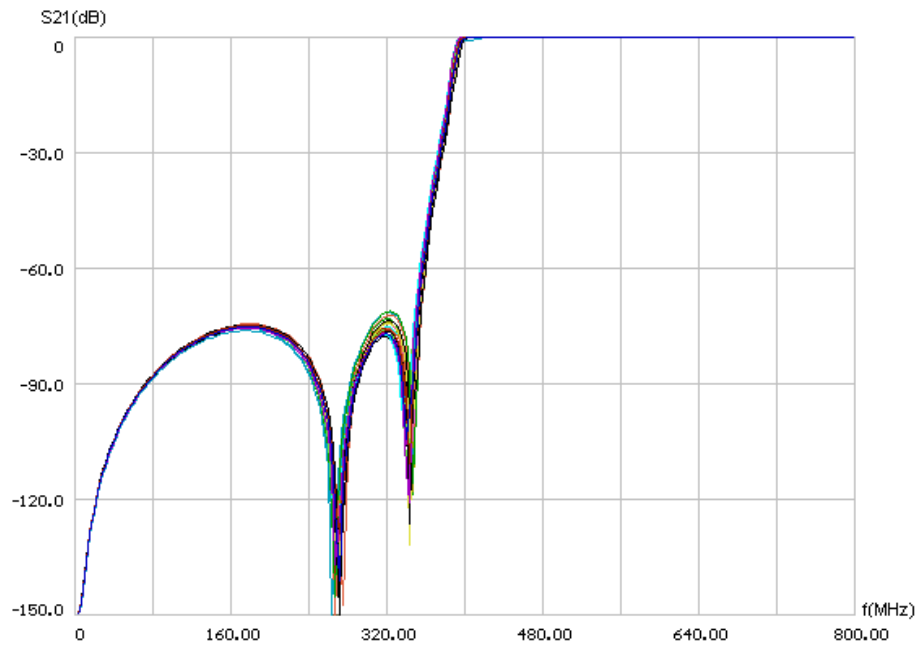


Figure 3.31: Monte Carlo analysis with 5% element deviation

The Monte Carlo analysis gave satisfactory results; the increase in stopband ripple is less than 5 dB, the corner frequency moves max 5 MHz in the worst case (Figure 3.31).

In Chapter 5, we will simulate this lumped filter by considering real life effects such as element parasitics, layout effects etc.

CHAPTER 4

DISTRIBUTED LOWPASS FILTER DESIGN TRIALS

4.1 Introduction

Having found a proper lumped structure for the highpass filter section of the hybrid bandpass filter structure in the previous chapter, we will start to synthesize the distributed lowpass part in this chapter. FILPRO is used to synthesize the lowpass filter trials, as in the previous chapter.

Similar to lumped element filters, we have also some criterions for the distributed filters, and we will decide on the proper filters using these criterions.

- **Element values:** For the distributed lowpass filter, very small and very high impedances are not feasible at the same substrate. High impedances results in thin transmission line (TL) pairs and low impedances results in very wide TLs that disturb quarter wavelength pairs. As a rule of thumb we can say that if width of a TL is greater than $\lambda/20$, then it may be considered as “wide”. At higher (quarter wave) frequencies this criteria is more evident since stub lengths decrease as the line widths remain same if same dielectric substance is used, this is one of the reasons why smaller height dielectrics are used at higher frequencies to decrease line widths. In Figure 4.1 it can be said that since $w_3 > \lambda/20$, the shunt stub may be considered as wide and it has a negative effect on the performance of adjacent $\lambda/4$ TLs.

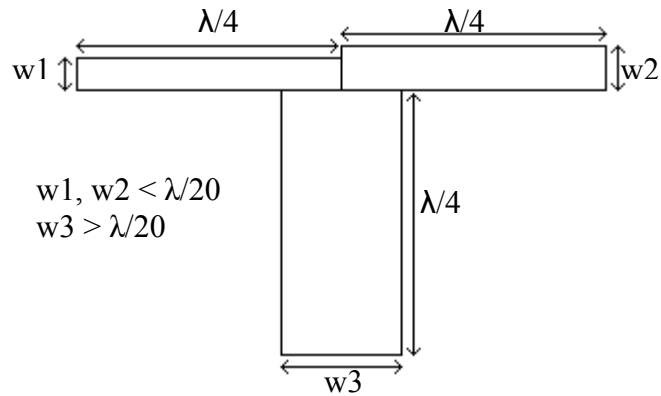


Figure 4.1: The wide shunt stub deteriorates the quarter wavelength behavior of the adjacent series TLs

Very high impedances results in very thin TLs which is difficult to realize. Usually lines that are thinner than 10 mils (0.254 mm) are difficult to realize and they are not reliable since bending of the dielectric substrate may cut the lines. As a rule of thumb, practical impedance range for striplines is 20Ω to 120Ω . For example for a stripline of width 62 mils and with a dielectric material having $\epsilon_r=2.2$, this impedance range results in line widths of 168 mils to 8 mils respectively.

- **Range of Element Values:** This criterion is important for distributed element filters especially, since spread impedances results in too narrow and too wide impedances.
- **Sensitivity of the filter response to element tolerances:** Distributed elements (stubs, TLs etc.) may deviate from the desired values due to production tolerances. These deviations are usually deterministic and should be taken care of. Response deviation of the distributed filters is less compared to lumped filters. A distributed filter should not be too sensitive to element tolerances; usually this implies that there shouldn't be very thin lines in a filter structure, since a constant production tolerance affects the width of the realized thin lines more compared to thick lines.

- **The order/complexity of the filter:** The order of the filter directly affects the size and the loss of the filter. Filters whose orders are greater than 15 are rarely used.

4.1 Design Trials of the Lowpass Distributed Filter

We should decide on the the filter structure before starting the distributed lowpass trials, because stub and TL widths of the synthesized filters depends on the structure to be used. For realization of distributed filters, it is common to use microstrip-like structures, such as basic microstrip, suspended microstrip, suspended-substrate stripline and stripline as shown in Figure 4.2 respectively.

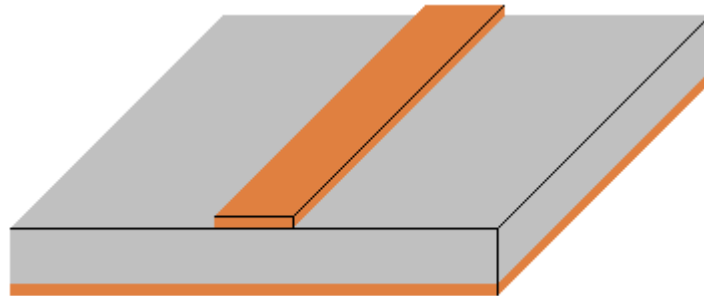


Figure 4.2.a: Microstrip

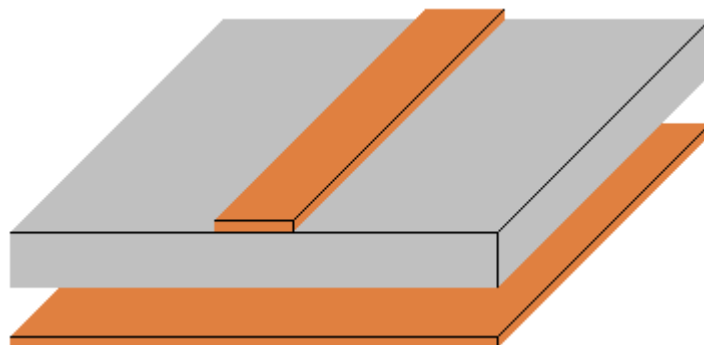


Figure 4.2.b: Suspended microstrip

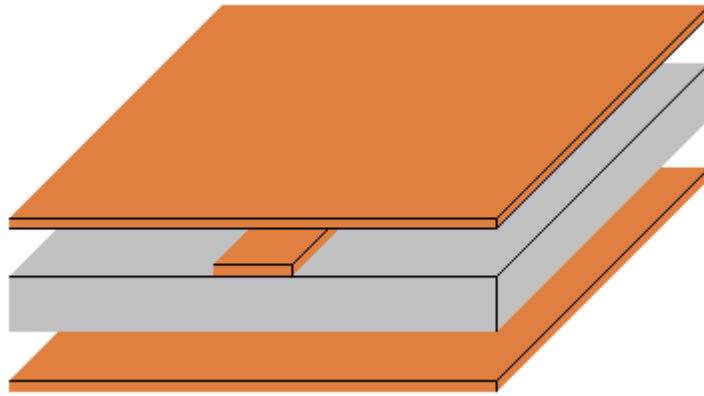


Figure 4.2.c: Suspended-Substrate Stripline

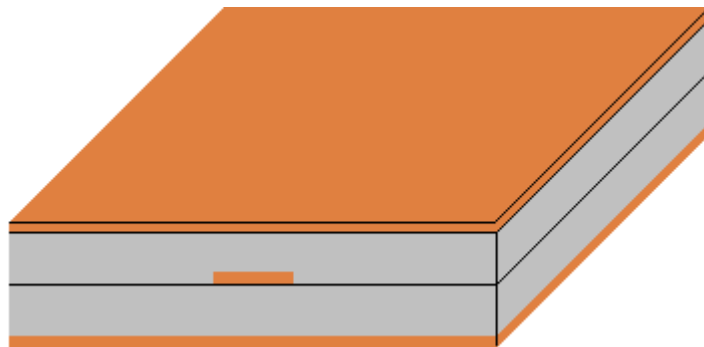


Figure 4.2.d: Stripline

Figure 4.2: Basic microstrip-like structures, the thin dark surfaces are conductors while the light color sections are the dielectric layers

For this thesis work, stripline structure is found proper for realization of the filters. Stripline is relatively easy to construct and the impedance range obtained with common dielectric thicknesses is satisfactory [5]. A cut-away view of a stripline filter is shown in Figure 4.3 below:

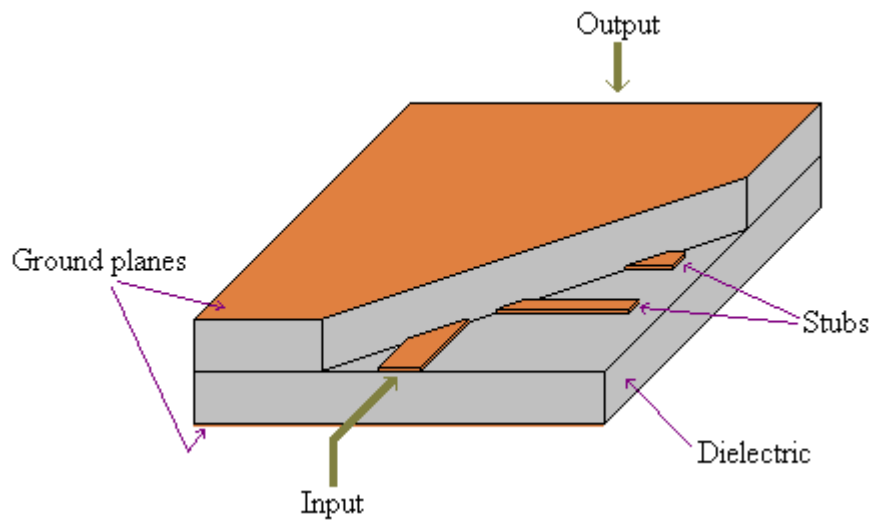


Figure 4.3: Cut-away view of a stripline filter

There are different topologies for lowpass distributed filters. Sharp skirt slopes and controlled (pass and stopband) responses can be obtained with small sizes by synthesizing Chebyshev filters with contributing unit elements and with carefully placed finite transmission zeros. Although all unit elements are chosen as non-redundant, if it eases some realization problems, one may also use some redundant unit elements and / or use the technique of replacing series SC stubs by transmission lines. A topology readily lending itself for realization comes out for lowpass filters with one transmission zero at infinity, if the number of unit elements are twice the number of finite transmission zeros, as shown in Figure 4.4. This effective topology is found most appropriate for the lowpass filter and will be used in the succeeding designs [1].

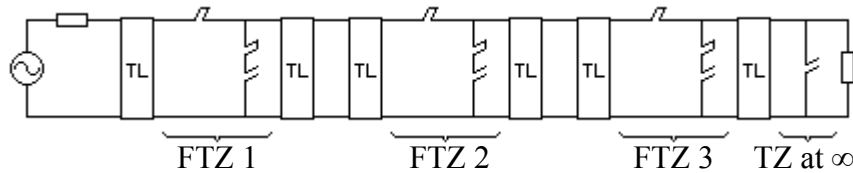


Figure 4.4: The selected topology for the distributed low pass structure

The lumped equivalent of that filter topology is as below:

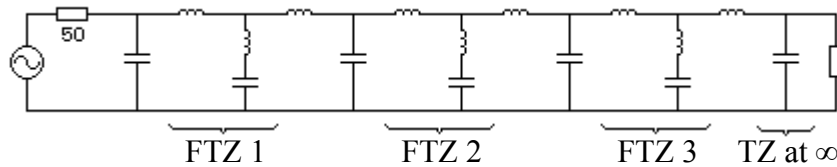


Figure 4.5: The lumped equivalent of the distributed lowpass filter. Six elements that are not indicated are TZs at ∞ , and they are the counterparts of the non-redundant UEs in the distributed filter

As an example, insertion loss response of a filter having f_c at 2 GHz, f_q at 5 GHz and three FTZs at 2350 MHz is shown in Figure 4.6. The lumped counterpart's (Figure 4.5) response is also shown in Figure 4.7.

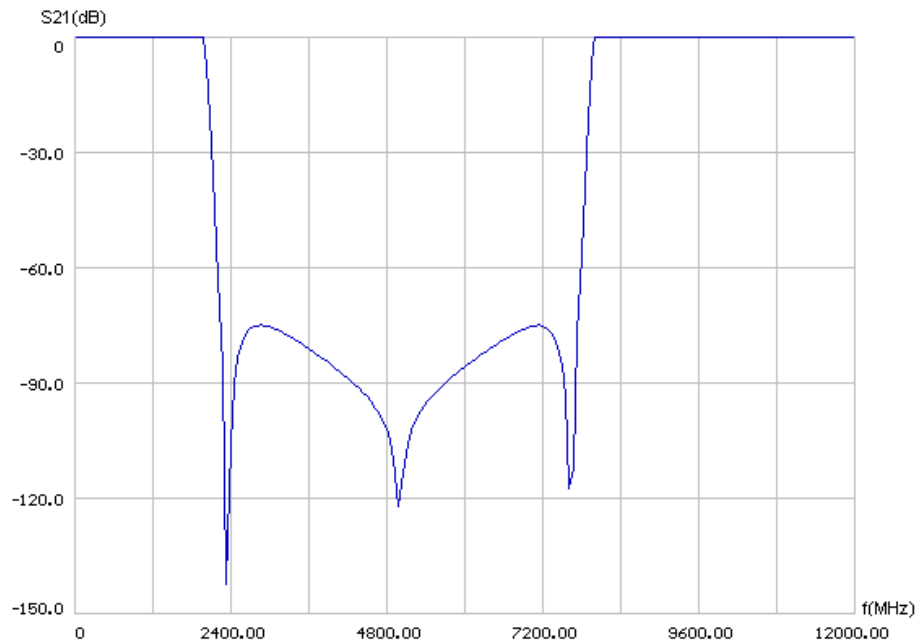


Figure 4.6: S21 of the distributed circuit

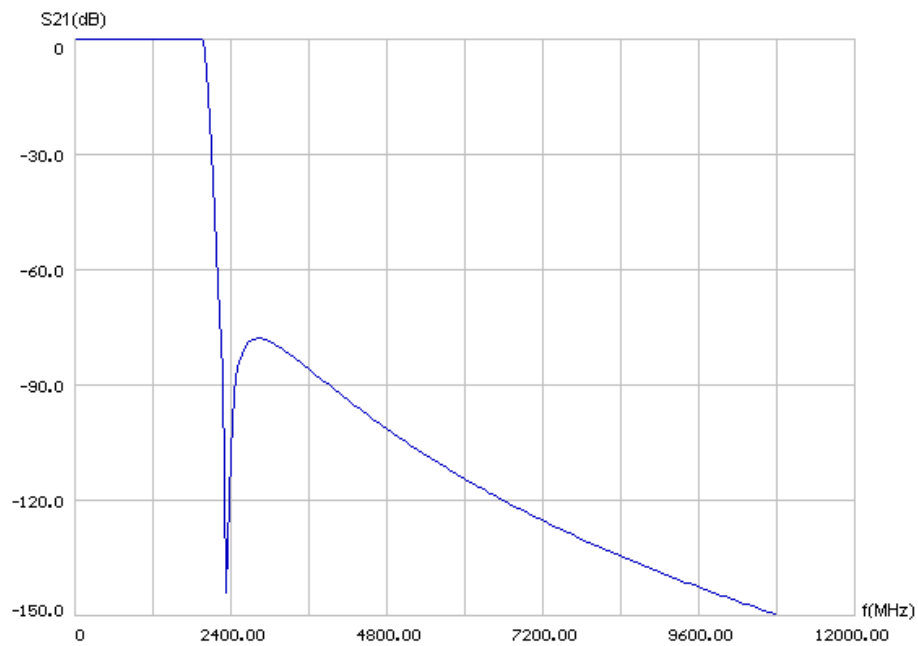


Figure 4.7: S21 of the lumped counterpart

The distributed filter has a repetitive characteristic and infinite frequency of the lumped circuit is mapped to the quarter wavelength frequency f_q for the distributed filter. The distributed filter has infinite attenuation at f_q although this is not so much apparent due to the quantization of the data points in the plot (Figure 4.6).

Series short circuited stubs are difficult to realize so by using Kuroda transformation and converting the obtained shunt resonators to step resonators [6], the initial form of the synthesized distributed filter structure in Figure 4.4 is translated into a more realizable one (Figure 4.8):

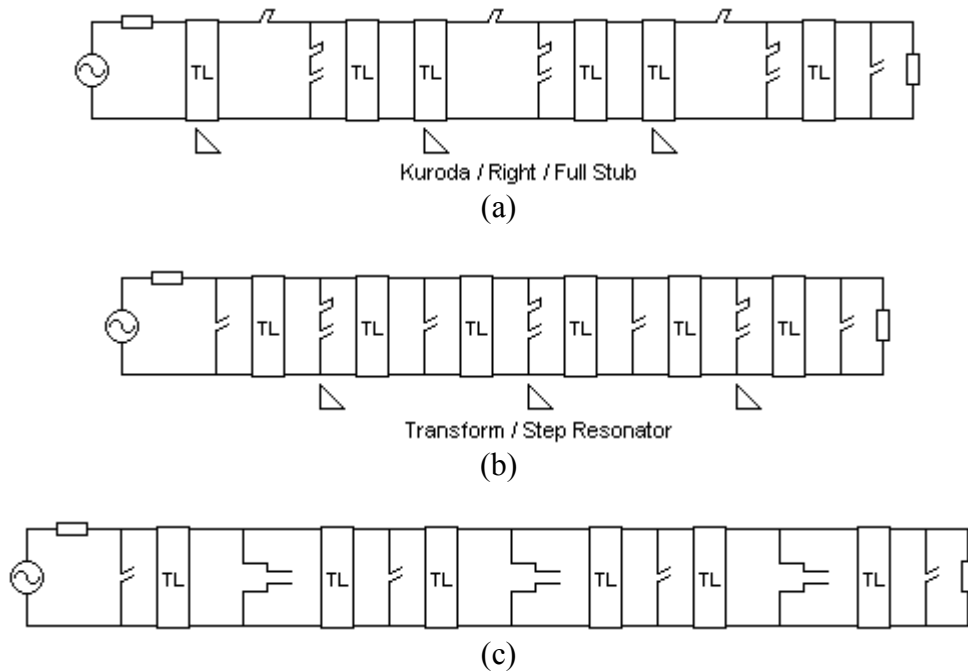


Figure 4.8: (a) Kuroda transformation is used to eliminate the series short-circuited stubs, (b) The shunt series short-circuited and open-circuited stub resonator is transformed to step resonator (c) The final structure where elements are easier to realize

4.2.1 Lowpass Filter Trial 1

In this initial trial, the filter is adjusted to have 70 dB stopband attenuation (Figure 4.10). S11 in the passband is around -16 dB (Figure 4.11).

Type	Distributed, Lowpass, Equiripple, Type B
Ripple(dB)	0.1
Corner Frequency(MHz)	2000
Quarter Wave Frequency(MHz)	4000
Order	13
Transmission Zeros with order of Extraction (MHz)	UE, 2200, 2xUE, 2500, 2xUE, 2200, UE, INF

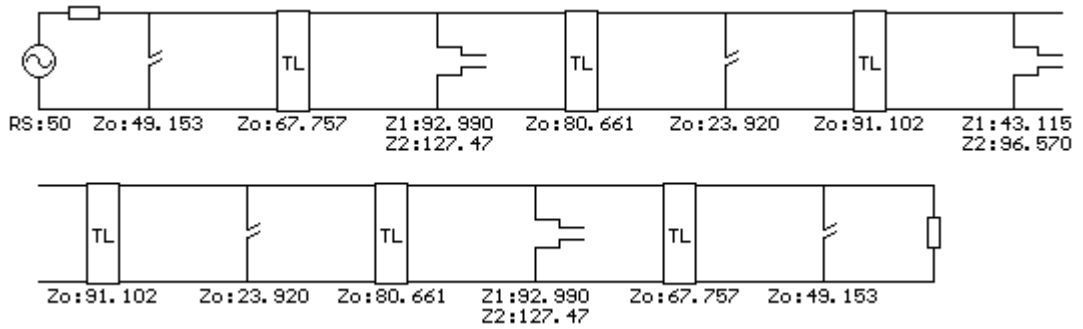


Figure 4.9: Elements of **Trial 1**

There are two element pairs that may be difficult to realize; one of them is the 23.920Ω shunt stubs and the other is 127.47Ω section of the step resonators. To realize the first one wide TLs are needed while for the second one narrow TLs are needed.

For example, for a stripline having 62 mils dielectric thickness with relative dielectric constant of 2.2, 23.920Ω is obtained by 133 mils stubs and 127.47Ω is obtained by 5.45 mils stubs. If we adjust the dielectric so that the thin stub gets wider, the already wide stub will also get wider by the same amount, so realization of this filter is difficult.

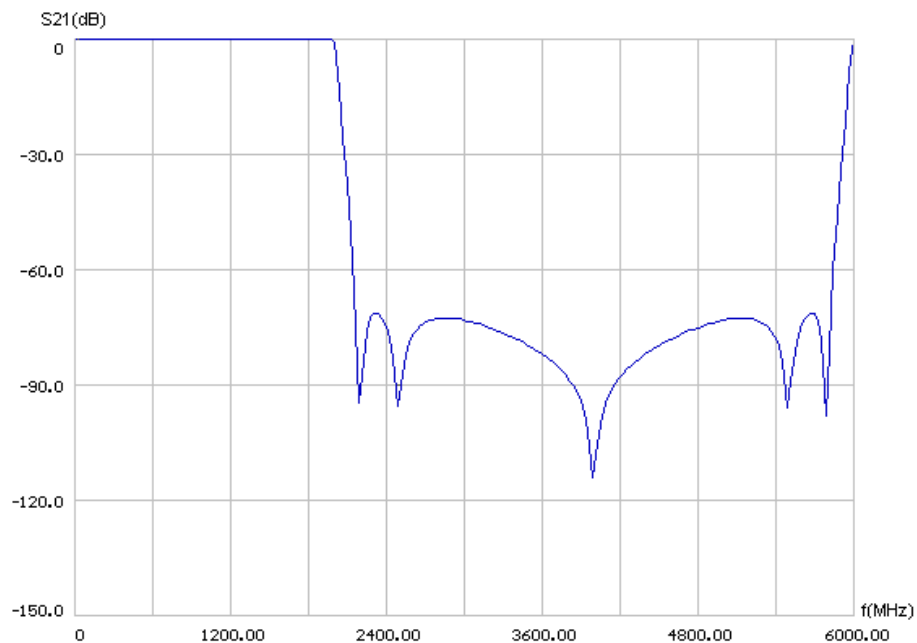


Figure 4.10: S21 graph of **Trial 1**

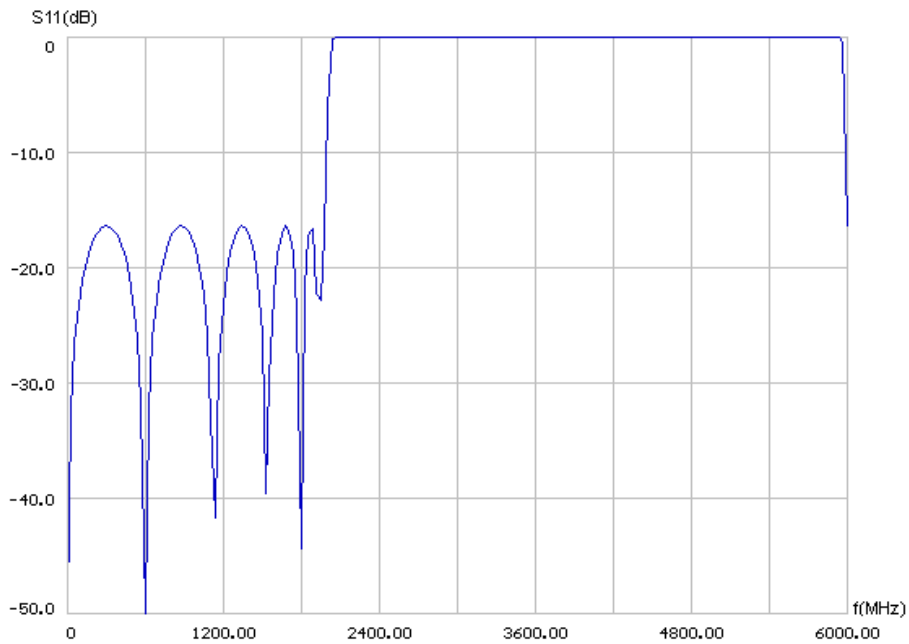


Figure 4.11: S11 graph **Trial 1**

It is possible to approximate the shunt open-circuited stubs by lumped capacitors. Since replace by lumped equivalent is an approximation around a specified frequency, the exact circuit is distorted and response changes. The 23.920 Ω shunt open circuited stubs are replaced by lumped capacitors as shown below:

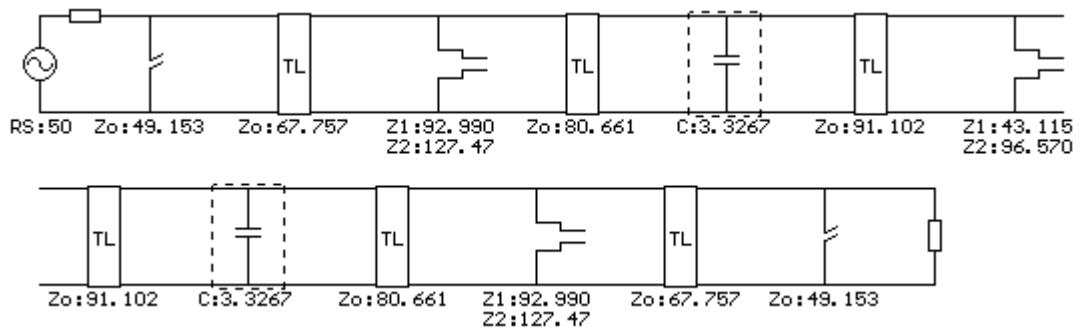


Figure 4.12: 23.920 Ω shunt open circuited stubs are replaced by lumped capacitors

The resulting 3.3267 pF capacitor is proper but the approximation distorts the response as shown in Figure 4.13.

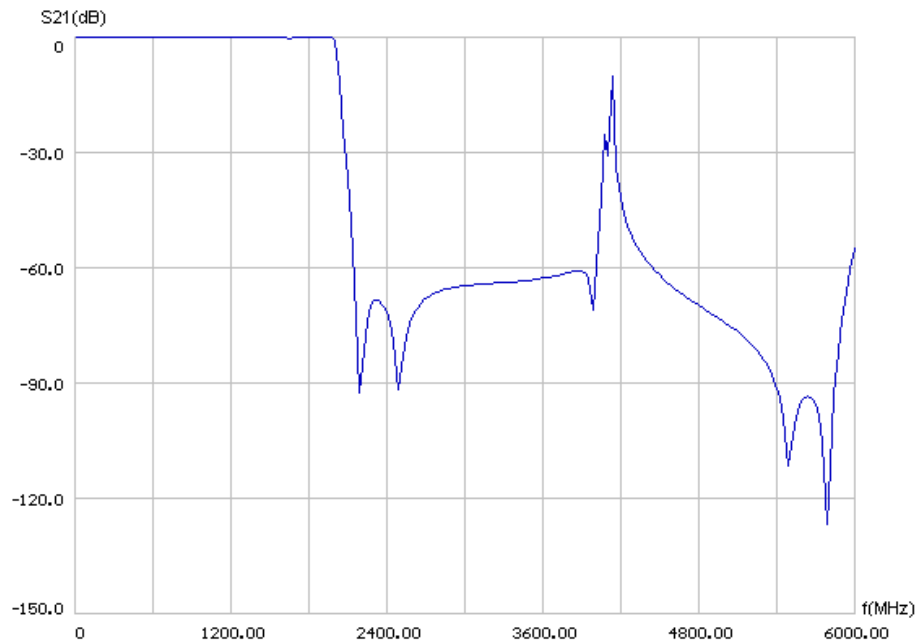


Figure 4.13: S21 graph of the modified circuit

We may also replace the 23.920Ω shunt OC stubs in Figure 4.9 by lumped LC resonators:

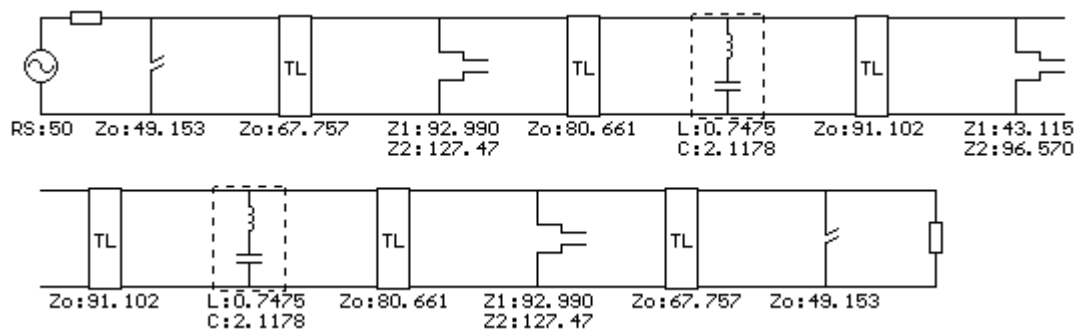


Figure 4.14: 23.920Ω shunt open circuited stubs are replaced by lumped resonators

Lumped LC section also distorts the response (Figure 4.15); the distortion is less compared to lumped capacitor replacement at the stopband region, but the corner of the filter response is distorted more.

Inserting lumped elements inside the stripline structure is difficult for realization, and considering the distortions, lumped element replacement of the step resonators is not practical. Stopband attenuation is min 67 dB (Figure 4.15).

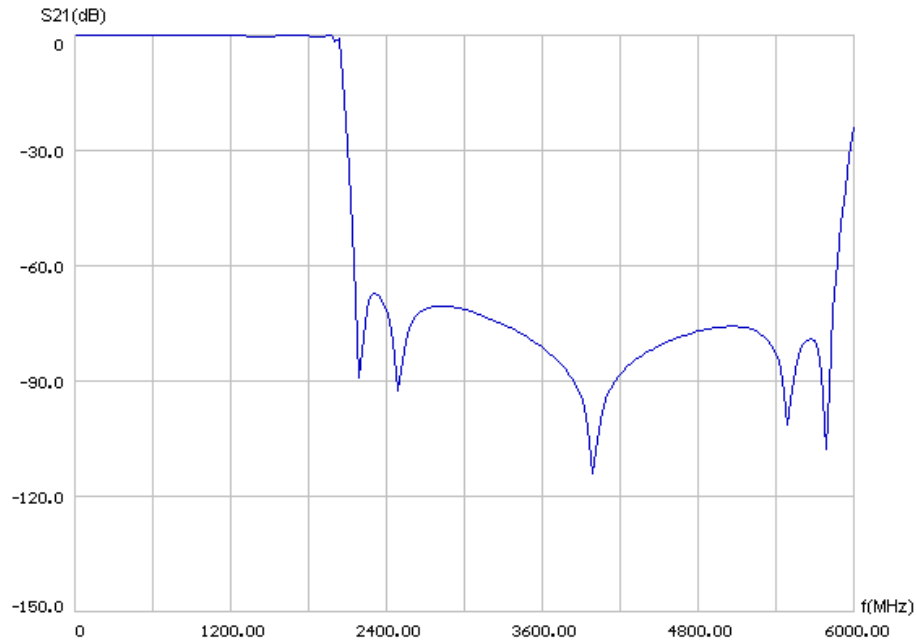


Figure 4.15: S21 graph when lumped resonators are used

4.2.2 Lowpass Filter Trial 2

The quarter wavelength frequency is shifted to 4500 MHz from 4000 MHz. All other design parameters are same with the previous filter.

Type	Distributed, Lowpass, Equiripple, Type B
Ripple(dB)	0.1
Corner Frequency(MHz)	2000
Quarter Wave Frequency(MHz)	4500
Order	13
Transmission Zeros with order of Extraction (MHz)	UE, 2200, 2xUE, 2500, 2xUE, 2200, UE, INF

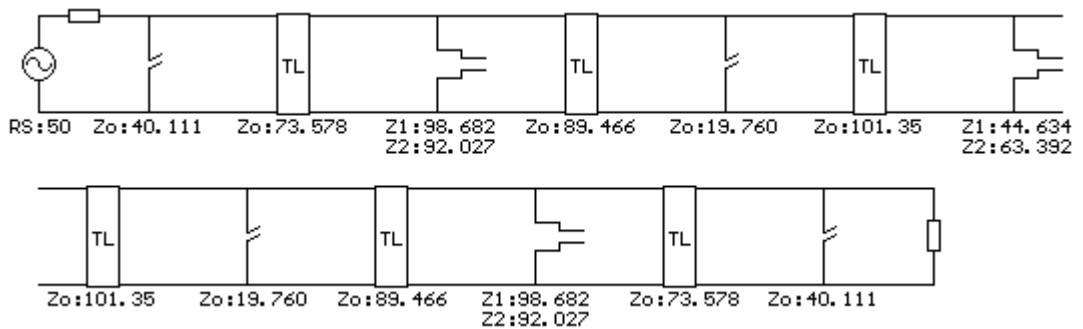


Figure 4.16: Elements of Trial 2

Compared to the previous design (Figure 4.9), it is seen that shunt stubs impedances decreases so the widths of the already wide stubs increases more (Figure 4.16). Stopband attenuation is min 71 dB (Figure 4.17).

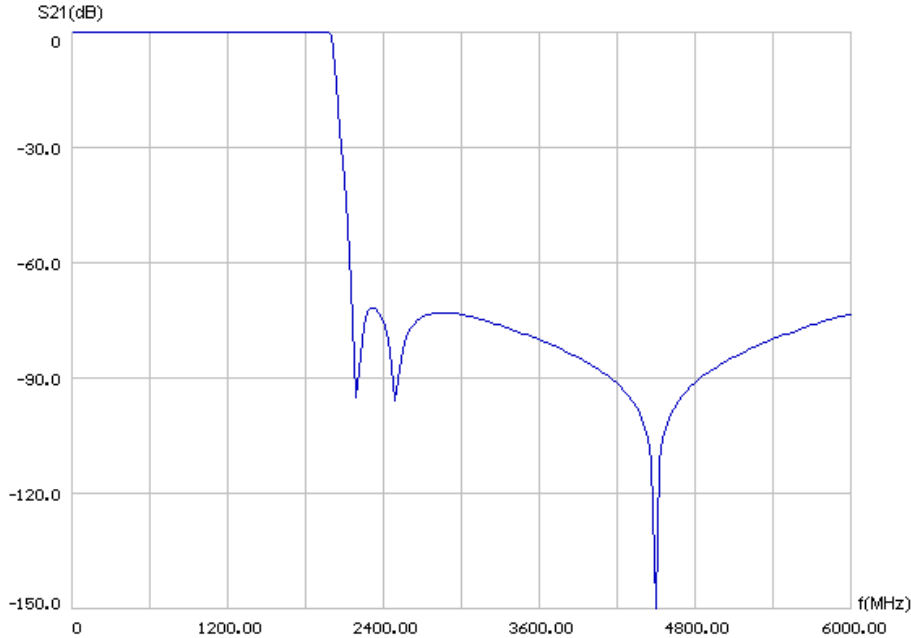


Figure 4.17: S21 graph of **Trial 2**

4.2.3 Lowpass Filter Trial 3

The quarter wavelength frequency is selected at 6 GHz, and the stopband attenuation is adjusted to be minimum 85 dB.

Type	Distributed, Lowpass, Equiripple, Type B
Ripple(dB)	0.1
Corner Frequency(MHz)	2000
Quarter Wave Frequency(MHz)	6000
Order	13
Transmission Zeros with order of Extraction (MHz)	UE, 2300, 2xUE, 2640, 2xUE, 2300, UE, INF

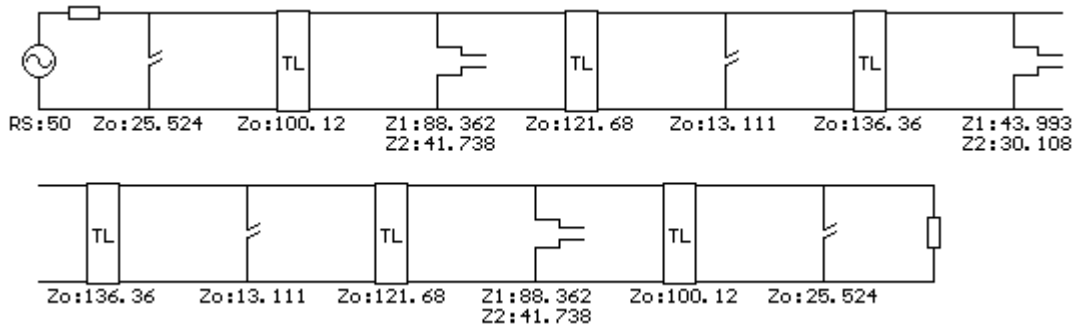


Figure 4.18: Elements of **Trial 3**

It is seen that shunt open-circuited stubs at the middle (13.111Ω) are completely unrealizable (Figure 4.18). Even if the stubs are divided into two equal pieces, the impedance is still difficult to realize (26.222Ω). Stopband attenuation is min 85 dB (Figure 4.19).

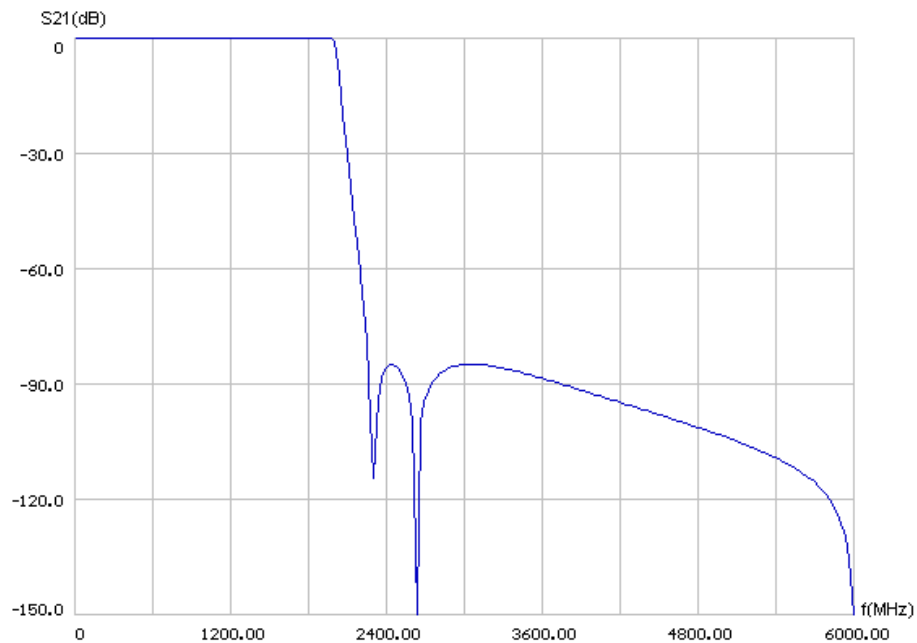


Figure 4.19: S21 graph of **Trial 3**

4.2.4 Lowpass Filter Trial 4

Compared to the previous trial, the finite transmission zeros are selected at lower frequencies. This results in an increase in the sharpness while decreasing the stopband attenuation (Figure 4.21). Stopband attenuation turns out to be min 65 dB.

Type	Distributed, Lowpass, Equiripple, Type B
Ripple(dB)	0.1
Corner Frequency(MHz)	2000
Quarter Wave Frequency(MHz)	6000
Order	13
Transmission Zeros with order of Extraction (MHz)	UE, 2150, 2xUE, 2400, 2xUE, 2150, UE, INF

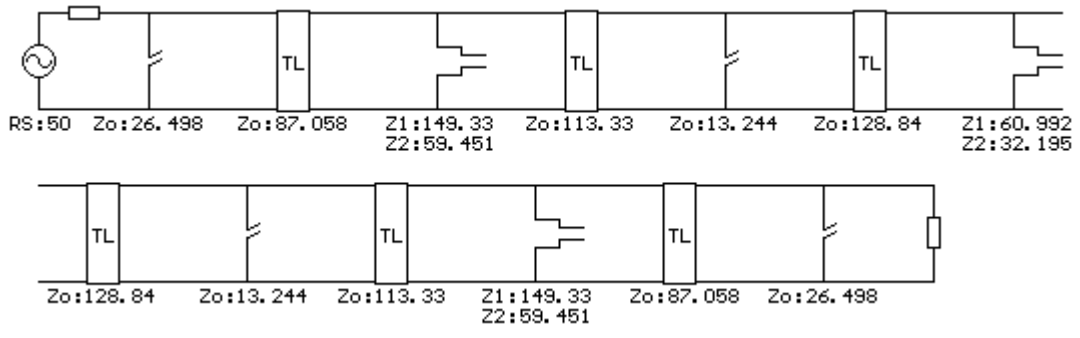


Figure 4.20: Elements of **Trial 4**

In addition to the shunt stubs at the middle (13.244 Ω), the 149.33 Ω stubs of the step resonators are also not feasible (Figure 4.20).

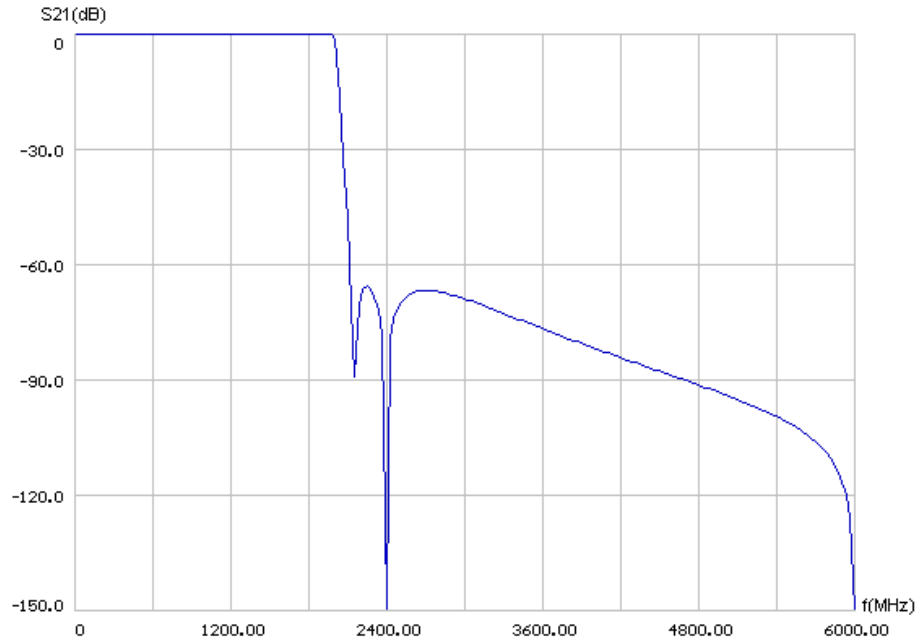


Figure 4.21: S21 graph of **Trial 4**

4.2.5 Lowpass Filter Trial 5

In this trial, two UEs and two TZs at ∞ are added.

Type	Distributed, Lowpass, Equiripple, Type B
Ripple(dB)	0.1
Corner Frequency(MHz)	2000
Quarter Wave Frequency(MHz)	4000
Order	17
Transmission Zeros with order of Extraction (MHz)	INF, 2xUE, 2200, 2xUE, 2480, 2xUE, 2200, UE, INF, UE, INF

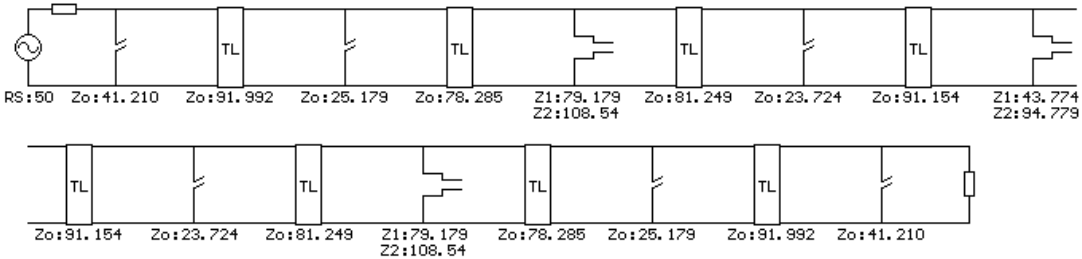


Figure 4.22: Elements of **Trial 5**

Despite the increasing order, the filter elements are more realizable than the previous ones. Stopband attenuation is min 93 dB (Figure 4.23). Note that the stopband response is not equiripple.

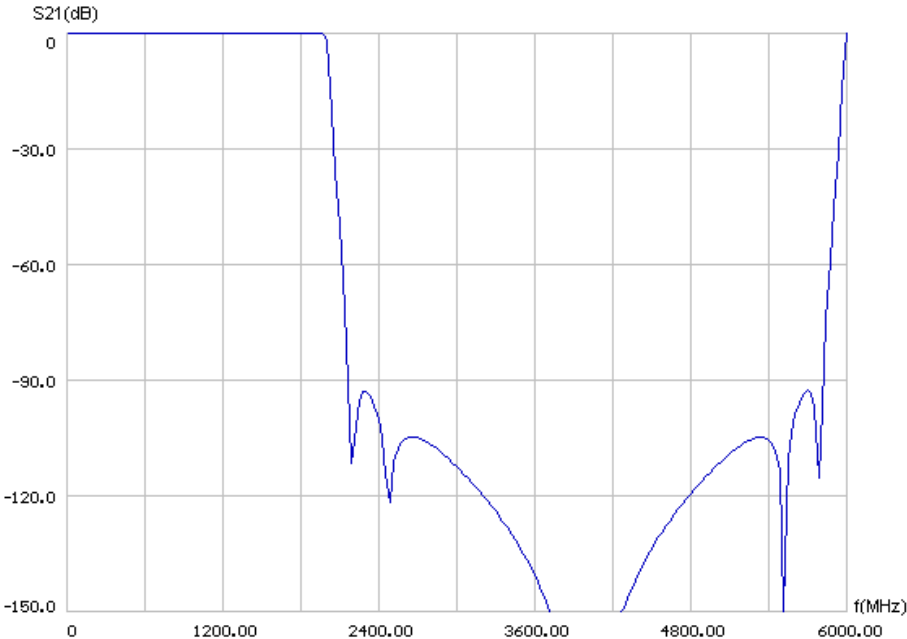


Figure 4.23: S21 graph of **Trial 5**

4.2.6 Lowpass Filter Trial 6

In this trial, the equiripple stopband version of the previous filter is analyzed.

Type	Distributed, Lowpass, Equiripple, Type B
Ripple(dB)	0.1
Corner Frequency(MHz)	2000
Quarter Wave Frequency(MHz)	4000
Order	17
Transmission Zeros with order of Extraction (MHz)	INF, 2xUE, 2200, 2xUE, 2375, 2xUE, 2200, UE, INF, UE, INF

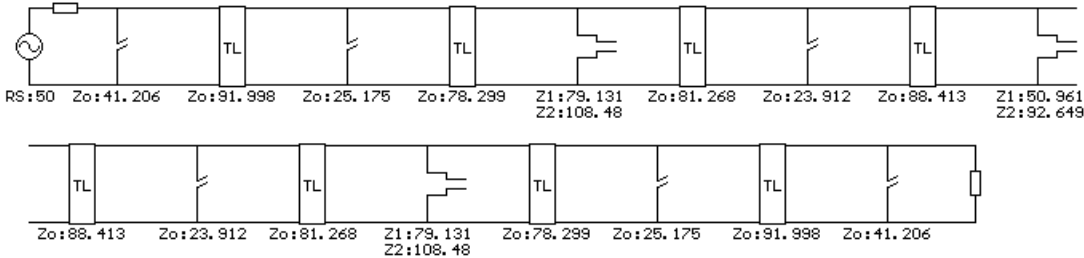


Figure 4.24: Elements of **Trial 6**

Stopband attenuation is min 98 dB (Figure 4.25).

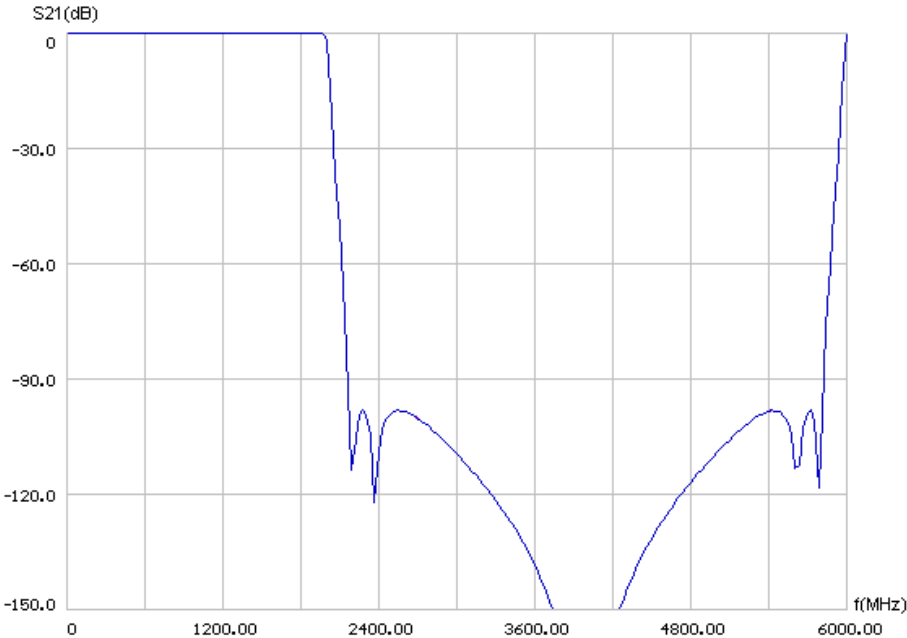


Figure 4.25: S21 graph of **Trial 6**

4.2.6 Lowpass Filter Trial 7

This trial is similar to **Trial 4**; the difference is the quarter wavelength frequency which is selected at 4500 MHz instead of 6000 MHz.

Type	Distributed, Lowpass, Equiripple, Type B
Ripple(dB)	0.1
Corner Frequency(MHz)	2000
Quarter Wave Frequency(MHz)	4500
Order	13
Transmission Zeros with order of Extraction (MHz)	UE, 2150, 2xUE, 2400, 2xUE, 2150, UE, INF

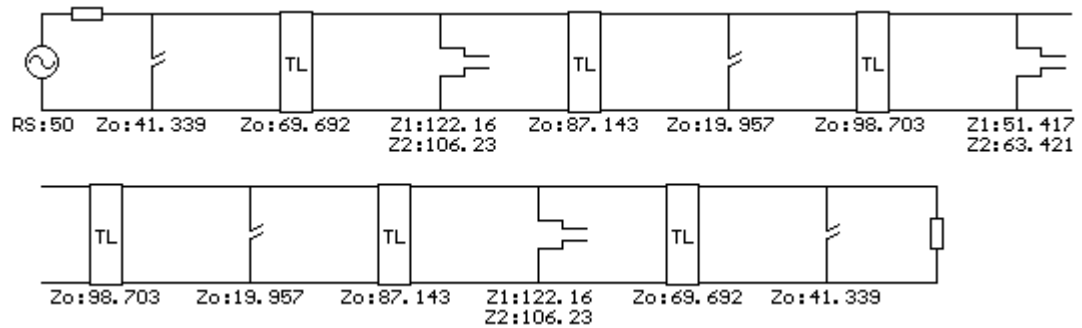


Figure 4.26: Elements of **Trial 7**

Compared to **Trial 4**, it is seen that the exterior step resonators' impedance values are relatively better, but still out of range. Stopband attenuation is min 65 dB (Figure 4.27).

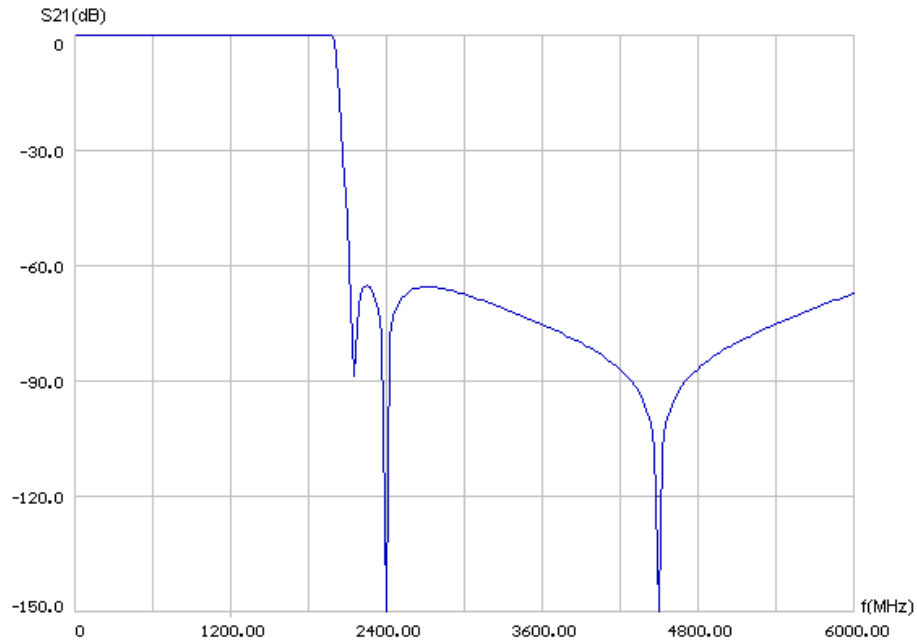


Figure 4.27: S21 graph of **Trial 7**

4.2.7 Lowpass Filter Trial 8

In this trial, compared to the previous filter the FTZ frequencies have increased with the other parameters being the same.

Type	Distributed, Lowpass, Equiripple, Type B
Ripple(dB)	0.1
Corner Frequency(MHz)	2000
Quarter Wave Frequency(MHz)	4500
Order	13
Transmission Zeros with order of Extraction (MHz)	UE, 2180, 2xUE, 2450, 2xUE, 2180, UE, INF

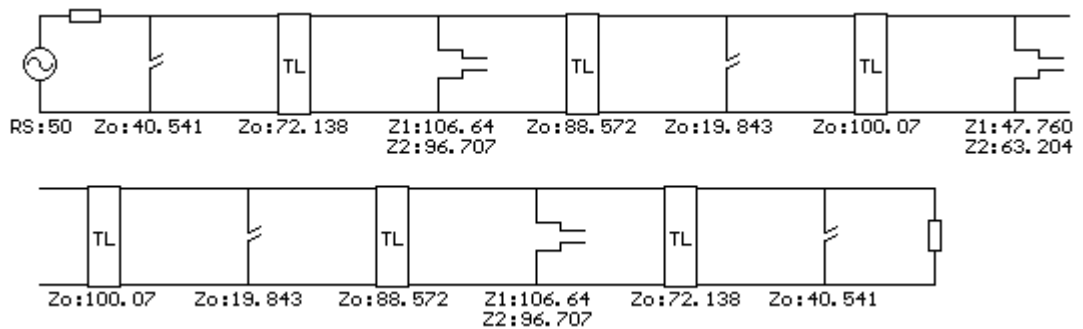


Figure 4.28: Elements of **Trial 8**

The exterior step resonators' impedance values decreased. Stopband attenuation is min 70 dB. Response is shown below (Figure 4.29).

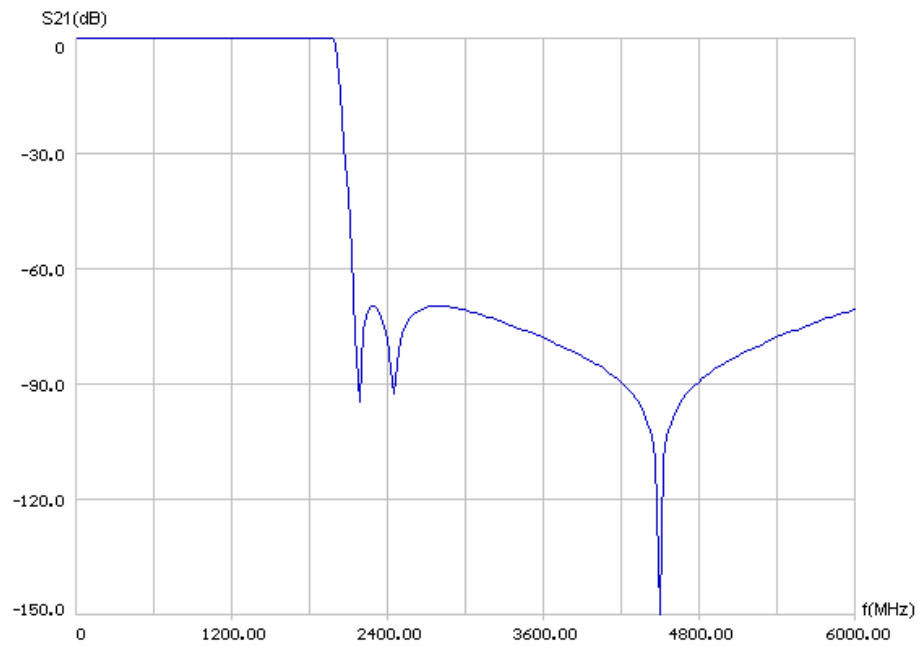


Figure 4.29: S21 graph of **Trial 8**

4.2.8 Lowpass Filter Trial 9

In the previous trials, the passband ripple was 0.1 dB. In order to see the effects of this parameter on element values the passband ripple is selected as 0.01 dB in this trial.

Type	Distributed, Lowpass, Equiripple, Type B
Ripple(dB)	0.01
Corner Frequency(MHz)	2000
Quarter Wave Frequency(MHz)	4500
Order	13
Transmission Zeros with order of Extraction (MHz)	UE, 2180, 2xUE, 2450, 2xUE, 2180, UE, INF

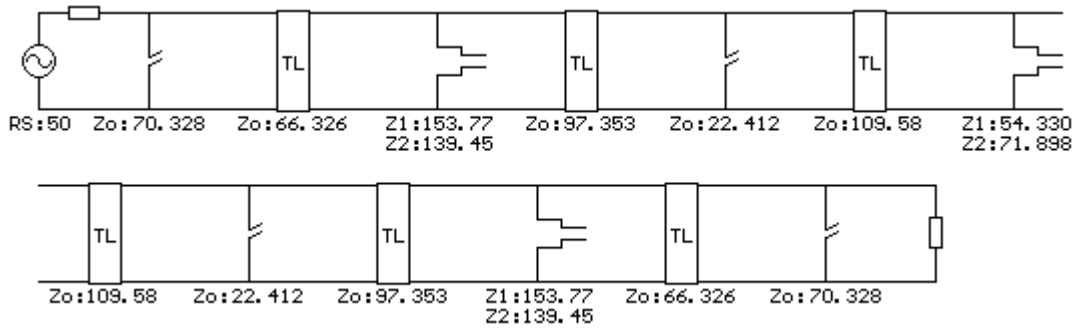


Figure 4.30: Elements of **Trial 9**

The exterior step resonator impedances are very high. Stopband attenuation is min 60 dB (Figure 4.31), 10 dB less compared to the previous trial (Figure 4.29).

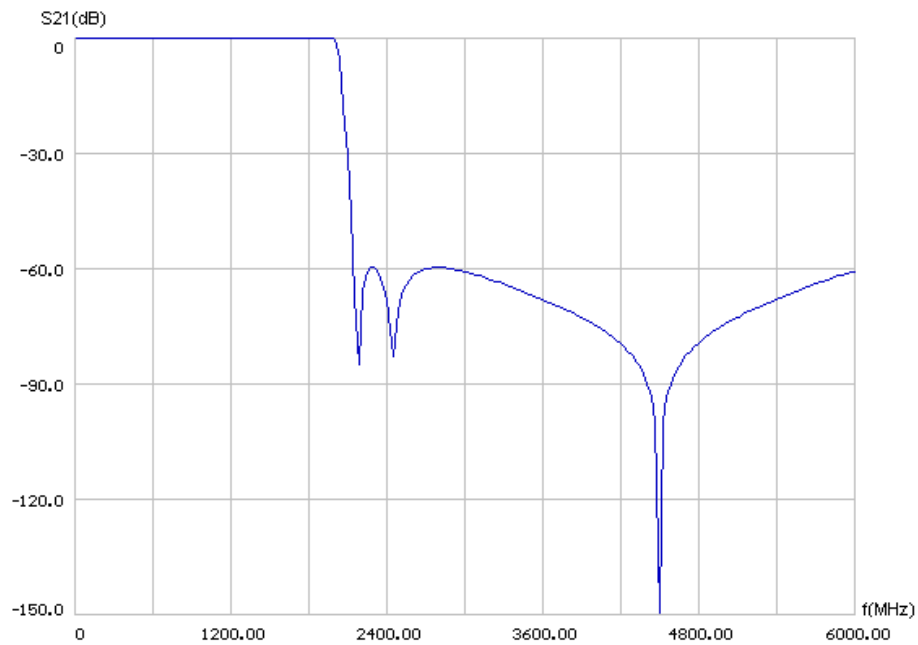


Figure 4.31: S21 graph of **Trial 9**

The stop band attenuation has decreased due to decrease in passband ripple.

4.2.9 Lowpass Filter Trial 10

In the previous example 0.01 dB ripple resulted in high step resonator impedances and have decreased the stopband attenuation, so in this example we used 0.1 dB passband ripple again.

Type	Distributed, Lowpass, Equiripple, Type B
Ripple(dB)	0.1
Corner Frequency(MHz)	2000
Quarter Wave Frequency(MHz)	4000
Order	13
Transmission Zeros with order of Extraction (MHz)	UE, 2200, 2xUE, 2200, 2xUE, 2200, UE, INF

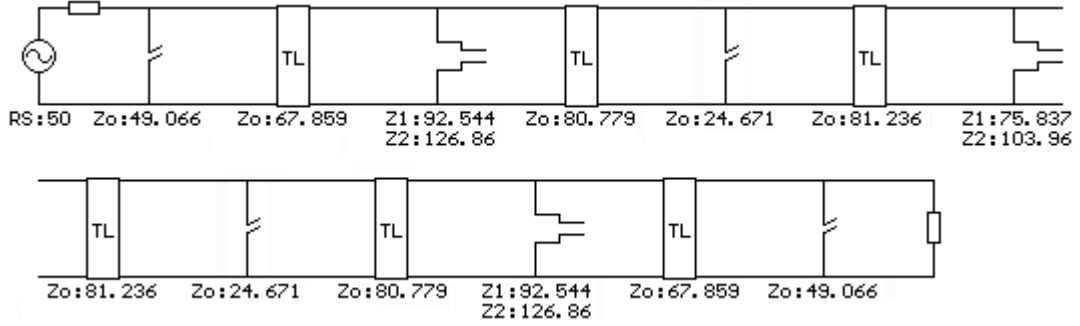


Figure 4.32: Elements of **Trial 10**

Except the 126.86 Ω arm of the step resonator, the element values are moderate (Figure 4.32). Stopband attenuation is min 61 dB (Figure 4.33).

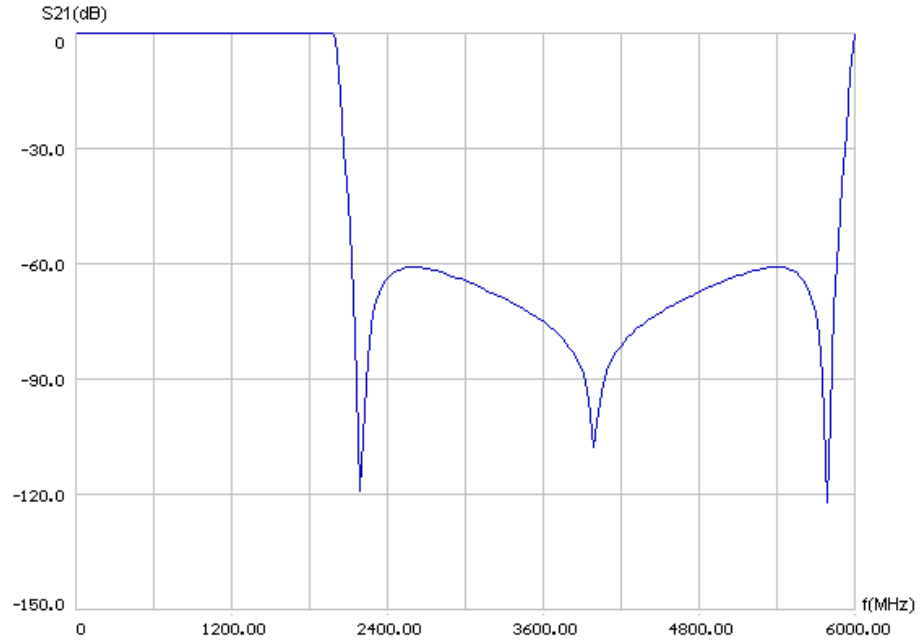


Figure 4.33: S21 graph **Trial 10**

As can be seen, selecting all of the FTZs at the same frequency decreases the stopband attenuation when compared to **Trial 8**, which have similar skirt slope.

But, on the other hand, the inner shunt OC stubs' impedances have increased from 19.843 Ω to 24.671 Ω .

4.2.11 Lowpass Filter Trial 11

In this trial, all the three FTZ's of the previous trial are shifted to 2310 MHz to see the effect on element values. All the other parameters are the same.

Type	Distributed, Lowpass, Equiripple, Type B
Ripple(dB)	0.1
Corner Frequency (MHz)	2000
Quarter Wave Frequency(MHz)	4000
Order	13
Transmission Zeros with order of Extraction (MHz)	UE, 2310, 2xUE, 2310, 2xUE, 2310, UE, INF

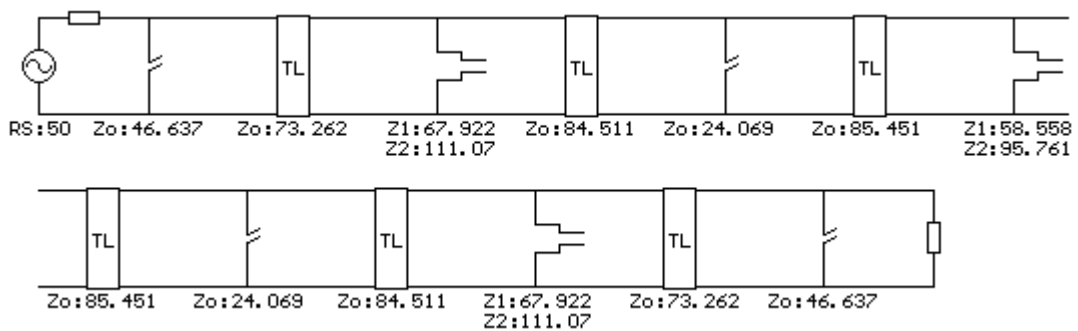


Figure 4.34: Elements of **Trial 11**

This filter has the best distributed element values up to now. This is one of the filters that will be simulated and realized as will be explained in the following chapter. Response is shown in Figure 4.35.

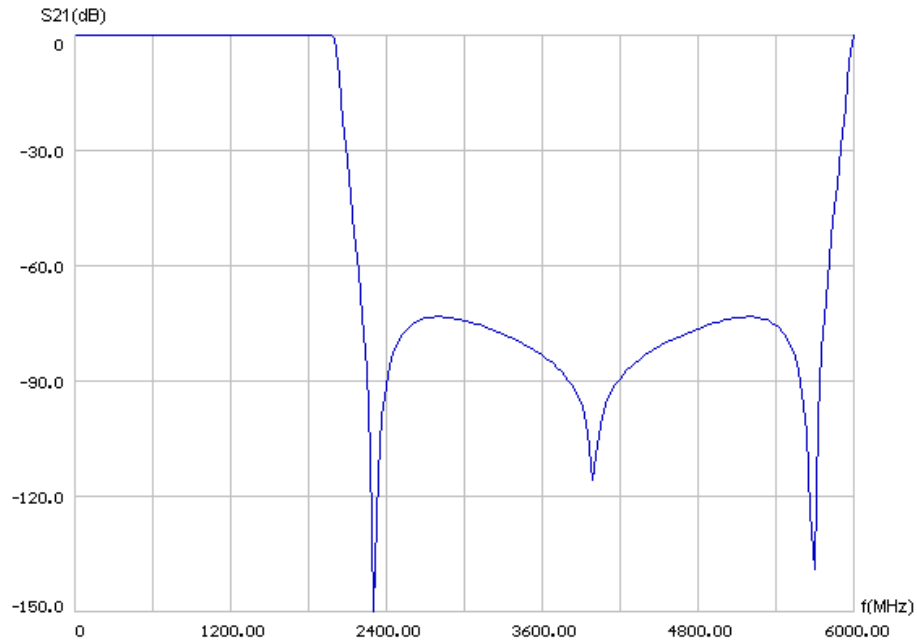


Figure 4.35: S21 graph of **Trial 11**

The skirt slope is similar to **Trial 3**, the stop band attenuation is min 73 dB instead of 85 dB in **Trial 3**, but since 73 dB is good enough this is not a problem.

4.2.12 Lowpass Filter Trial 12

In this trial f_q is selected at 4620 MHz, two times the FTZ frequencies.

Type	Distributed, Lowpass, Equiripple, Type B
Ripple(dB)	0.1
Corner Frequency(MHz)	2000
Quarter Wave Frequency(MHz)	4620
Order	13
Transmission Zeros with order of Extraction (MHz)	UE, 2310, 2xUE, 2310, 2xUE, 2310, UE, INF

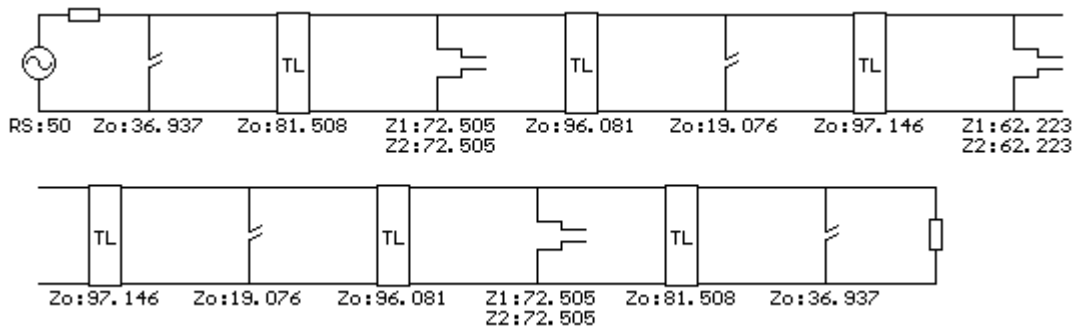


Figure 4.36: Elements of **Trial 12**

It is seen that, the two impedances of the step resonators are equal. This is the result of choosing FTZ at half the frequency of f_q . The only problematic element of the filter is the mid shunt open-circuited stubs (19.076Ω). Stopband attenuation is min 73 dB (Figure 4.37).

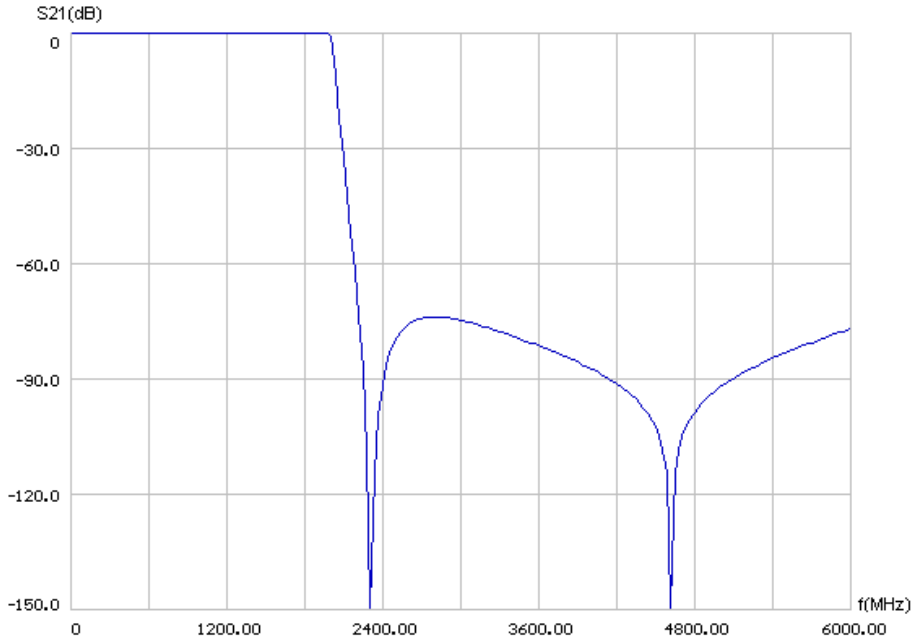


Figure 4.37: S21 graph of **Trial 12**

4.2.13 Lowpass Filter Trial 13

The FTZs are increased to 2370 MHz, and f_q is at 4740 MHz.

Type	Distributed, Lowpass, Equiripple, Type B
Ripple(dB)	0.1
Corner Frequency(MHz)	2000
Quarter Wave Frequency(MHz)	4740
Order	13
Transmission Zeros with order of Extraction (MHz)	UE, 2370, 2xUE, 2370, 2xUE, 2370, UE, INF

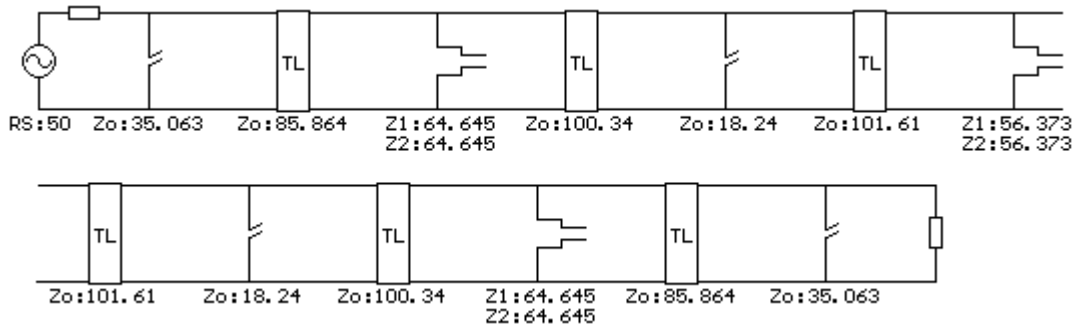


Figure 4.38: Elements of **Trial 13**

It is seen that, the two impedances of the step resonators are equal. The only problematic element of the filter is the mid shunt open-circuited stubs (18.24Ω). Stopband attenuation is min 79 dB (Figure 4.39).

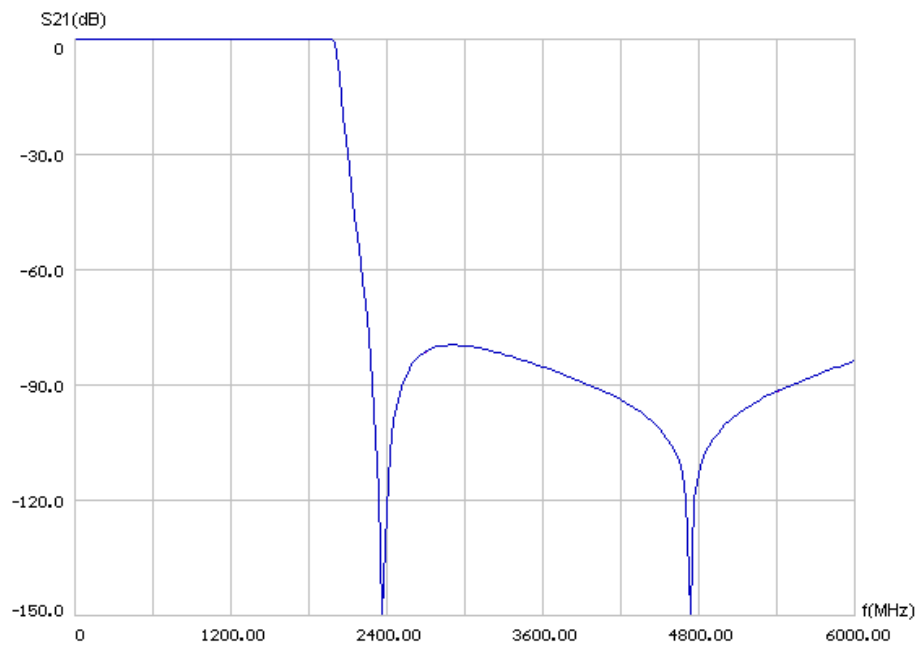


Figure 4.39: S21 graph of **Trial 13**

4.2.14 Lowpass Filter Trial 14

This trial is similar to the previous one; the difference is that f_q is shifted to 5000 MHz.

Type	Distributed, Lowpass, Equiripple, Type B
Ripple(dB)	0.1
Corner Frequency(MHz)	2000
Quarter Wave Frequency(MHz)	5000
Order	13
Transmission Zeros with order of Extraction (MHz)	UE, 2370, 2xUE, 2370, 2xUE, 2370, UE, INF

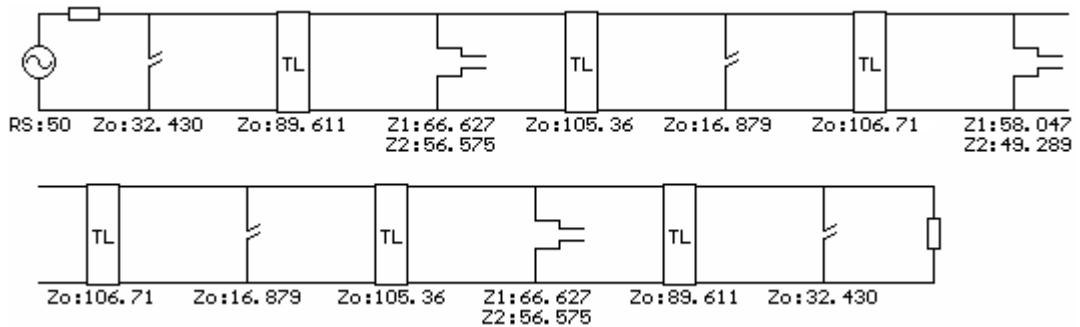


Figure 4.40: Elements of **Trial 14**

The increase in f_q resulted in a decrease in stub impedances. Stopband attenuation is min 80 dB (Figure 4.41).

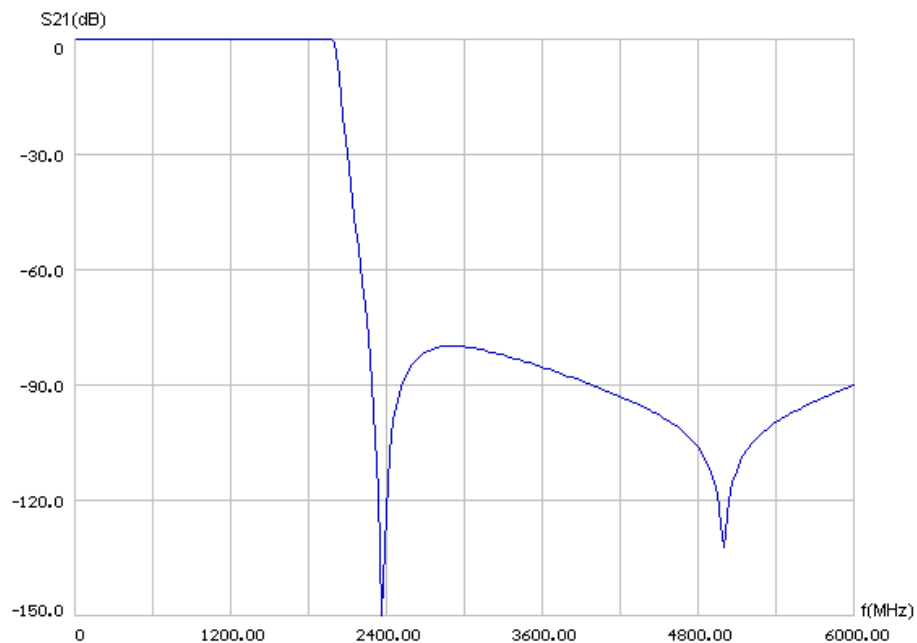


Figure 4.41: S21 graph of **Trial 14**

4.2.15 Lowpass Filter Trial 15

Compared to the previous filter the FTZs are decreased to 2270 MHz from 2370 MHz just to see the variations on element values.

Type	Distributed, Lowpass, Equiripple, Type B
Ripple(dB)	0.1
Corner Frequency(MHz)	2000
Quarter Wave Frequency(MHz)	5000
Order	13
Transmission Zeros with order of Extraction (MHz)	UE, 2270, 2xUE, 2270, 2xUE, 2270, UE, INF

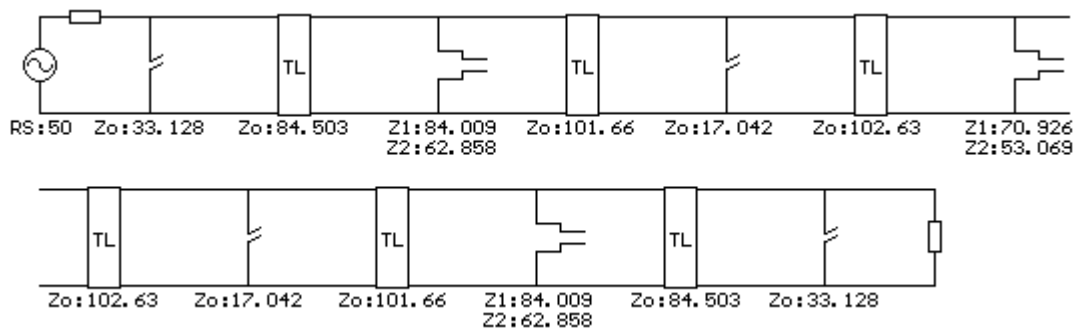


Figure 4.42: Elements of **Trial 15**

Change in impedances is not noteworthy (Figure 4.42). Stopband attenuation is min 70 dB (Figure 4.43).

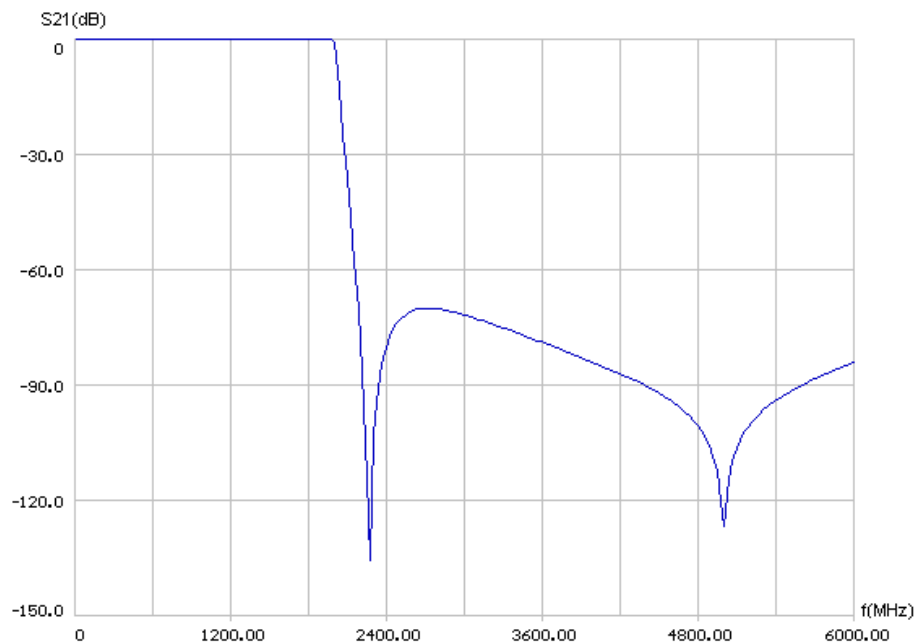


Figure 4.43: S21 graph of **Trial 15**

4.2.16 Lowpass Filter Trial 16

The effect of increasing f_q from 5000 MHz to 5500 MHz is analyzed in this trial.

Type	Distributed, Lowpass, Equiripple, Type B
Ripple(dB)	0.1
Corner Frequency(MHz)	2000
Quarter Wave Frequency(MHz)	5500
Order	13
Transmission Zeros with order of Extraction (MHz)	UE, 2270, 2xUE, 2270, 2xUE, 2270, UE, INF

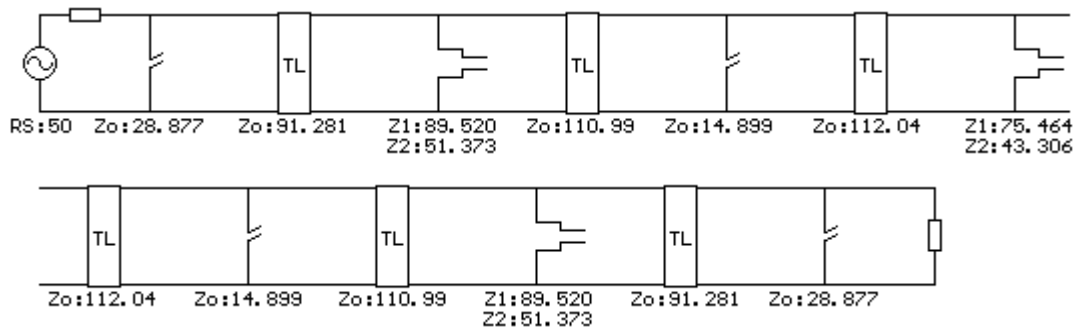


Figure 4.44: Elements of **Trial 16**

As can be seen the stub impedances decreased considerably to unrealizable levels. Stopband attenuation is min 70 dB (Figure 4.45).

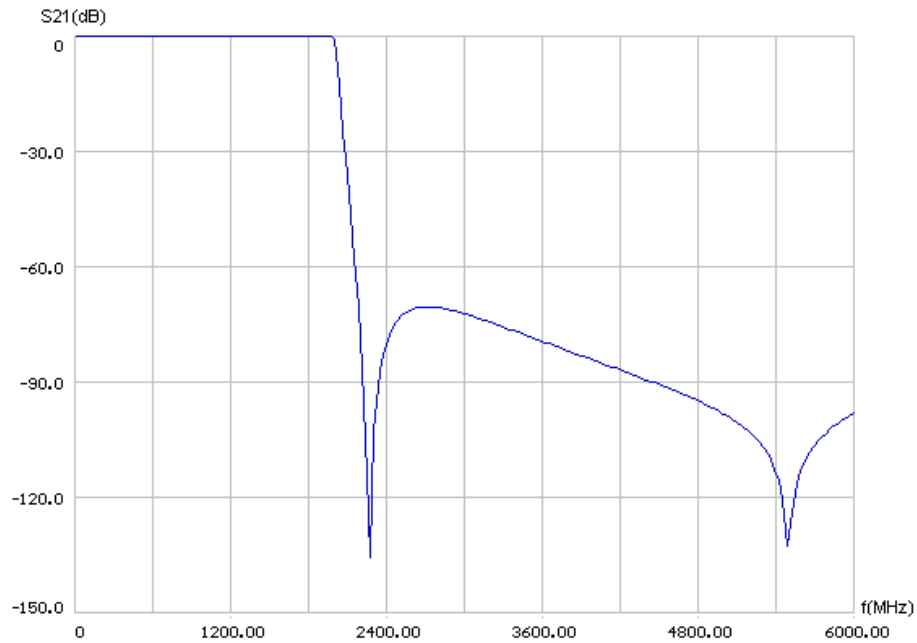


Figure 4.45: S21 graph **Trial 16**

4.2.17 Lowpass Filter Trial 17

The quarter wavelength frequency is selected at 5053 MHz which results in a 10mm quarter wavelength commensurate lines in an $\epsilon_r=2.2$ medium. Generating layout files is easier if the commensurate lines are selected rounded integer numbers.

Type	Distributed, Lowpass, Equiripple, Type B
Ripple(dB)	0.1
Corner Frequency(MHz)	2000
Quarter Wave Frequency(MHz)	5053
Order	13
Transmission Zeros with order of Extraction (MHz)	UE, 2310, 2xUE, 2310, 2xUE, 2310, UE, INF

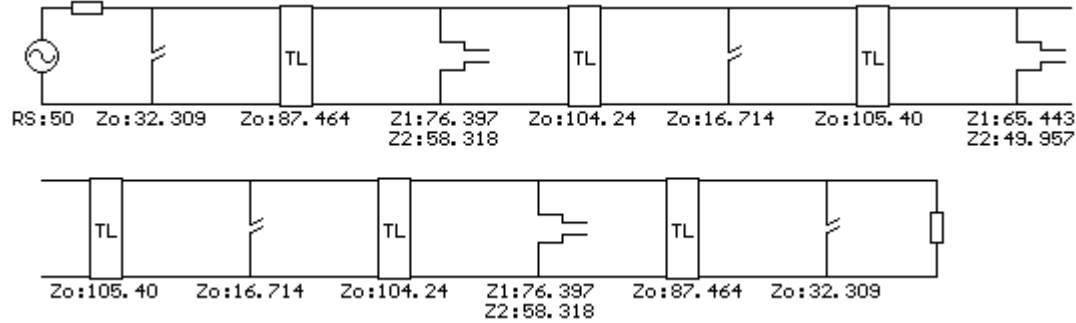


Figure 4.46: Elements of **Trial 17**

Other than the OC shunt stubs that are 16.714 Ω , the element values are proper.

Stopband attenuation is min 74 dB (Figure 4.47).

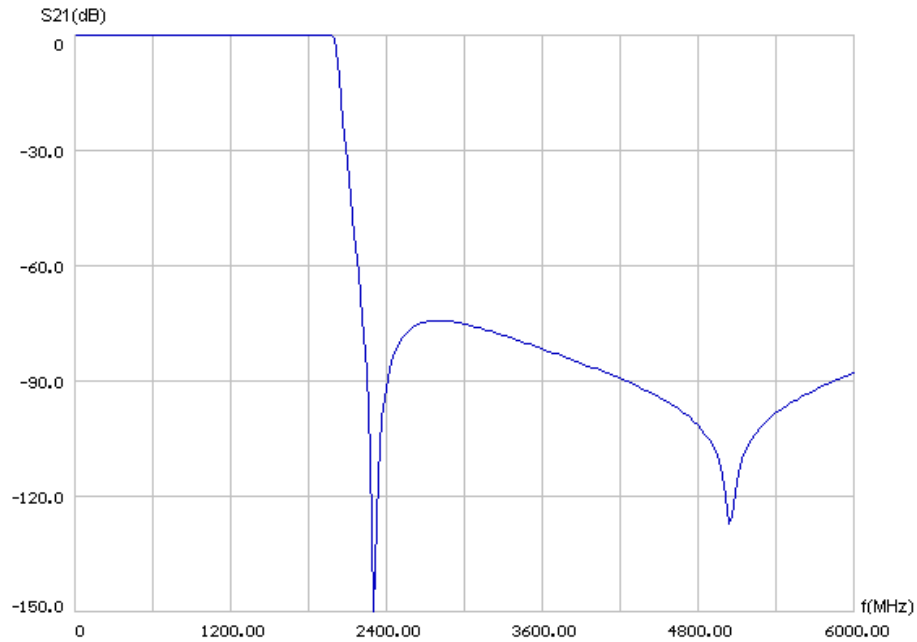


Figure 4.47: S21 graph of **Trial 17**

4.2.18 Lowpass Filter Trial 18

This filter is very similar to the previous filter; FTZs are selected at 2250 MHz instead of 2310 MHz, to see the change in element values.

Type	Distributed, Lowpass, Equiripple, Type B
Ripple(dB)	0.1
Corner Frequency(MHz)	2000
Quarter Wave Frequency(MHz)	5053
Order	13
Transmission Zeros with order of Extraction (MHz)	UE, 2250, 2xUE, 2250, 2xUE, 2250, UE, INF

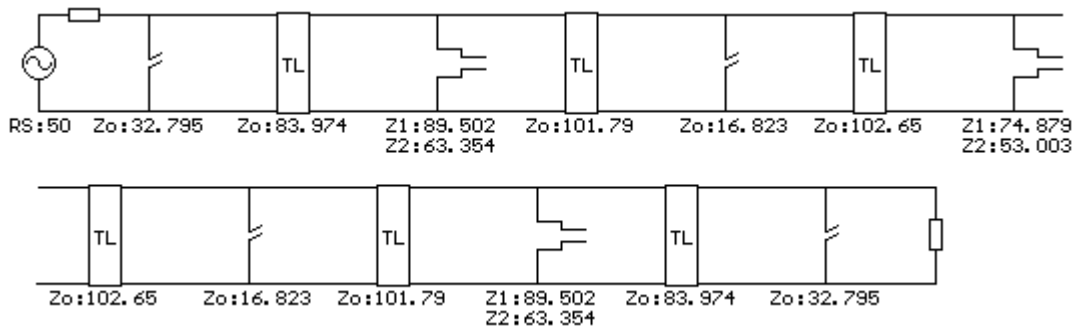


Figure 4.48: Elements of **Trial 18**

Naturally the element values are nearly the same with the previous trial. Stopband attenuation is min 68 dB (Figure 4.49).

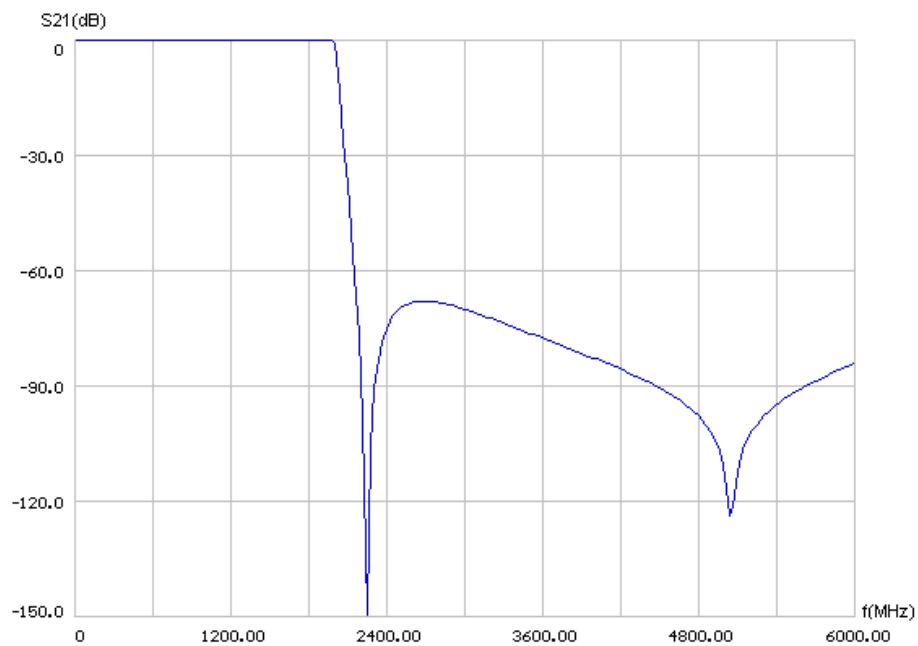


Figure 4.49: S21 graph **Trial 18**

4.2.19 Lowpass Filter Trial 19

FTZs are moved to 2370 MHz to adjust the TL impedances.

Type	Distributed, Lowpass, Equiripple, Type B
Ripple(dB)	0.1
Corner Frequency(MHz)	2000
Quarter Wave Frequency(MHz)	5053
Order	13
Transmission Zeros with order of Extraction (MHz)	UE, 2370, 2xUE, 2370, 2xUE, 2370, UE, INF

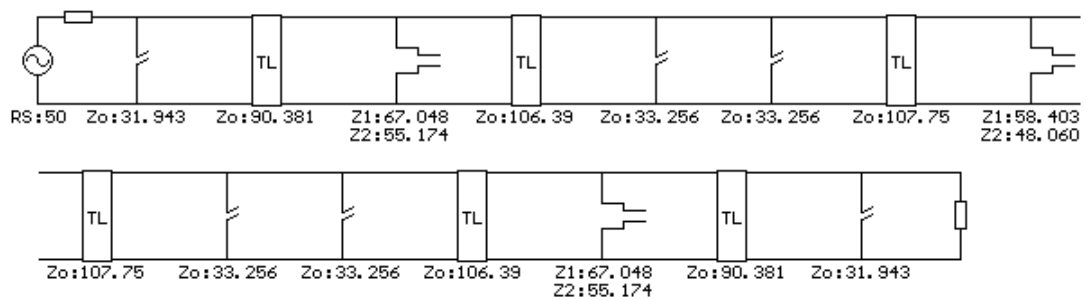


Figure 4.50: Elements of **Trial 19** with the inner shunt stubs divided into two equal parts.

The inner small valued OC shunt stubs are separated into two equal pieces of 33.256Ω (Figure 4.50). These stubs are the only problematic elements in this filter.

Stopband attenuation is min 80 dB (Figure 4.51). Due to increased frequency of FTZs (2370 MHz), the skirt slope is relatively low.

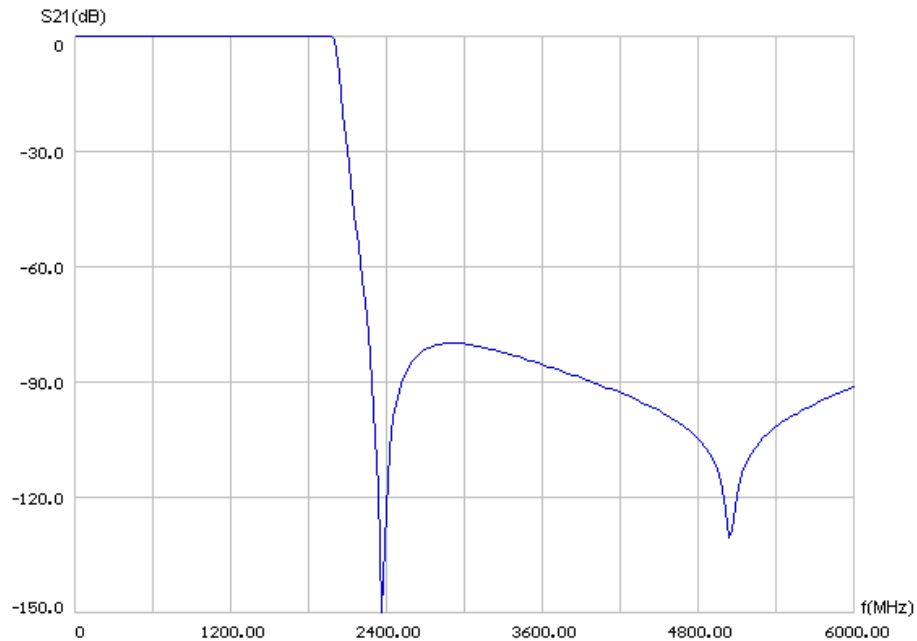


Figure 4.51: S21 graph **Trial 19**

4.2.20 Lowpass Filter Trial 20

f_q is decreased to see the effect on element values.

Type	Distributed, Lowpass, Equiripple, Type B
Ripple(dB)	0.1
Corner Frequency(MHz)	2000
Quarter Wave Frequency(MHz)	4930
Order	13
Transmission Zeros with order of Extraction (MHz)	UE, 2370, 2xUE, 2370, 2xUE, 2370, UE, INF

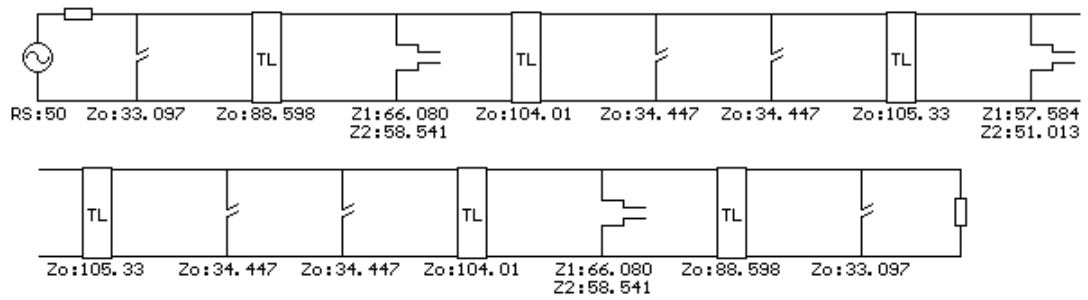


Figure 4.52: Elements of **Trial 20**

There is slight improvement in element values compared to the previous trial. Stopband attenuation is min 80 dB (Figure 4.53).

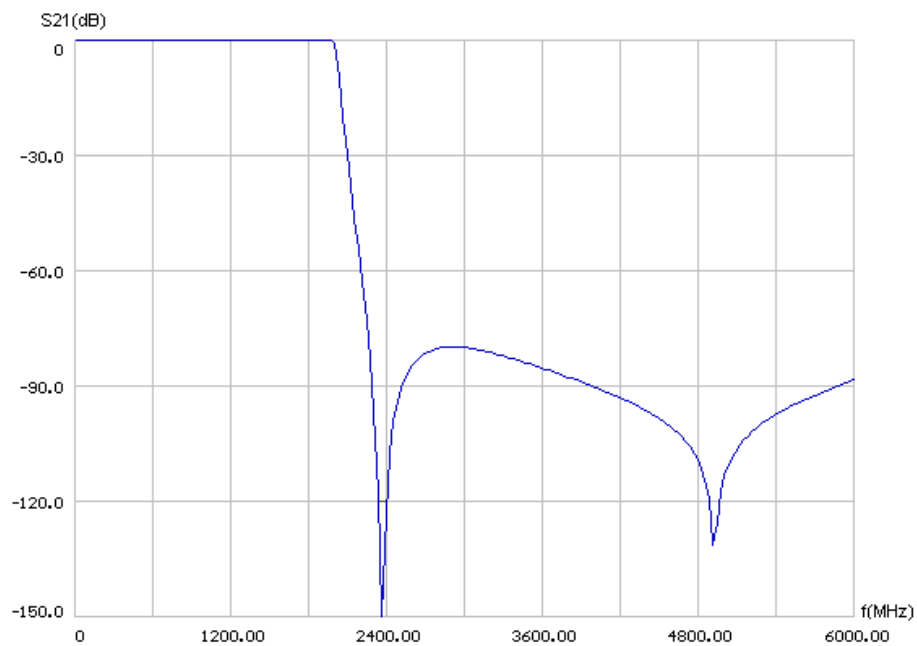


Figure 4.53: S21 graph **Trial 20**

4.2.21 Lowpass Filter Trial 21

f_q is further decreased to 4740 MHz, twice the FTZ frequency, to equate the step resonator impedances.

Type	Distributed, Lowpass, Equiripple, Type B
Ripple(dB)	0.1
Corner Frequency(MHz)	2000
Quarter Wave Frequency(MHz)	4740
Order	13
Transmission Zeros with order of Extraction (MHz)	UE, 2370, 2xUE, 2370, 2xUE, 2370, UE, INF

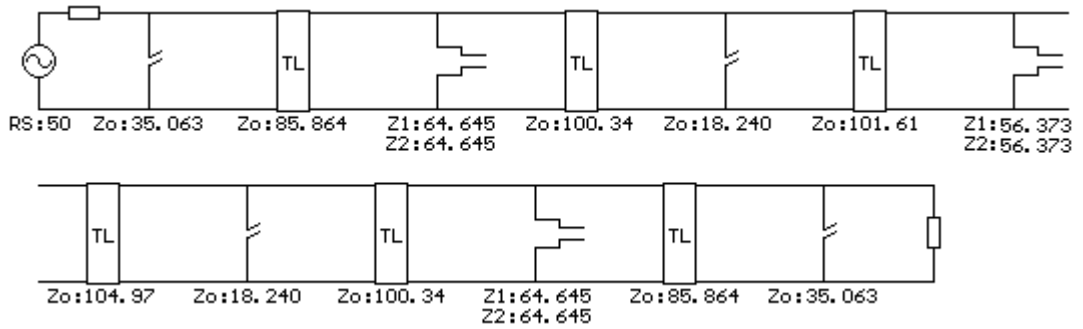


Figure 4.54: Elements of **Trial 21**

Selecting f_q at twice the frequency of FTZs, better element values have obtained compared to the previous filter. The 18.240Ω stub impedance is the only element that may be difficult to realize even if we split into two equal stub pieces. Stopband attenuation is min 80 dB (Figure 4.55).

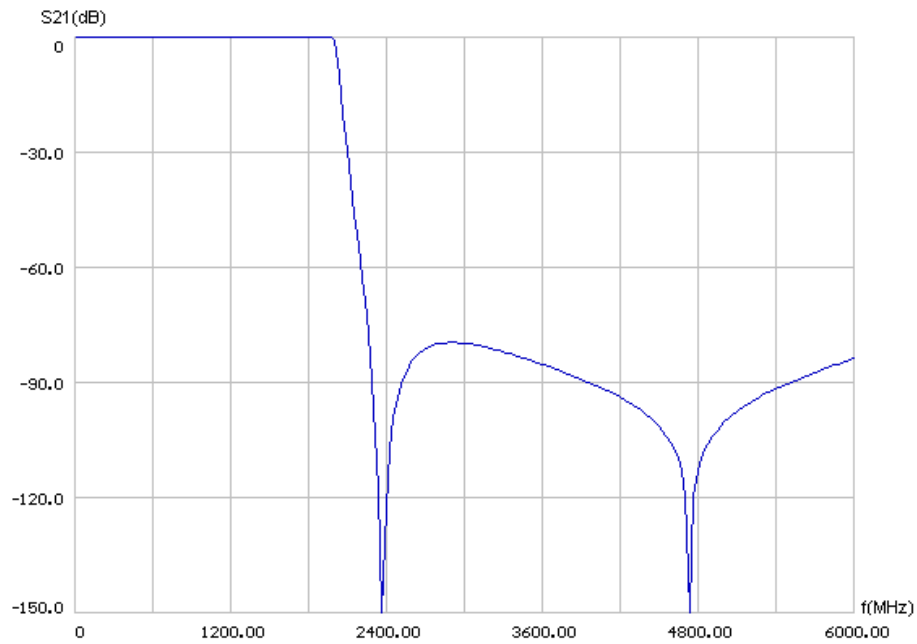


Figure 4.55: S_{21} graph **Trial 21**

4.2.22 Lowpass Filter Trial 22

In this trial FTZ's are kept at 2400 MHz and f_q is adjusted to 4800 MHz, two times the frequency of the FTZs, to obtain uniform step resonators.

Type	Distributed, Lowpass, Equiripple, Type B
Ripple(dB)	0.1
Corner Frequency(MHz)	2000
Quarter Wave Frequency(MHz)	4800
Order	13
Transmission Zeros with order of Extraction (MHz)	UE, 2400, 2xUE, 2400, 2xUE, 2400, UE, INF

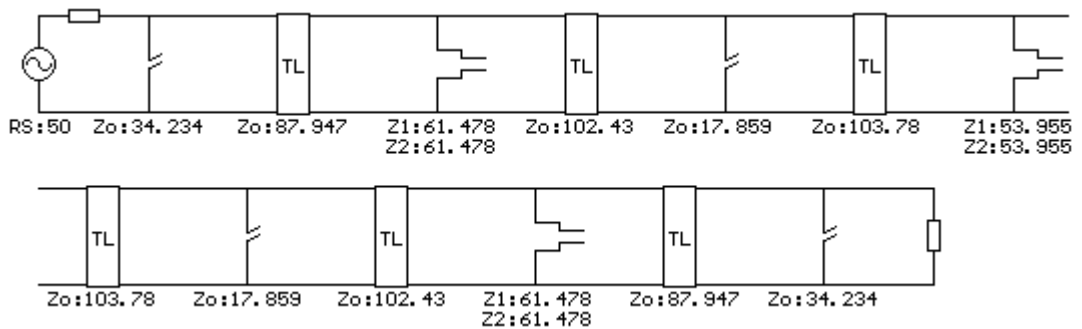


Figure 4.56: Elements of **Trial 22**

Except the middle stubs of 17.859 Ω , the other impedances are feasible. Stopband attenuation is min 82 dB (Figure 4.57).

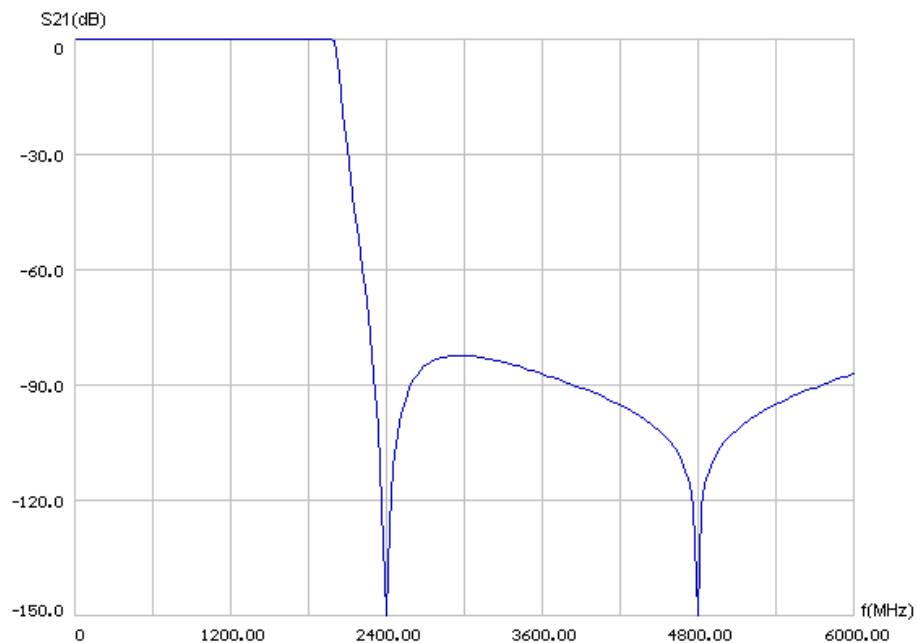


Figure 4.57: S21 graph of **Trial 22**

4.2.23 Lowpass Filter Trial 23

This is another version with stepped resonator of equal step impedances. In this trial the FTZ's are set at 2562.5 MHz and fq is twice the FTZ frequency, 5053 MHz. However, the impedances of shunt OC stubs came out to be too low.

Type	Distributed, Lowpass, Equiripple, Type B
Ripple(dB)	0.1
Corner Frequency(MHz)	2000
Quarter Wave Frequency(MHz)	5053
Order	13
Transmission Zeros with order of Extraction (MHz)	UE, 2526.5, 2xUE, 2526.5, 2xUE, 2526.5, UE, INF

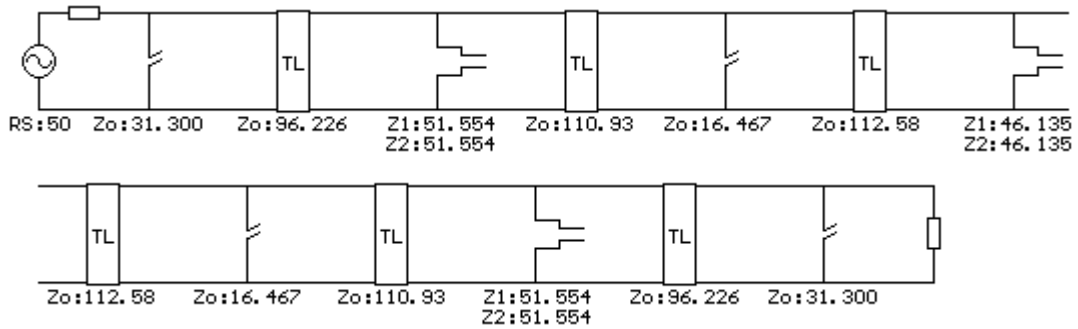


Figure 4.58: Elements of **Trial 23**

Stopband attenuation is min 82 dB (Figure 4.59).

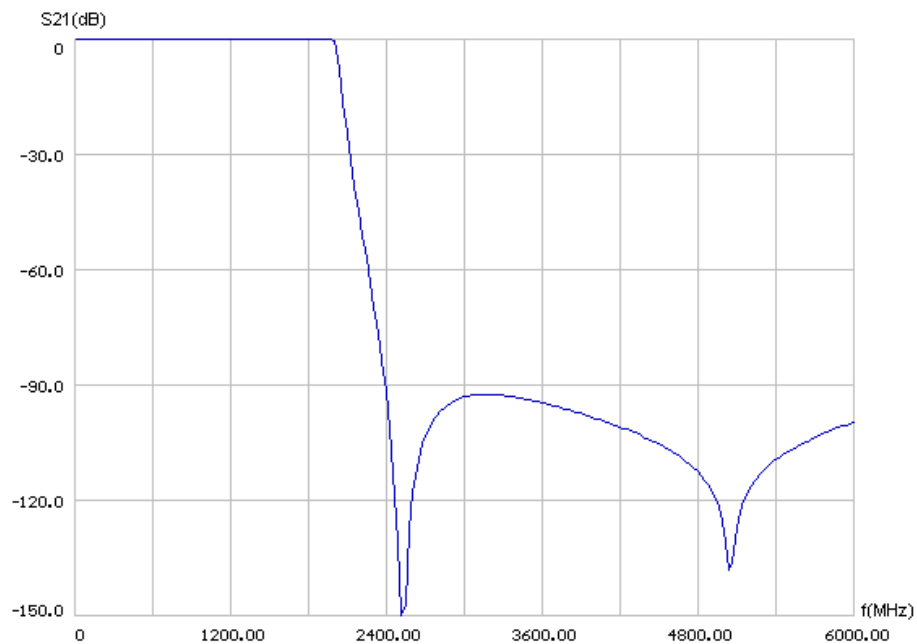


Figure 4.59: S21 graph of **Trial 23**

4.2.24 Lowpass Filter Trial 24

The passband ripple is changed to 0.07 dB from 0.1 dB to see its effect on the outermost element values.

Type	Distributed, Lowpass, Equiripple, Type B
Ripple(dB)	0.07
Corner Frequency(MHz)	2000
Quarter Wave Frequency(MHz)	5053
Order	13
Transmission Zeros with order of Extraction (MHz)	UE, 2526.5, 2xUE, 2526.5, 2xUE, 2526.5, UE, INF

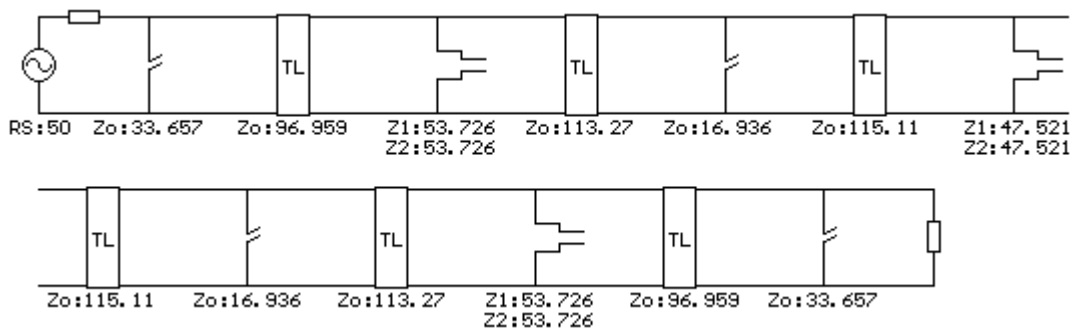


Figure 4.60: Elements of **Trial 24**

The outermost OC shunt stub impedances have increased which is desired change. Stopband attenuation is min 90 dB (Figure 4.61).

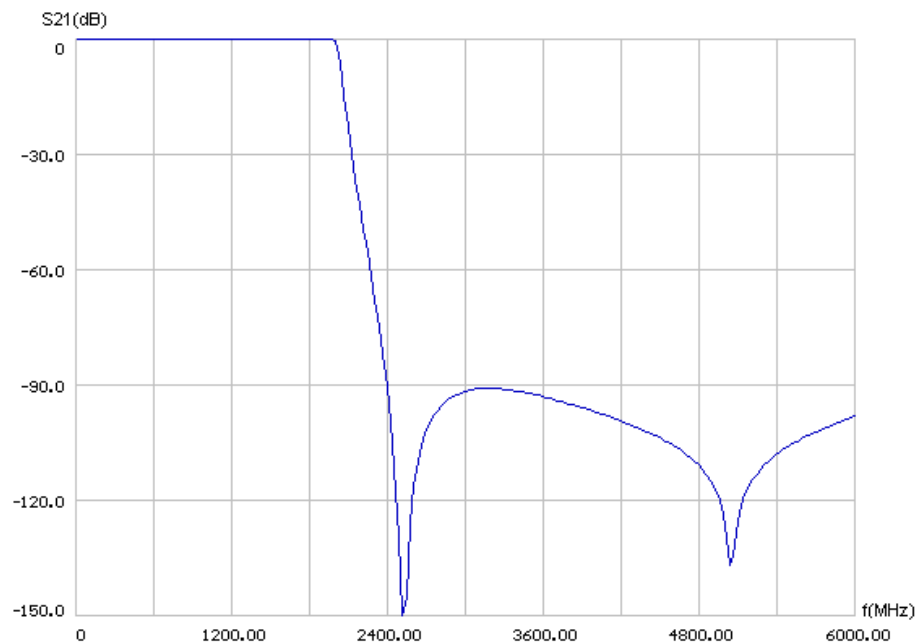


Figure 4.61: S21 graph of **Trial 24**

4.2.25 Lowpass Filter Trial 25

The f_q and FTZs are selected at lower frequencies to see their effects:

Type	Distributed, Lowpass, Equiripple, Type B
Ripple(dB)	0.07
Corner Frequency(MHz)	2000
Quarter Wave Frequency(MHz)	4740
Order	13
Transmission Zeros with order of Extraction (MHz)	UE, 2370, 2xUE, 2370, 2xUE, 2370, UE, INF

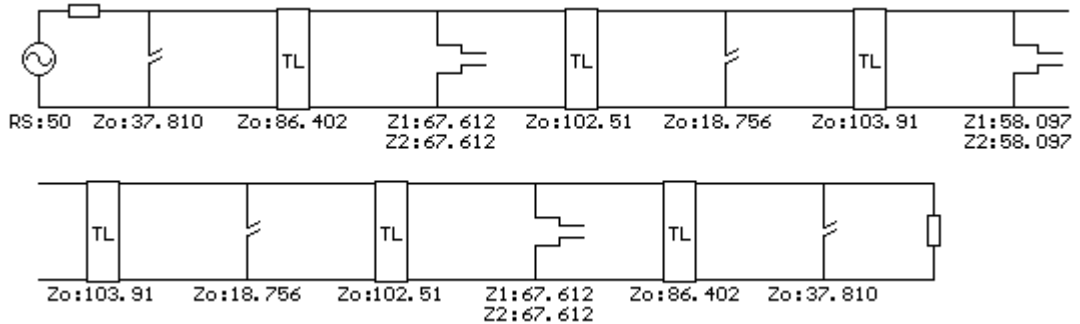


Figure 4.62: Elements of **Trial 25**

The decrease in FTZ and quarter wavelength frequencies resulted in better element values. Stopband attenuation is min 78 dB.

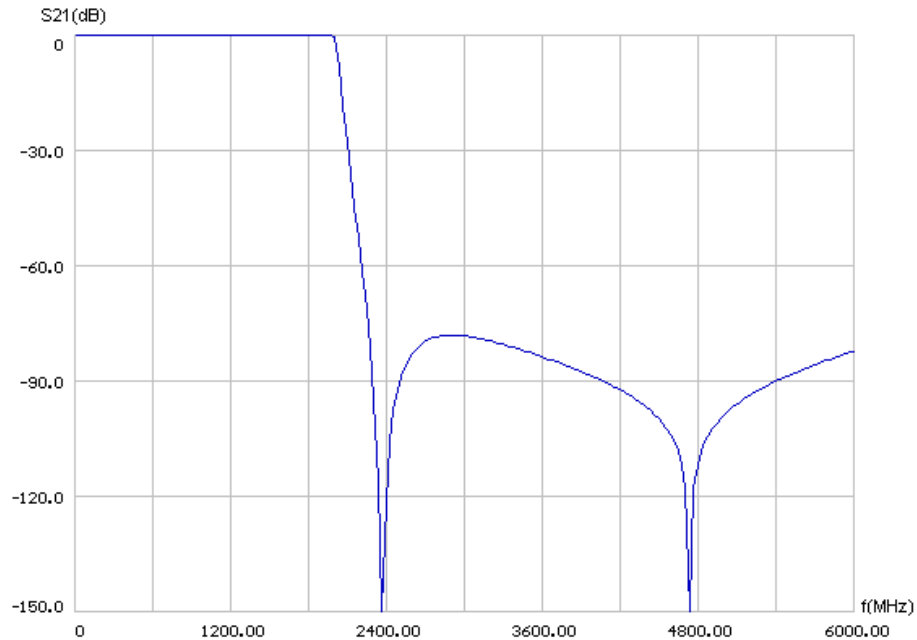


Figure 4.63: S21 graph of **Trial 25**

4.2.26 Lowpass Filter Trial 26

The passband ripple is dropped to 0.05 dB.

Type	Distributed, Lowpass, Equiripple, Type B
Ripple(dB)	0.05
Corner Frequency(MHz)	2000
Quarter Wave Frequency(MHz)	4740
Order	13
Transmission Zeros with order of Extraction (MHz)	UE, 2370, 2xUE, 2370, 2xUE, 2370, UE, INF

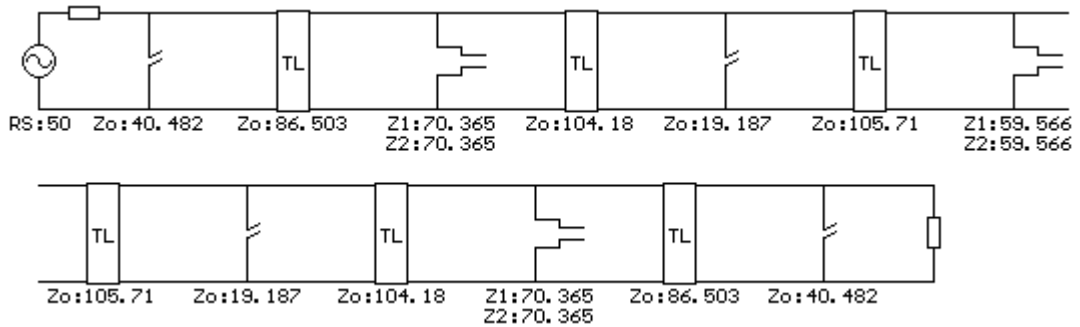


Figure 4.64: Elements of **Trial 26**

A slight decrease in ripple increased the impedance of OC shunt stubs but the TL impedances have also increased, the maximum TL impedance is 105.71 Ω . We want to decrease the ripple more in order not to increase the highest impedance level. The 105.71 Ω transmission lines can be realized by 10.2 mils width lines on a stripline whose dielectric height is 62 mils. This is the minimum width that we can realize reliably. Stopband attenuation is min 76 dB (Figure 4.65).

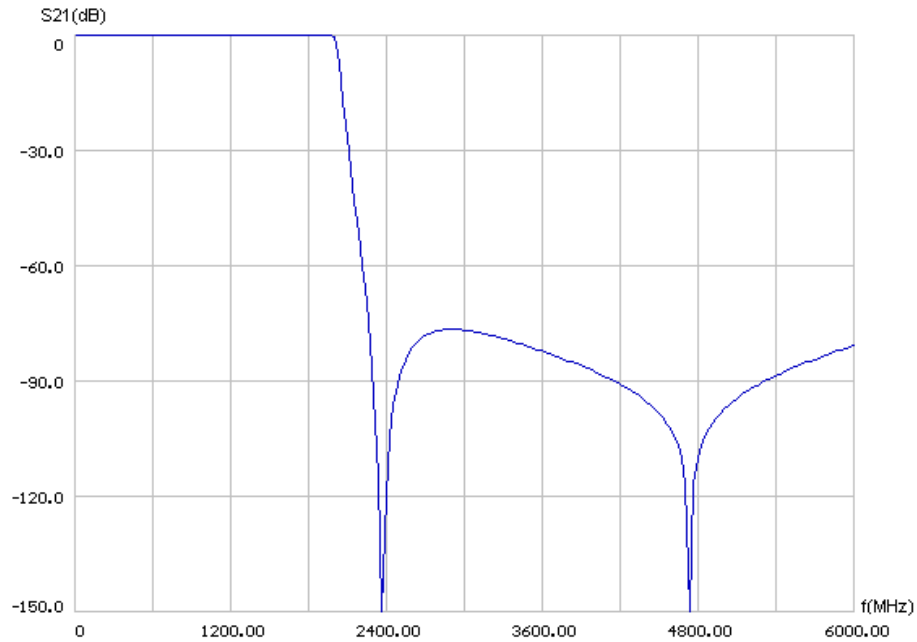


Figure 4.65: S21 graph of **Trial 26**

4.2.27 Lowpass Filter Trial 27

A very similar filter to the previous filter is as follows:

Type	Distributed, Lowpass, Equiripple, Type B
Ripple(dB)	0.05
Corner Frequency(MHz)	2000
Quarter Wave Frequency(MHz)	4684
Order	13
Transmission Zeros with order of Extraction (MHz)	UE, 2342, 2xUE, 2342, 2xUE, 2342, UE, INF

The inner open-circuited stubs are splitted into two equal pieces in order to have relatively thin stubs.

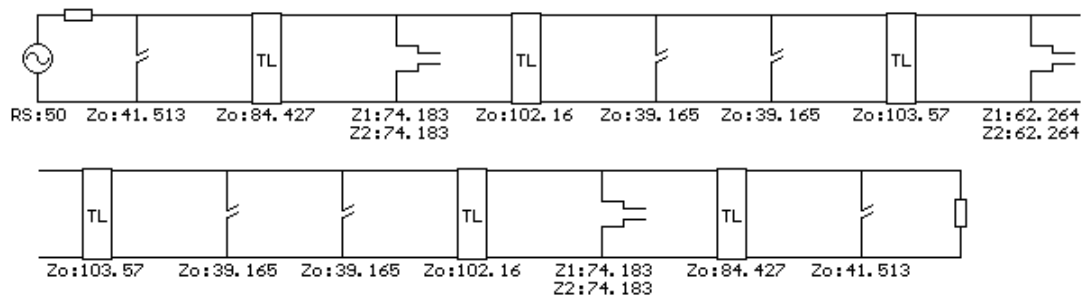


Figure 4.66: Elements of **Trial 27**

Stopband attenuation is min 74 dB (Figure 4.67).

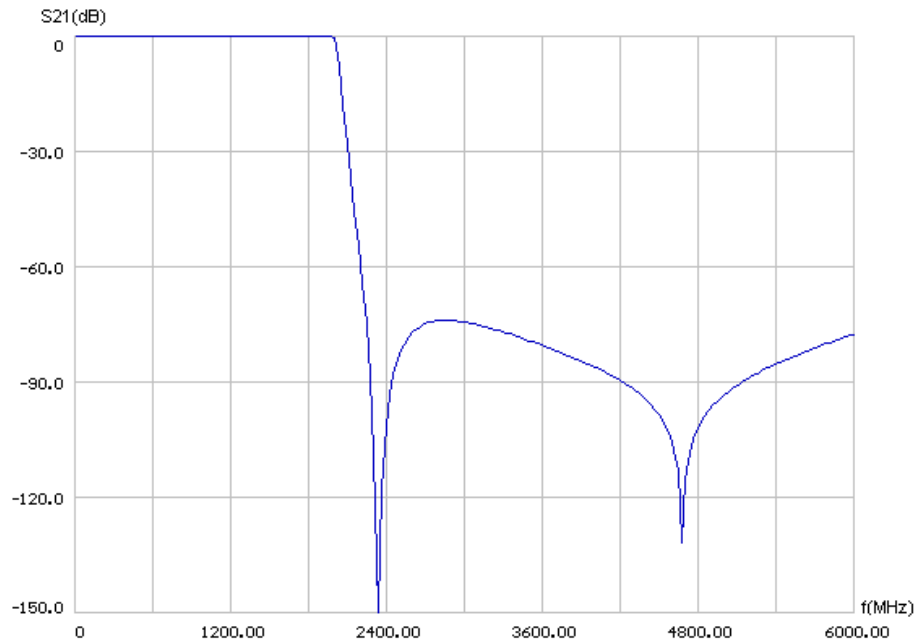


Figure 4.67: S21 graph **Trial 27**

This filter has nice element values; in the following trial, we will modify this trial in order to obtain rounded commensurate line lengths.

4.2.28 Lowpass Filter Trial 28

To have a round number for the stub lengths f_q is selected at 4736.6 MHz, at which the quarter wavelength becomes 420 mils.

Type	Distributed, Lowpass, Equiripple, Type B
Ripple(dB)	0.05
Corner Frequency(MHz)	2000
Quarter Wave Frequency(MHz)	4736.6
Order	13
Transmission Zeros with order of Extraction (MHz)	UE, 2368.3, 2xUE, 2368.3, 2xUE, 2368.3, UE, INF

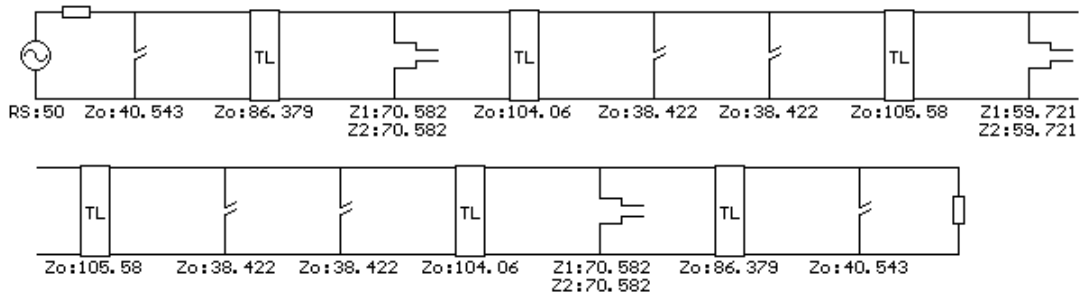


Figure 4.68: Elements of **Trial 28**

The impedance range of this filter is from 38.422 Ω to 105.58 Ω , the ratio is smaller than three which shows that element values are not too spread. Attenuation is min 76 dB (Figure 4.69).

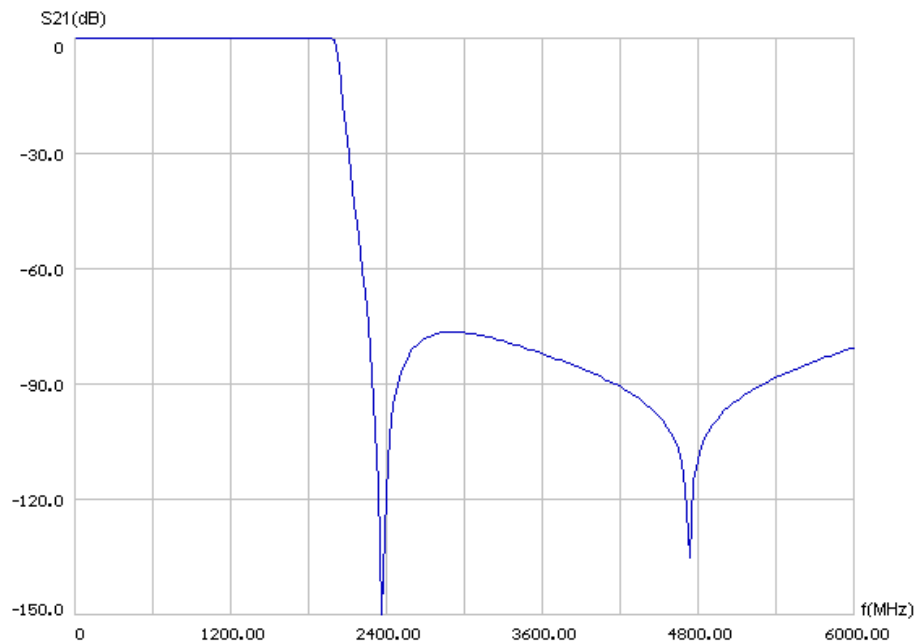


Figure 4.69: S21 graph of **Trial 28**

This filter is selected for further analysis that will be performed in the following chapter.

4.2.29 Lowpass Filter Trial 29

This is the same filter with the previous one; the difference is the outer stubs. The outer shunt open-circuited stubs of the previous filter are divided into two equal pieces to have thinner lines.

Type	Distributed, Lowpass, Equiripple, Type B
Ripple(dB)	0.05
Corner Frequency(MHz)	2000
Quarter Wave Frequency(MHz)	4736.6
Order	13
Transmission Zeros with order of Extraction (MHz)	UE, 2368.3, 2xUE, 2368.3, 2xUE, 2368.3, UE, INF

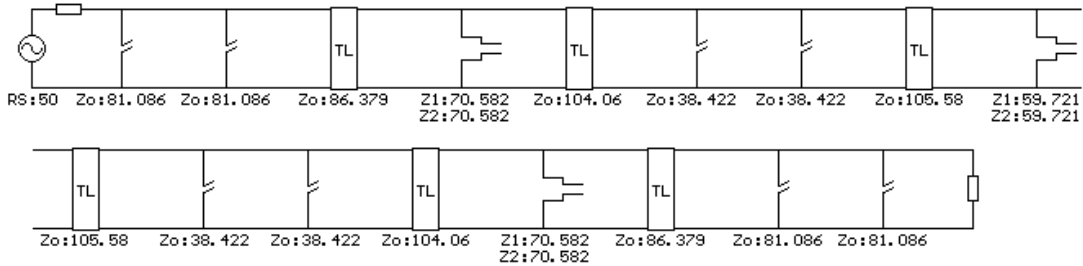


Figure 4.70: Elements of **Trial 29**

Response is same with **Trial 28** (Figure 4.69).

This filter is also selected for further analysis that will be performed in the flowing chapter.

4.3 Selected Filter Versions

In this chapter 29 filter trials are performed. Out of them, three distributed lowpass filters are selected for further analysis, optimization and electromagnetic simulations. The selected filters provide the desired responses with optimal impedances. From now on these distributed filters will be named as Selected Lowpass Filter 1, 2, 3. They are as follows:

4.3.1 Selected Lowpass Filter 1 (Trial 11)

Type	Distributed, Lowpass, Equiripple, Type B
Ripple(dB)	0.1
Corner Frequency (MHz)	2000
Quarter Wave Frequency(MHz)	4000
Order	13
Transmission Zeros with order of Extraction (MHz)	UE, 2310, 2xUE, 2310, 2xUE, 2310, UE, INF

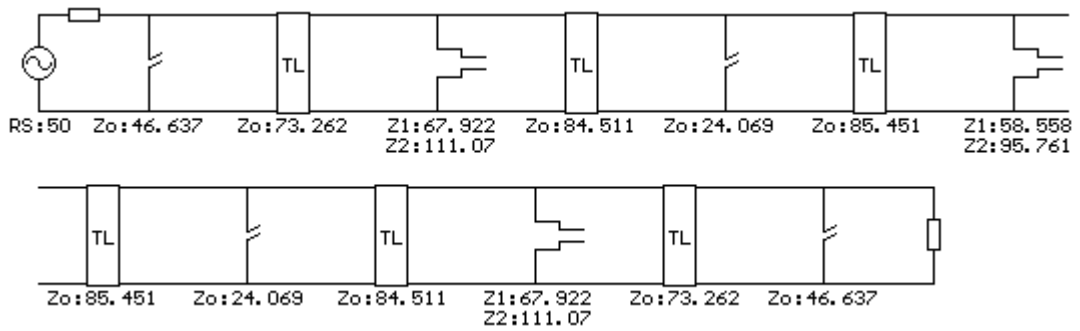


Figure 4.71: Elements of **Selected Lowpass Filter 1**

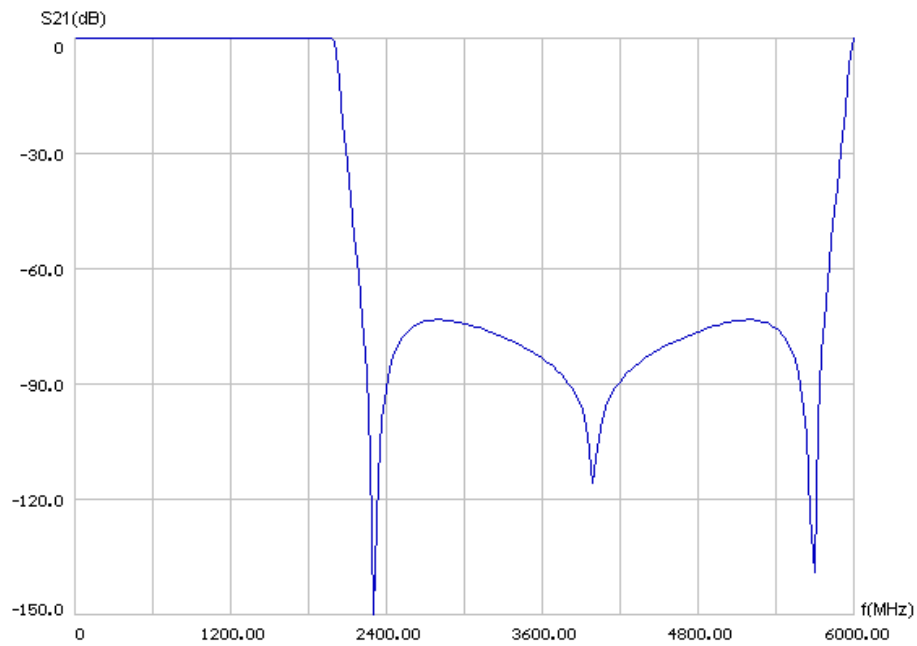


Figure 4.72: S21 response of the **Selected Lowpass Filter 1**

4.3.2 Selected Lowpass Filter 2 (Trial 28)

Type	Distributed, Lowpass, Equiripple, Type B
Ripple(dB)	0.05
Corner Frequency(MHz)	2000
Quarter Wave Frequency(MHz)	4736.6
Order	13
Transmission Zeros with order of Extraction (MHz)	UE, 2368.3, 2xUE, 2368.3, 2xUE, 2368.3, UE, INF

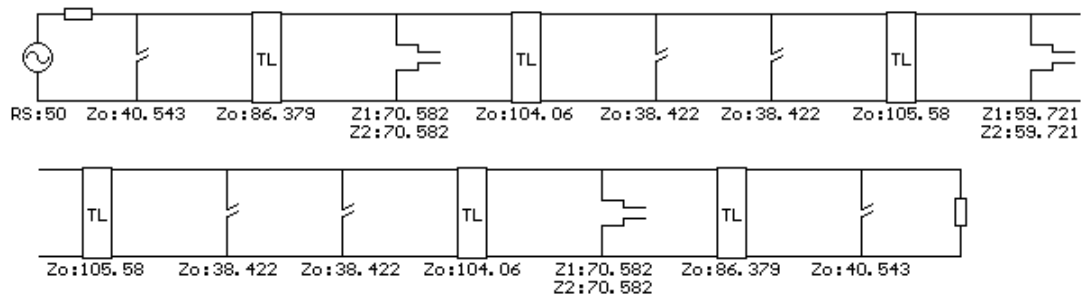


Figure 4.73: Elements of **Selected Lowpass Filter 2**

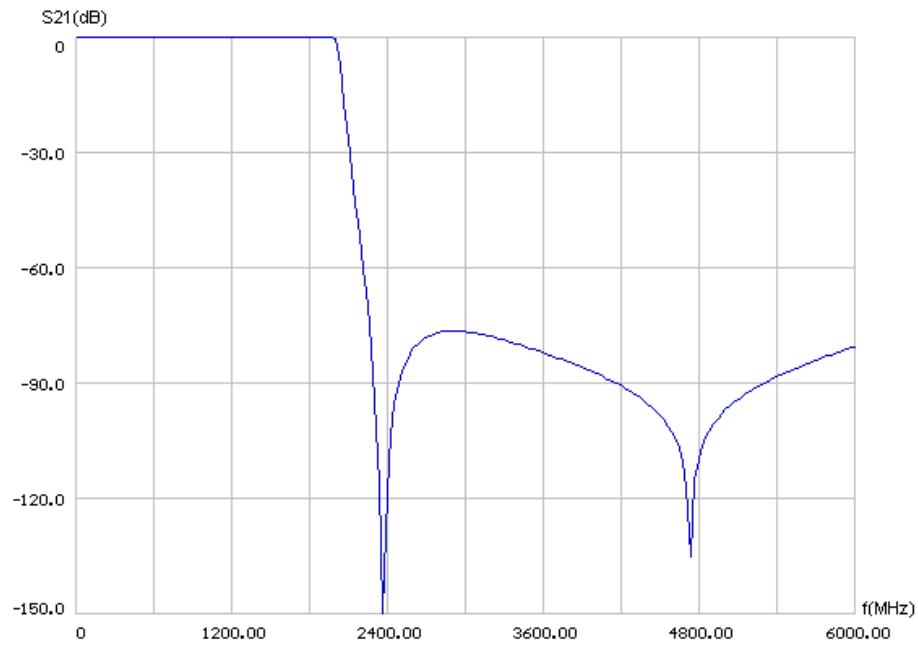


Figure 4.74: S21 graph of **Selected Lowpass Filter 2**

4.3.3 Selected Lowpass Filter 3 (Trial 29)

Type	Distributed, Lowpass, Equiripple, Type B
Ripple(dB)	0.05
Corner Frequency(MHz)	2000
Quarter Wave Frequency(MHz)	4736.6
Order	13
Transmission Zeros with order of Extraction (MHz)	UE, 2368.3, 2xUE, 2368.3, 2xUE, 2368.3, UE, INF

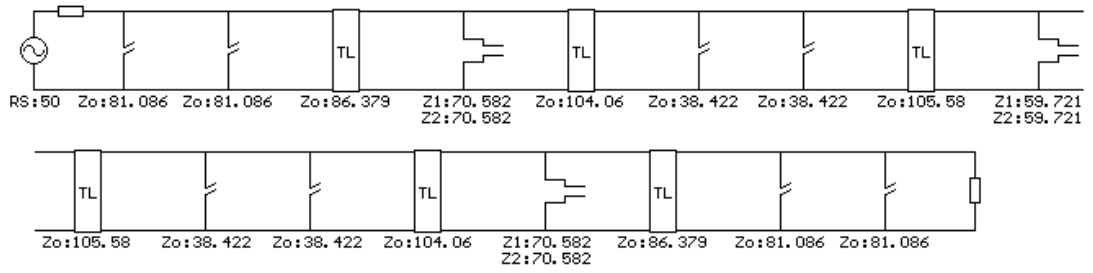


Figure 4.75: Elements of **Selected Lowpass Filter 3**

Response is same with **Selected Lowpass Filter 3**'s response (Figure 4.74).

CHAPTER 5

OPTIMIZATION, SIMULATION AND REALIZATION OF THE SELECTED FILTERS

5.1 Introduction

In the previous two chapters, different kinds of filters are synthesized and analyzed using FILPRO and some filter structures appeared to be more advantageous. These filters are selected for optimization and electromagnetic simulation.

Optimization and simulation is an important part of the recent filter design process. For the last two decades, with the availability of desktop computers, the way engineers design electrical filters has changed. Without performing any bulky calculations, we can now synthesize any type of analog filters in seconds with programs such as FILPRO. Instead of trial and error, with the help of electromagnetic simulation tools such as EAGLE, SONNET and HFSS we can now simulate the real behavior of the filters and see the responses before realizing the filter. We can tune the filters according to the simulation results and continue this process until we get the desired response. These results in reduction in time and expenditures needed to design the filter.

In order to obtain realistic simulation results some basic factors that may affect simulation results should be considered. First, the user should have a basic understanding of how the program performs the simulations. He/she should be aware of the strong and weak points of the program. The parameters of the filter

must be precisely known, and the physical structure of the filter must be properly modeled. Considering the computer sources and needs, an optimum decision should be made between accuracy and time.

Simulation programs model the filters using small elements, called meshes. Dividing the structure into lots of smaller regions (meshes) allows the system to compute the field solution separately in each element [17]. For 2D simulators meshes are surfaces, whereas for 3D simulators they may also be volumetric objects.

Meshing may be considered as an approximation, a structure that may be considered to be formed of infinite number of infinitesimal elements, but the simulation program's model is a finite approximation of the real structure. As an example a real 90 degree bend and two common modeling approximations to this structure are as shown (Figure 4.1):

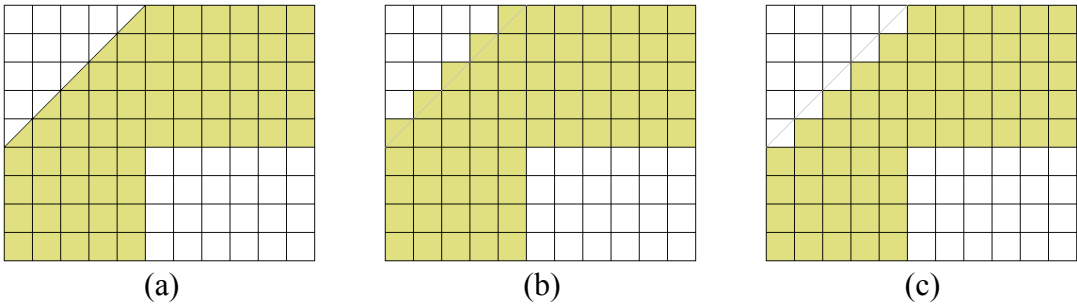


Figure 5.1: In (a) the real structure is shown, and (b) and (c) are two different approximations that can be used in simulations

The situation may be different from above. In the above picture except the slant sides, the sizes of the rectangular parts are integer multiples of the grid size, but this may not be the case in all situations as below:

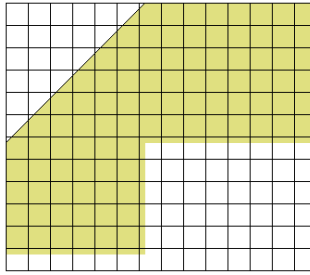


Figure 5.2: A meshing example where the grids do not fit the structure

If possible it is should be tried to adjust the grid size so that the lengths and width of the structure are integer multiples of the grid size.

The above meshes are square; it is also possible to define rectangular meshes as may be seen in Figure 4.3 if variations in one dimension are less compared to other:

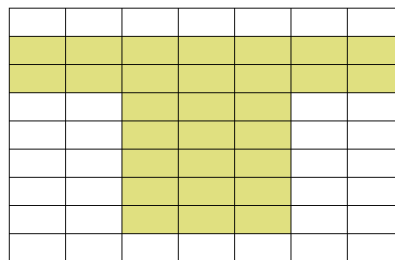


Figure 5.3: Rectangular mesh

Non-rectangular and non-uniform adaptive meshing is also possible with some simulation programs such as HFSS. In non-uniform meshing, the meshes are chosen smaller at surfaces where high density and rapidly changing fields exist, and large meshes are used for other parts so that the simulation is optimized.

As seen, due to meshing, the structure entered to the simulating program may differentiate from the real structure, especially if the structure has a complex geometry. By selecting the meshes small enough the difference between the real and simulated structure may be reduced, but this results in an increase in mesh size; which results in an increase of simulation time and required computing power.

Simulations are performed mainly on three computers:

Computer 1:

Type: HP® KAYAK Workstation
Processor: Intel® Pentium2 266 MHz
Memory: 192MB 100 MHz RAM
Disk: 2 GB IDE
Operating system: Windows® NT Workstation 4.0
Simulation Program Installed: SONNET®

Computer 2:

Type: HP® 2100 Workstation
Processor: Intel® Pentium4 1.9 GHz
Memory: 1.5 GB 400 MHz RAM
Disk: 34GB SCSI
Operating system: Windows® XP Professional
Simulation Program Installed: EAGLEWARE GENESYS®

Computer 3:

Type: HP® 2100 Workstation
Processor: Intel® Pentium4 1.7 GHz
Memory: 1.0 GB 400 MHz RAM
Disk: 34GB SCSI
Operating system: Windows® XP Professional
Simulation Program Installed: ANSOFT HFSS®

Simulation programs are mainly classified as 2D and 3D. Since most 2D simulators have some capabilities for considering the effect of simple uniform extensions in the third dimension, they may be called as 2.5D simulators.

2.5D simulators are good at simulating planar circuit layouts and microstrip/stripline like structures such as filters, dividers and couplers. The dielectric medium above and below the structure can be defined in these simulators. Outside the dielectric, vacuum and/or other dielectrics may be selected. 2.5D simulators are generally faster for the structures that they are intended to be used for.

With 3D simulators, all physical objects can be simulated and analyzed, since they do not have a limitation on any of the dimensions. Mainly, these simulators use 3D meshes. Due to the addition of the third dimension, more

computational power is needed. The simulation of 2.5D structures with 3D simulators may take longer times.

Sonnet may be considered as a 2.5 D simulator. It uses Finite Element Method (FEM) to simulate the structures [3]. This is a simple and an effective method.

Empower electromagnetic simulator of GENESYS is also a 2.5D simulator. It uses a rather different method called the “Method of Lines”. It is claimed to have good error convergence property and allows code optimization to decrease complexity and so simulation time [2].

Ansoft HSSS uses 3D Finite Element Method (FEM). In Ansoft HFSS, the geometric structures are divided into large numbers of tetrahedrons, where a single tetrahedron is a four-sided pyramid [17]. HFSS is used only for one of the selected distributed filters to compare the consistency of this program with GENESYS and SONNET.

The electromagnetically simulated filters are prototyped using milling technique. A machine having a drill that can be positioned with high precision is used to cut out unwanted copper parts of the substrate. Compared to etching this technique is faster.

5.2 Lumped Highpass Filter

In Chapter 3, sixteen highpass lumped filter trials are performed. The last one of these trials is selected to be used as the highpass part of the final bandpass filter. The synthesized filter is as follows:

Type	Lumped, Highpass, Equiripple, Type A
Ripple(dB)	0.1
Corner Frequency(MHz)	400
Order	11
Transmission Zeros with order of extraction (MHz)	Zero, Zero, 250, 360, 360, 320, Zero

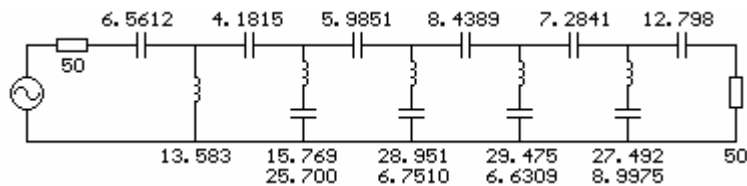


Figure 5.4: Elements of lumped highpass filter

The element values of the filter in Figure 5.4 are not standard. The elements of this filter is transformed into standard E12 values (1, 1.2, 1.5, 1.8, 2.2, 2.7, 3.3, 3.9, 4.7, 5.6, 6.8, 8.2 and ten multiples of these numbers). Since capacitors are easier to use, inductors are pulled to the closest value and the relevant capacitances are adjusted to preserve the initial response. Optimization of capacitors may also be performed keeping the inductors fixed. GENESYS software is used during these linear analysis and optimization stages. The optimized filter is as shown below (Figure 5.5):

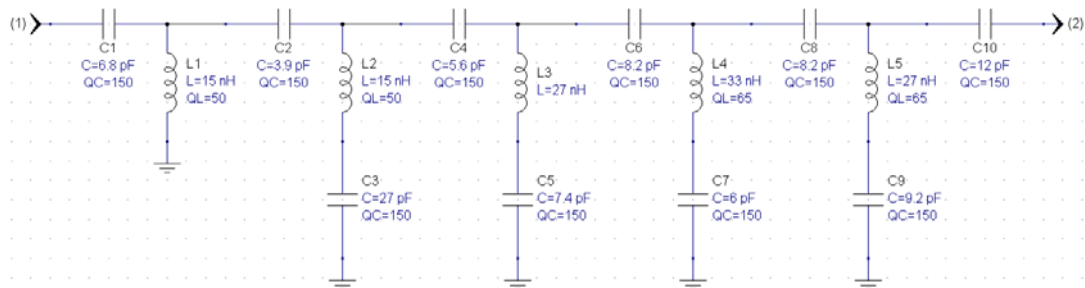


Figure 5.5: Tuned filter with E12 element values using GENESYS

During optimization stage, all element values are set to the available standard values including their losses. For inductor's, Q values are entered from manufacturer's (Coilcraft) data sheet. For capacitors a Q value of 150 is found convenient, which is the result of many previous impedance analyzer measurements.

In Figure 5.6 and 5.7 the ideal responses of the synthesized filter obtained from FILPRO are shown. In Figure 5.8 and 5.9 the optimized filter's responses are shown. It is seen that negligible shifts are observed on FTZ's and the sharp corners are rounded due to finite Q of elements.

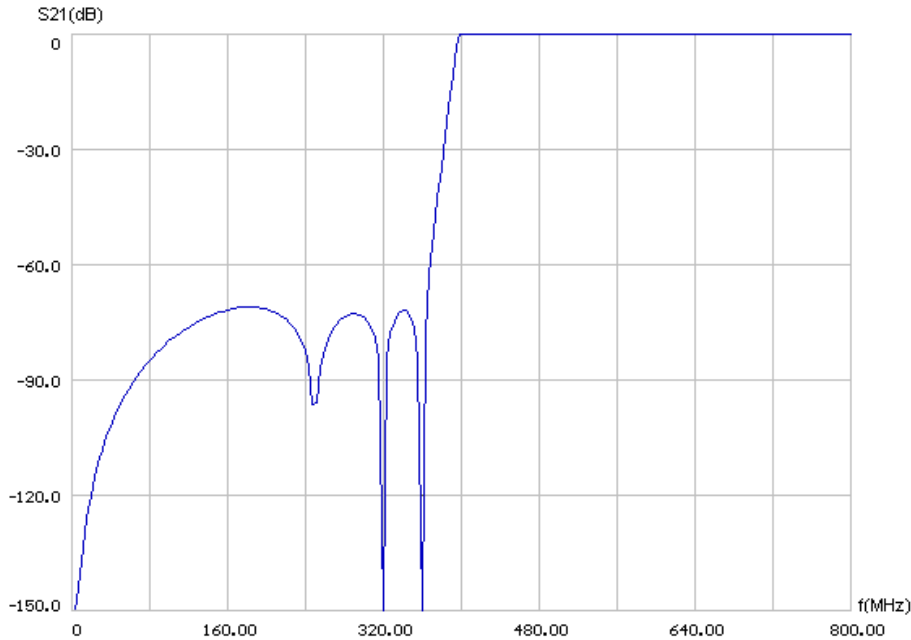


Figure 5.6: Ideal S₂₁ of the highpass filter

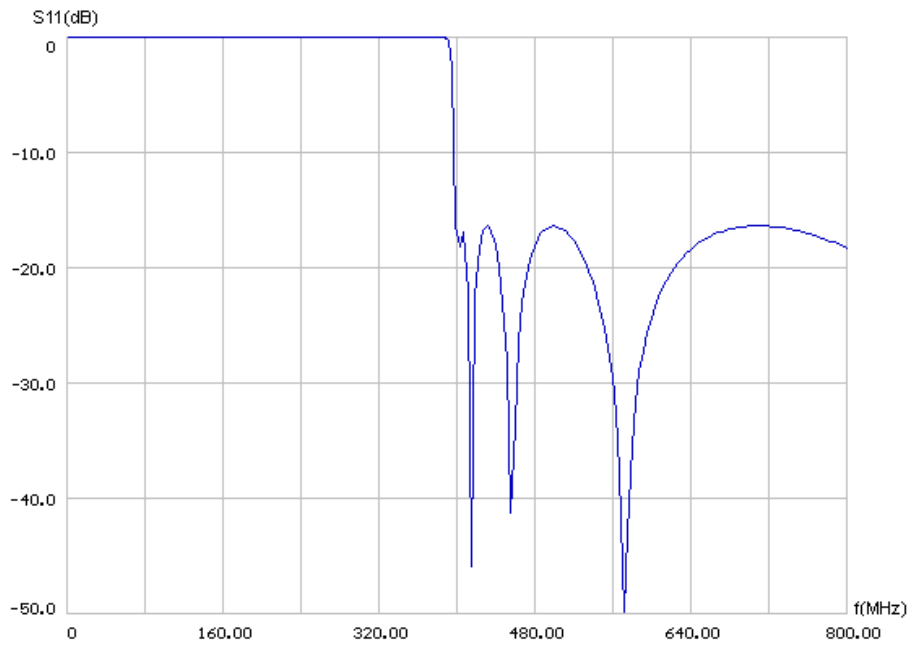


Figure 5.7: Ideal S11 of the lowpass filter

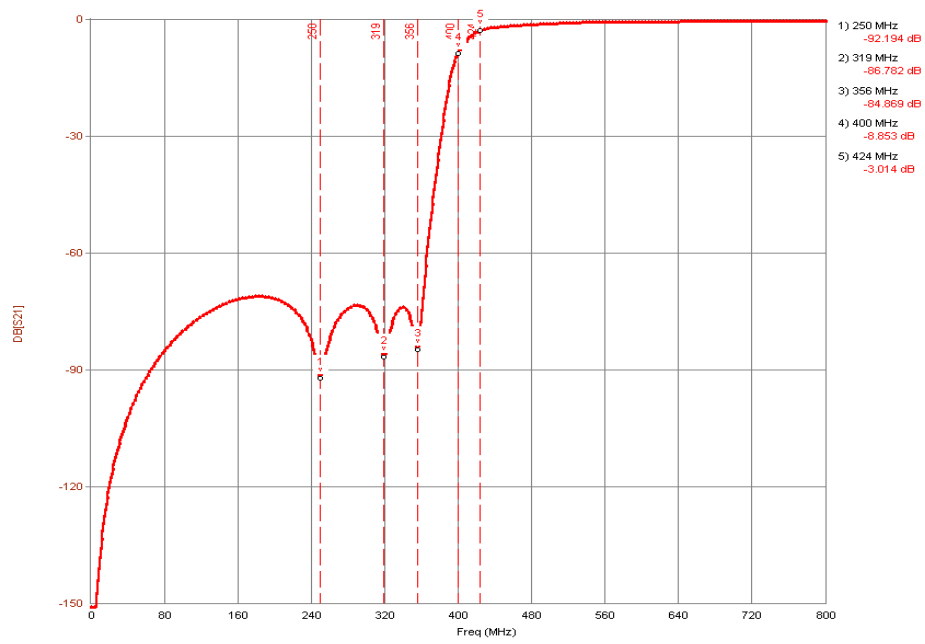


Figure 5.8: S21 response of the optimized lowpass filter

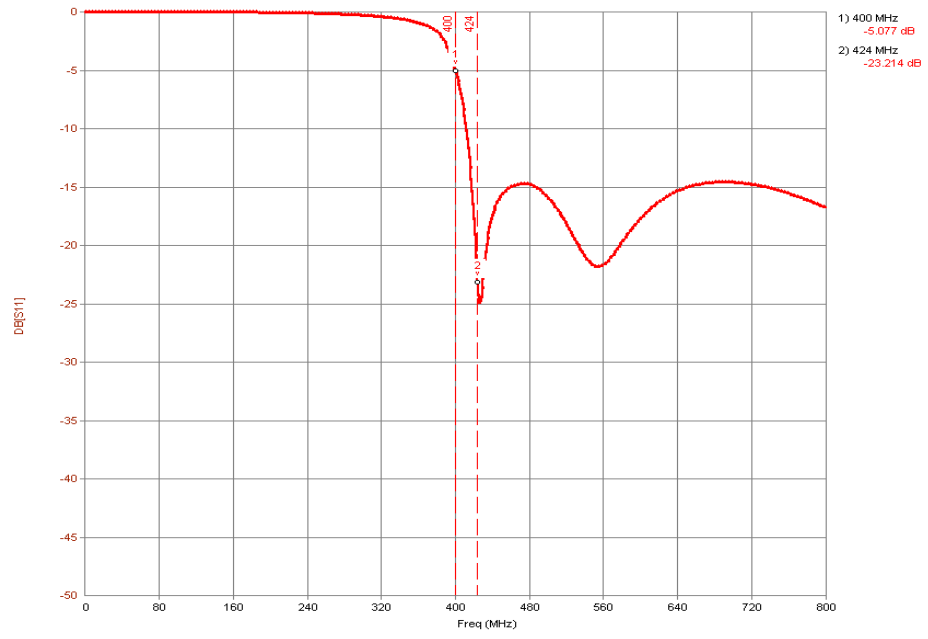


Figure 5.9: S11 response of the optimized lowpass filter

5.2.1 First Layout

Two different layouts are tried. Layouts are drawn using GENESYS. The first layout is constructed using FR4 substrate whose relative dielectric constant is around 4.5. The thickness of the dielectric is 31 mils. The pictures of top layer, bottom layer and combined versions of the first layout are shown in Figure 5.10, 5.11 and 5.12.

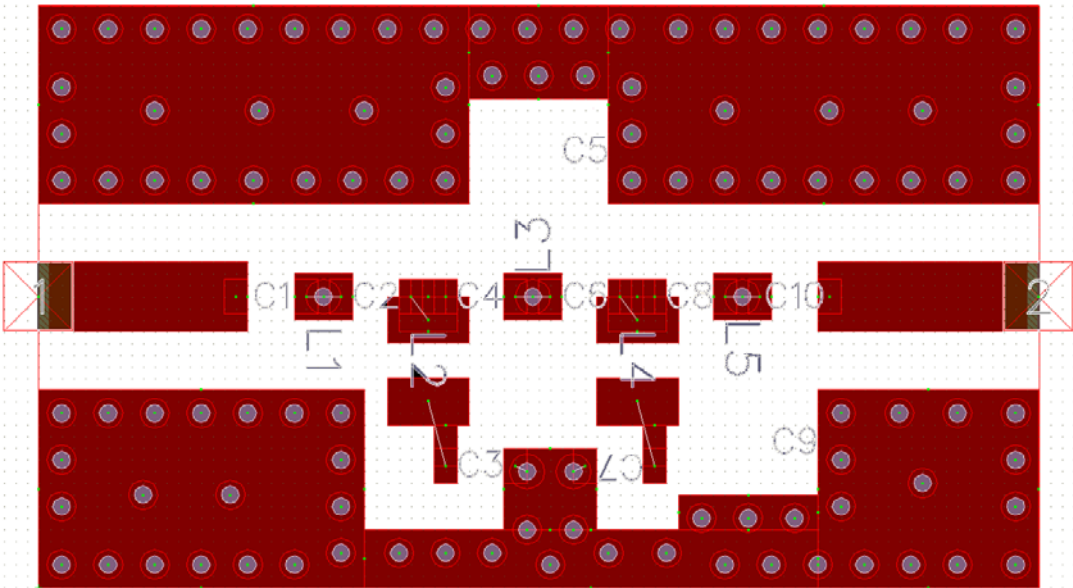


Figure 5.10: The upper side of the first lumped HP layout

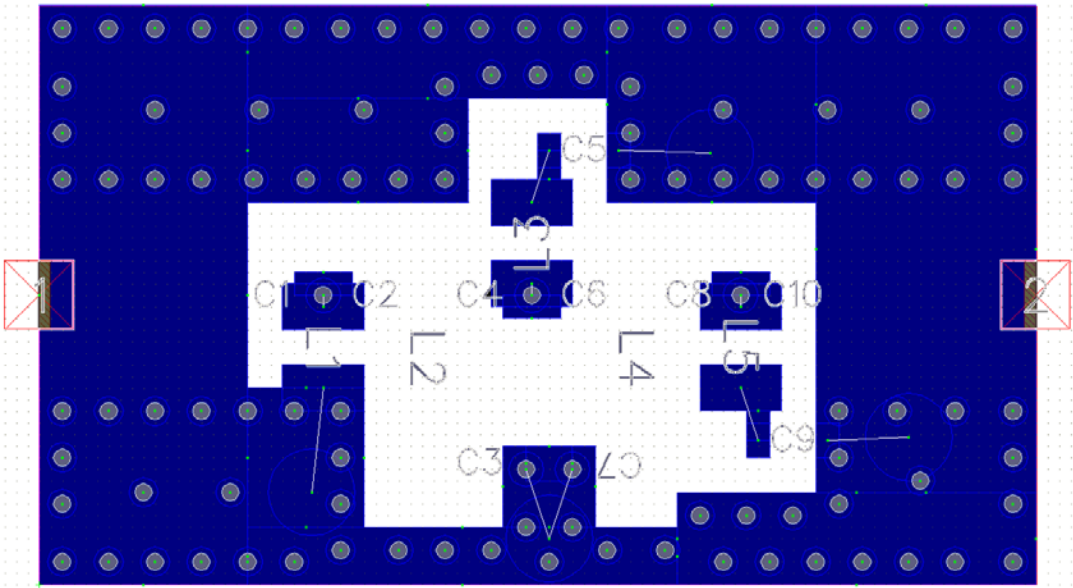


Figure 5.11: The bottom side of the first lumped HP layout

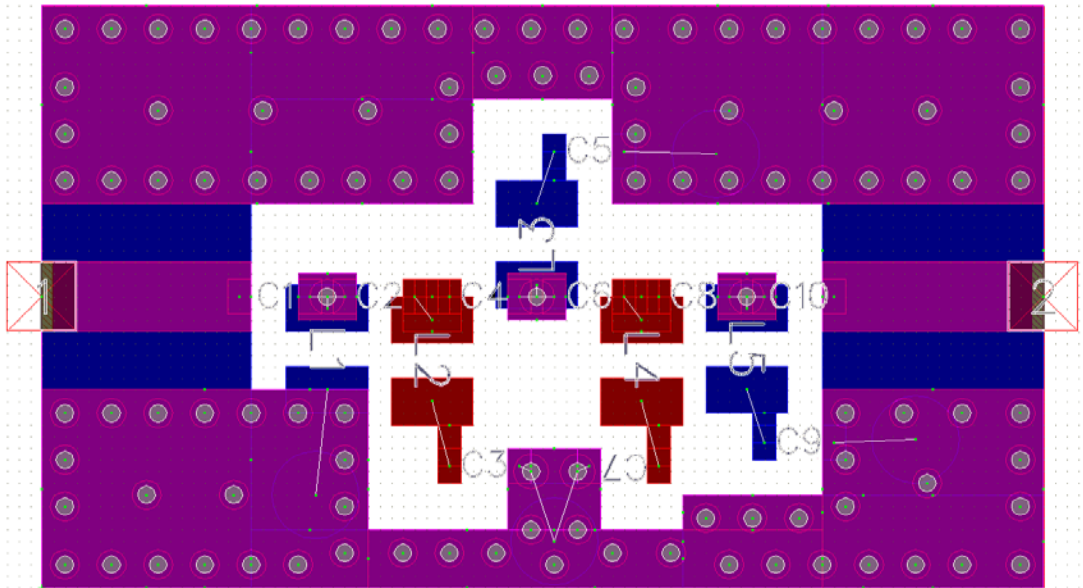


Figure 5.12: Combined view of the 0.4 GHz highpass filter

The electromagnetic simulation of this layout is performed using EMPOWER® tool of GENESYS. Electromagnetic parameters are selected as follows (Table 5.1 and Figure 5.13):

	Horizontal	Vertical
Cell Size (mil)	10	10
Box Size (mil)	860	500
# of cells	86	50

Table 5.1: Layout and grid sizes. The dimensions are in mils.

Name	Use	Slot-type	Use 1/2 Height	Type	Height or Thickness	Er	Tand/Sigma	Ur	Rho	Rough
Top Cover				Electrical						
Air Above	<input checked="" type="checkbox"/>				200					
TOP METAL [3]	<input checked="" type="checkbox"/>	<input type="checkbox"/>		Sub: Untitled 1	1.42			1	0.094	
SUBSTRATE [4]	<input checked="" type="checkbox"/>		<input type="checkbox"/>	Sub: Untitled 1	31	4.6	0.0004	1		
BOT METAL [5]	<input checked="" type="checkbox"/>	<input type="checkbox"/>		Sub: Untitled 1	1.42			1	0.094	
Air Below	<input checked="" type="checkbox"/>				200					
Bottom Cover				Sub: Default	1.42			1	0.094	

Figure 5.13: Layout parameters of the first layout

Simulation resulted in 20 hours because of inclusion of top and bottom ground planes and vias. The simulation results compared with the linear analysis is as shown in Figure 5.14 and 5.15.

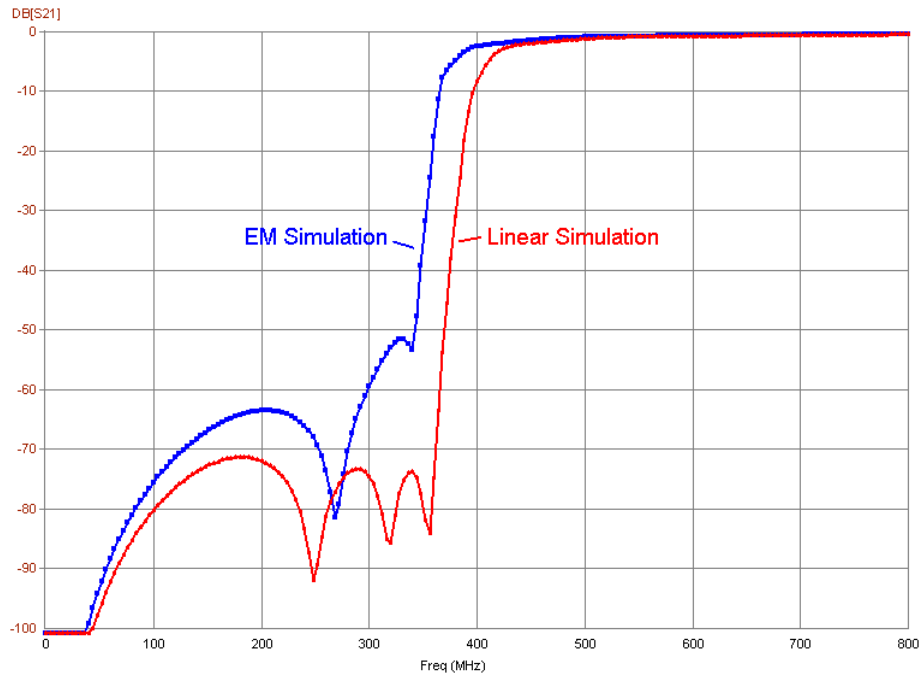


Figure 5.14: Insertion loss result of the EM simulation compared with the linear analysis

It is seen that the sharpness of skirt is decreased due to parasitic capacitances of pads to ground.

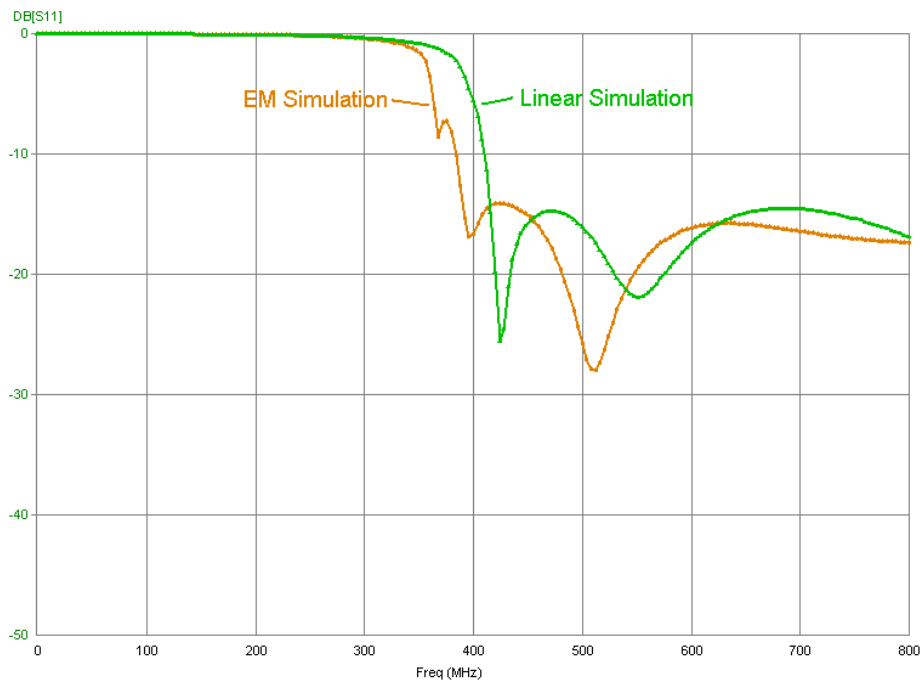


Figure 5.15: Return loss result of the EM simulation compared to linear analysis

The EM simulations are satisfactory so the first layout of the lumped highpass filter is realized. The first layout with elements and connectors mounted is shown in Figure 5.16 and 5.17.

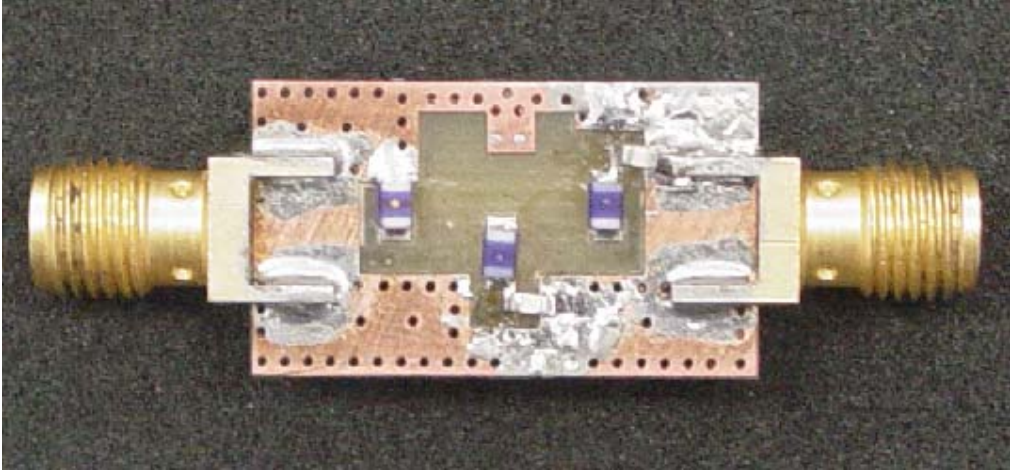


Figure 5.16: Top view of the first 400 MHz HP filter layout

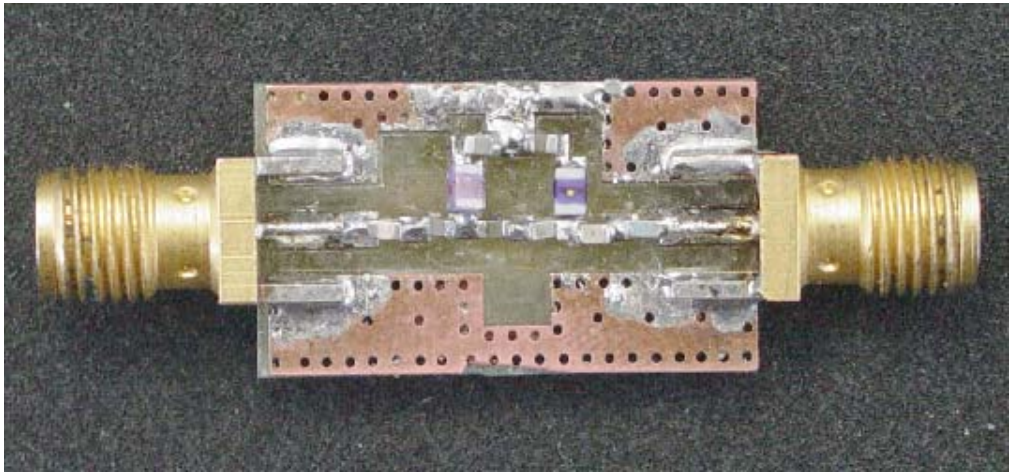


Figure 5.17: Bottom view of the first 400 MHz HP filter layout

Miniature elements are used to keep the size of the filter small. The capacitors are 0603 size (6x3 mils) and the inductors are 0805 size (8x5 mils). These elements have high series resonance frequencies and higher Qs compared to the most elements. The properties of the 0805 inductors are shown in Appendix C. Three of the inductors are located at the top surface (Figure 5.16) while the remaining two is at the bottom surface to decrease mutual coupling (Figure 5.17).

The measured responses are shown in Figure 5.18, 5.19, 5.20 and 5.21:

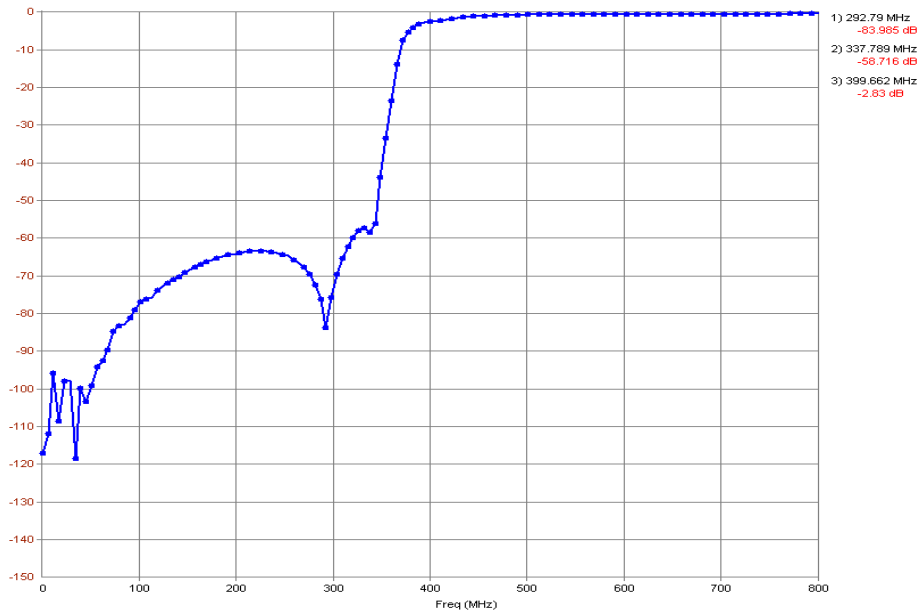


Figure 5.18: Measured S21 up to 800 MHz

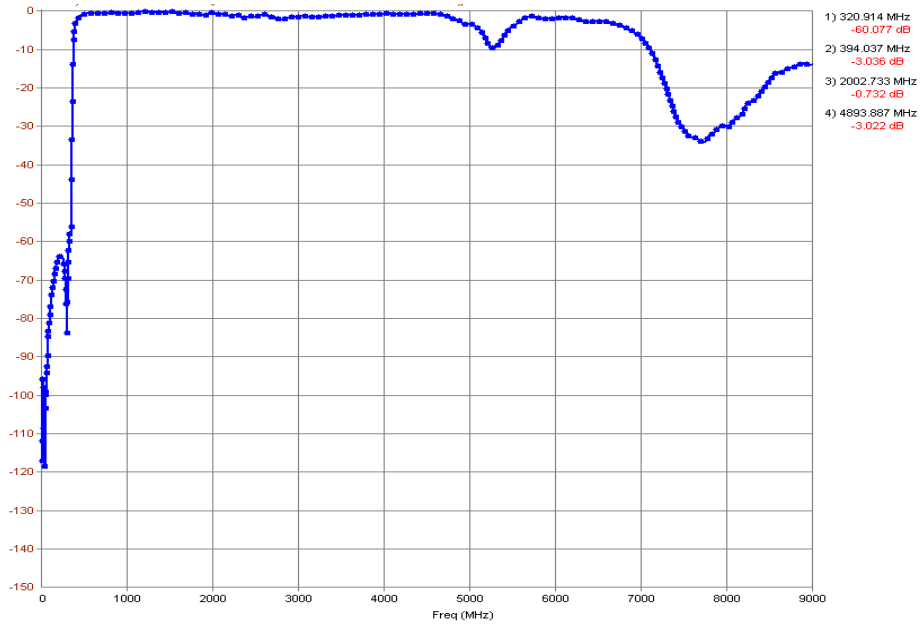


Figure 5.19: Measured S21 up to 9 GHz

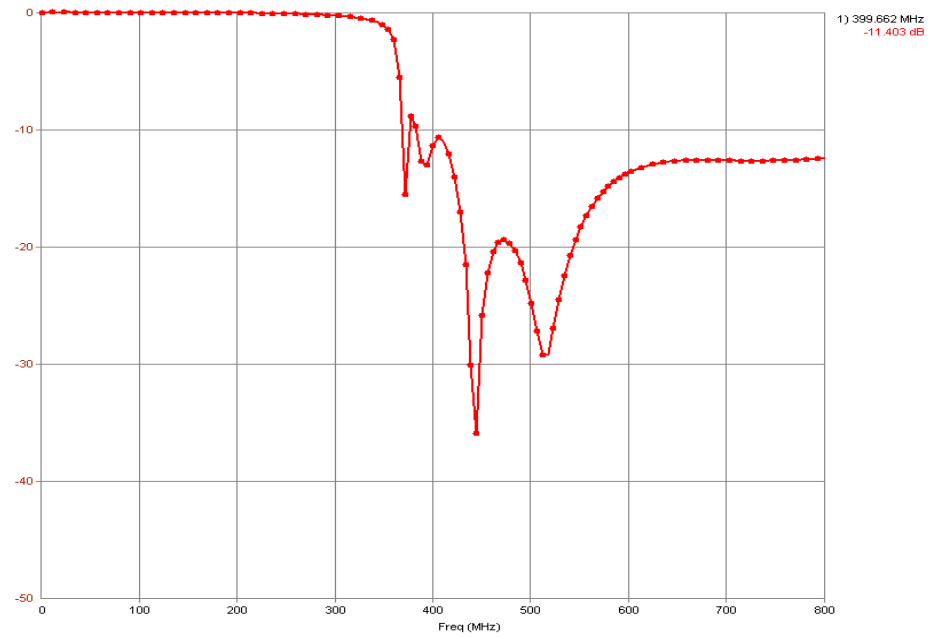


Figure 5.20: Measured S11 up to 800 MHz

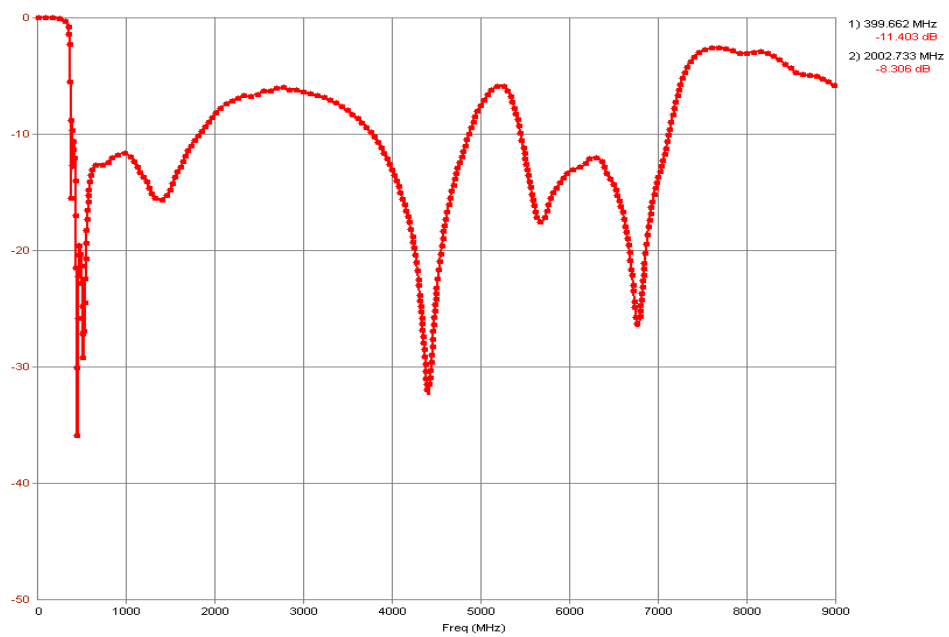


Figure 5.21: Measured S11 up to 9 GHz

The measured results are consistent with the simulations.

5.2.2 Second Layout

In order to be able combine the highpass lumped filter with the distributed lowpass filter on the same substrate, the lumped filter is also realized using the Rogers® 5880 substrate with relative dielectric constant 2.2. The thickness of the dielectric is 31 mils and the metallization thickness is 0.7 mils. Loss tangent is 0.0004. The detailed properties of the substrate are shown in Appendix B.

Name	Use	Slot-type	Type	Height or Thickness	Er	Tand/Sigma	Ur	Rho	Rough
Top Cover			Lossless						
Air Above	<input checked="" type="checkbox"/>			200					
TOP METAL [3]	<input checked="" type="checkbox"/>	<input type="checkbox"/>	Sub: 5880_31mil	0.71				1	0.094
SUBSTRATE [4]	<input checked="" type="checkbox"/>		Sub: 5880_31mil	31	2.2	0.0004	1		
BOT METAL [5]	<input type="checkbox"/>	<input type="checkbox"/>							
Air Below	<input type="checkbox"/>								
Bottom Cover			Lossless						

Figure 5.22: Parameters of the EM simulation in GENESYS

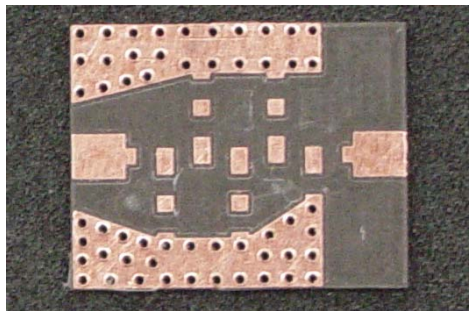


Figure 5.23: Top view of the second HP filter layout

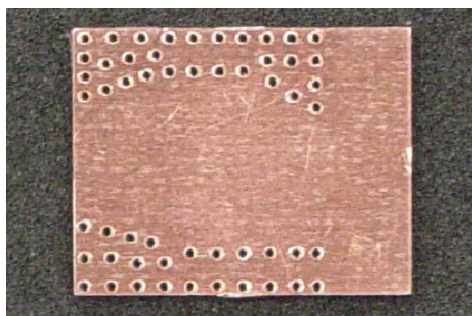


Figure 5.24: Bottom view of the second HP filter layout

The holes are used for connecting top and bottom layers via small copper wires in order to equate the ground potential everywhere. In Table 2 below, the layout and grid sizes are shown.

	Horizontal	Vertical
Cell Size (mil)	10	10
Box Size (mil)	630	500
# of cells	63	50

Table 5.2: Layout and grid sizes. The dimensions are in mils.

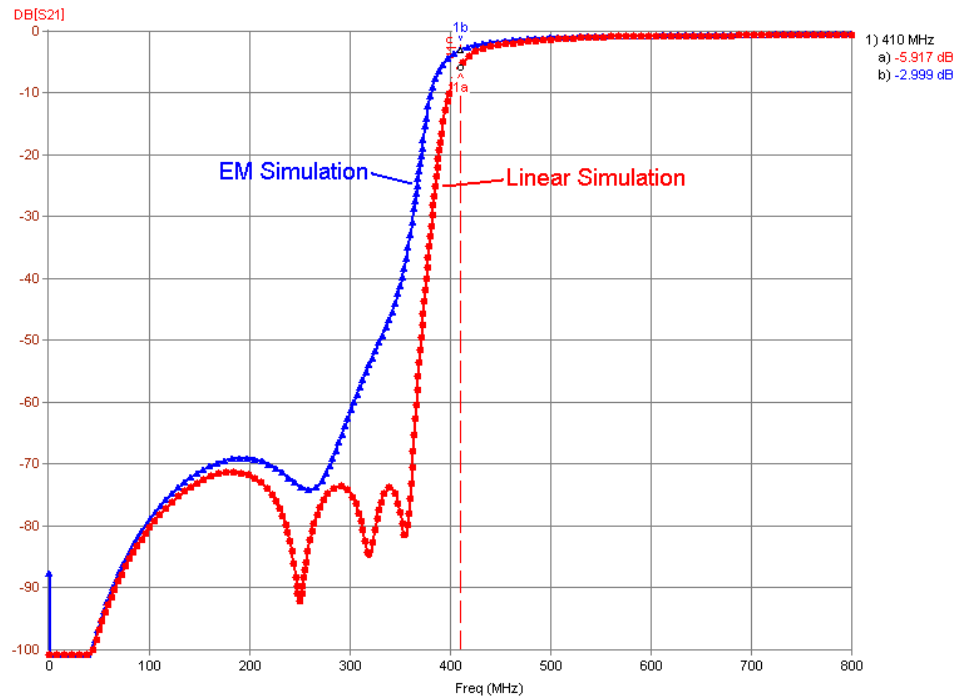


Figure 5.25: Insertion loss result of the EM simulation compared with the linear analysis.

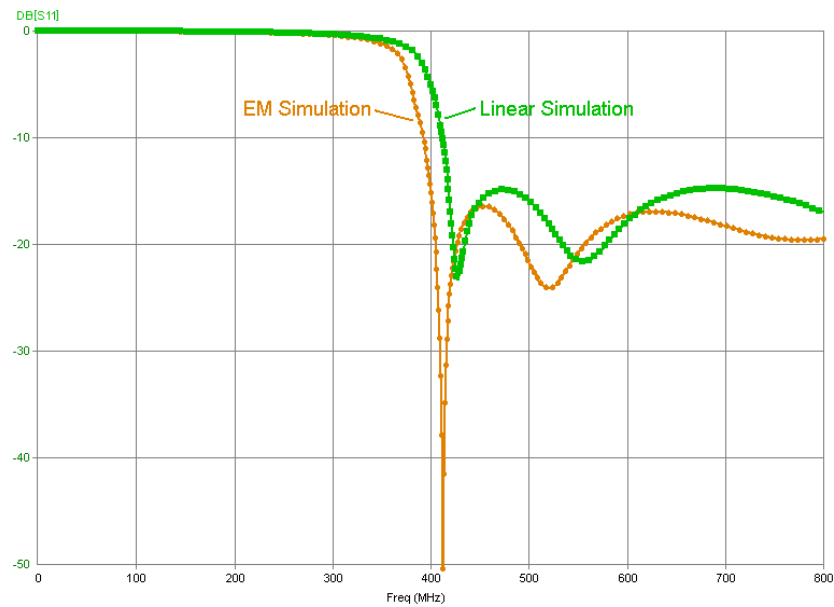


Figure 5.26: Return loss result of the EM simulation compared to linear analysis

The HP filter with the elements soldered is as shown below (Figure 5.24). Note that elements are soldered on only top layer instead of two (as in the first layout) to make the construction easier.



Figure 5.27: Top view of the second HP filter with elements and connectors soldered



Figure 5.28: Bottom view of the second HP filter with elements and connectors soldered

For this filter, to obtain a smaller size, 0603 inductors are used instead of 0805 size inductors. The capacitors are still 0603 size. The properties of 0603 inductors are shown in Appendix C.

Since the Teflon based dielectric is easy to bend a supporting part is soldered from the connectors as shown below to make the filter stable during measurements (Figure 5.25).



Figure 5.29: Filter with the soldered supporting structure

The network analyzer measurements of this filter are given in figures below:

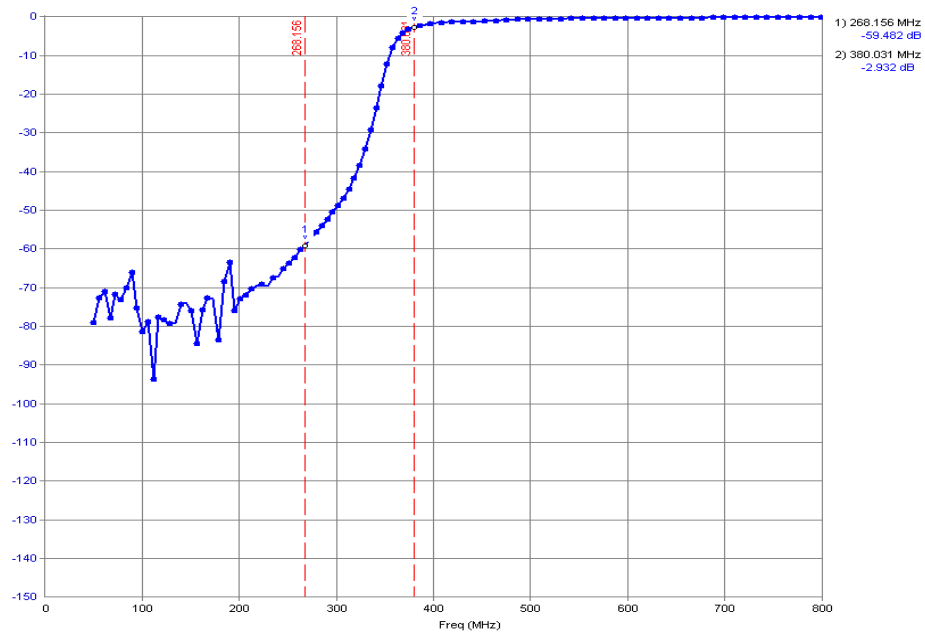


Figure 5.30: Measured insertion loss of the second lumped HP filter up to 800 MHz

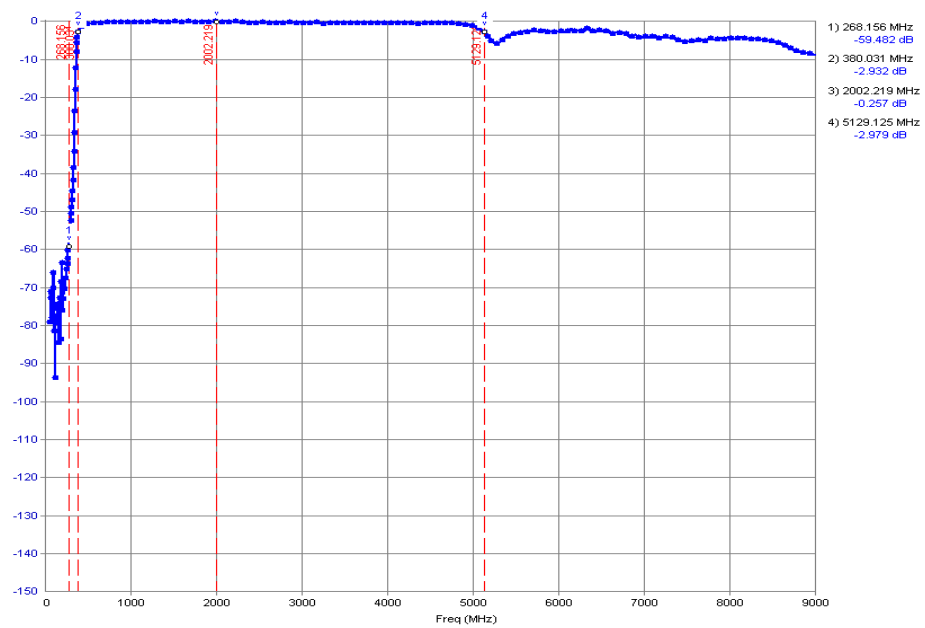


Figure 5.31: Measured insertion loss of the second lumped HP filter up to 9 GHz

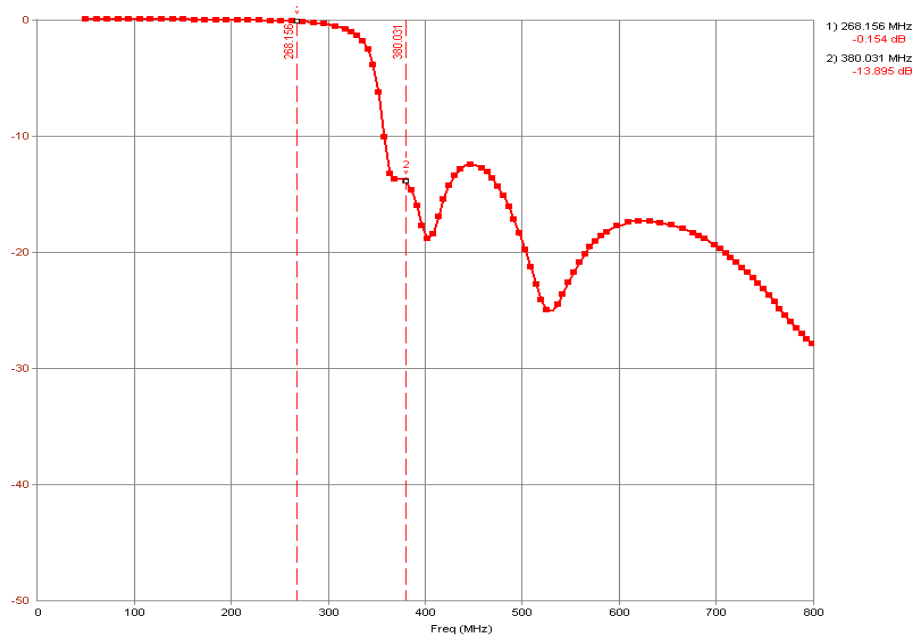


Figure 5.32: Measured return loss of the second lumped HP filter up to 800 MHz

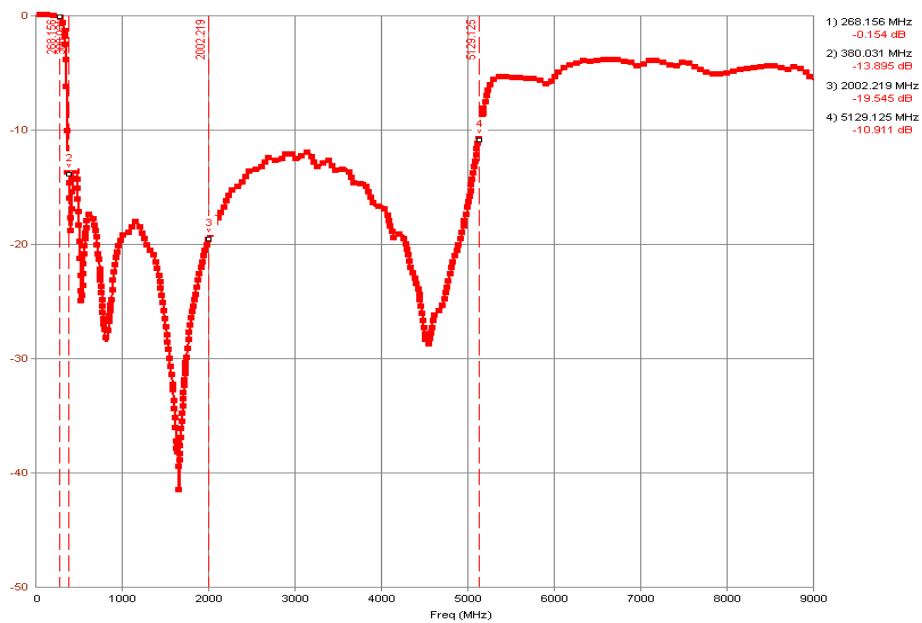


Figure 5.33: Measured return loss of the second lumped HP filter up to 9 GHz

This filter's response is distorted compared to the first trial. This is mainly due to mutual coupling of the inductances and pad impedances. It is seen that passband limit is increased up to 5129 MHz (Figure 5.27) compared to the first layout version (which was 4894 MHz).

This is not due to stray capacitances, $h=62$ mils selected, similar results obtained. Mutual coupling of inductors is not dominant. Coupling from the closely placed element pads seems to be the dominant factor. Poor grounding also results in distortion.

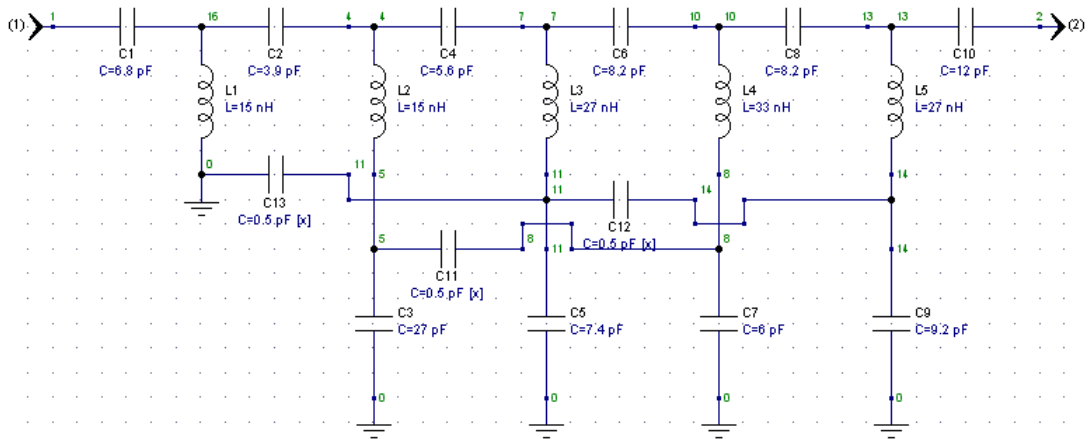


Figure 5.34: Schematic with 0.5 pF coupling capacitors

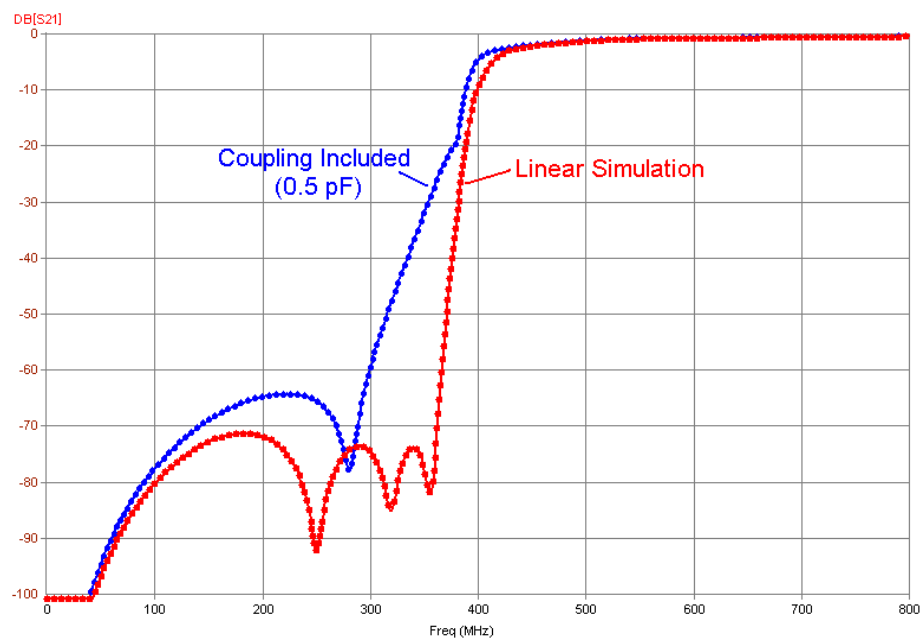


Figure 5.35: Distortion in insertion loss due to simulated coupling

5.3 Selected Lowpass Filter 1

The filter is as follows:

Type	Distributed, Lowpass, Equiripple, Type B
Ripple(dB)	0.1
Corner Frequency(MHz)	2000
Quarter Wave Frequency(MHz)	4000
Order	13
Transmission Zeros with order of Extraction (MHz)	UE, 2310, 2xUE, 2310, 2xUE, 2310, UE, INF

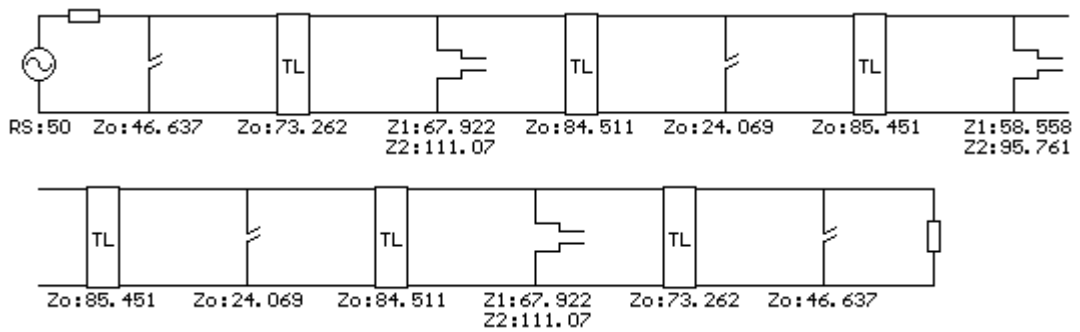


Figure 5.36: Elements of **Selected Lowpass Filter 1**

Using GENESYS it is possible to analyze the effect of changes in TL widths and lengths entering a scheme as shown below:

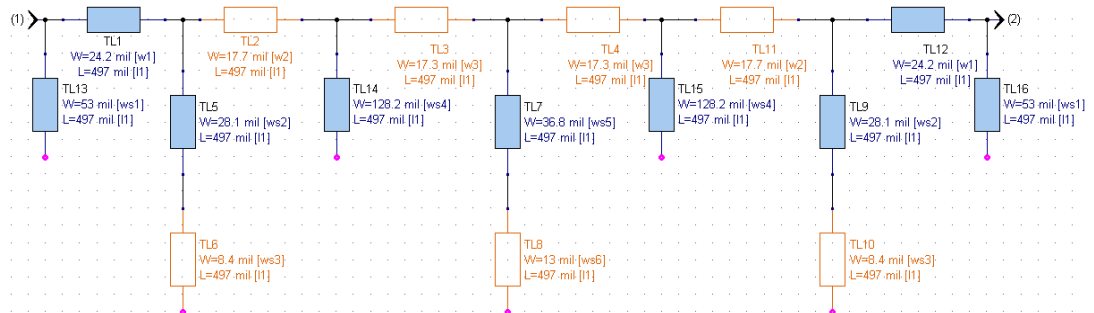


Figure 5.37: Linear scheme of **Selected Lowpass Filter 1**

Machined circuit boards generally have about 1 mil (0.0254 mm) of board material stripped off [7]. Considering this effect, the 31 mil dielectric thickness of each substrate becomes 30 mils, so the total dielectric thickness of the stripline turns out to be 60 mils and line widths should be chosen accordingly.

When Rogers 5880® dielectric substrate is used, using Transmission Line tool of GENESYS, stub and transmission line widths for the stripline turns out to be as follows:

Impedance (Ω)	Line width (mils) for h=62 mils	Line width (mils) for h=60 mils
46.637	54.8702	53.0419
73.262	25.0383	24.1839
67.923	29.0815	28.095
111.074	8.7671	8.44614
84.512	18.3428	17.7074
24.070	132.581	128.216
85.451	17.8746	17.2544
58.559	38.066	36.7862
95.762	13.4514	12.9762
50.000	49.3107	47.6638

Table 5.3: Equivalent widths of TLs and stubs

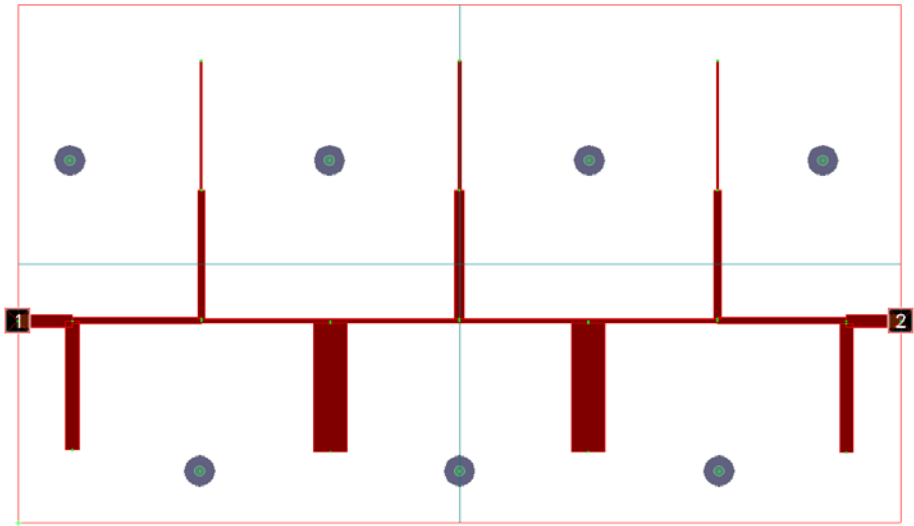


Figure 5.38: Layout view of Selected Lowpass Filter 1

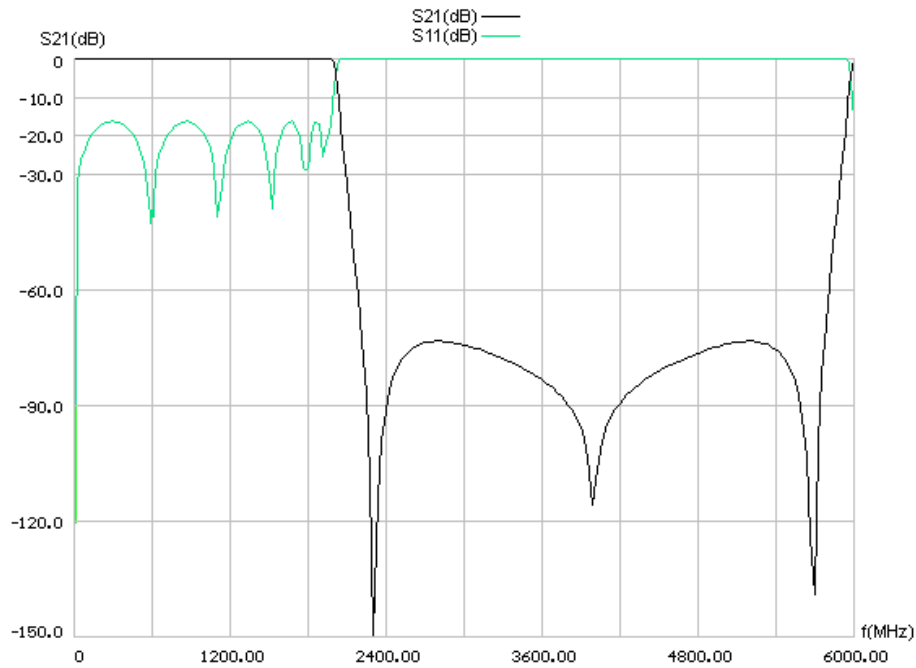


Figure 5.39: Linear analysis S21 and S11 responses of **Selected Lowpass Filter 1**

Layout and grid sizes for GENESYS and SONNET simulations are as follows:

	Horizontal	Vertical
Cell Size(mil)	4.3	3.5
Box Size(mil)	3440	2030
# of cells	800	580

Table 5.4: Layout and grid sizes. The dimensions are in mils.

In Figure 5.40 parameters of the layout is shown which is used for GENESYS simulation. Figure 5.41 shows the simulation output.

Name	Use	Slot-type	Use 1/2 Height	Type	Height or Thickness	Er	Tand/Sigma	Ur	Rho	Rough
Top Cover				Lossless						
Air Above	<input type="checkbox"/>									
SUBSTRATE [3]	<input checked="" type="checkbox"/>		<input type="checkbox"/>	Sub: Rogers 588	30	2.2	0.0004	1		
TOP METAL [4]	<input checked="" type="checkbox"/>	<input type="checkbox"/>		Sub: Rogers 588	0.71				1	0.094
SUBSTRATE [5]	<input checked="" type="checkbox"/>		<input type="checkbox"/>	Sub: Rogers 588	30	2.2	0.0004	1		
BOT METAL [6]	<input type="checkbox"/>	<input checked="" type="checkbox"/>								
Air Below	<input type="checkbox"/>									
Bottom Cover				Lossless						

Figure 5.40: Parameters of the layout in GENESYS

The result of the SONNET simulation is shown in Figure 5.42.

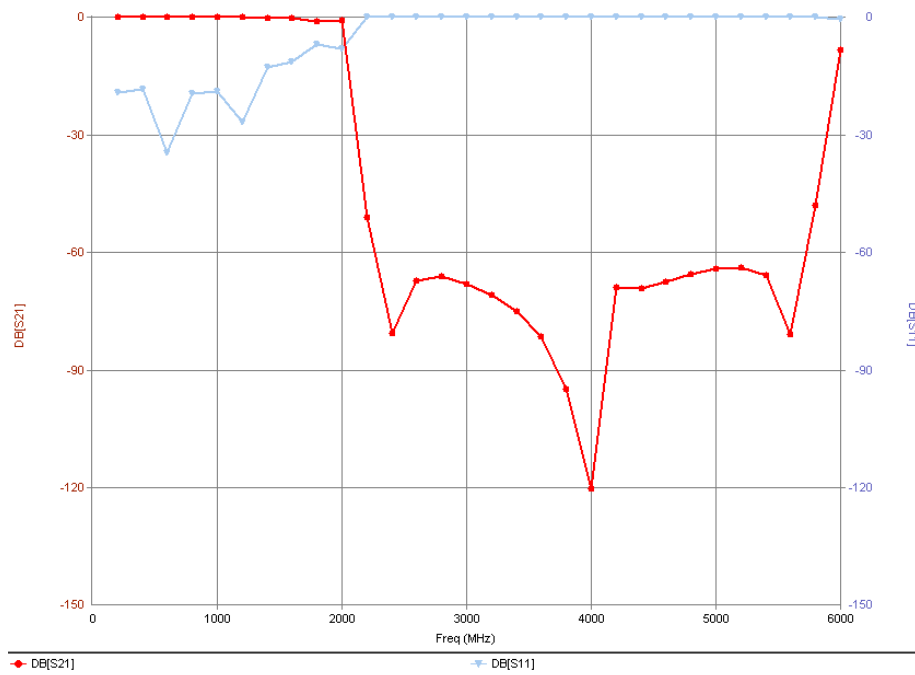


Figure 5.41: EM simulation output obtained from GENESYS

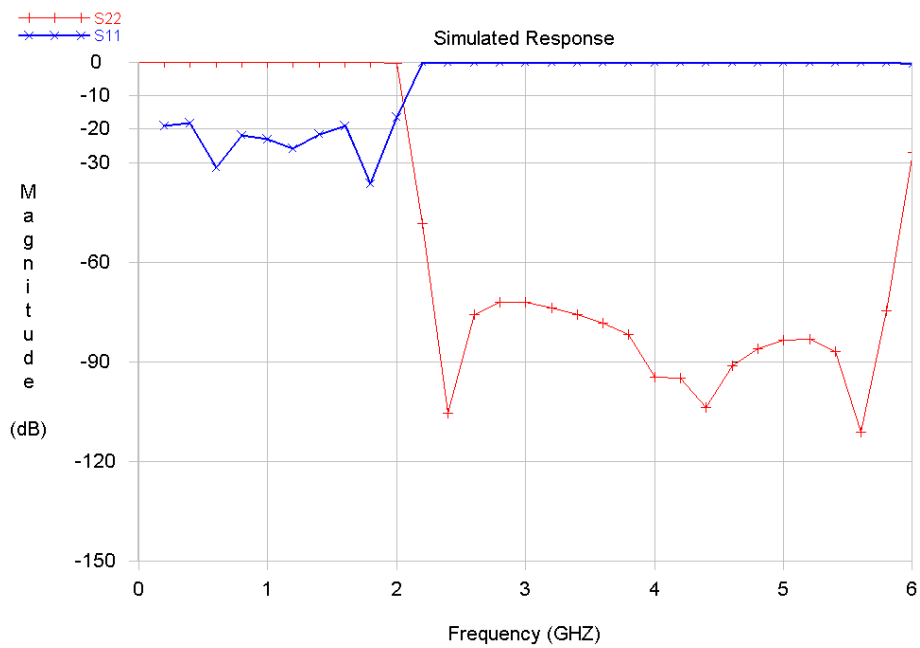


Figure 5.42: EM simulation output obtained from SONNET

The realized **Selected Lowpass Filter 1** is as follows Figure 5.43, 5.44, 5.45 and 5.46:

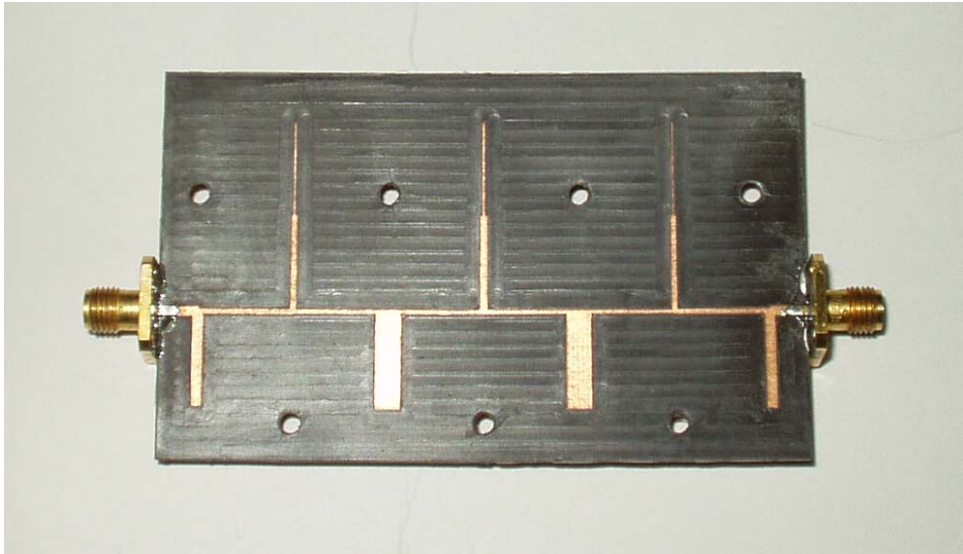


Figure 5.43: View of TLs and stubs of **Selected Lowpass Filter 1**



Figure 5.44: Connected view of **Selected Lowpass Filter 1**

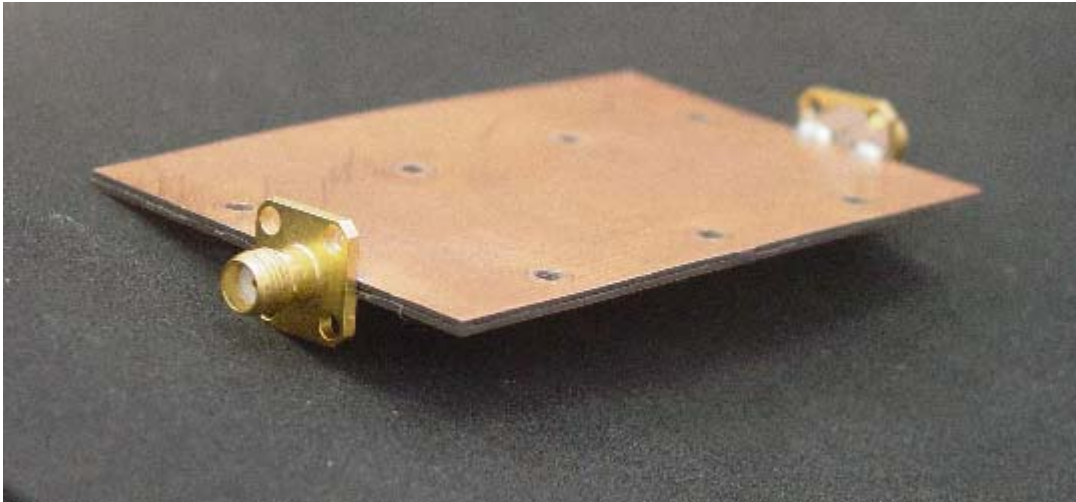


Figure 5.45: Side view of **Selected Lowpass Filter 1**

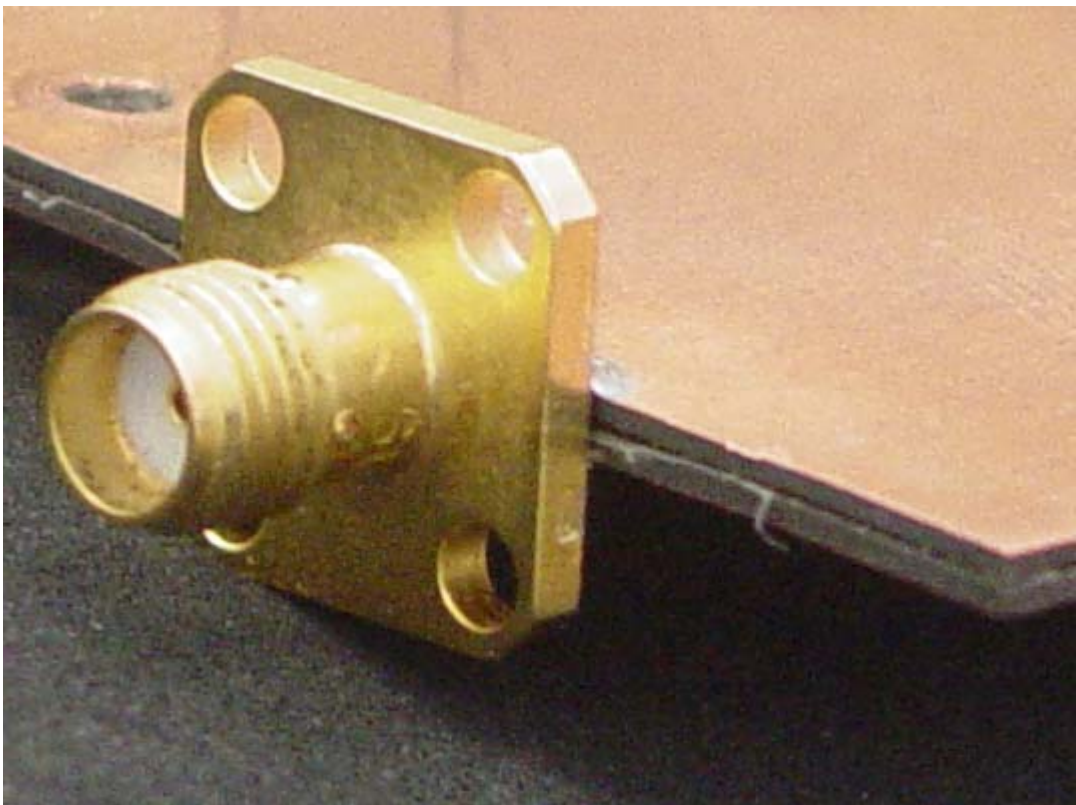


Figure 5.46: Near the connector due to soldering the top and bottom parts may not be connected properly, the filter is resoldered to correct this error.

Measured results of this filter is shown in Figure 5.47, 5.48.

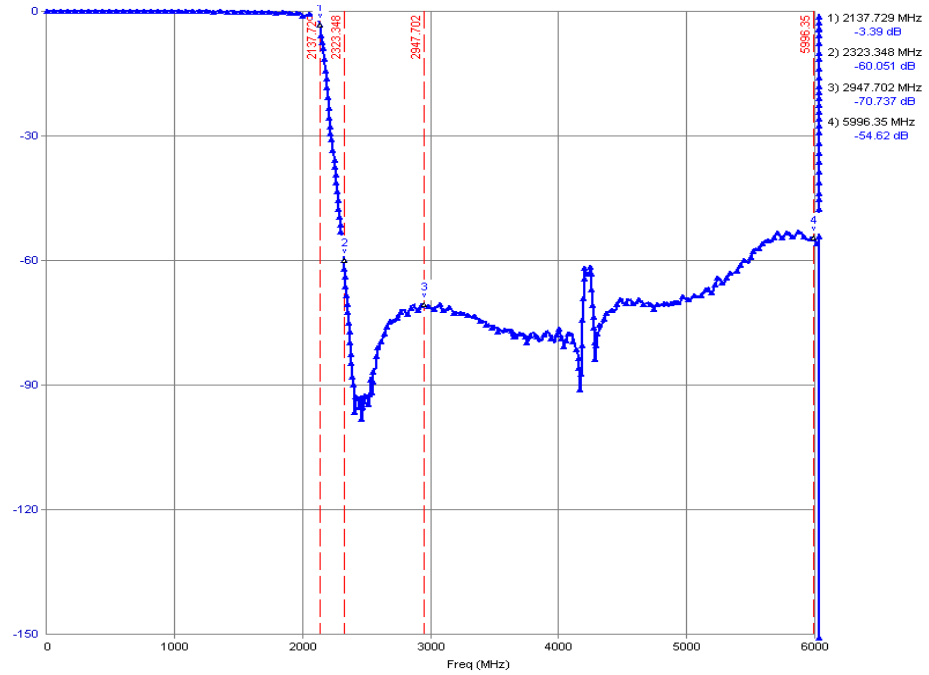


Figure 5.47: Measured insertion loss of **Selected Lowpass Filter 1** up to 6 GHz

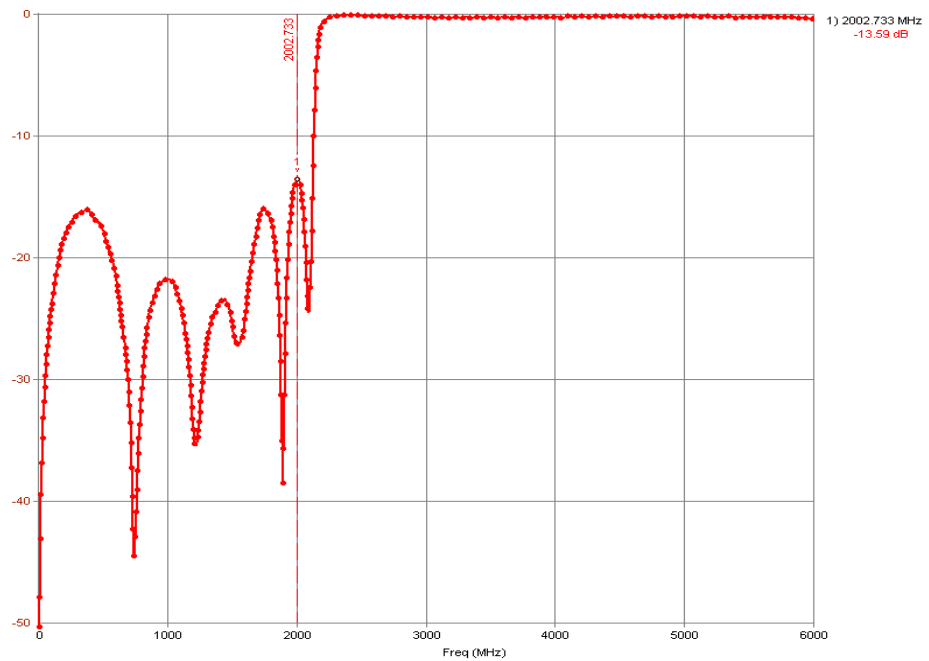


Figure 5.48: Measured return loss of **Selected Lowpass Filter 1** up to 6 GHz

The measurements are consistent with the simulations, stop band attenuation after f_q increases and is more than the simulated response, this is probably due to internal coupling of TL and stubs, which are not exactly included in the simulations.

5.4 Selected Lowpass Filter 2

The filter is as follows:

Type	Distributed, Lowpass, Equiripple, Type B
Ripple(dB)	0.05
Corner Frequency(MHz)	2000
Quarter Wave Frequency(MHz)	4736.6
Order	13
Transmission Zeros with order of Extraction (MHz)	UE, 2368.3, 2xUE, 2368.3, 2xUE, 2368.3, UE, INF

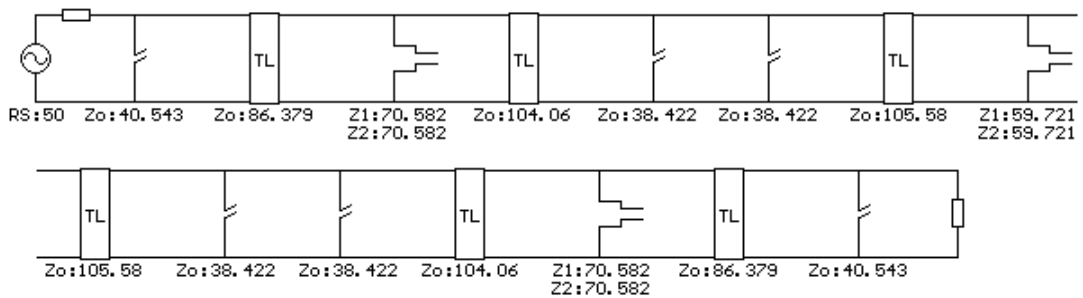


Figure 5.49: Elements of Selected Lowpass Filter 2

The scheme to analyze the effect of changes in TL widths and lengths is as shown below:

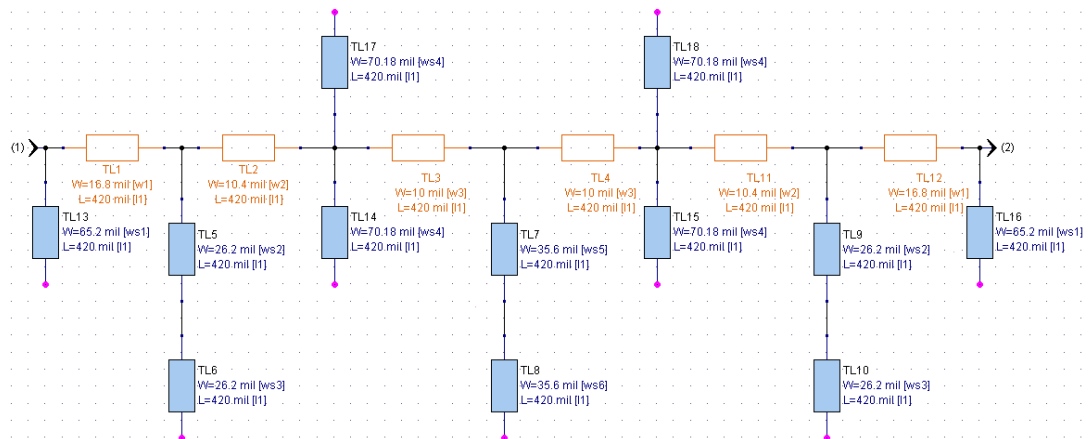


Figure 5.50: Linear scheme of Selected Lowpass Filter 2 constructed in GENESYS

Stub and transmission line widths for Rogers 5880® dielectric and 2x31mil stripline width is as follows:

Impedance (Ω)	Line width (mils) for h=62 mils
40.543	65.096
86.379	16.8372
70.582	26.0882
104.067	10.3116
19.211	167.771
105.587	9.88123
59.721	35.5763
50.000	47.6883

Table 5.5: Equivalent widths of TLs and stubs

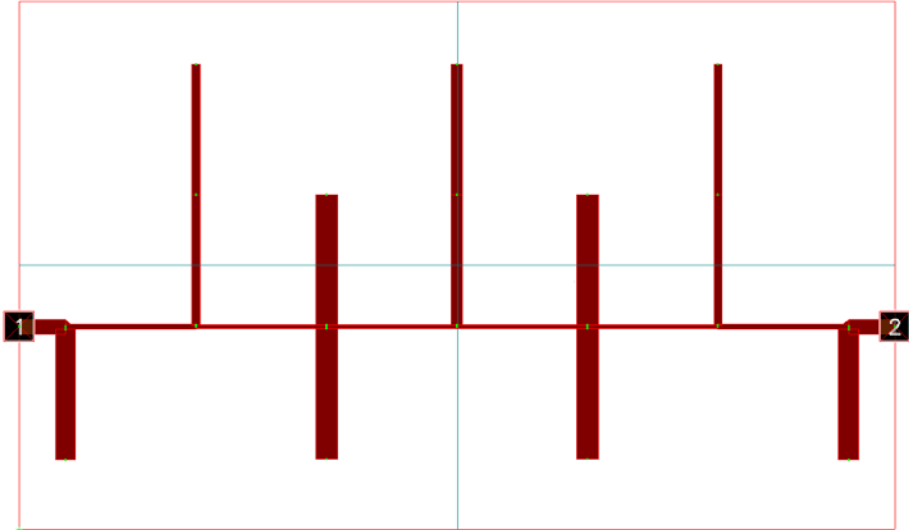


Figure 5.51: Layout view of Selected Lowpass Filter 2

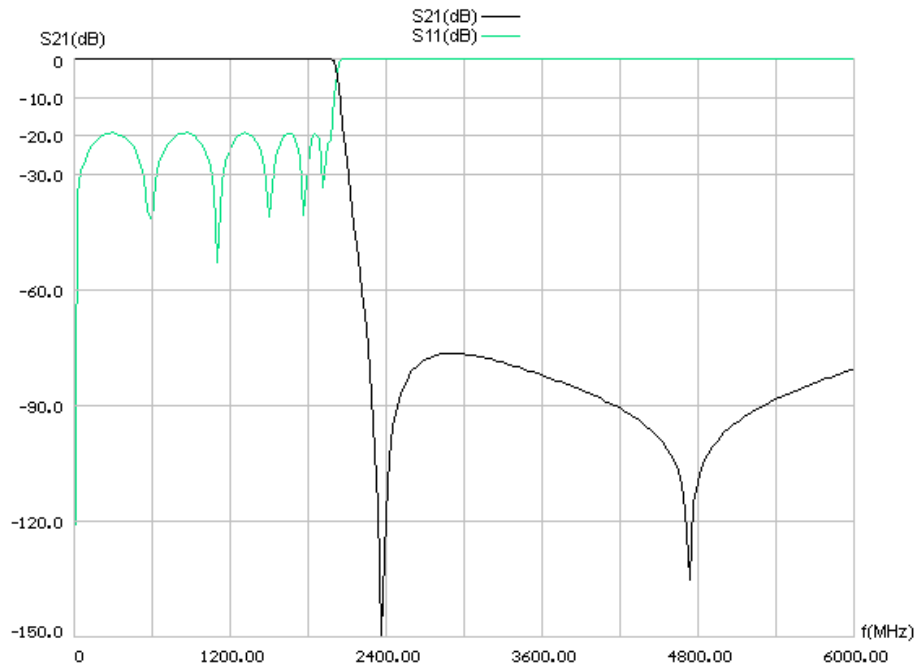


Figure 5.52: Linear analysis S21 and S11 responses of **Selected Lowpass Filter 2**

Layout and grid sizes for GENESYS and SONNET simulations are as follows:

	Horizontal	Vertical
Cell Size(mil)	7.05	7.5
Box Size(mil)	2820	1500
# of cells	400	200

Table 5.6: Layout and grid sizes. The dimensions are in mils.

In Figure 5.53 parameters of the layout is shown which is used for GENESYS simulation. Figure 5.54 shows the simulation output.

Name	Use	Slot-type	Use 1/2 Height	Type	Height or Thickness	Er	Tand/Sigma	Ur	Rho	Rough
Top Cover				Lossless						
Air Above	<input type="checkbox"/>									
SUBSTRATE [3]	<input checked="" type="checkbox"/>		<input type="checkbox"/>	Sub: Rogers 588	30	2.2	0.0004	1		
TOP METAL [4]	<input checked="" type="checkbox"/>	<input type="checkbox"/>		Sub: Rogers 588	0.71				1	0.094
SUBSTRATE [5]	<input checked="" type="checkbox"/>		<input type="checkbox"/>	Sub: Rogers 588	30	2.2	0.0004	1		
BOT METAL [6]	<input type="checkbox"/>	<input checked="" type="checkbox"/>								
Air Below	<input type="checkbox"/>									
Bottom Cover				Lossless						

Figure 5.53: Parameters of the EM simulation in GENESYS

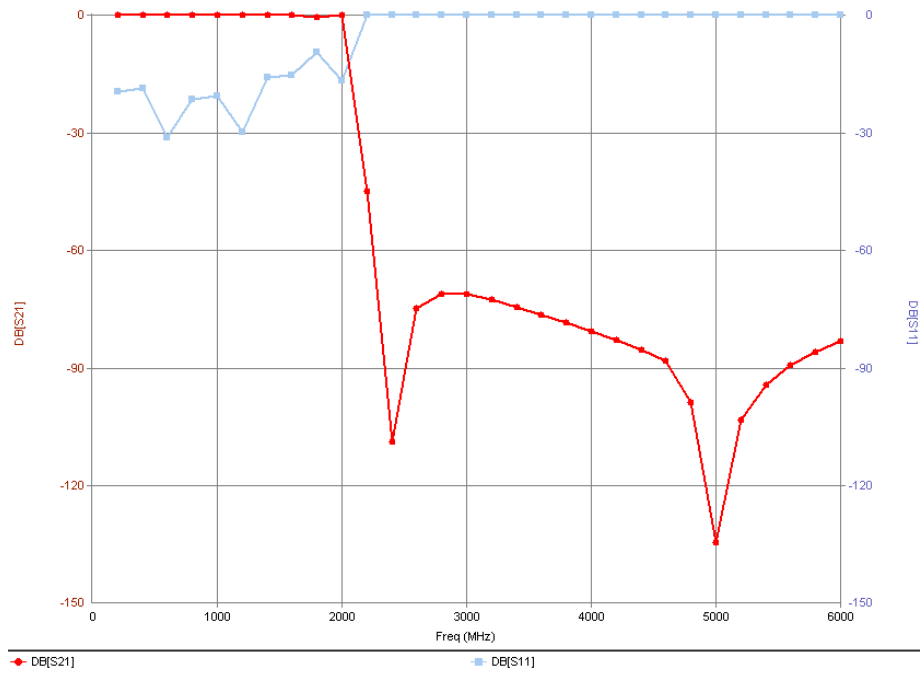


Figure 5.54: EM simulation output obtained from GENESYS

The result of the SONNET simulation is shown in Figure 5.55.

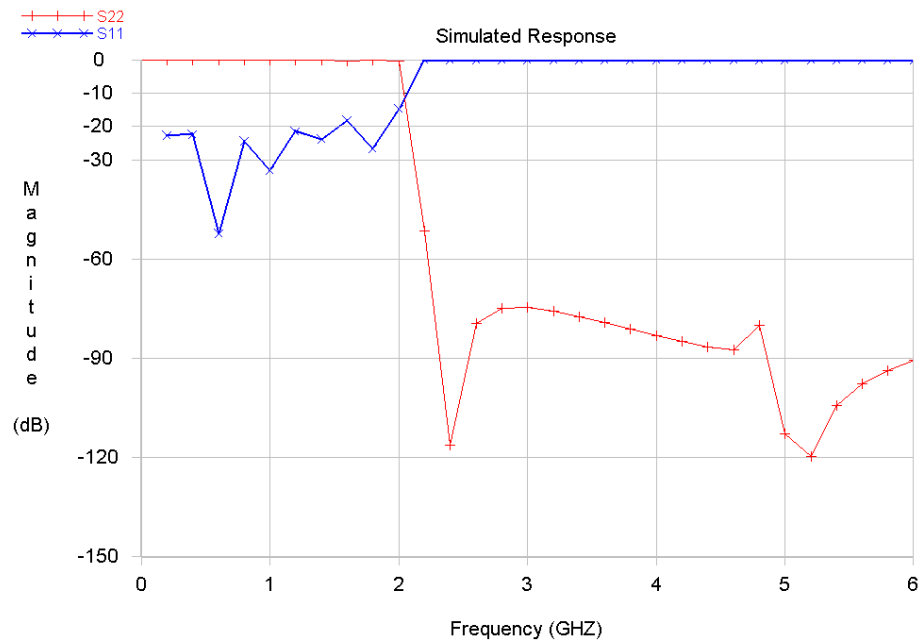


Figure 5.55: EM simulation output obtained from SONNET

The realized **Selected Lowpass Filter 2** is as follows:

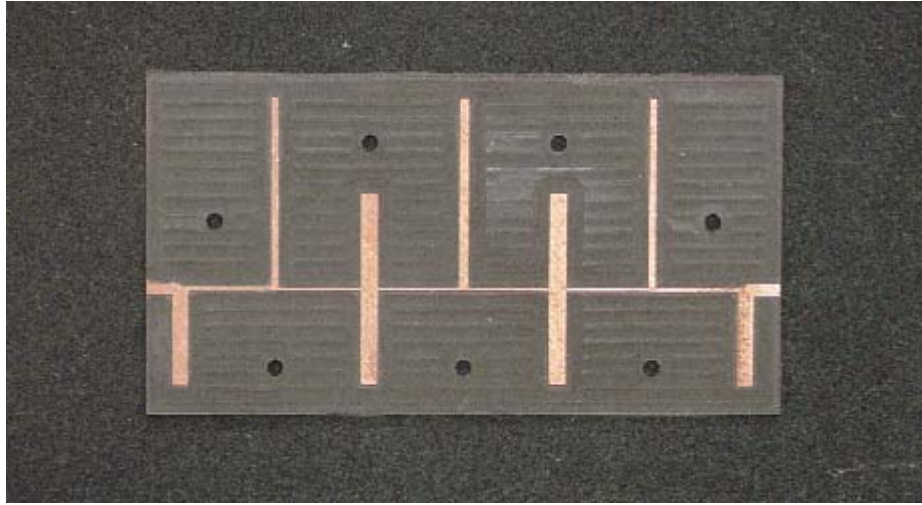


Figure 5.56: TLs and stubs of **Selected Lowpass Filter 2**

Measured results of this filter are shown in Figure 5.53, 5.54.

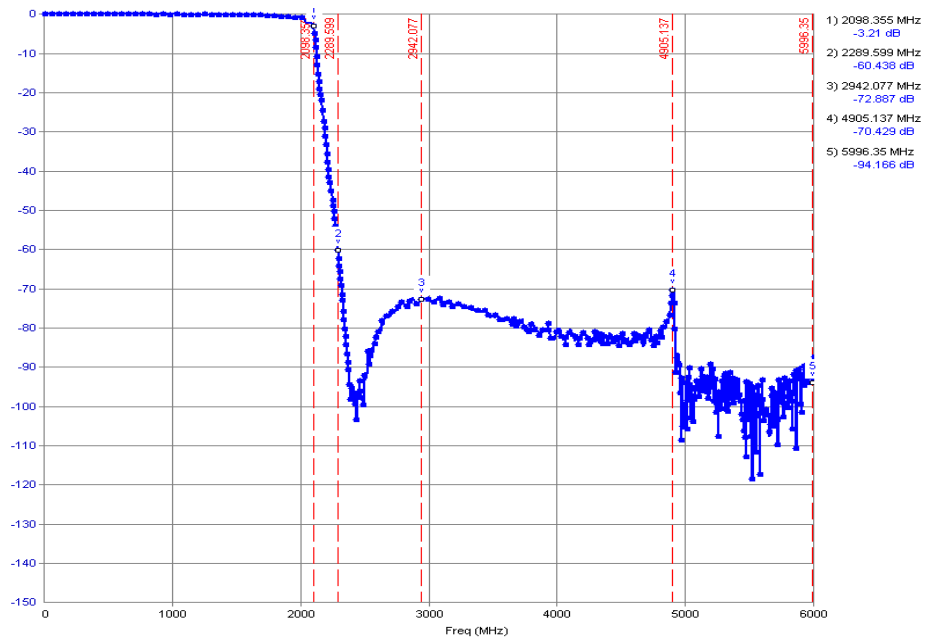


Figure 5.57: Measured insertion loss of **Selected Lowpass Filter 2** up to 6 GHz

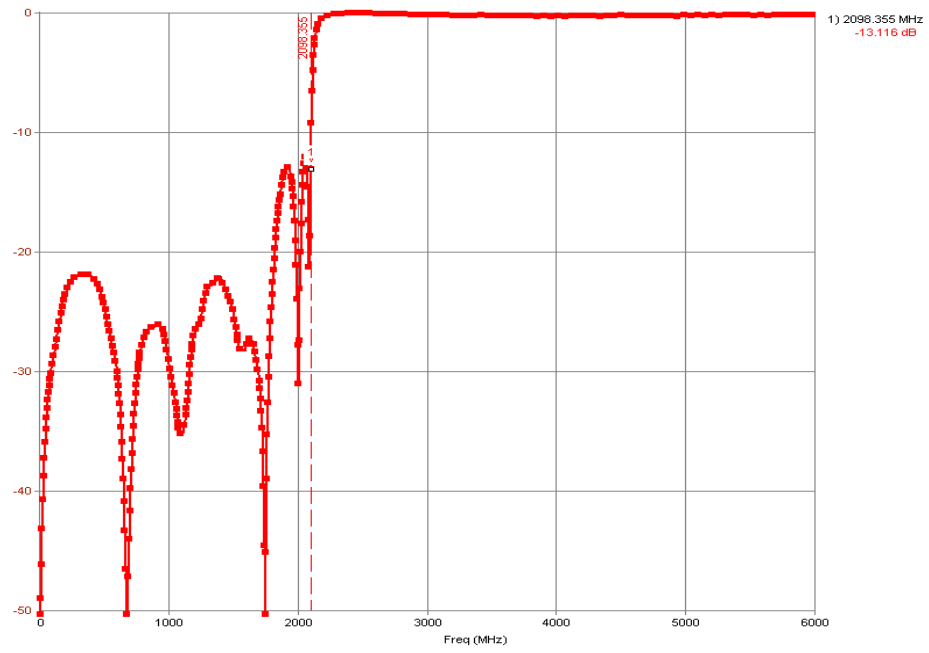


Figure 5.58: Measured return loss of **Selected Lowpass Filter 2** up to 6 GHz

It is seen that the measurements are consistent again with the simulations.

5.5 Selected Lowpass Filter 3

40.543 Ω lines of **Selected Lowpass Filter 2** are splitted into two equal pieces of 81.086 Ω 's whose equivalent line widths are 19.4837mils for 62mil height stripline. The filter is as follows:

Type	Distributed, Lowpass, Equiripple, Type B
Ripple(dB)	0.05
Corner Frequency(MHz)	2000
Quarter Wave Frequency(MHz)	4736.6
Order	13
Transmission Zeros with order of Extraction (MHz)	UE, 2368.3, 2xUE, 2368.3, 2xUE, 2368.3, UE, INF

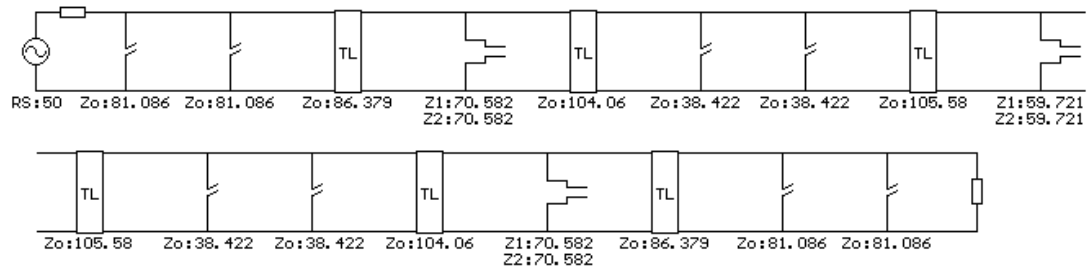


Figure 5.59: Elements of **Selected Lowpass Filter 3**

The scheme to analyze the effect of changes in TL widths and lengths is as shown below:

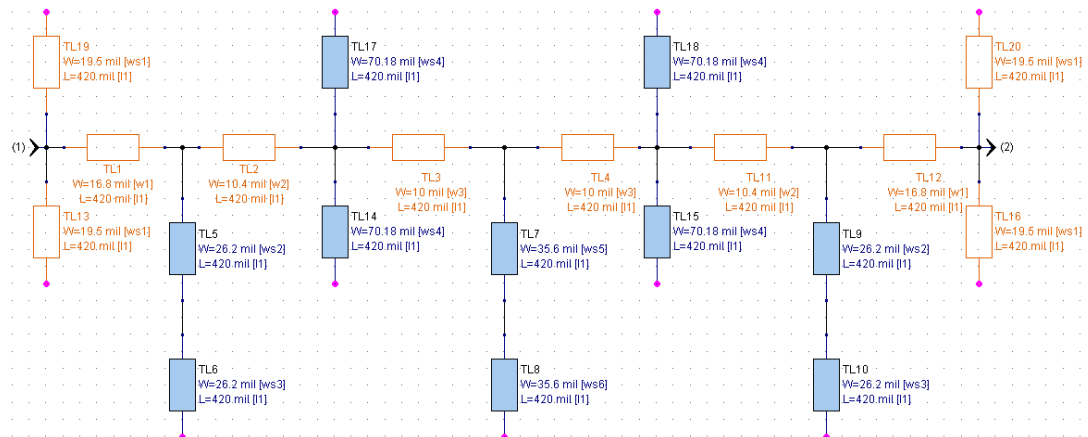


Figure 5.60: Linear scheme of **Selected Lowpass Filter 3** in GENESYS

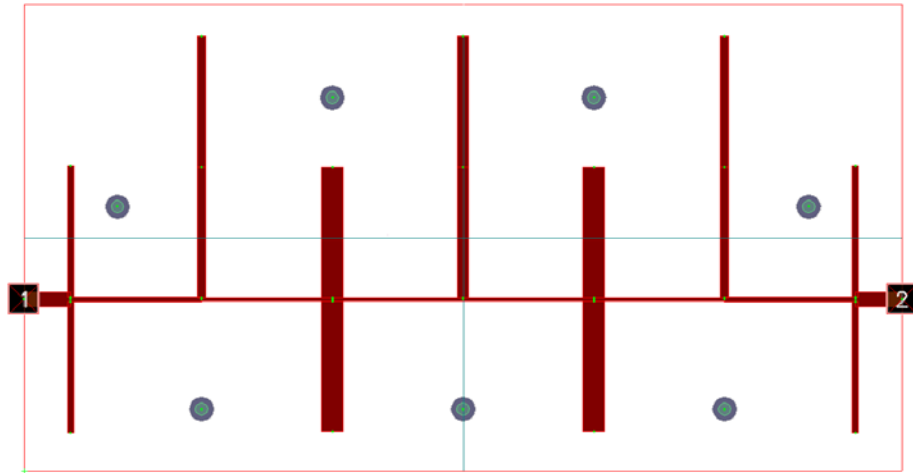


Figure 5.61: Layout view of **Selected Lowpass Filter 3**

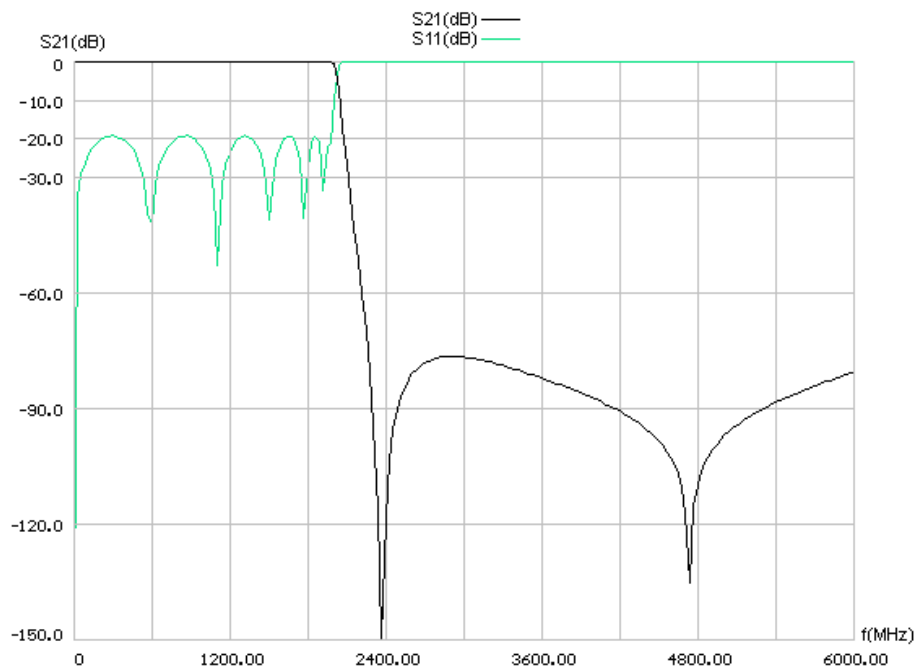


Figure 5.62: Linear analysis S21 and S11 responses of **Selected Lowpass Filter 3**

Grid sizes for GENESYS and SONNET simulations are as follows:

	Horizontal	Vertical
Cell Size(mil)	7.05	7.5
Box Size(mil)	2820	1500
# of cells	400	200

Table 5.7: Layout and grid sizes. The dimensions are in mils.

In Figure 5.63 parameters of the layout is shown which is used for GENESYS simulation. Figure 5.64 shows the simulation output.

Name	Use	Slot-type	Use 1/2 Height	Type	Height or Thickness	Er	Tand/Sigma	Ur	Rho	Rough
Top Cover				Lossless						
Air Above	<input type="checkbox"/>									
SUBSTRATE [3]	<input checked="" type="checkbox"/>		<input type="checkbox"/>	Sub: Rogers 588	30	2.2	0.0004	1		
TOP METAL [4]	<input checked="" type="checkbox"/>	<input type="checkbox"/>		Sub: Rogers 588	0.71				1	0.094
SUBSTRATE [5]	<input checked="" type="checkbox"/>		<input type="checkbox"/>	Sub: Rogers 588	30	2.2	0.0004	1		
BOT METAL [6]	<input type="checkbox"/>	<input checked="" type="checkbox"/>								
Air Below	<input type="checkbox"/>									
Bottom Cover				Lossless						

Figure 5.63: Parameters of the EM simulation in GENESYS

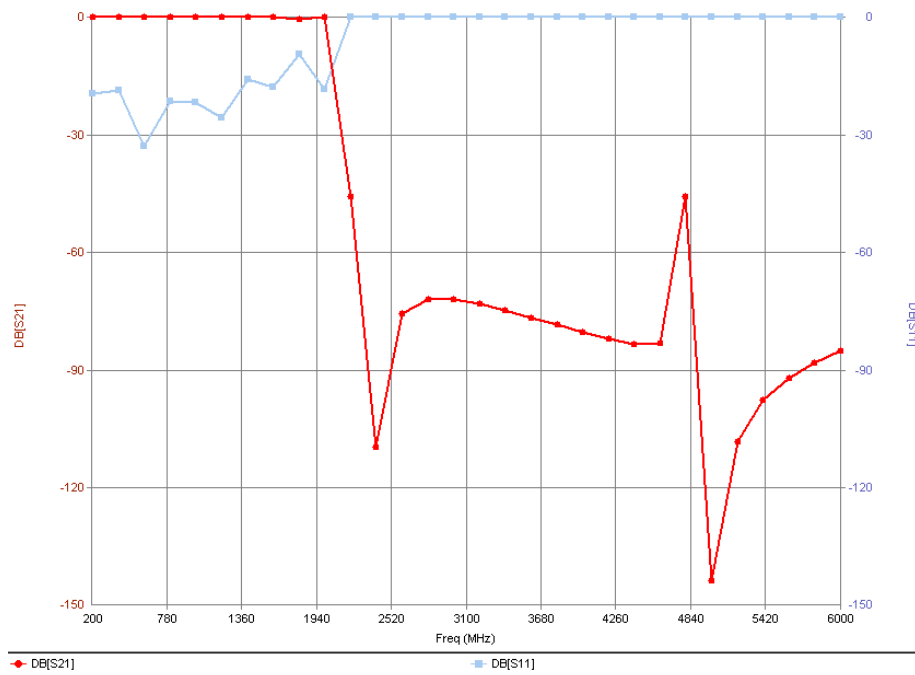


Figure 5.64: EM simulation output obtained from GENESYS

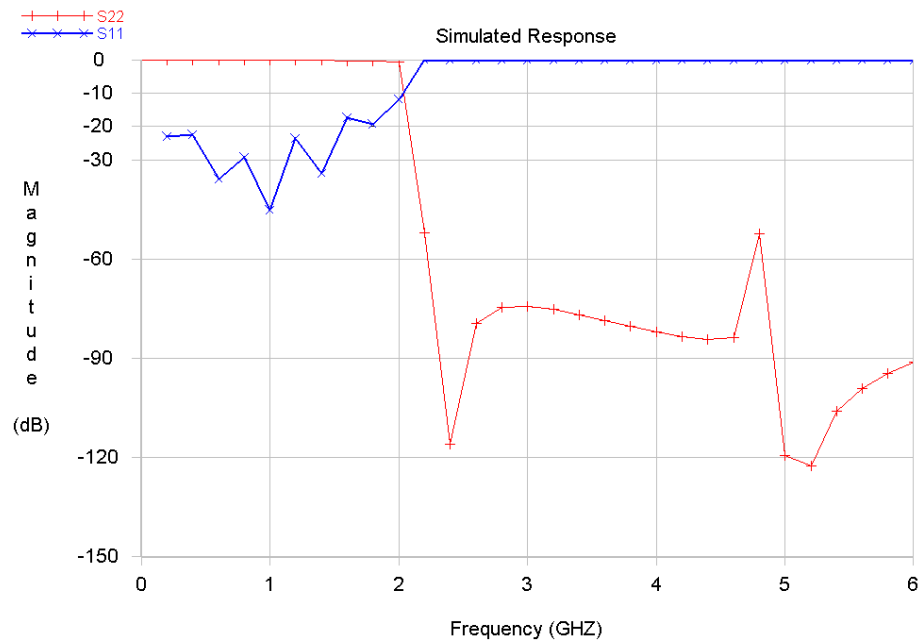


Figure 5.65: EM simulation output obtained from SONNET

The realized **Selected Lowpass Filter 3** is as follows:

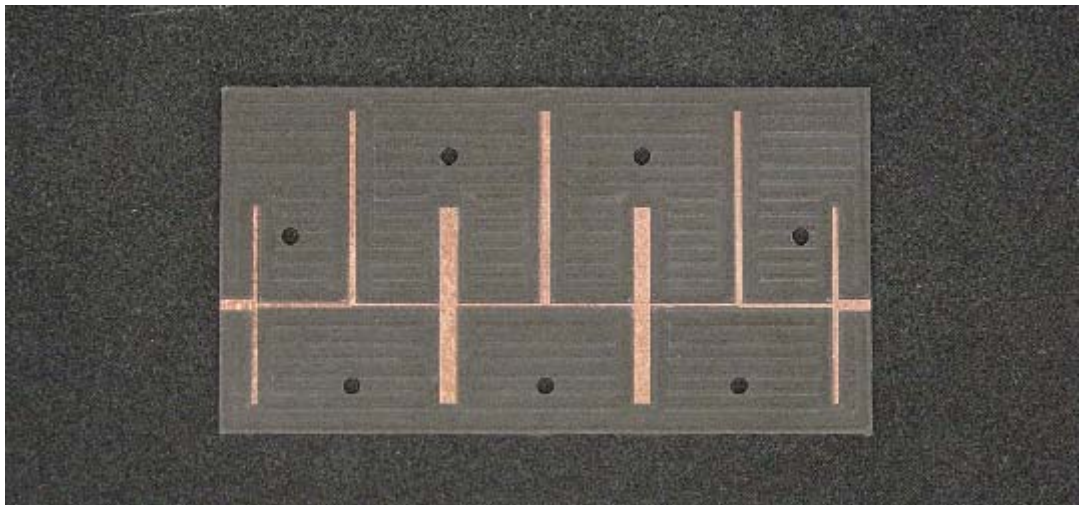


Figure 5.66: TLs and stubs of **Selected Lowpass Filter 3**

Note that the effects of machining process are very apparent in this figure. There are some horizontal hills produced by the drill machine's machining process.

Measured results of this filter are shown in Figure 5.67, 5.68.

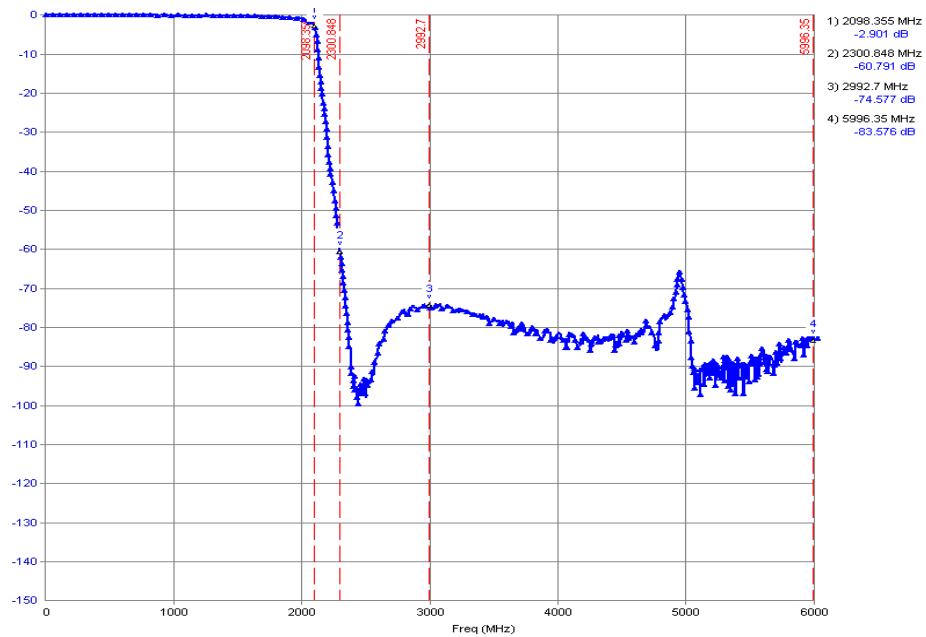


Figure 5.67: Measured insertion loss of **Selected Lowpass Filter 3** up to 6 GHz

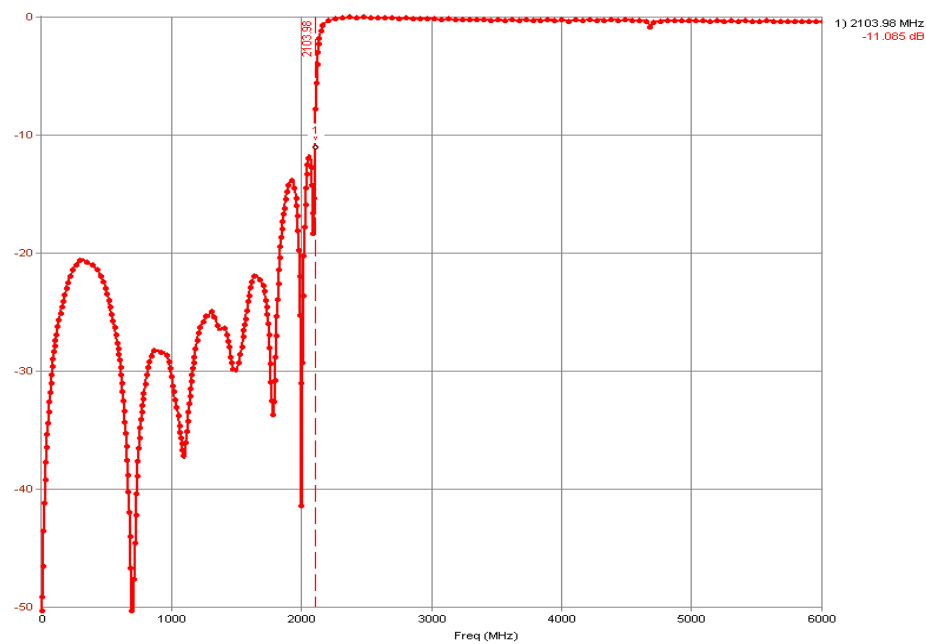


Figure 5.68: Measured insertion loss of **Selected Lowpass Filter 3** up to 6 GHz

Both GENESYS and SONNET EM simulations and the measurements showed that **Selected Lowpass Filter 3** has a peak at the quarter wavelength frequency, so 0041 counterpart will be selected for realization.

5.6 Combination of Lowpass and Highpass Filters to form Bandpass Filter

The lowpass filter with second layout and **Selected Lowpass Filter 2** are combined to form the bandpass filter. The pictures of the final BP filter layout are shown in Figure 5.69, 5.70, 5.71, 5.72 and 5.73.

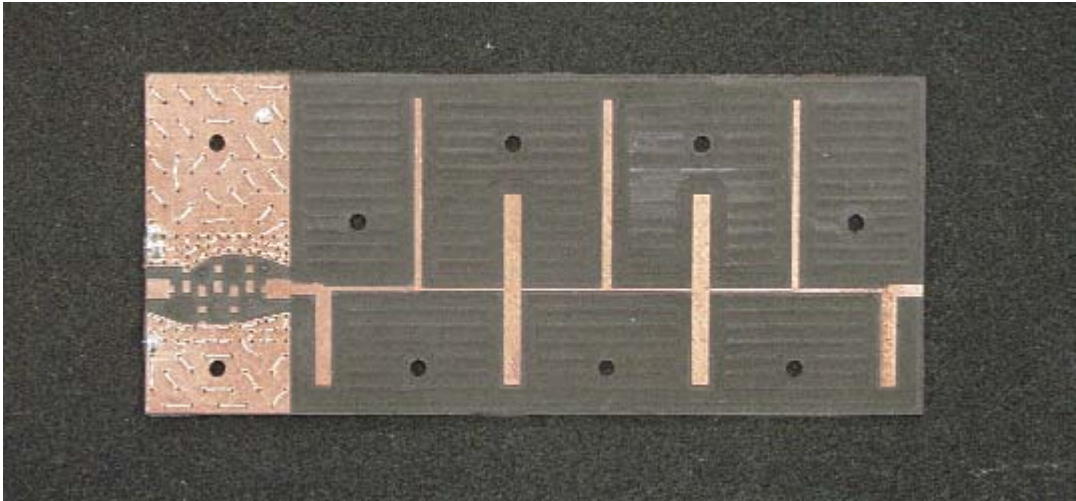


Figure 5.69: Lower part's top layout before soldering

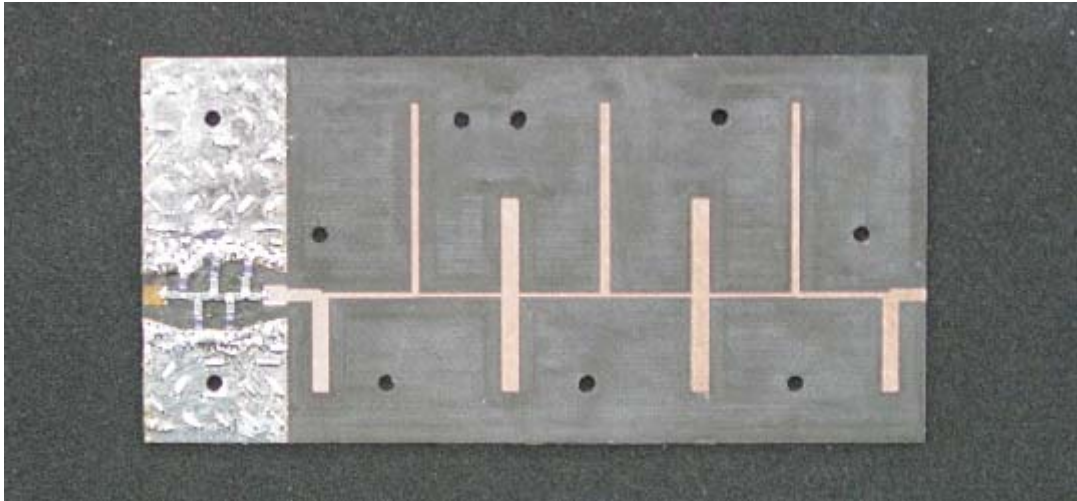


Figure 5.70: Lower part's top layout after soldering

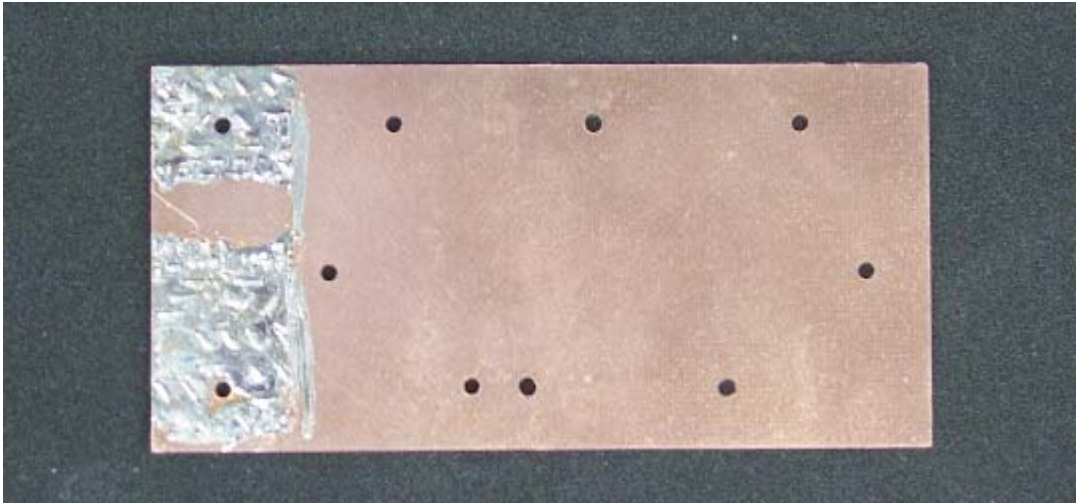


Figure 5.71: Lower part's bottom side after soldering

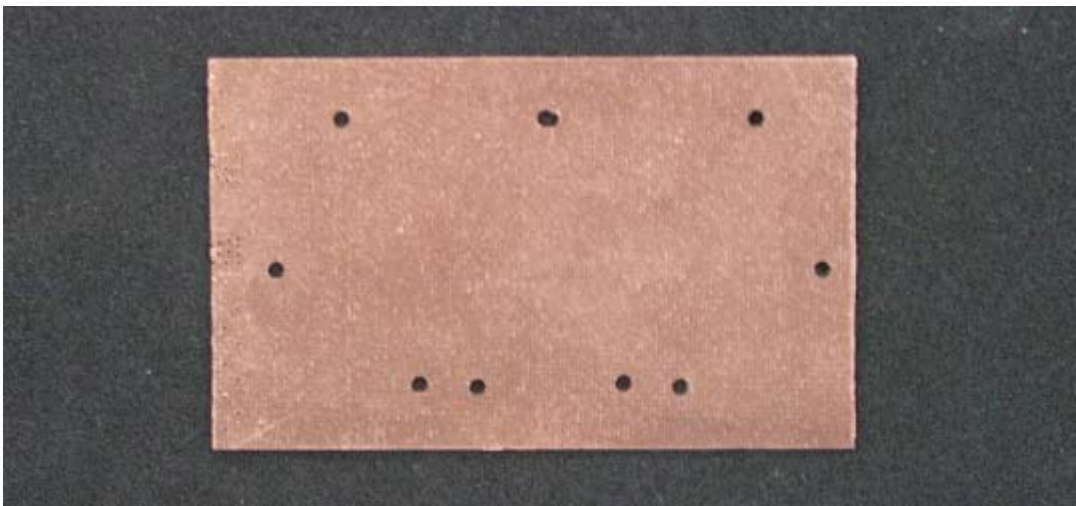


Figure 5.72: Upper part's top side

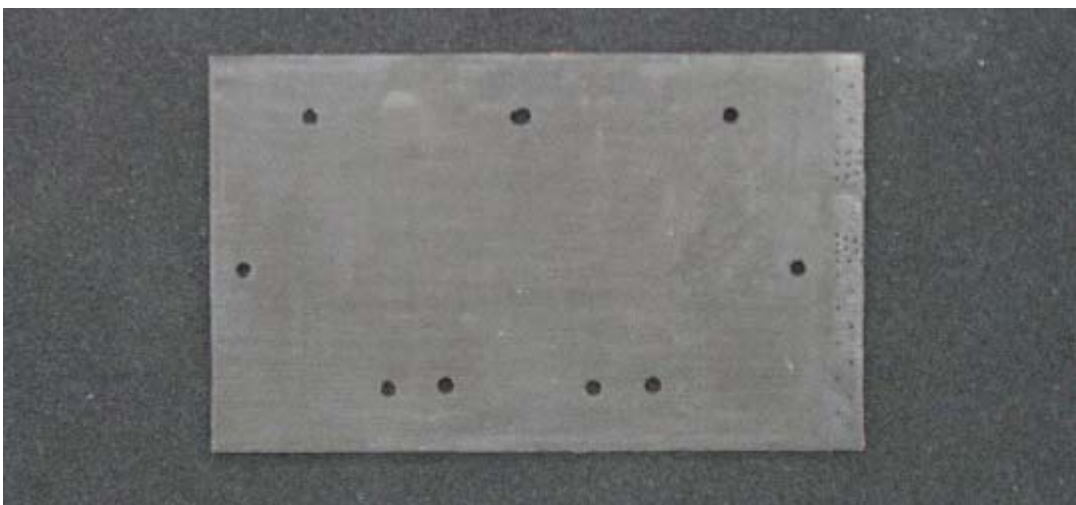


Figure 5.73: Upper part's bottom side

The response of the bandpass filter is as below:

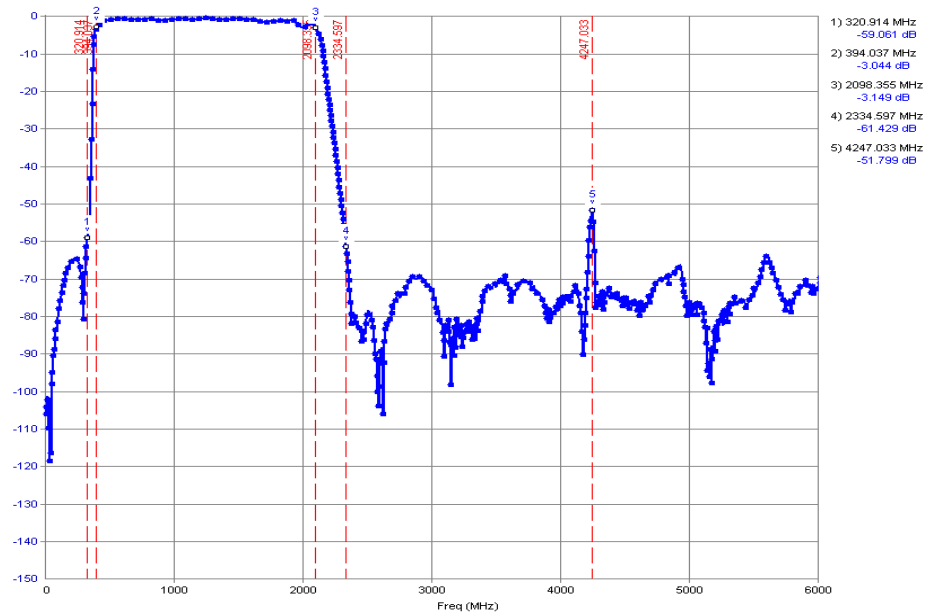


Figure 5.74: Measured S21 response of the connected filters up to 6 GHz

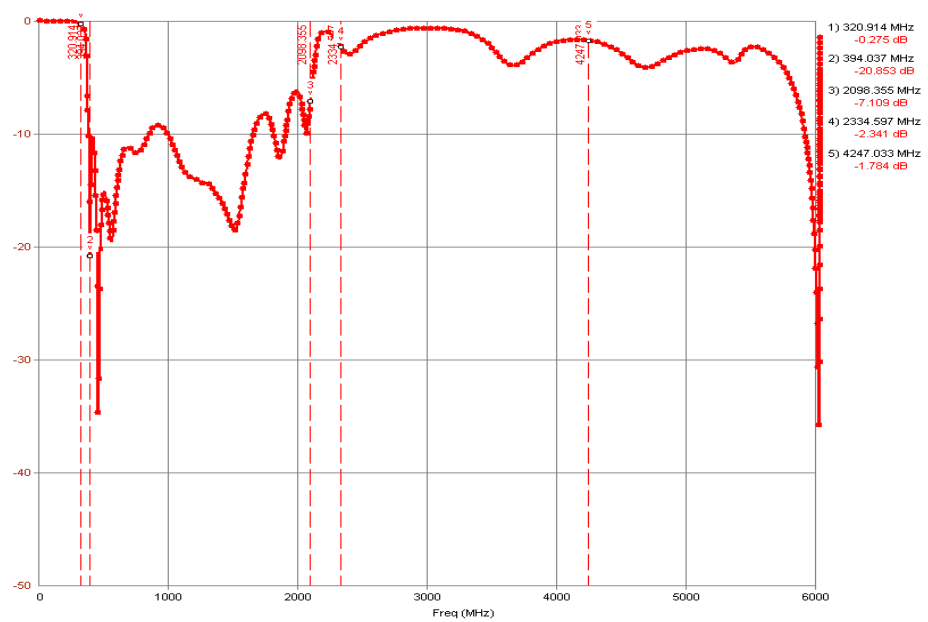


Figure 5.75: Measured S11 response of the connected filters up to 6 GHz

It is seen that the response is satisfactory and no deviation from the individual responses is observed.

As a last stage the filter is placed in a box, the box is shown in Figure 5.76. The final boxed filter is shown in Figure 5.77, 5.78 and 5.79. The details of the filter substrate dimensions and drill holes are shown in Appendix A.

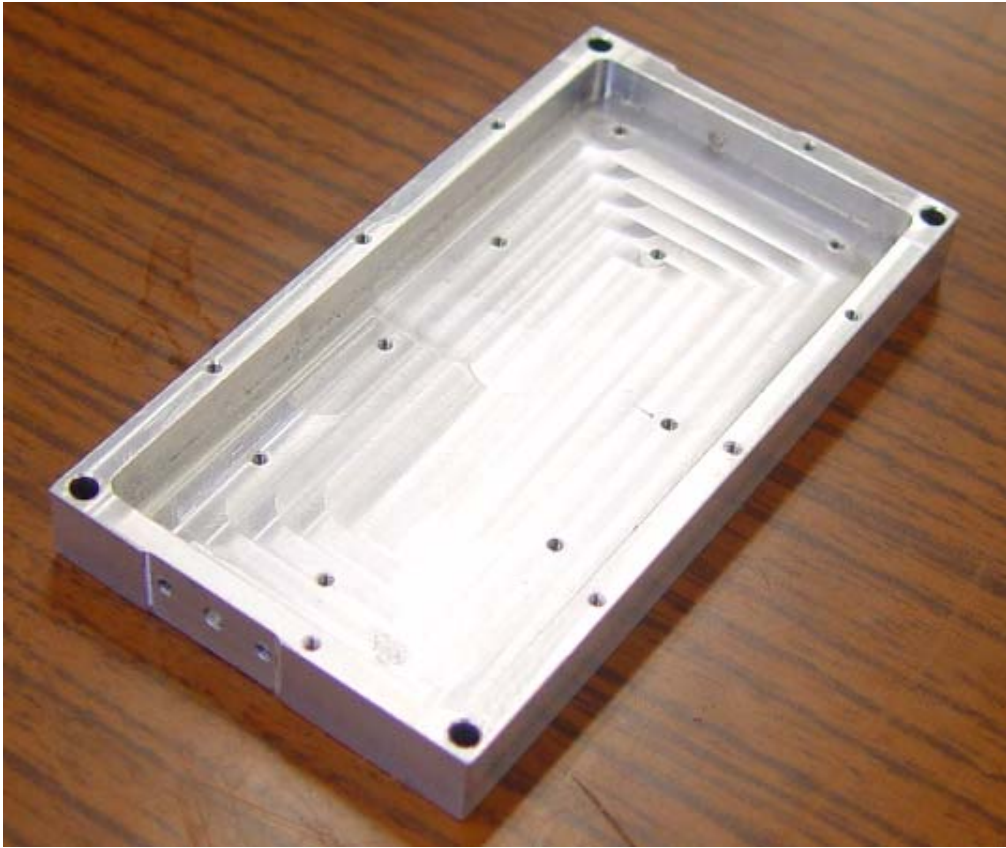


Figure 5.76: Inside view of the box



Figure 5.77: Side view of the BP filter box



Figure 5.78: Top view of the BP filter box

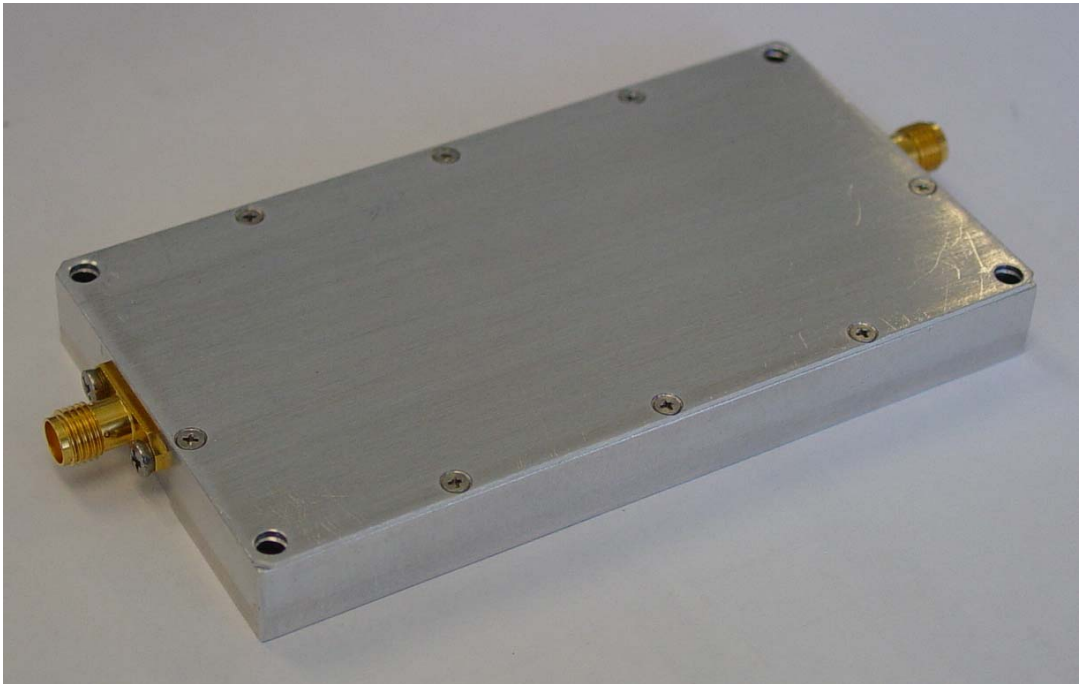


Figure 5.79: Oblique view of the BP filter box

The response of the boxed filter is shown in Figure 5.80 and 5.81.

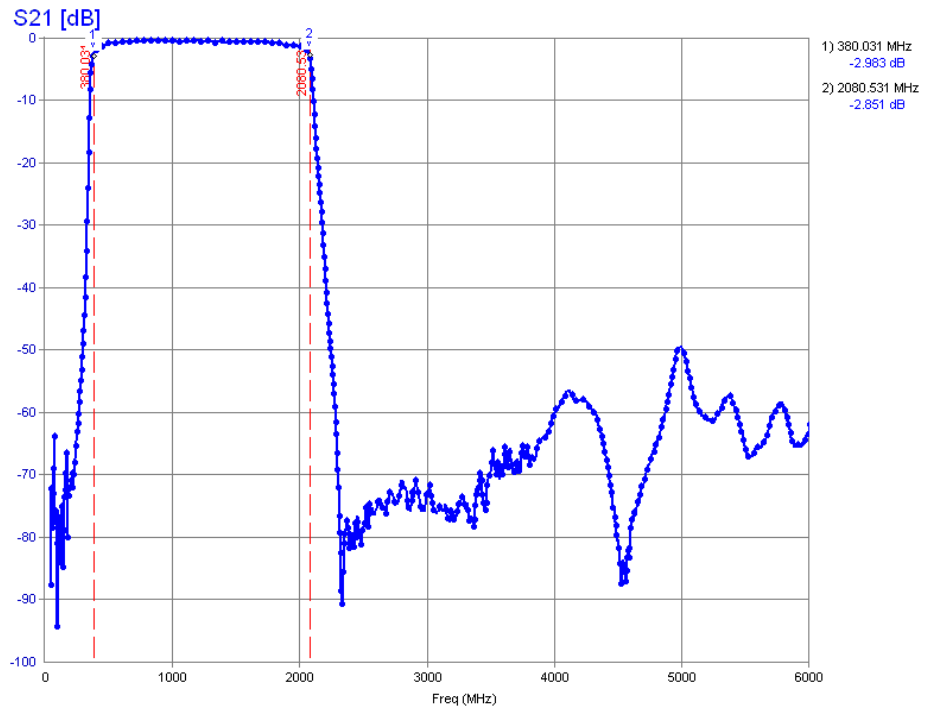


Figure 5.80: Measured S21 response of the final boxed BP filter up to 6 GHz

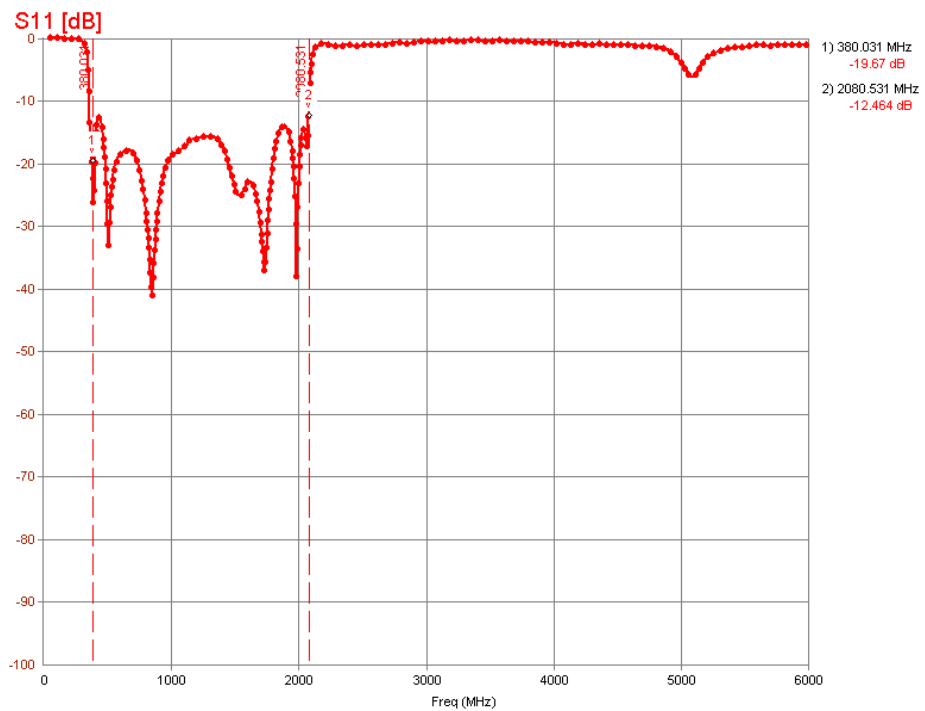


Figure 5.81: Measured S11 response of the final boxed BP filter up to 6 GHz

Compared to Figure 5.74, in figure 5.80 above it is seen that the stopband response is distorted especially after the quarter wavelength frequency (4736.6 MHz). This is due to poor grounding from the connectors to the top and bottom

sides of the stripline structure. This effect may be tolerated using through connectors that allow soldering of top and bottom sides of the stripline.

CHAPTER 6

CONCLUSION

In this thesis work, a design method has been presented to realize a highly selective mixed element broadband microwave bandpass filter. The method combines separate highpass and lowpass filters to form the bandpass filter. Small size, low passband loss and high stopband attenuation are aimed initially. A bandpass filter with a passband from 0.4 GHz to 2 GHz is selected for the thesis work. A 0.4 GHz highpass lumped filter is combined with a 2.0 GHz lowpass distributed filter to obtain the desired bandpass filter.

Due to broadband response of the desired bandpass filter, since the corner frequencies are separated too much, highpass and lowpass filters are designed independently. More than forty design trials are performed using FILPRO. According to the resulting responses of the trials, one lumped highpass filter and three distributed lowpass filters are selected for optimization, simulation and realization.

Various design considerations, computer simulations and experimental studies have been carried out on the selected filters. Electromagnetic simulation results are included in the optimization of the lumped filter. For distributed lowpass filter simulations, both GENESYS and SONNET are used. GENESYS and SONNET gave very similar simulation results. One of the distributed lowpass filters is also simulated using HFSS program and the result of this simulation is found very consistent with GENESYS and SONNET's results. Having seen that the

simulation results are consistent in each other and are satisfactory, realization studies started.

The distributed lowpass filter is realized in stripline form using Teflon based Rogers® 5880 substrate, whose relative dielectric constant is 2.2. The initial lumped highpass filter is realized using ordinary two sided FR4 substrate, whose relative dielectric constant is roughly 4.5. In later stages, lumped filter is also adapted to Rogers 5880 substrate, with some performance degradation, to be able to combine lowpass and highpass filters on the same printed circuit substrate. Lumped topology resulted in a very small size as expected.

Drilling method is used to realize the filters. Some modifications are made to cancel the deteriorating effects of drilling such as decrease in dielectric thickness.

Realized filters are tested with a network analyzer. It is seen that the measurements are in agreement with simulation results. Some further modifications are performed on the filters according to the measurement results.

When the lowpass and highpass filters are combined to form the bandpass filter, no degradation in filter performances is observed, due to the broadband nature of the bandpass filter. According to the measurements, insertion loss of the final bandpass filter is 1 dB in the passband and more than 60 dB in the stopband, and return loss is less than 10 dB in the passband. These results show that initial aims are obtained.

Even though initial aims were very high, this thesis shows that after encountering several different problems, highly selective mixed element broadband microwave filters can be produced on a single substrate with a performance which surpasses expectations.

Finally, it can be said that, this thesis generally gives the necessary information and experience to design and realize a mixed element broadband bandpass filter.

As a future work, appropriate topologies to extend the stopband limit may be searched and an additional lowpass filter may be embedded to the 0.4-2.0 GHz bandpass filter for rejection of bands from 6 GHz up to 18GHz. The performance of the lumped highpass part may also be improved.

REFERENCES

- [1] FILPRO Manual, METU, 2002.
- [2] GENESYS User's Manual, Eagleware Software Inc, 2002.
- [3] SONNET User's Manual, Sonnet Software Inc, 2000.
- [4] Dean J.E., "Microwave Integrated Circuit Broadband Filters and Contiguous Multiplexers", Ph. D. Thesis in Electrical and Electronics Engineering Dept., University of Leeds, Leeds, England, October 1979.
- [5] Yıldız İrfan, "Realization of a Stripline Switched Multiplexer", M.S. Thesis in Electrical and Electronics Engineering Dept., Middle East Technical University, Ankara, Turkey, December 2001.
- [6] Bağdat A. Dilara, "Design of Highly Selective Broadband Suspended Substrate Triplexers", M.S. Thesis in Electrical and Electronics Engineering Dept., Middle East Technical University, Ankara, Turkey, June 2001.
- [7] Randall W. Rhea, "HF Filter Design and Computer Simulation", Noble Publishing Corp., Atlanta, USA, 1994.
- [8] Arslan Ali, "Design and Realization of Microwave Bandpass Filters Using Sine-Plane Approach", M.S. Thesis in Electrical and Electronics Engineering Dept., Middle East Technical University, Ankara, Turkey, February 1989.
- [9] Karaaslan Mehmet, "Network Transformations for Realization of Lumped and Distributed Filters", M.S. Thesis in Electrical and Electronics Engineering Dept., Middle East Technical University, Ankara, Turkey, September 1994.
- [10] Çağlar Ü. Kenan, "Generalized Chebychev Low Pass Filter Design and Construction Using Suspended Stripline Structure", M.S. Thesis in Electrical and Electronics Engineering Dept., Middle East Technical University, Ankara, Turkey, September 1987.

- [11] Richards, P.I., "Resistor Transmission Line Circuits" Proc. IRE, Vol 36 1948, pp.217-220.
- [12] Wenzel, R. J., "General Theory and Design of Optimum Quarter Wave TEM Filters" IEEE Microwave Theory Tech., May 1965.
- [13] Rhodes, J.D., "Suspended Substrates Provide Alternative to Coax" Microwave Systems News, Aug. 1979.
- [14] Agilent S-Parameter Design Application Note, AN-154.
- [15] Uzun Remzi, "Computer Aided Microwave Filter Design", M.S. Thesis in Electrical and Electronics Engineering Dept., Middle East Technical University, Ankara, Turkey, June 1990.
- [16] Donald R.J. White, "A Handbook on Electrical Filters", 1976, Germantown, Maryland 20767, TK 7872.F5 W47 1980.
- [17] Ansoft HFSS Getting Started Manual An Antenna Problem
- [18] Agilent S-Parameter Design Application Note, AN-154.
- [19] Helszajn Joseph, "Synthesis of Lumped Element, Distributed and Planar Filters", McGraw-Hill Book Company (UK) Limited, TK7872.F5H393 1990.

APPENDIX A

STRIPLINE SUBSTRATE AND DRILL HOLE DIMENSIONS

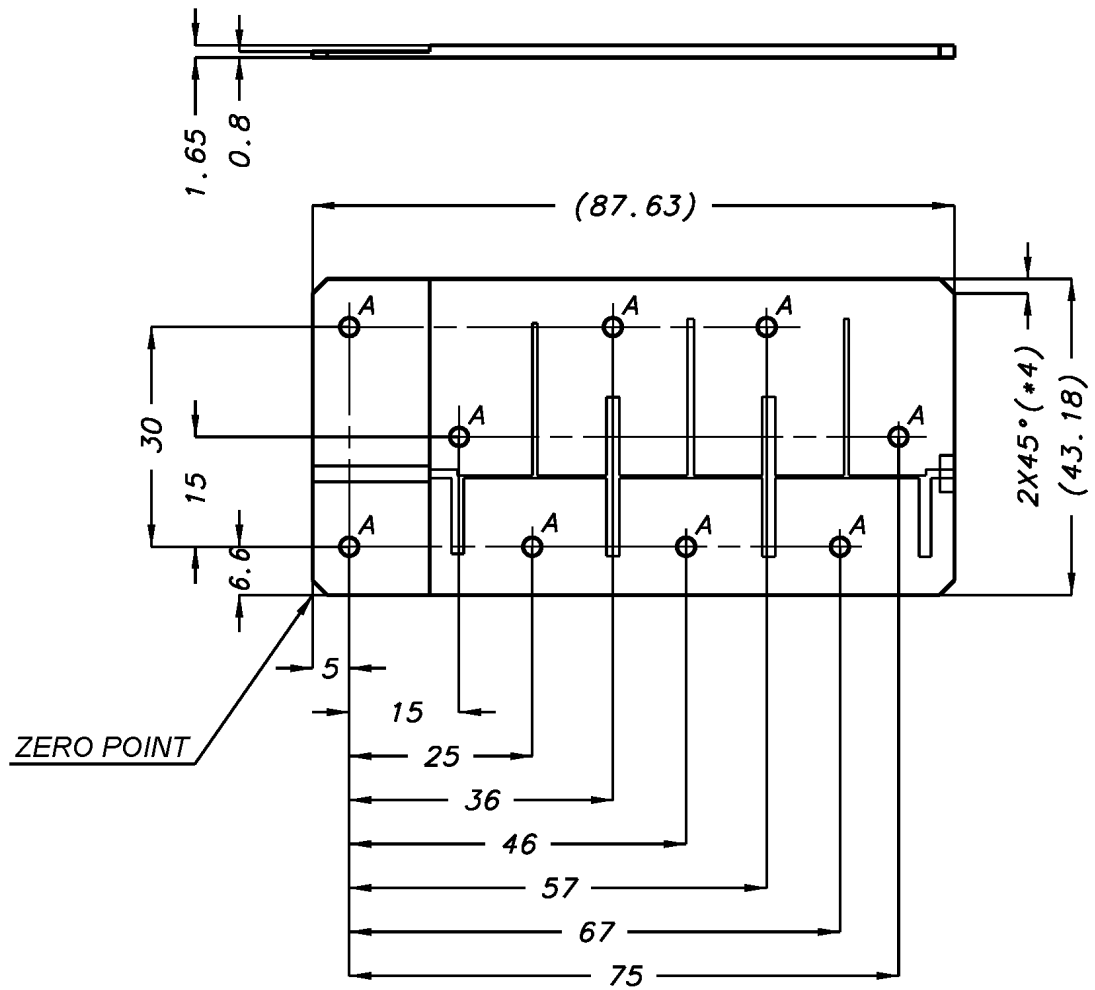


Figure A.1: Dimensions of the stripline substrate and locations of the drill holes for aluminum box

APPENDIX B

PROPERTIES OF STRIPLINE DIELECTRIC MATERIAL

RT/duroid® 5870 /5880 High Frequency Laminates

Features:

- Lowest electrical loss for reinforced PTFE material.
- Low moisture absorption.
- Isotropic
- Uniform electrical properties over frequency.
- Excellent chemical resistance.

Some Typical Applications:

- Commercial Airline Telephones
- Microstrip and Stripline Circuits
- Millimeter Wave Applications
- Military Radar Systems
- Missile Guidance Systems
- Point to Point Digital Radio Antennas

RT/duroid® 5870 and 5880 glass microfiber reinforced PTFE composites are designed for exacting stripline and microstrip circuit applications.

Glass reinforcing microfibers are randomly oriented to maximize benefits of fiber reinforcement in the directions most valuable to circuit producers and in the final circuit application.

The dielectric constant of RT/duroid 5870 and 5880 laminates is uniform from panel to panel and is constant over a wide frequency range. Its low dissipation factor extends the usefulness of RT/duroid 5870 and 5880 to Ku-band and above.

RT/duroid 5870 and 5880 laminates are easily cut, sheared and machined to shape. They are resistant to all solvents and reagents, hot or cold, normally used in etching printed circuits or in plating edges and holes.

Normally supplied as a laminate with electrodeposited copper of $\frac{1}{4}$ to 2 ounces/ft.² (8 to 70 μ m) on both sides, RT/duroid® 5870 and 5880 composites can also be clad with rolled copper foil for more critical electrical applications. Cladding with aluminum, copper or brass plate may also be specified.

When ordering RT/duroid 5870 and 5880 laminates, it is important to specify dielectric thickness, tolerance, rolled or electrodeposited copper foil, and weight of copper foil required.

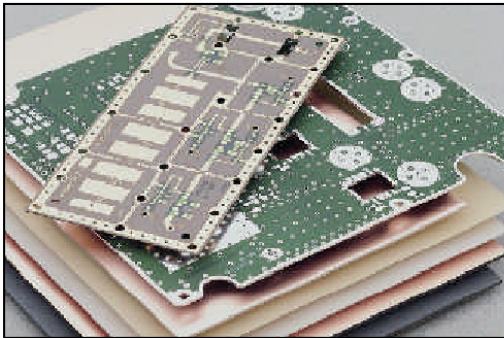


Figure B.1: Rogers 5870/5880 substrates

PROPERTY	TYPICAL VALUE						DIRECTION	UNITS	CONDITION	TEST METHOD
	RT/duroid® 5870			RT/duroid® 5880						
Dielectric Constant, ϵ_r	2.35 2.33 ± 0.02 spec.			2.20 2.20 ± 0.02 spec.			Z	—	C24/23/50 C24/23/50	1 MHz IPC-TM-650 2.5.5.3 10 GHz IPC-TM-650 2.5.5.5
Dissipation Factor, $\tan \delta$	0.0005 0.0012			0.0004 0.0009			Z	—	C24/23/50 C24/23/50	1 MHz IPC-TM-650 2.5.5.3 10 GHz IPC-TM-650 2.5.5.5
Thermal Coefficient of ϵ_r	-115			-125				ppm/°C	-50 - 150°C	IPC-TM-650 2.5.5.5
Volume Resistivity	2 X 10 ⁷			2 X 10 ⁷			Z	Mohm•cm	C96/35/90	ASTM D257
Surface Resistivity	3 X 10 ⁶			3 X 10 ⁶			Z	Mohm	C96/35/90	ASTM D257
Tensile Modulus	Test at 23°C 1300(189) 1280(185)	Test at 100°C 490 (71) 430 (63)	Test at 23°C 1070 (156) 860 (125)	Test at 100°C 450 (65) 380 (55)			X Y	MPa (kpsi)		
ultimate stress	50 (7.3) 42 (6.1)	34 (4.8) 34 (4.8)	29 (4.2) 27 (3.9)	20 (2.9) 18 (2.6)			X Y	MPa (kpsi)	A	ASTM D638
ultimate strain	9.8 9.8	8.7 8.6	6.0 4.9	7.2 5.8			X Y	%		
Compressive Modulus	1210 (176) 1360 (198) 803 (120)	680 (99) 860 (125) 520 (76)	710 (103) 710 (103) 940 (136)	500 (73) 500 (73) 670 (97)			X Y Z	MPa (kpsi)		
ultimate stress	30 (4.4) 37 (5.3) 54 (7.8)	23 (3.4) 25 (3.7) 37 (5.3)	27 (3.9) 28 (5.3) 52 (7.5)	22 (3.2) 21 (3.1) 43 (6.3)			X Y Z	MPa (kpsi)	A	ASTM D695
ultimate strain	4.0 3.3 8.7	4.3 3.3 8.5	8.5 7.7 12.5	8.4 7.8 17.6			X Y Z	%		
Deformation Under Load				Test at 150°C 1.0			Z	%	24 hr/14 MPa (2kpsi)	ASTM D621
Heat Distortion Temperature	>260 (>500)			>260 (>500)			X,Y	°C (°F)	1.82 MPa (264 psi)	ASTM D648
Specific Heat	0.96 (0.23)			0.96 (0.23)				J/g/K (BTU/lb/°F)		Calculated
Moisture Absorption Thickness = 0.8 mm (0.031) Thickness = 1.6 mm (0.062)	0.9 (0.02) 13 (0.015)			0.9 (0.02) 13 (0.015)				mg (%)	D24/23	ASTM D570
Thermal Conductivity	0.22			0.20			Z	W/m/K		ASTM C518
Thermal Expansion	X	Y	Z	X	Y	Z	<<<	mm/m		
	-5.0	-5.5	-11.6	-6.1	-8.7	-18.7			-100°C	
	-0.6	-0.9	-4.0	-0.9	-1.8	-6.9			15	
	-0.3	-0.4	-2.6	-0.5	-0.9	-4.5			25	
	0.7	0.9	7.5	1.1	1.5	8.7			75	
	1.8	2.2	22.0	2.3	3.2	28.3			150	
	3.4	4.0	58.9	3.8	5.5	69.5			250	
Density	2.2			2.2						ASTM D792
Copper Peel	20.8 (3.7)			22.8 (4.0)				pli (N/mm)	after solder float	IPC-TM-650 2.4.8
Flammability	94V-0			94V-0						UL

[1] SI unit given first with other frequently used units in parentheses.
[2] References: Internal TR's 1430, 2224, 2854. Test were at 23°C unless otherwise noted.
Typical values should not be used for specification limits.

Table B.2: Material properties of Rogers 5870/5880 substrates

APPENDIX C

PROPERTIES OF LUMPED INDUCTORS

Chip Inductors—0603CS Series (1608)

Ultra small size, exceptional Q and high SRFs make these inductors ideal for high frequency applications where size is at a premium. They also have excellent DCR and current carrying characteristics.

Part Number ¹	Inductance ² (nH)	Percent Tolerance ³	Q Min ⁴	SRF ⁵ Min (MHz)	R _{DC} Max ⁶ (Ohms)	I _{PC} Max ⁷ (mA)	900 MHz		1.7 GHz		Color Code
							L Typ	Q Typ	L Typ	Q Typ	
0603CS-1N6X_BC	1.6 @ 250 MHz	10.5	24	12500	.030	700	1.67	49	1.65	63	Red
0603CS-1N8X_BC	1.8 @ 250 MHz	10.5	16	12500	.045	700	1.63	35	1.66	50	Black
0603CS-3N6X_BC	3.6 @ 250 MHz	10.5	22	5900	.063	700	3.72	53	3.71	65	Red
0603CS-3N9X_BC	3.9 @ 250 MHz	10.5	22	6900	.080	700	3.95	49	3.96	67	Brown
0603CS-4N3X_BC	4.3 @ 250 MHz	10.5	22	5900	.063	700	4.32	50	4.33	70	Orange
0603CS-4N7X_BC	4.7 @ 250 MHz	10.5	20	5800	.116	700	4.72	47	4.75	57	Violet
0603CS-5N1X_BC	5.1 @ 250 MHz	10.5	20	5700	.140	700	4.93	47	4.95	56	Green
0603CS-6N8X_BC	6.8 @ 250 MHz	10.5,2	27	5800	.110	700	6.75	60	7.10	81	Red
0603CS-7N5X_BC	7.5 @ 250 MHz	10.5,2	28	4800	.106	700	7.70	60	7.82	65	Brown
0603CS-8N7X_BC	8.7 @ 250 MHz	5,2	28	4600	.109	700	8.86	62	9.32	58	Yellow
0603CS-9N5X_BC	9.5 @ 250 MHz	5,2	28	5400	.135	700	9.7	59	9.92	61	Blue
0603CS-10NX_BC	10 @ 250 MHz	5,2	31	4800	.130	700	10.0	66	10.6	83	Orange
0603CS-11NX_BC	11 @ 250 MHz	5,2	33	4000	.086	700	11.0	53	11.5	56	Gray
0603CS-12NX_BC	12 @ 250 MHz	5,2	35	4000	.130	700	12.3	72	13.5	83	Yellow
0603CS-15NX_BC	15 @ 250 MHz	5,2	35	4000	.170	700	15.4	64	16.8	89	Green
0603CS-16NX_BC	16 @ 250 MHz	5,2	34	3300	.104	700	16.2	55	17.3	52	White
0603CS-18NX_BC	18 @ 250 MHz	5,2	35	3100	.170	700	18.7	70	21.4	69	Blue
0603CS-22NX_BC	22 @ 250 MHz	5,2	38	3000	.190	700	22.8	73	26.1	71	Violet
0603CS-24NX_BC	24 @ 250 MHz	5,2	37	2650	.135	700	24.5	45	28.7	39	Black
0603CS-27NX_BC	27 @ 250 MHz	5,2	40	2800	.220	600	29.2	74	34.6	65	Gray
0603CS-30NX_BC	30 @ 250 MHz	5,2	37	2250	.144	600	31.4	47	39.9	28	Brown
0603CS-33NX_BC	33 @ 250 MHz	5,2	40	2300	.220	600	36.0	67	49.5	42	White
0603CS-36NX_BC	36 @ 250 MHz	5,2	38	2080	.250	600	39.4	47	52.7	24	Red
0603CS-39NX_BC	39 @ 250 MHz	5,2	40	2200	.250	600	42.7	60	60.2	40	Black
0603CS-43NX_BC	43 @ 250 MHz	5,2	39	2000	.280	600	47.0	44	64.9	21	Orange
0603CS-47NX_BC	47 @ 200 MHz	5,2	38	2000	.280	600	52.2	62	77.2	35	Brown
0603CS-56NX_BC	56 @ 200 MHz	5,2	38	1900	.310	600	62.5	56	97.0	26	Red
0603CS-68NX_BC	68 @ 200 MHz	5,2	37	1700	.340	600	80.5	54	168	21	Orange
0603CS-72NX_BC	72 @ 150 MHz	5,2	34	1700	.490	400	82.0	53	135	20	Yellow
0603CS-82NX_BC	82 @ 150 MHz	5,2	34	1700	.540	400	96.2	54	177	21	Green
0603CS-R10X_BC	100 @ 150 MHz	5,2	34	1400	.580	400	124	49	—	—	Blue
0603CS-R11X_BC	110 @ 150 MHz	5,2	32	1350	.610	300	138	43	—	—	Violet
0603CS-R12X_BC	120 @ 150 MHz	5,2	32	1300	.650	300	166	39	—	—	Gray
0603CS-R15X_BC	150 @ 150 MHz	5,2	28	990	.920	280	250	25	—	—	White
0603CS-R18X_BC	180 @ 100 MHz	5,2	25	990	1.25	240	305	22	—	—	Black
0603CS-R22X_BC	220 @ 100 MHz	5,2	25	900	2.10	200	480	8	—	—	Brown
0603CS-R27X_BC	270 @ 100 MHz	5,2	24	900	2.30	170	980	4	—	—	Red

1. Tolerance and packaging codes:

0603CS-R12X_BC

L Packaging

C = EIA RS-481 clear tape and reel (standard).
For orders of less than a full reel, there is a \$25 per reel charge to make them machine-ready.
B = In a carrier tape but without leader or trailer.

Inductance tolerance

G=2%, J=5%, K=10%
Table above shows stock tolerances in bold.
Other tolerances shown are available on special order.

2. Inductance measured using Coilcraft SMD-A fixture in HP4286 impedance analyzer with Coilcraft-provided correlation pieces. For recommended test procedures, contact Coilcraft.

3. Tolerances in bold are stocked for immediate shipment.

4. Q measured using HP4291A with HP16193 test fixture and on HP8753D with Coilcraft SMD-D test fixture.

5. SRF measured using HP8753D network analyzer and Coilcraft SMD-D test fixture.

6. R_{DC} measured on Cambridge Technology micro-ohmmeter and Coilcraft CCF58 test fixture.

7. For 15°C rise.

8. Operating temperature range -40°C to +125°C.

9. Electrical specifications at 25°C.

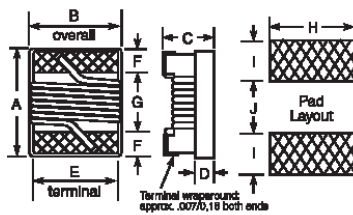
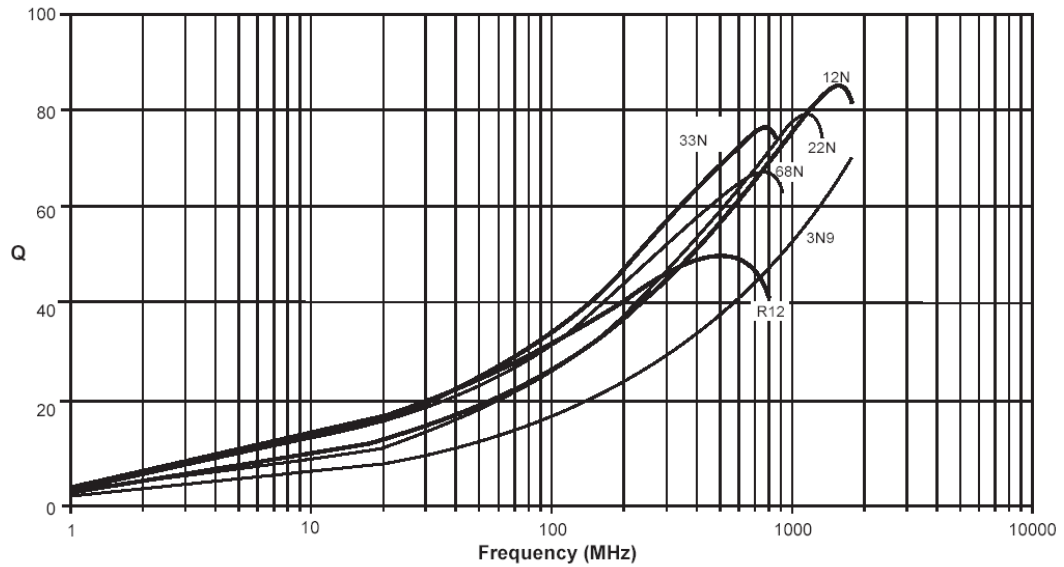
Document 195-2 Revised 5/19/99

1102 Silver Lake Road Cary, Illinois 60013 Phone 847/839-6400 Fax 847/839-1469
E-mail info@coilcraft.com Web http://www.coilcraft.com

Figure C.1: Coilcraft 0603CS inductors

0603CS Series (1608)

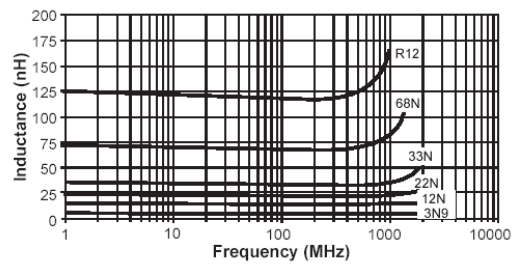
TYPICAL Q vs FREQUENCY



A	B	C	D	E	F	G	H	I	J
Max. .071	Max. .044	Max. .040	Ref. .015	.030	.013	.034	.040	.025	.025
1.80	1.12	1.02	0.38	0.76	0.33	0.86	1.02	0.64	0.64

Parts/reel: 7" 2,000; 13" 7,500 Tape width: 8mm

L vs FREQUENCY



Coilcraft

Document 195-2 Revised 5/19/99

1102 Silver Lake Road Cary, Illinois 60013 Phone 847/839-6400 Fax 847/839-1469
E-mail info@coilcraft.com Web http://www.coilcraft.com

Figure C.2: Coilcraft 0603CS inductors' Q and L curves

Chip Inductors – 0805CS Series (2012)

These ultra-compact inductors provide exceptional Q values, even at high frequencies. They have a ceramic body and wirewound construction to provide the highest SRFs available in 0805 size.

Part Number ¹	Inductance ² (nH)	Percent Tolerance ³	Q Min ⁴	SRF Min ⁵ (MHz)	R _{dc} Max ⁶ (Ohms)	I _{dc} Max ⁷ (mA)	Color Code
0805CS-020X _BC	2.8 @ 250 MHz	20, 10, 5	80 @ 1500 MHz	7900	.06	800	Gray
0805CS-3N0X _BC	3.0 @ 250 MHz	20, 10, 5	65 @ 1500 MHz	7900	.06	800	White
0805CS-030X _BC	3.3 @ 250 MHz	20, 10, 5	50 @ 1500 MHz	7900	.08	600	Black
0805CS-050X _BC	5.6 @ 250 MHz	20, 10, 5	65 @ 1000 MHz	5500	.08	600	Orange
0805CS-060X _BC	6.8 @ 250 MHz	20, 10, 5	50 @ 1000 MHz	5500	.11	600	Brown
0805CS-070X _BC	7.5 @ 250 MHz	20, 10, 5	50 @ 1000 MHz	4500	.14	600	Green
0805CS-080X _BC	8.2 @ 250 MHz	20, 10, 5, 2	50 @ 1000 MHz	4700	.12	600	Red
0805CS-100X _BC	10 @ 250 MHz	20, 10, 5, 2	60 @ 500 MHz	4200	.10	600	Blue
0805CS-120X _BC	12 @ 250 MHz	20, 10, 5, 2	50 @ 500 MHz	4000	.15	600	Orange
0805CS-150X _BC	15 @ 250 MHz	20, 10, 5, 2	50 @ 500 MHz	3400	.17	600	Yellow
0805CS-180X _BC	18 @ 250 MHz	20, 10, 5, 2	50 @ 500 MHz	3300	.20	600	Green
0805CS-220X _BC	22 @ 250 MHz	20, 10, 5, 2	55 @ 500 MHz	2600	.22	500	Blue
0805CS-240X _BC	24 @ 250 MHz	20, 10, 5, 2	50 @ 500 MHz	2000	.22	500	Gray
0805CS-270X _BC	27 @ 250 MHz	20, 10, 5, 2	55 @ 500 MHz	2500	.25	500	Violet
0805CS-330X _BC	33 @ 250 MHz	20, 10, 5, 2, 1	60 @ 500 MHz	2050	.27	500	Gray
0805CS-360X _BC	36 @ 250 MHz	20, 10, 5, 2, 1	55 @ 500 MHz	1700	.27	500	Orange
0805CS-390X _BC	39 @ 250 MHz	20, 10, 5, 2, 1	60 @ 500 MHz	2000	.29	500	White
0805CS-430X _BC	43 @ 200 MHz	20, 10, 5, 2, 1	60 @ 500 MHz	1650	.34	500	Yellow
0805CS-470X _BC	47 @ 200 MHz	20, 10, 5, 2, 1	60 @ 500 MHz	1650	.31	500	Black
0805CS-500X _BC	50 @ 200 MHz	20, 10, 5, 2, 1	60 @ 500 MHz	1550	.34	500	Brown
0805CS-680X _BC	68 @ 200 MHz	10, 5, 2, 1	60 @ 500 MHz	1450	.38	500	Red
0805CS-820X _BC	82 @ 150 MHz	10, 5, 2, 1	65 @ 500 MHz	1300	.42	400	Orange
0805CS-910X _BC	91 @ 150 MHz	20, 10, 5, 2, 1	65 @ 500 MHz	1200	.48	400	Black
0805CS-101X _BC	100 @ 150 MHz	10, 5, 2, 1	65 @ 500 MHz	1200	.46	400	Yellow
0805CS-111X _BC	110 @ 150 MHz	20, 10, 5, 2	50 @ 250 MHz	1000	.48	400	Brown
0805CS-121X _BC	120 @ 150 MHz	10, 5, 2, 1	50 @ 250 MHz	1100	.51	400	Green
0805CS-151X _BC	150 @ 100 MHz	10, 5, 2, 1	50 @ 250 MHz	920	.56	400	Blue
0805CS-181X _BC	180 @ 100 MHz	10, 5, 2, 1	50 @ 250 MHz	870	.64	400	Violet
0805CS-221X _BC	220 @ 100 MHz	10, 5, 2	50 @ 250 MHz	850	.70	400	Gray
0805CS-241X _BC	240 @ 100 MHz	20, 10, 5, 2	44 @ 250 MHz	690	1.0	350	Red
0805CS-271X _BC	270 @ 100 MHz	10, 5, 2	48 @ 250 MHz	650	1.0	350	White
0805CS-331X _BC	330 @ 100 MHz	10, 5, 2	48 @ 250 MHz	600	1.4	310	Black
0805CS-391X _BC	390 @ 100 MHz	10, 5, 2	48 @ 250 MHz	560	1.5	290	Brown
0805CS-471X _BC	470 @ 50 MHz	10, 5	33 @ 100 MHz	375	1.76	250	Violet
0805CS-561X _BC	560 @ 25 MHz	10, 5	23 @ 50 MHz	340	1.90	230	Orange
0805CS-681X _BC	680 @ 25 MHz	10, 5	23 @ 50 MHz	188	2.20	190	Green
0805CS-821X _BC	820 @ 25 MHz	10, 5	23 @ 50 MHz	215	2.35	180	Blue

1. Tolerance and packaging codes:

0805CS-391X_BC

Packaging

C = EIA RS-481 clear tape and reel (standard).
For orders of less than a full reel, there is a \$25 per reel charge to make them machine-ready.
B = In a carrier tape but without leader or trailer.

Inductance tolerance

F=1%, G=2%, J=5%, K=10%, M=20%
Table above shows stock tolerances in bold.
Other tolerances shown are available on special order.

- Inductance measured using Coilcraft SMD-A fixture in HP4286A impedance analyzer with Coilcraft-provided correlation pieces. For recommended test procedures, contact Coilcraft.
- Tolerances in bold are stocked for immediate shipment.
- Q measured using HP4291A with HP16193 test fixture and on HP8753D with Coilcraft SMD-D test fixture.
- SRF measured using HP8753D network analyzer and Coilcraft SMD-D test fixture.
- R_{dc} measured on Cambridge Technology micro-ohmmeter and Coilcraft CCF858 test fixture.
- For 15°C rise.
- Operating temperature range -40° to +125°C.
- Electrical specifications at 25°C.

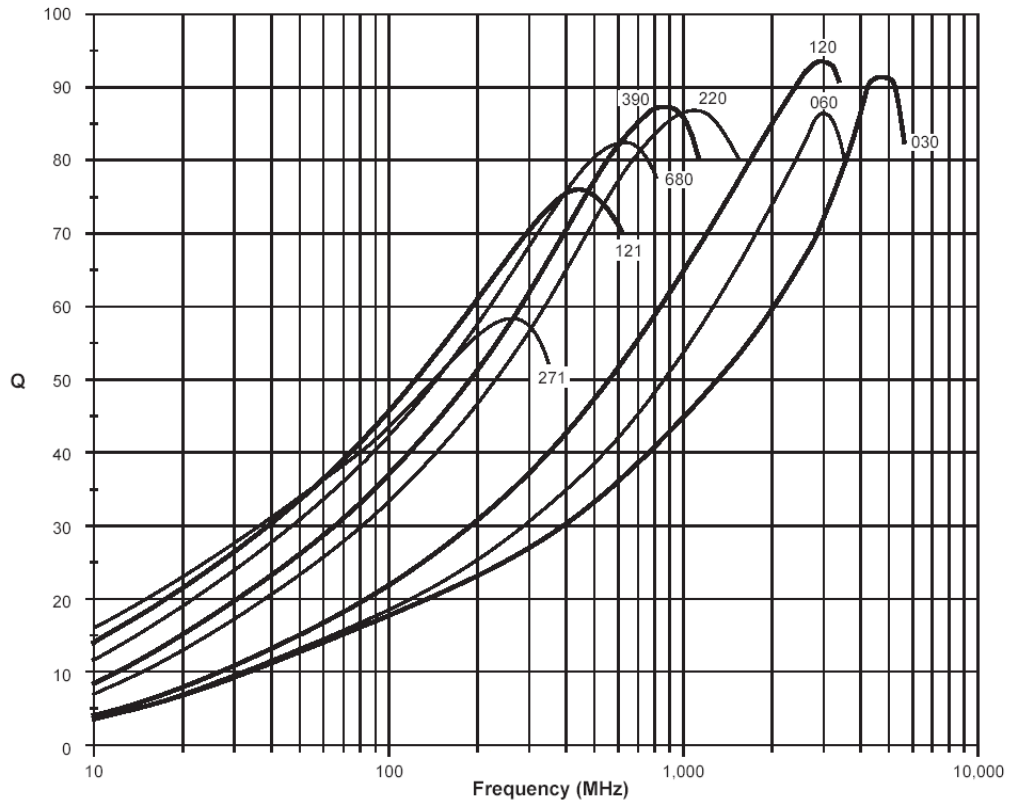
Document 100-1 Revised 3/1/00

1102 Silver Lake Road Cary, Illinois 60013 Phone 847/639-6400 Fax 847/639-1469

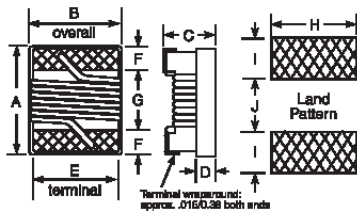
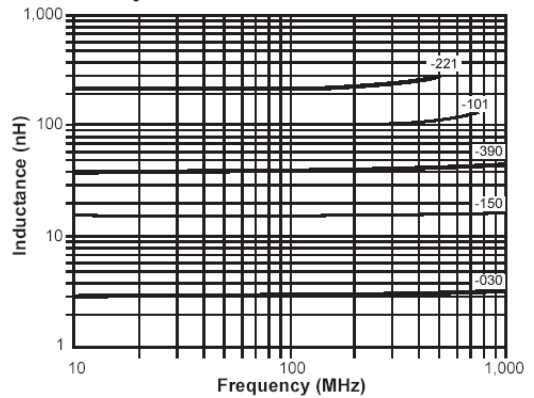
Figure C.3: Coilcraft 0805CS inductors

0805CS Series (2012)

TYPICAL Q vs FREQUENCY



L vs FREQUENCY



A	B	C	D	E	F	G	H	I	J
Max.	Max.	Max.	Ref.						
.090	.068	.060	.020	.050	.020	.040	.070	.040	.030
2.29	1.73	1.52	0.51	1.27	0.51	1.02	1.78	1.02	0.76

Parts/reel: 7" 2,000; 13" 7,500 Tape width: 8mm

Coilcraft

Document 100-2 Revised 5/19/99

1102 Silver Lake Road Carv, Illinois 60013 Phone 847/639-6400 Fax 847/639-1469

Figure C.4: Coilcraft 0805CS inductors' Q and L curves